

**Energy Storage and Dissipation in Deformed
Protein-based Networks on Seconds Time Scale
is Controlled by Submicron Length Scales**

Claire Darizu Munialo

Thesis committee

Promotor

Prof. Dr E. van der Linden
Professor of Physics and Physical Chemistry of Foods
Wageningen University

Co-promotor

Dr H.H.J. de Jongh
Senior Scientist, Physics and Physical Chemistry of Foods
Wageningen University

Other members

Dr J. Engmann, Nestlé Research Center, Lausanne, Switzerland
Prof. Dr M. Langton, Swedish University of Agricultural Sciences, Uppsala, Sweden
Prof. Dr J. van der Gucht, Wageningen University
Prof. Dr H. Gruppen, Wageningen University

This research was conducted under the auspices of the Graduate School VLAG (Advanced studies in Food Technology, Agrobiotechnology, Nutrition and Health Sciences).

Energy Storage and Dissipation in Deformed Protein-based Networks on Seconds Time Scale is Controlled by Submicron Length Scales

Claire Darizu Munialo

Thesis

submitted in fulfilment of the requirements for the degree of doctor
at Wageningen University

by the authority of the Rector Magnificus

Prof. Dr M.J. Kropff,

in the presence of the

Thesis Committee appointed by the Academic Board

to be defended in public

on Friday 22 May 2015

at 1:30 p.m. in the Aula.

Claire Darizu Munialo

Energy Storage and Dissipation in Deformed Protein-based Networks on
Seconds Time Scale is Controlled by Submicron Length Scales
280 pages.

PhD thesis, Wageningen University, Wageningen, NL (2015)
With references, with summaries in Dutch and English
ISBN 978-94-6257-310-9

***Especially dedicated to my best friend and love Josh Onyango
and my parents Andrew and Ruth Munialo***

I have fought a good fight, I have finished the race and kept the faith.

TABLE OF CONTENTS

	PAGE
Chapter 1. General introduction	9
Chapter 2. Modulation of the gelation efficiency of fibrillar and spherical aggregates by means of thiolation	27
Chapter 3. Fibril formation from pea protein and subsequent gel formation	53
Chapter 4. The ability to store energy in pea protein gels is set by network dimensions smaller than fifty nanometers	77
Chapter 5. Quantitative analysis of the network structure that underlines the transitioning in mechanical responses of pea protein gels	99
Chapter 6. Modification of ovalbumin with fructooligosaccharides: consequences for network morphology and mechanical deformation responses	129
Chapter 7. Modulation of the serum phase viscosity and its contribution to energy dissipation upon mechanical deformation of whey protein gels	169
Chapter 8. Activation energy of the disruption of gel networks in relation to elastically stored energy in fine-stranded ovalbumin gels	209
Chapter 9. General discussion	233
Summary	261
Samenvatting	265
Acknowledgements	271
List of publications	275
Curriculum vitae	277
Overview of completed training activities	278

Chapter I

General Introduction

Foods and food products are multi-component systems, whose spatial volume is often set by a protein-continuous network, such as in dairy products like cheese and butter, jellies, tofu, or confectionary products¹. However, with an increase in human population and a concurrent increase in demand for protein, the food industry is challenged to diversify the available protein sources or to come up with alternative proteins to meet the increasing demand. The alternative proteins should have a similar functionality to the original protein and, most importantly, the end products should still have a similar texture. However, proteins from different sources such as animal or plant protein sources have inherent functional properties that profoundly differ e.g. in solubility, denaturation, aggregation propensity, and thereby the network-forming properties. This makes the exchangeability of protein sources without altering the textural and sensorial properties of the final product a difficult target.

To feed the growing population, there are a number of routes that the food industry can adopt. It can introduce alternative proteins into the food chain, modify the proteins, or exchange the protein with proteins from a different source, given that proteins can be used as structuring and texturing components in food products. This can however, result in variation of the texture of the final product, making it difficult to develop products with textural properties that are acceptable to the consumer. Additionally, the use of alternative proteins in the food chain increases the need to understand protein-specific behavior that results in variation of the material responses during several processes, such as oral processing or in the manufacturing of the product¹.

To efficiently search for alternative protein sources for food gels, the relation between protein network properties and texture must be better understood. This provides a challenge to understand the fundamental relations between characteristics of the constituting proteins and the conditions of the network formation, such as pH, ionic strength, protein concentration, and incubation temperature, to produce a wide range of network properties. Such knowledge will give guidelines on the limits of exchangeability of protein sources in food products and can be used to tailor products accordingly.

Animal proteins are often used for human consumption. It is estimated that about 2 billion people live mainly on meat-based diets in comparison to 4 billion who live on plant-protein based diets². With a global increase in middle class population, the total population feeding on meat-based diets is expected to increase, which will result in a concurrent increase in the demand for animal proteins. Meat production in general puts a large footprint on natural resources such as land, energy, and water². Another downside, of animal production is that it causes high greenhouse gas emissions³.

Plant proteins have become more important in human nutrition because they are more available, cost effective, and the method for their utilization is more sustainable than animal proteins. Legumes such as lentils, beans, and peas, have been used in the diets of people from many cultures especially where animal proteins are expensive or scarce⁴. Plant proteins can contribute to a more sustainable production, because direct human consumption of plants proteins is far more efficient than conversion of plant protein into animal protein and subsequent consumption thereof⁵. However, in order to make plant proteins such as legumes more attractive as a food ingredient, an understanding and the improvement of their functional characteristics is essential⁴.

In the study of functional characteristics of protein-based gels, an understanding of how the gels behave under deformation is important, as this provides information that can be useful to understand the textural attributes of the gels. The resilience, or the materials ability to recover to its original dimensions after deformation, is a key criterion in understanding the energy balance in spatial gel networks. If food gels exhibit time-dependent deformation, i.e. viscoelasticity, it is common that upon deformation, the energy that is applied can either be dissipated or stored⁵. One of the prerequisites for the optimal use of proteins in food applications is directing their ability to store energy upon mechanical deformation. The ability to store energy, often measured in terms of recoverable energy in gels, has been correlated to a crumbly perception of food gels⁶. Crumbliness, which is defined as the effort needed to break the sample into (small) pieces between the tongue and the palate⁶, is one of the textural attributes that determines consumer acceptance of several food products such as processed meat or confectionary, and hence it is often used as a parameter for quality control during manufacture⁶. However, mechanical responses that relate to crumbliness such as the recoverable energy have to be understood in terms of gel composition to use this parameter for predictive and directive purposes in tailoring food products.

The aim of this thesis is to understand how structural aspects affect the ability of protein gels to store versus dissipate energy. Special attention is given to understanding how these structural aspects of protein networks can be varied and how this eventually affects the ability of the networks to store energy.

In this chapter, we first address the proteins that were studied in this thesis, and give a more detailed account of the formation of (stranded) networks. After that, we outline the approaches to prepare protein networks that vary in structure, the fracture properties of gel networks, and the energy balance i.e. the balance between storage and dissipated energy which arises from the application of energy to deform gels. Furthermore the techniques that can be used to study the networks formed are discussed. In the final part of this chapter, the outline of the thesis is presented.

Types of proteins

Proteins are macromolecules that are made of one or more long chains of amino acid residues. Proteins can be divided mainly into fibrous or globular. Fibrous proteins form long, elongated rod-like structures that provide structural support for cells and tissue^{7, 8, 9}. Typical examples of fibrous proteins include collagen and fibrinogen (a blood serum protein). Globular proteins are typically more 'spherical' in shape and can have densities approaching crystalline hydrocarbons and amino acids¹⁰. Globular proteins include whey proteins, egg white proteins, and plant seed storage proteins.

Proteins studied in this thesis

Whey proteins

Whey protein (hereafter referred to as WPI) is a mixture of globular proteins isolated from whey – a liquid by-product of cheese production¹¹. WPI is important in the food industry, not only as a component of dairy products, but also as an ingredient in many non-dairy food products,^{12, 13} due to its nutritional and functional properties¹¹. The main proteins present in WPI are β -lactoglobulin, which is a small dimeric protein (molecular weight of around 36 kDa (2 x 18 kDa)) that consists of 162 amino acid residues, two disulfide bonds (Cys66 – Cys160 and Cys106–Cys119), and a free thiol group (Cys121)¹⁴, with an isoelectric point (IEP) of 5.2, and a defined secondary and tertiary structure, accounting for > 60 % of WPI i.e. ~3.2 g/ kg. α -Lactalbumin is a Ca^{2+} binding protein that accounts for ~ 22 % of WPI i.e. 1.2 g/ kg, with IEP 4.8 - 5.1¹⁵ and a molecular weight of around 14 kDa. Immunoglobulin makes up ~ 9.1 % WPI totaling to 0.7 g/ kg, with an IEP 5.5 - 6.8¹⁶ and 0.4 g/ kg bovine serum albumin (amounting to ~ 5.5 % of WPI) with an IEP 4.8 - 5.1¹⁶. The heat denaturation of whey proteins starts at 65 °C, but during the heating of milk denaturation mostly occurs at temperatures above 80 °C¹⁷.

Egg white proteins

Egg white proteins (albumins) are applied in a wide range of foods because of their functional properties such as solubility, gelling, emulsification, and water binding ability¹⁸. Ovalbumin, the major egg white protein, is a glycoprotein with a molecular mass of 45 kDa that has 386 amino acids, an IEP of about 4.7, and a denaturation temperature of around 80 °C¹⁹. Ovalbumin belongs to the serine protease inhibitor (serpin) super family, although it does not exhibit any protease-inhibitory activity due to failure of insertion of the cleaved reactive loop into a β -sheet²⁰. Ovalbumin has 4 free thiol groups with a single internal disulfide bond between Cys 74 and Cys 121²¹. Ovalbumin has 2 potential phosphorylation sites at serine 69 and 345 and different degrees of phosphorylation may occur: zero, one or two phosphate groups per molecule²⁰.

Soy storage proteins

Soy proteins are applied in a wide range of food products because of their ability to improve the texture of foods and their high nutritive value²². Soy protein isolate consists of two major globulin components, β -conglycinin (7 S) and glycinin (11 S), whose composition and structure determine the functional properties of soy based protein products. The network formation by soy proteins or their individual components such as glycinin or β -conglycinin has been extensively investigated²³⁻²⁵. Glycinin is a hexameric protein with 350 – 400 kDa molecular weight²⁶ and has a compact quaternary structure which is stabilized via disulfide, electrostatic and hydrophobic interactions, and it is made up of six A-B subunits²⁷. Each subunit is composed of an acid polypeptide with a molecular weight of ~38 kDa, and a basic polypeptide which has a molecular weight of ~20 kDa, each linked by single disulfide bond, except for the acid polypeptide -A₄⁻²⁷. β -Conglycinin is a major protein of 7 S fraction²⁸ that has a molecular weight of 150 -180 kDa²⁹. It is composed of three subunits, - α ' - (molecular weight 72 kDa), - α - ' - (molecular weight 62 kDa), and - β - ' - (molecular weight 52 kDa), which interact to produce seven isomers (Bo - B6)²⁷. β -conglycinin is less heat-stable than glycinin; with an onset denaturation temperature of about 70 °C compared to that of glycinin which is over 80 °C (at neutral pH and low ionic strength)³⁰.

Pea storage proteins

Storage proteins of pea (*Pisum sativum* L.) have the potential of being used in the food industry as alternatives for soy proteins for the formulation of new food products because of their high nutritive value and non-allergenic character³¹. Pea proteins were identified in the 1960s - 70s as a potential alternative to soy bean proteins and consist predominantly of legumin (11S), vicilin (7S) and a minor protein, convicilin. Pea legumin is a hexamer of subunit pairs, each consisting of a basic subunit of ~ 20 kDa, and an acidic subunit of ~ 40 kDa³². Vicilin consists mainly of ~ 30, ~ 34, ~ 47, and ~ 50 kDa subunits³³, whereas convicilin is an α -subunit of vicilin³³. Pea proteins have a peak denaturation temperature of around 85 °C^{34, 35}, and an IEP between pH 4.8 – 5.5³⁶.

Protein aggregation and network formation

A gel can be described as colloidal particles sticking together to form a three-dimensional spatial network that fills the entire volume of the system³⁷. Gel formation can be achieved by heating proteins above the denaturation temperature³⁸, slow acidification towards the IEP using glucono- δ -lactone (GDL)^{37, 39} just adjusting the pH, or by the addition of salts such as NaCl³⁷. The formed gel networks can be classified as either fine or coarse-stranded and these networks are made up of different structural elements. Fine-stranded networks are made up of flexible strands or more rigid fibrils that can be around 5 - 12 nm in diameter depending on pH and ionic strength^{40, 41}. Such networks are formed when the gel formation is initiated at pHs far away from the IEP of the protein, or at low ionic strength⁴².

These gels have a transparent appearance because of the low light scattering efficiency of the thin strands⁴³. When low concentration protein solutions are heated at pHs away from the IEP, fibrillar (fibrils) aggregates which are few nm thick and few μm long can be formed^{42, 44-46}. Fibrillar networks are an example of an extreme type of a fine-stranded network.

Coarse networks which are often turbid in appearance are formed at pHs close to the IEP or at higher ionic strength⁴⁷. Coarse-stranded networks are often composed of relatively large particulate (spherical) aggregates with diameters in the range of 100 – 1000 nm^{42, 48} (as determined by the gelling conditions). The aggregates that form coarse-stranded networks are often loosely bound to each other in a random manner⁴⁸. Increasing the particulate nature of a gel network can however transform the network into micro phase-separated structure⁴⁹ resulting in an increased permeability of the gels⁵⁰.

The functionalization of the specific structural elements that constitute a stranded network and their interactions can be used as a tool in understanding which length scales are relevant for tuning textural and deformation properties of food gels⁵¹. The type, shape, and dimensions of these network structures can determine the efficiency and gel strength of the formed spatial gel network. In this thesis, the networks that are formed at varying length scales will be divided into fibrils and fine/coarse-stranded networks as illustrated in **Fig. 1**.

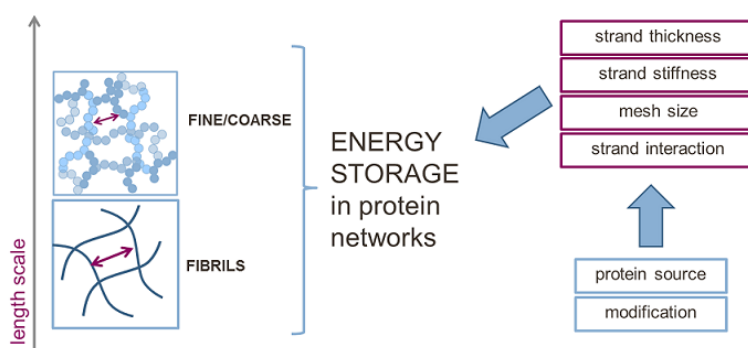


Figure 1: Schematic overview of stranded networks that can be formed at varying length scales, the relevant aspects of stranded networks, and how these aspects can be tuned to result in an influence on the ability of the networks to store energy.

Approaches to realize network structures

The assembly of the networks into fine or coarse-stranded can influence the ability of the networks to store energy, once energy is supplied to the system via mechanical deformation of the material.

The structural aspects dominating a gelled network include the strand thickness⁵², strand stiffness²², the interaction energy in the interaction points of the individual strands making up the spatial structure⁵¹, and the mesh size⁵³. It is however, important to note that these aspects are all interrelated, and hence changes in the network structure will result in subsequent changes in more than one aspect. Structural aspects are affected by the protein source e.g. animal protein vs. plant protein.

Due to inherent differences between these two different protein sources, the networks prepared from the proteins may vary in the structural aspects.

Various chemical modifications of proteins such as thiolation³⁹, oligofructosylation/Maillardation⁵⁴ and succinylation⁵⁵ can result in variations in the structural aspects of the network structure. As a consequence the mechanical deformation properties of the gels, such as the ability to store energy will be altered. The relevance of such chemical modifications for food applications has been recently discussed⁵⁶.

Fracture properties of gels

Covalent (disulfide bonds) and non-covalent (hydrogen bonds, hydrophobic interactions, and electrostatic interactions) interactions play a role in the formation of protein gels. During deformation of food gels, non-covalent cross-linked gels dissipate some energy because of bending, breaking and reforming of low energy bonds^{57, 58}.

The formation of self-supporting gels allows for the study of the mechanical deformation and fracture properties. The fracture properties of food gels have a significant influence on the texture, which in turn affects the sensorial perception of food products⁵⁹. The fracturing of materials usually occurs when the bonds between structural elements of the material break in a given macroscopic plane, leading to the structural breakdown over length scales larger than the structural elements, resulting in the material falling apart⁵⁷. The theory of crack initiation and propagation assumes that solid materials contain heterogeneities in the forms of pores, cracks, or flaws⁶⁰. During deformation, these cracks spread resulting in the formation of new surfaces which cause the material to eventually breakdown⁶¹. Fracture begins when the local stress at the tip of a crack or defect exceeds the cohesion and adhesion forces between the structural elements¹⁶. Therefore, for fracture to occur, the stress intensity at the tip of the crack has to supersede a critical value, K_{Ic} , which is known as the fracture toughness. Subsequently, the crack propagates spontaneously if the strain energy applied to the crack tip exceeds a critical value, G_{Ic} ⁶².

In describing the fracture behavior and the large deformation properties of food materials, several parameters are important. In addition to the true fracture stress and the true fracture (**Hencky**) strain, other mechanical responses that can be measured before, during, and after fracture provide insights on the relationship between the textural perception and mechanical properties of foods.

Mechanical responses such as Young's modulus, which is the measure of stiffness of a material, the recoverable energy, which is the measure of the energy that is stored within the network⁶³, serum release⁶⁴, and the critical stress intensity factor⁶⁵ are all relevant in foods and model systems as they have an impact on the sensorial perception of food products.

Previous studies show that network chains of visco-elastic materials become fully extended first, following viscoelastic rearrangement, before breaking, which suggests that deformation is a rate or time dependent behavior⁵⁷. Very small deformation rates were reported to provide the material enough time to relax before a considerable strain is attained¹⁶. An increase in fracture stress accompanied by a decrease in fracture strain has been observed with increasing strain rate⁶⁶. In the oral cavity, slipperiness perception was observed in the mixed lubrication regime at typical entrainment speeds between 10 and 100 mm/s⁶⁷ with tongue-palate contact pressures of 10 – 33 kPa⁶⁸. The energy that is built-up under these conditions can thus be used for the fracture of solid foods, whereas for fluid or semi-solids, the deformation will occur with the movement of the tongue by compressing it towards the upper palate and moving to the side of the mouth at the back⁶⁹. This differs depending on the type of protein.

Several empirical methods have been developed to establish the relationship between textural perception and the measurement of the mechanical properties of gels. Texture Profile Analysis (TPA), is the most commonly used method, which utilizes a two-cycle uniaxial compression test to characterize texture features that include cohesiveness, hardness, brittleness, gumminess, adhesiveness, chewiness and elasticity⁷⁰. The large deformation rheological tests used in the investigation of food textures often result in the breakdown of the samples into pieces, and this provides a good indication of the force, and the deformation that is associated with the “first bite”⁷¹. Performing real-time measurements on the mechanical behavior of gels provides a unique opportunity to explore the relationship between structural characteristics and the rheological properties of the gels. Thus, an understanding of the physical properties of the food at nano and micro length scale (structure), and the structural breakdown properties (rheological properties) of the gels is important to take into account all the factors that affect texture perception of food products⁷⁰.

The energy balance

Energy is the ability to do work, where work is defined as the ability to provide force and a displacement in distance of an object. The energy balance model described by van Vliet and co-workers⁵ shows that when energy is applied on most visco-elastic materials such as food gels, only part of the total supplied energy is stored, the remainder being dissipated. The energy balance can thus be expressed as:

$$W_{\text{applied}} = W_{\text{stored}} + W_{\text{dissipated}} \quad (1)$$

The energy that is stored is referred to as the recoverable energy. The applied energy can dissipate according to:

$$W_{\text{dissipated}} = W_{\text{fr}} + W_{\text{db}} + W_{\text{mf}} + W_{\text{sf}} + W_{\text{pd}} + W_{\text{sr}} \quad (2)$$

where W_{fr} is the contribution of energy that is used for the initiation and propagation of fracturing events at length scales larger than the microstructures of the network. W_{db} is the energy that causes de-bonding and subsequent re-hydration of physical contacts between microstructural elements of the network. W_{mf} represents energy that is lost by friction between microstructural elements during deformation. W_{sf} reflects the contribution of the viscous flow of the liquid entrapped by the network. W_{pd} denotes the energy that leads to plastic deformation of the material beyond the yielding-point, and W_{sr} is the energy that is lost via relaxation of elements within the network¹. A detailed explanation of how these dissipation modes contribute to the dissipation of energy can be found elsewhere¹.

The recoverable energy

The characterization of the large deformation and fracture behavior of foods cannot be carried out by determining only the fracture stress (gel strength) and strain (brittleness). Consumer perception of fracture during the handling and chewing of food is not predominantly determined by the stress at which the bonds between the structural elements rupture, but by the energy balance which governs the crack propagation, and as such, the falling apart of the foods into pieces⁷². An understanding of the energy that is stored and dissipated during the breakdown of gels upon deformation is thus important as this can provide a better understanding of the relation between textural and sensorial qualities of food products.

During deformation of gels, the ratio of the energy that is stored and dissipated defines the fracture characteristics of the gels⁷³. In a uniaxial compression test, the recoverable work represents the contribution of the energy that is stored while that of the irrecoverable work represents the dissipated energy⁷⁴. The recoverable energy is normally determined as the ratio of the energy recovered during decompression over the energy invested during compression of the gels⁶. During the compression of a specimen to a given compressive strain, the work necessary to compress the specimen up to this point (W_{loading}) is calculated from the area below the stress versus the strain loading curves. After reaching the set strain, the samples are unloaded at the same rate and the work ($W_{\text{unloading}}$) released by the gel specimen is determined in the same way. The recoverable energy is thus expressed as $100\% \times (W_{\text{unloading}}/W_{\text{loading}})^1$.

The ability of gels to store energy within their network has been related to the breakdown pattern of the gels. The crumbliness of WPI/polysaccharide mixed gels was found to be highly correlated with the recoverable energy measured by compression-decompression test⁶.

Gels having a high stored energy have been reported as showing a rapid decrease in normalized force after fracture, and this allows the material to fracture via free-running cracks^{16, 75} and therefore, these gels were perceived as being more crumbly than gels with a slower normalized force decrease and a high serum release⁷⁰.

Techniques for measuring the structural length scales of stranded networks

Depending on the structural length scales of the network structures that can be classified into microscopic and macroscopic structures, various techniques can be employed to characterize the dimensionalities of these structures. For microscopic structures between 1 – 100 μm , suitable techniques may include light microscopy and confocal laser scanning microscopy. For structures such as proteins and polymers that fall within the so-called “mesoscopic” region, which is typically the intermediate domain that describes properties of the microscopic and the macroscopic structures⁷⁶, techniques such as dynamic and static light scattering, transmission, and scanning electron microscopy, can be employed to characterize the structures whose sizes lie within the sub-micron level such as between 1 – 1000 nm. The use of electron microscopy allows for the visualization of network structures at high resolution and this provides a detailed account of the structural aspects of the networks.

The use of microscopy to image the network structure provides important parameters of the structure such as the coarseness, defined as the inhomogeneity of the gel networks as related to the strands that span the networks³⁴, porosity of the networks, and the typical length scales of the networks. The quantification of the network structure to obtain details on the typical length scales can be performed by measuring characteristics of the networks such as strand thickness or pore sizes, using public domain ImageJ software⁷⁷ with custom-made macro-instructions. Depending on whether images/micrographs are two or three-dimensional, the use of the pair correlation function can also be applied to quantify the network structures⁷⁸. In the case of two-dimensional images, treatment of the images should however be employed to overcome the shadowing and relief effect that is inherent in two-dimensional images⁷⁹, allowing the use of the pair correlation.

Objective and Outline of the thesis

The aim of this thesis is to understand how the structural aspects of a stranded protein network affect the ability of such networks to store energy. Special attention is given to understanding by which means these structural aspects can be varied and how this eventually affects the ability of the networks to store energy. A graphical illustration of the thesis outline is presented in **Fig. 2**.

In Chapter 2, the modification of supramolecular structures i.e. whey protein fibrillar and spherical aggregates and the consequences to the rheological behavior of the formed gels is presented.

In this chapter, an investigation was carried out to determine whether strands of network structures can be thickened using modification. Subsequently, gel formation was carried out to evaluate the rheological behavior of the gels that were formed from the modified protein aggregates. It is hypothesized that more impact on rheological behavior of gels can be achieved by thiolation when using fibrillar as opposed to spherical aggregates.

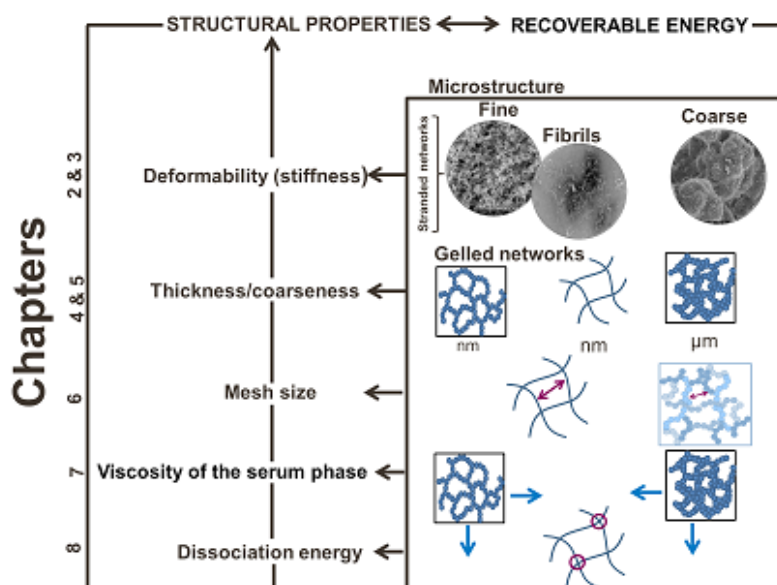


Figure 2: Short graphical presentation of thesis content.

This might be related to higher excluded volumes in fibrillar compared to spherical aggregates at the same protein concentration.

In Chapter 3, the protein source is shifted from whey protein (animal protein) to pea protein (plant storage protein) and fibrillar aggregates are formed. The reason for the shifting from animal to plant storage proteins was to get insights on whether the inherent differences between animal and plant storage proteins such as differences in the quaternary structures and solubility, can result in differences in structural aspects, such as strand stiffness and thickness. The rheological properties of gels made from fibrillar aggregate building blocks were determined and compared to protein fibrils made from proteins of different sources such as whey and soy proteins.

In Chapter 4, pea protein gels varying in coarseness were prepared to study whether changing the coarseness of the network structure will affect the ability of the networks to store energy. In Chapter 5, the quantification of the network structures that underline the transition in mechanical deformation properties of pea protein gels is carried out.

The studies carried out in Chapters 4 and 5 were aimed at understanding the length scales that set the ability to store energy in pea protein gels and to determine the pH at which precise structural transition from a fine to coarse stranded networks occurs.

In Chapter 6, ovalbumin networks are formed from proteins modified by conjugation with oligo-sugars via the Maillard reaction, and the effect of the mesh size on the rheological responses of the spatial networks is studied. It is hypothesized that an increase in the mesh size will result in a reduction of the ability of the gels to store energy, measured in terms of the recoverable energy as a result of an increase in energy dissipation, as water becomes more able to move with the network in relative motions. This will in turn result in an increase in the energy dissipated via viscous flow. Conjugation of sugar moieties to pre-aggregated ovalbumin was also carried out in the appendix to Chapter 6. This study was aimed at determining the impact of Maillardation on rheological responses of fibrillar aggregates made from ovalbumin.

The role of the serum phase viscosity on energy dissipation upon mechanical deformation of whey protein gels is studied in Chapter 7. In this chapter, the main research question was to find out how the serum phase viscosity contributes to energy dissipation in whey protein gels. To test the genericity of the insights obtained from Chapter 7, a study on the impact of the serum phase viscosity on rheological properties of pea protein gels was carried out and the findings of this study are presented in the appendix to Chapter 7.

The relationship between dissociation and elastically store energy in ovalbumin gels is discussed in Chapter 8. The study in Chapter 8 was carried out to determine the dissociation energy in a network by the use of activation energy. Special attention is given to understanding how the gel disruption energy is related to energy storage and dissipation upon mechanical deformation of fine-stranded ovalbumin gels.

In the final chapter (Chapter 9), the findings of this thesis are integrated and discussed in a coherent view on the application of protein networks in food applications with a tailored mechanical response. A summary of the major findings discussed in thesis is also presented.

References

- (1) de Jong, S.; van Vliet, T.; de Jongh, H. J. H., The contribution of time-dependent stress relaxation in protein gels to the recoverable energy that is used as tool to describe food texture **Mech. Time-Depend. Mater.** 2015, *In press*.
- (2) Pimentel, D.; Pimentel, M., Sustainability of meat-based and plant-based diets and the environment. **Am. J. Clin. Nutr.** 2003, **78**, 660S-663S.
- (3) Smil, V., Worldwide transformation of diets, burdens of meat production and opportunities for novel food proteins. **Enzyme Microb. Technol.** 2002, **30**, 305-311.
- (4) Johnson, E. A.; Brekke, C. J., Functional properties of acylated pea protein isolates. **J. Food Sci.** 1983, **48**, 722-725.
- (5) van Vliet, T.; Luyten, H.; Walstra, P., **Fracture and yielding of gels**. 1991; p 392-403.
- (6) van den Berg, L.; Carolas, A. L.; van Vliet, T.; van der Linden, E.; van Boekel, M. A. J. S.; van de Velde, F., Energy storage controls crumbly perception in whey proteins/polysaccharide mixed gels. **Food Hydrocolloid** 2008, **22**, 1404-1417.
- (7) Huggins, M. L., The structure of fibrous proteins. **Chem. Rev.** 1943, **32**, 195-218.
- (8) Muiznieks, L. D.; Keeley, F. W., Molecular assembly and mechanical properties of the extracellular matrix: A fibrous protein perspective. **Biochim. Biophys. Acta** 2013, **1832**, 866-875.
- (9) Pauling, L.; Corey, R. B., The structure of fibrous proteins of the collagen-gelatin group. **PNAS** 1951, **37**, 272-281.
- (10) Dill, K. A., Theory for the folding and stability of globular proteins. **Biochemistry** 1985, **24**, 1501-1509.
- (11) Smithers, G. W., Whey and whey proteins—From ‘gutter-to-gold’. **Int. Dairy J.** 2008, **18**, 695-704.
- (12) Flett, K. L.; Corredig, M., Whey protein aggregate formation during heating in the presence of κ -carrageenan. **Food Chem.** 2009, **115**, 1479-1485.
- (13) Li, J.; Ould Eleya, M. M.; Gunasekaran, S., Gelation of whey protein and xanthan mixture: Effect of heating rate on rheological properties. **Food Hydrocolloid** 2006, **20**, 678-686.
- (14) Sakai, K.; Sakurai, K.; Sakai, M.; Hoshino, M.; Goto, Y., Conformation and stability of thiol-modified bovine lactoglobulin. **Protein Sci.** 2000, **9**, 1719-1729.
- (15) Permyakov, E. A.; Berliner, L. J., α -Lactalbumin: structure and function. **FEBS Lett.** 2000, **473**, 269-274.
- (16) Walstra, P., **Physical chemistry of foods**. CRC Press: 2002; Vol. 121.

- (17) Jovanović, S.; Barać, M.; Mačej, O., Whey proteins-properties and possibility of application. **Млјехарство** 2005, **55**, 215-233.
- (18) Kato, A.; Ibrahim, H. R.; Watanabe, H.; Honma, K.; Kobayashi, K., Enthalpy of denaturation and surface functional properties of heated egg white proteins in the dry state. **J. Food Sci.** 1990, **55**, 1280-1283.
- (19) Photchanachai, S.; Mehta, A.; Kitabatake, N., Heating of an ovalbumin solution at neutral pH and high temperature. **Biosci., Biotechnol., Biochem.** 2002, **66**, 1635-1640.
- (20) Stein, P. E.; Leslie, A. G. W.; Finch, J. T.; Carrell, R. W., Crystal structure of uncleaved ovalbumin at 1.95 Å resolution. **J. Mol. Biol.** 1991, **221**, 941-959.
- (21) Kitabatake, N.; Tahara, M.; Doi, E., Thermal denaturation of soybean protein at low water contents (Food & Nutrition). **Agric. Biol. Chem.** 1990, **54**, 2205-2212.
- (22) Renkema, J. M. S.; van Vliet, T., Heat-induced gel formation by soy proteins at neutral pH. **J. Agric. Food. Chem** 2002, **50**, 1569-1573.
- (23) Renkema, J. M. S., Relations between rheological properties and network structure of soy protein gels. **Food Hydrocolloid** 2004, **18**, 39-47.
- (24) Renkema, J. M. S.; Gruppen, H.; van Vliet, T., Influence of pH and ionic strength on heat-induced formation and rheological properties of soy protein gels in relation to denaturation and their protein compositions. **J. Agric. Food Chem.** 2002, **50**, 6064-6071.
- (25) Renkema, J. M. S.; Lakemond, C. M. M.; de Jongh, H. H. J.; Gruppen, H.; van Vliet, T., The effect of pH on heat denaturation and gel forming properties of soy proteins. **J. Biotechnol.** 2000, **79**, 223-230.
- (26) Hudson, B. J. F.; Gueguen, J.; Cerletti, P., Proteins of some legume seeds: soybean, pea, faba-bean and lupin. In **New and Developing Sources of Food Proteins**, Springer US: 1994; pp 145-193.
- (27) Barać, M. B.; Stanojević, S. P.; Jovanović, S. T.; Pešić, M. B., Soy protein modification: A review. **Acta periodica technologica** 2004, 3-16.
- (28) Riblett, A. L.; Herald, T. J.; Schmidt, K. A.; Tilley, K. A., Characterization of β -conglycinin and glycinin soy protein fractions from four selected soybean genotypes. **J. Agric. Food. Chem** 2001, **49**, 4983-4989.
- (29) Dréau, D.; Lallès, J.-P., Contribution to the study of gut hypersensitivity reactions to soybean proteins in peruminant calves and early-weaned piglets. **Livest. Prod. Sci.** 1999, **60**, 209-218.
- (30) Hermansson, A. M., Physico-chemical aspects of soy proteins structure formation. **J. Texture Stud.** 1978, **9**, 33-58.
- (31) Gharsallaoui, A.; Saurel, R.; Chambin, O.; Voilley, A., Pea (*Pisum sativum*, L.) protein isolate stabilized emulsions: A novel system for microencapsulation of lipophilic ingredients by spray drying. **Food Bioprocess Technol.** 2012, **5**, 2211-2221.

- (32) Barac, M.; Cabrilo, S.; Pesic, M.; Stanojevic, S.; Zilic, S.; Macej, O.; Ristic, N., Profile and functional properties of seed proteins from six pea (*Pisum sativum*) genotypes. **Int. J. Mol. Sci.** **2010**, **11**, 4973-4990.
- (33) Croy, R.; Gatehouse, J. A.; Tyler, M.; Boulter, D., The purification and characterization of a third storage protein (convicilin) from the seeds of pea (*Pisum sativum* L.). **Biochem. J** **1980**, **191**, 509-516.
- (34) Munialo, C. D.; van der Linden, E.; de Jongh, H. H. J., The ability to store energy in pea protein gels is set by network dimensions smaller than 50 nm. **Food Res. Int.** **2014**, **64**, 482-491.
- (35) Shand, P. J.; Ya, H.; Pietrasik, Z.; Wanasundara, P. K. J. P. D., Physicochemical and textural properties of heat-induced pea protein isolate gels. **Food Chem.** **2007**, **102**, 1119-1130.
- (36) Bacon, J. R.; Noel, T. R.; Lambert, N., Preparation of transparent pea protein gels: a comparison of isolation procedures. **Int. J. Food Sci. Technol.** **1990**, **25**, 527-537.
- (37) Alting, A. C.; Hamer, R. J.; de Kruif, C. G.; Visschers, R. W., Cold-set globular protein gels: Interactions, structure and rheology as a function of protein concentration. **J. Agric. Food. Chem** **2003**, **51**, 3150-3156.
- (38) Alting, A. C.; Hamer, R. J.; de Kruif, C. G.; Paques, M.; Visschers, R. W., Number of thiol groups rather than the size of the aggregates determines the hardness of cold set whey protein gels. **Food Hydrocolloid** **2003**, **17**, 469-479.
- (39) Munialo, C. D.; de Jongh, H. H. J.; Broersen, K.; van der Linden, E.; Martin, A. H., Modulation of the gelation efficiency of fibrillar and spherical aggregates by means of thiolation. **J. Agric. Food. Chem** **2013**, **61**, 11628-11635.
- (40) Durand, D.; Gimel, J. C.; Nicolai, T., Aggregation, gelation and phase separation of heat denatured globular proteins. **Phys. A** **2002**, **304**, 253-265.
- (41) Veerman, C.; Ruis, H.; Sagis, L. M. C.; van der Linden, E., Effect of electrostatic interactions on the percolation concentration of fibrillar β -lactoglobulin gels. **Biomacromolecules** **2002**, **3**, 869-873.
- (42) Langton, M.; Hermansson, A. M., Fine-stranded and particulate gels of beta-lactoglobulin and whey protein at varying pH. **Food Hydrocolloid** **1992**, **5**, 523-539.
- (43) Barbut, S.; Foegeding, E. A., Ca^{2+} -induced gelation of pre-heated whey protein isolate. **J. Food Sci.** **1993**, **58**, 867-871.
- (44) Bolder, S. G.; Hendrickx, H.; Sagis, L. M. C.; van der Linden, E., Fibril assemblies in aqueous whey protein mixtures. **J. Agric. Food. Chem** **2006**, **54**, 4229-4234.
- (45) Arnaudov, L. N.; de Vries, R., Thermally induced fibrillar aggregation of hen egg white lysozyme. **Biophys. J.** **2005**, **88**, 515-526.
- (46) Akkermans, C.; van der Goot, A. J.; Venema, P.; Gruppen, H.; Vereijken, J. M.; van der Linden, E.; Boom, R. M., Micrometer-sized fibrillar protein aggregates from soy glycinin and soy protein iso-

late. **J. Agric. Food. Chem.** 2007, **55**, 9877-9882.

(47) Clark, A. H.; Judge, F. J.; Richards, J. B.; Stubbs, J. M.; Suggett, A., Electron microscopy of network structures in thermally-induced globular protein gels. **Int. J. Pept. Protein Res.** 1981, **17**, 380-392.

(48) Stading, M.; Hermansson, A.-M., Large deformation properties of β -lactoglobulin gel structures. **Food Hydrocolloid** 1991, **5**, 339-352.

(49) Ako, K.; Nicolai, T.; Durand, D.; Brotons, G., Micro-phase separation explains the abrupt structural change of denatured globular protein gels on varying the ionic strength or the pH. **Soft Matter** 2009, **5**, 4033-4041.

(50) Verheul, M.; Roefs, S. P., Structure of particulate whey protein gels: effect of NaCl concentration, pH, heating temperature, and protein composition. **J. Agric. Food Chem.** 1998, **46**, 4909-4916.

(51) Martin, A. H.; Baigts Allende, D.; Munialo, C. D.; Urbonaite, V.; Pouvreau, L.; de Jongh, H. H. J., Modulating protein interaction on a molecular and microstructural level for texture control in protein based gels. In **Gums and Stabilisers for the Food Industry 17: The Changing Face of Food Manufacture: The Role of Hydrocolloids**, RSC: 2014; pp 64-70.

(52) Kitabatake, N.; Tani, Y.; Doi, E., Rheological properties of heat-induced ovalbumin gels prepared by two-step and one-step heating methods. **J. Food Sci.** 1989, **54**, 1632-1638.

(53) Hinsch, H.; Wilhelm, J.; Frey, E., Quantitative tube model for semiflexible polymer solutions. **Eur. Phys. J. E** 2007, **24**, 35-46.

(54) Munialo, C. D.; Ortega, R. G.; van der Linden, E.; de Jongh, H. H. J., Modification of ovalbumin with fructooligosaccharides: Consequences for network morphology and mechanical deformation responses. **Langmuir** 2014.

(55) Walker, J.; Aitken, A.; Learmonth, M., Succinylation of proteins. In **The Protein Protocols Handbook**, Humana Press: 1996; pp 343-344.

(56) de Jongh, H. H.; Broersen, K., **Application potential of food protein modification**. INTECH Open Access Publisher: 2012.

(57) van Vliet, T.; Walstra, P., Large deformation and fracture behaviour of gels. **Faraday Discuss.** 1995, **101**, 359-370.

(58) Foegeding, E. A.; Gonzalez, C.; Hamann, D. D.; Case, S., Polyacrylamide gels as elastic models for food gels. **Food Hydrocolloid** 1994, **8**, 125-134.

(59) Montejano, J. G.; Hamann, D. D.; Lanier, T. C., Comparison of two instrumental methods with sensory texture of protein gels. **J. Texture Stud.** 1985, **16**, 403-424.

(60) Öhgren, C.; Langton, M.; Hermansson, A. M., Structure-fracture measurements of particulate gels. **J. Mater. Sci.** 2004, **39**, 6473-6482.

(61) van Vliet, T.; Luyten, H.; Walstra, P., Fracture and yielding of gels. **Food Polymers, Gels and**

Colloids 1991, 392-403.

- (62) Alvarez, M. D.; Saunders, D. E. J.; Vincent, J. F. V.; Jeronimidis, G., An engineering method to evaluate the crisp texture of fruit and vegetables. **J. Texture Stud.** 2000, **31**, 457-473.
- (63) van den Berg, L.; van Vliet, T.; van der Linden, E.; van Boekel, M. A. J. S.; van de Velde, F., Breakdown properties and sensory perception of whey proteins/polysaccharide mixed gels as a function of microstructure. **Food Hydrocolloid** 2007, **21**, 961-976.
- (64) van den Berg, L.; van Vliet, T.; van der Linden, E.; van Boekel, M. A. J. S.; van de Velde, F., Serum release: The hidden quality in fracturing composites. **Food Hydrocolloid** 2007, **21**, 420-432.
- (65) Vincent, J.; Saunders, D.; Beyts, P., The use of critical stress intensity factor to quantify "hardness" and "crunchiness" objectively. **J. Texture Stud.** 2002, **33**, 149-159.
- (66) Lowe, L. L.; Allen Foegeding, E.; Daubert, C. R., Rheological properties of fine-stranded whey protein isolate gels. **Food Hydrocolloid** 2003, **17**, 515-522.
- (67) Prakash, S.; Tan, D. D. Y.; Chen, J., Applications of tribology in studying food oral processing and texture perception. **Food Res. Int.** 2013, **54**, 1627-1635.
- (68) Kieser, J.; Singh, B.; Swain, M.; Ichim, I.; Waddell, J. N.; Kennedy, D.; Foster, K.; Livingstone, V., Measuring intraoral pressure: Adaptation of a dental appliance allows measurement during function. **Dysphagia** 2008, **23**, 237-243.
- (69) van Aken, G. A.; Vingerhoeds, M. H.; de Hoog, E. H. A., Food colloids under oral conditions. **Curr. Opin. Colloid Interface Sci.** 2007, **12**, 251-262.
- (70) Cakir, E. Understanding textural properties of protein-based soft-solid structures using oral processing. Raleigh, North Carolina, 2011.
- (71) Borwankar, R. P., Food texture and rheology: A tutorial review. **J. Food Eng.** 1992, **16**, 1-16.
- (72) van Vliet, T., **Rheology and fracture mechanics of foods**. CRC Press: Boca Raton, FL, USA, 2013; p 363.
- (73) Çakir, E.; Daubert, C. R.; Drake, M. A.; Vinyard, C. J.; Essick, G.; Foegeding, E. A., The effect of microstructure on the sensory perception and textural characteristics of whey protein/κ-carrageenan mixed gels. **Food Hydrocolloid** 2012, **26**, 33-43.
- (74) Kaletunc, G.; Normand, M. D.; Nussinovitch, A.; Peleg, M., Determination of elasticity of gels by successive compression–decompression cycles. **Food Hydrocolloid** 1991, **5**, 237-247.
- (75) van Vliet, T.; Luyten, H.; Walstra, P.; Dickinson, E., Fracture and Yielding of Gels. In **Food Polymers, Gels and Colloids**, Woodhead Publishing: 1991; pp 392-403.
- (76) Weijers, M. Aggregate morphology and network properties of ovalbumin. Wageningen University, 2005.
- (77) Rasband, W. 2009. ImageJ, U.S National Institutes of Health, Bethesda, Maryland, USA.

<http://rsb.info.nih.gov/ij/>

(78) Ako, K.; Durand, D.; Nicolai, T.; Becu, L., Quantitative analysis of confocal laser scanning microscopy images of heat-set globular protein gels. **Food Hydrocolloid** 2009, **23**, 1111-1119.

(79) Munialo, C. D.; Ortega, R. G.; van der Linden, E.; de Jongh, H. H. J., Modification of ovalbumin with fructooligosaccharides: Consequences for network morphology and mechanical deformation responses. **Langmuir** 2014, **30**, 14062-14072.

Chapter 2

Modulation of the gelation efficiency of fibrillar and spherical aggregates by means of thiolation

Fibrillar and spherical aggregates were prepared from whey protein isolate (WPI) and thiolated to a substantial degree to observe any impact on functionality. Changes on a molecular and microstructural level were studied using tryptophan fluorescence, transmission electron microscopy, and particle size analysis. The size of spherical aggregates increased from 38 nm to 68 nm for the blocked variant and 106 nm for the deblocked variant after thiolation. Rheological characterization of these variants showed that thiolation decreased the gelation concentration and increased gel strength for both WPI fibrillar and spherical aggregates, with the observed effects being more pronounced for thiolation of preformed fibrillar aggregates.

This chapter is published as:

Munialo, C.D.; de Jongh, H. H. J.; Broersen, K.; van der Linden, E.; Martin, A.H. Modulation of the gelation efficiency of fibrillar and spherical aggregates by means of thiolation.

***Journal of Agricultural and Food Chemistry* 2013, 61, (47), 11628-11635.**

Introduction

Whey proteins (WP) are widely used as food ingredients because of their nutritional and functional properties¹. Past research has yielded valuable information on structural changes in WP as a function of protein concentration, pH, and ionic strength upon exposure to heat²⁻⁴. The behavior of WP upon heating is of interest because, when well understood, protein denaturation and aggregation events can be directed to result in novel materials^{5, 6} with diversity in size and functional properties. Micrometer scale three dimensional amorphous particles whose internal structure is not strictly spherical, but will be referred to as 'spherical' aggregates in this article, are claimed to be used in applications that may vary from thickening agents⁷ to carriers for encapsulation⁸, and fat substitutes to improve creaminess⁸. Fibrillar aggregates (fibrils) which are a few nm thick, may be used in low-caloric products because of their functionality that ranges from gelling agents to stabilizers of foams and emulsions⁹. Past research on fibrillar^{1, 10-12} and spherical¹³ aggregates has reported their assembly process.

Protein gelation is the result of aggregation in which polymer to solvent interactions are balanced and a network is formed¹⁴. Both fibrillar and spherical aggregates can be organized into three-dimensional gel networks. The condition at which the transformation from aggregates to gel networks occurs largely determines visual and rheological properties of the resulting gel networks¹⁴. Fibrils can be organized into a network by different approaches^{15, 16}. Apart from these reports^{15, 16}, limited attention has been given to the formation of gels from preformed fibrils. Turbid, particulate gels are formed by spherical aggregates for instance by adding high salt concentrations¹³, by slow acidification towards iso-electric point (IEP) using glucono- δ -lactone¹⁴, or by heat induced gelation¹³. It is generally found that cold-set gelation of spherical aggregates results in gels with superior strength over heat-induced ones^{13, 14}.

Sulfhydryl (SH) groups and disulfide bonds (S-S) play a significant role in the formation of protein gels¹⁷⁻¹⁹. A number of functional properties such as viscosity, texturization, thermal stability, and elasticity have been directly or indirectly linked to sulfhydryl content of proteins²⁰. The number as well as reactivity of thiol groups has been reported to have an influence on rheological behavior of proteins²¹. Studies into the role of thiol groups and disulfide bridges in aggregation and gelation processes, have been performed by either the blocking of the thiol groups naturally present in the protein molecule¹³, or by the introduction of thiol groups (thiolation) using **S**-acetylmercaptosuccinic anhydride (S-AMSA)^{22, 23}. The mechanism of this reaction is shown in **Fig. 1**. The relevance of such modifications for food applications has been recently discussed by de Jongh and Broersen (2012)²⁴.

In most studies, native proteins were used as a starting point for the thiolation procedure, after which the aggregation and consequently gel formation properties of the protein were evaluated^{21, 25}. A concomitant impact on gelation was however reported due to the formation of different type of aggregates²³.

2,2V-dipyridyldisulfide (PDS) was obtained from Alfa Aesar (Karlsruhe, Germany). Thioflavin T (Th T) was obtained from Acros organics (Geel, Belgium). All reagents were of analytical grade and used without further purification.

WPI fibril preparation

Protein solutions of 9 wt % WPI were prepared by dispersing WPI powder in MilliQ water adjusted to pH 2 using HCl, followed by overnight stirring at 300 rpm and 4 °C. The obtained solutions were then centrifuged at $15000 \times g$ for 30 min at 4 °C to remove traces of insoluble material. The supernatant was filtered through a 0.45 μm (Millex-SV, Millipore Corp., Bedford, MA) filter. The final protein concentration was corrected to 2.5 wt % unless stated otherwise. Protein content was determined using DUMAS (NA 2100 Protein, CE instruments, Milan, Italy) with a conversion factor of 6.38.

Fibril preparation was carried out according to a previously described protocol¹. In summary, 20 mL aliquots of 2.5 wt % protein solutions prepared as described above were incubated at 80 °C for 24 h at pH 2 in a temperature-controlled water bath, and continuously stirred at 300 rpm. After the heat treatment, samples were cooled in an ice bath and stored at 4 °C until further use. Thioflavin T (Th T) fluorescence assay was used to evaluate the formation of WPI fibrils as previously described⁹. After 24 h of heating, a volume of 48 μL of heated WPI samples was mixed with 4 mL of filtered (0.2 μm , Schleicher and Schuell) 60 μM Th T solution in phosphate buffer (10 mM phosphate, 150 mM NaCl at pH 7.0), and incubated for 10 min at 25 °C. Fluorescence intensity was measured using a fluorescence spectrophotometer (Perkin-Elmer LS 50 B) at an excitation wavelength of 460 nm (slit width 2.5 nm) and emission wavelength from 465 to 550 nm (slit width 2.5 nm). Controls included the fluorescence intensity of Th T solution without the addition of protein solution and unheated WPI solutions.

WPI spherical aggregate preparation

WPI spherical aggregate solutions were prepared by dispersing 9 wt % WPI powder in MilliQ water (Millipore Corp., Billerica, MA), followed by stirring at 25 °C, 300 rpm for 2 h. Portions of 100 mL protein solutions at an initial pH 7 were incubated in a water bath at 68.5 °C for 2.5 h. This heat treatment has been shown to result in over 95 % aggregation of the proteins¹⁴. WPI aggregate solutions were then cooled using running tap water for 30 min and subsequently stored overnight at 4 °C.

Determination of hydrodynamic diameters of the protein aggregates was carried out using dynamic light scattering (Zetasizer Nano ZS, Malvern Instruments, Worcestershire, UK). The spherical aggregate solutions at pH 7 were diluted to 0.5 wt % using MilliQ water and triplicate measurements were carried out at 25 °C. Reported values are the average hydrodynamic diameters of the largest intensity peak as found in the distribution analysis using Malvern DTS 5.03 software.

Thiolation of WPI structural building blocks into blocked (SX) and reactive (SH) variants

Thiolation was carried out on the above derived structural building blocks (fibrillar and spherical aggregates) as previously described²⁶. The pH of a 50 mL of a 2.5 wt % WPI fibrillar and spherical aggregates protein solution was adjusted to pH 8 using 6 M NaOH. Aliquots of the solutions were kept separate and used without further treatment to serve as unmodified controls. Optimization of S-AMSA to amines ratio was performed initially with regard to degree of substitution (DS) and reactivity. This led to selection of a ratio of 1:8 (S-ASMA: amines) to obtain medium DS of around 60 %.

S-AMSA reagent was added to the protein solutions in aliquots of 5 mg to a total of 97.5 mg while maintaining a constant pH 8.0 (± 0.1). After adding S-AMSA reagent, the solution was stirred for 24 h at room temperature followed by extensive dialysis against distilled water at 4 °C (MWCO 12-14,000 Da dialysis membrane). Dialyzed solutions were separated into two fractions. To the first fraction, a final concentration of 0.01 M hydroxylamine hydrochloride was added to aid in deblocking of thiol groups by removal of the acetyl groups. This sample contained exposed thiol groups (SH). After addition of 0.01 M hydroxylamine hydrochloride, the SH fraction was stirred (25 °C, 1 h, 300 rpm), followed by dialysis against distilled water for 24 h at 4 °C (MWCO 12-14,000 Da dialysis membrane). To the second fraction, no further treatment was carried out, thus yielding a fraction in which thiol groups were present in a 'blocked' form, still containing the acetyl group (SX). The samples were subsequently stored at 4 °C and used within 2 weeks. Thiolation carried out in this way resulted in the formation of six WPI variants as presented in **Table 1**.

Table 1: Overview of unmodified and thiolated (SX-blocked and SH-deblocked variants) WPI fibrillar and spherical aggregates as used in this work. Where F is fibrillar aggregates, A is spherical aggregates.

	blocked/deblocked	Variant abbreviation
WPI fibrils	Unmodified	F
Thiolated WPI fibrils	Blocked	FSX
Thiolated WPI fibrils	Deblocked	FSH
Spherical WPI aggregates	Unmodified	A
Thiolated spherical WPI aggregates	Blocked	ASX
Thiolated spherical WPI aggregates	Deblocked	ASH

Analytical characterization of WPI structural building blocks

The total number of sulfhydryl groups was determined using Ellman's reagent²⁷. The number of primary amines (lysines and the protein N-terminal amine groups) was determined using chromogenic ortho-phthaldialdehyde (OPA) assay as previously described²⁸. OPA results were used to determine the degree of substitution (DS) of amines with thiol groups. Apparent chemical reactivity of thiol groups was measured for each sample using the sulfhydryl–disulfide exchange index (SEI) as previously described²⁹. SEI determines the reactivity of blocked and deblocked protein variants based on the reaction between 2,2V-dipyridyldisulfide (PDS) and free –SH groups³⁰. Ellman's, OPA and SEI assays were all carried out in duplicate.

Microscopic and spectrophotometric characterization of WPI structural building blocks

Unmodified and thiolated WPI fibrillar and spherical aggregates were prepared for transmission electron microscopy (TEM) by negative staining according to the previously described protocol¹⁵. In summary, a 10 μL aliquot of 0.025 wt % protein solution was deposited onto a carbon support film on a copper grid (Aurion-Immuno Gold Reagents & Accessories, Wageningen, The Netherlands). The excess protein solution was removed after 30 s using filter paper (Whatman No. 1, 512-1002, VWR International Europe BVBA, Leuven, 3001, Belgium). A droplet of 2 % uranyl acetate, pH 3.8, was added for 30 s for improved contrast, and any excess was removed by use of filter paper. Electron micrographs were obtained using a Jeol JEM1011 transmission electron microscope (Tokyo, Japan) operating at 80 kV.

Intrinsic tryptophan fluorescence spectra of 50 $\mu\text{g}/\text{mL}$ WPI sample solutions in MilliQ water were obtained using a Cary eclipse fluorescence spectrophotometer (Agilent technologies, The Netherlands) upon excitation at a wavelength of 280 nm, and the emission spectra were recorded at a wavelength range from 300 to 400 nm at 25 °C. Quartz cuvettes with an optical path of 1 cm were used. The excitation and emission slit widths were 5 nm and a scan speed of 120 nm/min was used. All spectra were recorded in duplicate and averaged.

Turbidity measurements at a protein concentration between 0.2 - 2.3 wt % were performed at 25 °C on a Shimadzu UV-1800 UV-VIS spectrophotometer (Shimadzu Corporation, Japan) equipped with a CPS-temperature controller. Changes in turbidity were measured by following the absorbance at 500 nm in time. Triplicate measurements were carried out on each sample and averaged.

Preparation of protein gels

Gelation of unmodified and thiolated structural building blocks prepared from WPI was carried out by acid-induced cold gelation using glucono- δ -lactone (GDL).

The concentrations of GDL added to the samples to induce gelation were determined using the formula $(\% \text{ GDL (wt/wt)}) = 0.0065 \times \text{Cprotein (g/L)} + 0.045$ ³¹. GDL was added to WPI solutions with a protein concentration ranging from ~0.2 – 2.5 wt % to induce gelation at 25 °C. The pH of all samples was determined after 24 h of incubation at 25 °C in identical samples placed in a water bath at 25 °C.

Rheological characterization of protein gels

A stress-controlled rheometer (ARG2, TA Instruments, Leatherhead, UK) with a concentric cylinder geometry (C14: cup diameter, 15.4 mm; bob diameter, 14.04 mm;) was used to determine storage modulus (G') as a function of time (frequency, 1 Hz; temperature, 25 °C; strain, 0.05, 24 h). After 24 h, oscillation amplitude was performed (frequency, 1 Hz; temperature, 25 °C; strain, 0.01 - 100). Duplicate measurements were performed on various batches of freshly thiolated aggregates to prevent the possibility of autoxidation of introduced thiol groups occurring during prolonged storage, which could mask the impact of thiolation on gelation efficiency. Measurements were performed within the linear region which was between a strain % of 0.001 and 10.

Results and Discussion

Thiolation of WPI based fibrillar and spherical aggregates to study its effect on the gelation behavior of WPI structural building blocks yielded blocked (SX) and reactive (SH) WPI variants. These variants were used to describe the impact of thiolation on gel formation.

Chemical characterization of WPI fibrils and spherical aggregates upon thiolation

The number of free –SH groups in unmodified and thiolated WPI fibrillar and spherical aggregates was determined using Ellman's reagent, whereas chemical reactivity of introduced thiol groups was determined using sulfhydryl–disulfide exchange index (SEI) (Table 2).

Native WPI had less exposed thiol groups than unmodified fibrils (F). Thiol groups in native β -lactoglobulin, the major fraction of WPI, are reported to be buried between the β -barrel and the C-terminal major α -helix^{32,33}, and may not be available for reaction with Ellman's reagent³³. Formation of fibrils from peptides following protein hydrolysis at pH 2 resulted in the increased exposure of thiol groups, suggesting firstly that conformation of proteins in the fibrillar aggregates may be different from that of the native protein, and secondly, that exposed thiol groups may function to stabilize interfibrillar interactions upon gel formation. The potential of this concept was further explored by introducing multiple thiol groups onto the fibrillar and spherical aggregates by means of thiolation. Generally, the thiolation procedure led to the introduction of thiol groups to modify approximately 60 % of the primary amines available in both WPI fibrillar and spherical aggregates.

Table 2: Chemical characterization of WPI samples modified with a ratio of 1:8 S-AMSA: amines – number of thiol groups as obtained by Ellman’s reagent, degree of substitution (DS) % as obtained by OPA assay, and thiol reactivity (%) as obtained by SEI.

	number of thiol groups (mM/mM of protein \pm stdev)	DS (%)	reactivity (SEI) %
Native	0.20 \pm 0.03	0	0 \pm 0.0
F	0.60 \pm 0.07	n.a	8 \pm 0.30
A	0.20 \pm 0.02	n.a	9 \pm 0.13
FSX	1.76 \pm 0.02	65 \pm 3.3	54 \pm 0.58
FSH	3.10 \pm 0.01	66 \pm 2.2	96 \pm 1.49
ASX	1.57 \pm 0.01	57 \pm 0.1	16 \pm 0.91
ASH	3.51 \pm 0.96	62 \pm 1.1	31 \pm 0.25

The number of thiol groups detected by Ellman’s reagent increased upon conversion of protected acetyl groups (SX) to SH groups in both fibrillar and spherical aggregates (**Table 2**).

Upon thiolation, FSX and FSH showed increased thiol reactivity compared to F, whereas, thiol reactivity of ASX and ASH was limited (**Table 2**). FSX showed thiol reactivity of about 50 %. The reactivity of FSX, in which thiol groups are blocked could be due to auto oxidation occurring in the acetyl groups either by reaction with oxygen or reaction of two thiol groups resulting in SH or S-S group¹³. Nevertheless, FSH variants showed higher reactivity compared to F and FSX variants. SEI results of spherical WPI aggregates show that although thiol groups were successfully introduced in the variants, thiolated spherical aggregates appear to have less reactivity than WPI fibrillar aggregates. Attachment of reactive thiol groups to WPI fibrils potentially results in cross-linking reactivity between thiol groups, resulting in disulfide bond formation. Thus, covalent cross-linking could have occurred between and within WPI fibrillar aggregates. These results show that (i) heating of native WPI to form fibrils (from peptides) or to form spherical aggregates increased the exposure of indigenous sulfhydryl groups, and that (ii), deblocking of the SX variant was successful and resulted in increased thiol reactivity.

Structural analysis of fibrillar and spherical aggregates

The changes in protein folding as a result of aggregate assembly of WPI structural building blocks were probed using intrinsic tryptophan fluorescence (**Fig. 2**).

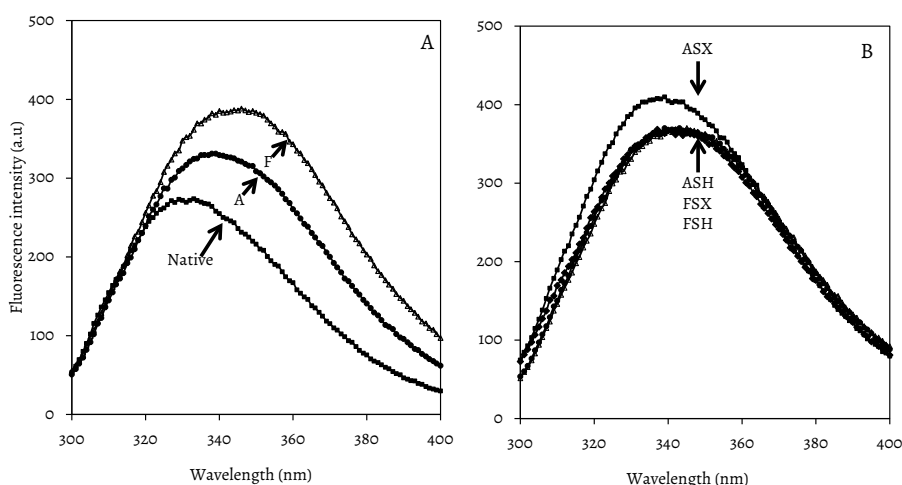


Figure 2: Analysis of tertiary structure probed by intrinsic fluorescence for A) native WPI (native), unmodified WPI fibrils (F), and unmodified spherical aggregates (A); B) blocked variant of modified fibrils (FSX), deblocked variant of modified fibrils (FSH), blocked variant of modified spherical aggregates (ASX), and deblocked variant of modified spherical aggregates (ASH) variants of WPI.

Native WPI exhibited a fluorescence emission maximum at 330 nm which is characteristic for a tertiary folded protein in which the tryptophans are buried in the interior of the molecule as reported for β -lactoglobulin³⁴. Conversion of native WPI to fibrillar or spherical aggregates induced a red-shift of the fluorescence maximum³⁵ due to conformational changes that occur as a result of aggregate assembly. The red shift in fluorescence maximum was more pronounced for fibrillar than for spherical aggregates. This observation illustrates that both fibrillar and spherical aggregate formation coincide with conformational change of the tryptophan residues resulting in more solvent exposure of the tryptophans³⁵. Unmodified and thiolated WPI fibrillar and spherical aggregates showed higher fluorescence intensity than native WPI.

Upon thiolation no further changes were observed in tertiary structure for FSX, FSH, and ASH variants of WPI fibrillar and spherical aggregates compared to unmodified variants (F and A). ASX variant showed the highest fluorescence intensity compared to FSX, FSH and ASH variants. Variation in fluorescence intensity may be the result of different energy transfer efficiency between tryptophan and tyrosine as a result of structural rearrangement upon fibrillar or spherical aggregate formation as reported for ovalbumin²³.

A Thioflavin T (Th T) assay was carried out on unmodified and thiolated WPI fibrillar and spherical aggregates to confirm the presence of β -sheet aggregates in protein solutions.

Upon association into either fibrillar or spherical aggregates, Th T fluorescence intensity increased compared to native variant, particularly for WPI fibrillar aggregates (**Fig. 3**).

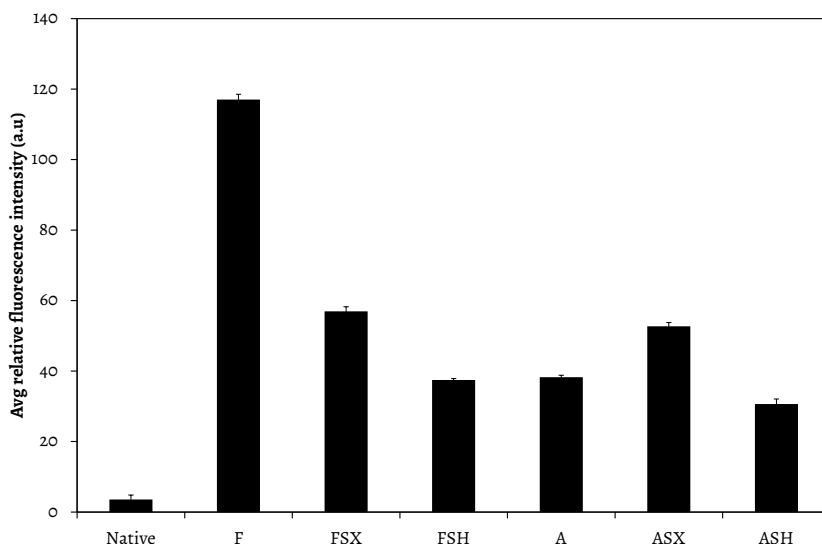


Figure 3: Average relative fluorescence intensities probed by Th T fluorescence at 485 nm wavelength for unmodified (A), thiolated blocked (ASX) and deblocked (ASH) variants of spherical WPI aggregates and unmodified (F), thiolated blocked (FSX) and deblocked (FSH) variants of WPI fibrils.

Modification of fibrils resulted in a decrease in the Th T intensity of FSX variant suggesting a partial disruption of β -sheet fibrillar structure upon thiolation. The partial disruption of β -sheet fibrillar structure could be related to pH changes occurring during the thiolation process. Partial disruption of β -sheet structure related to pH changes has been reported for fibrils made from insulin³⁶. A slight increase in Th T intensity was observed in ASX whereas a reduction in fluorescence intensity was observed in FSH and ASH. The reduction in relative fluorescence intensity in FSH and ASH variants may be due to reduced efficiency of Th T to bind to the protein as a result of inaccessibility of Th T binding groves³⁷.

Effect of thiolation on the morphology of WPI aggregates

Fibril morphology was probed using TEM. Fibrils from unmodified WPI (F) show long linear fibrillar aggregates (**Fig. 4 a (A)**) that resemble the general kind of fibrils reported before¹. The ability to form fibrils from WPI that had been thiolated in its 'monomeric' state was first assessed (**Fig. 4 b**).

The TEM micrographs show a mixture of fibrils and small aggregated clusters suggesting a reduced propensity for fibril formation. Hence, the prospects of thiolation of preformed fibrils were evaluated. The conversion of unmodified fibrils (F) to FSX and FSH resulted in some changes at the fibrillar scale (**Figs. 4 a panels B and C**).

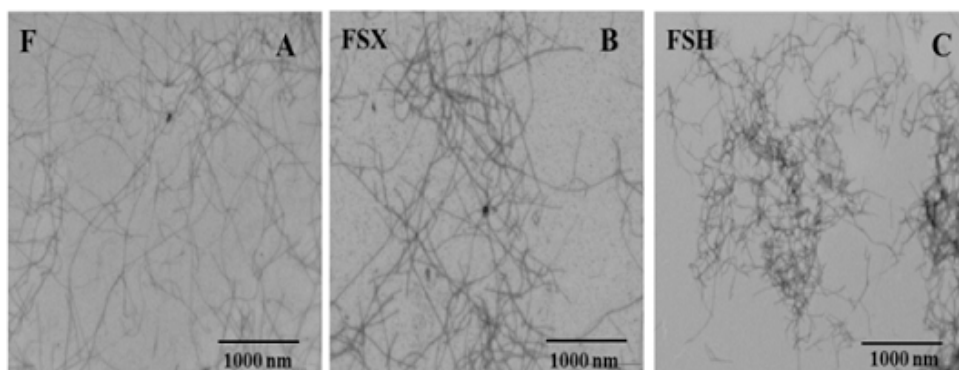
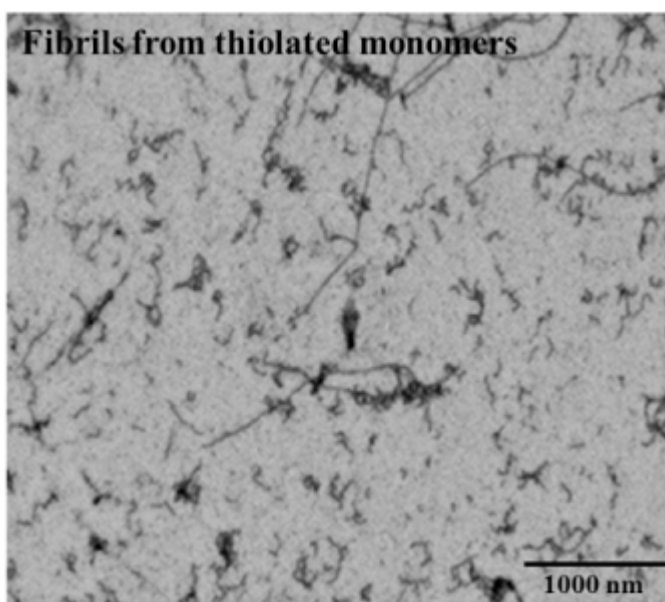
Fig. 4a**Fig. 4b**

Figure 4: TEM micrographs for a) unmodified fibrils (F), thiolated fibrils after fibril formation blocked variant (FSX), and deblocked variant (FSH); b) monomeric WPI thiolated before fibril formation was carried out; at pH \sim 7. Scale bars represent 1000 nm.

An apparent increase in clustering and tightening of the adjacent fibrils occurred in FSH as deduced from TEM images suggesting that enhancement of physical interactions occur following unblocking of the introduced thiol groups.

The use of TEM to study the effect of thiolation on microstructure of spherical aggregates did not show differences between unmodified and thiolated spherical aggregates. Cryo-TEM images for spherical WPI aggregates have been reported before¹³. The expected high level of clustering for spherical aggregates resulted in the use of dynamic light scattering instead of TEM to evaluate the aggregate size upon thiolation. The average hydrodynamic diameters of the largest intensity peak were 38 nm for A (with a % polydispersity index of 62), 68 nm for ASX (with a % polydispersity index of 62) and 106 nm for ASH (with a % polydispersity index of 64) (**Fig. 5**).

Thiolation increased the spherical aggregate size and their clustering. These observations suggest that physical interactions occur upon thiolation that result in the clustering of adjacent aggregates.

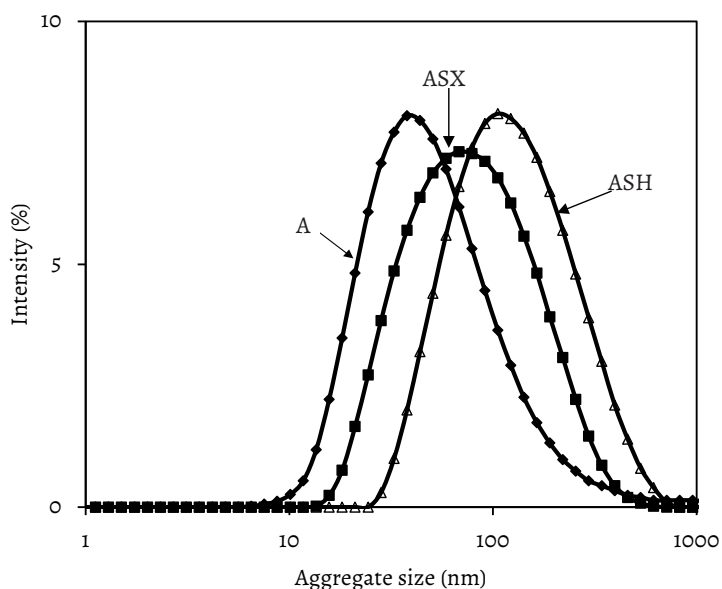


Figure 5: Aggregate size of unmodified spherical WPI aggregates (A), blocked (ASX), and deblocked variants (ASH) of thiolated spherical aggregates determined by dynamic light scattering.

Effect of thiolation on gelation of WPI fibrils and spherical aggregates

Evaluation of whether thiolated preformed WPI fibrils are capable of forming gels at lower protein concentrations than unmodified preformed fibrils (F) was carried out. The spatial clustering of aggregates and gelation of a range of protein concentrations of F were investigated using turbidimetry and small deformation rheology.

The turbidity and storage modulus (G') were followed as a function of time, after the addition of GDL to induce the gelation process. During acidification, an initial increase in turbidity was observed for all concentrations indicating an increase in aggregate size (**Fig. 6**).

As the pH values decreased to below the IEP of WPI, turbidity of 0.2, 0.3, 0.7 and 0.9 wt % of F decreased. The decrease in turbidity could be related to solubilisation of the fibrils that are clustered at pH around the IEP. A similar observation of disassociation at $\text{pH} < \text{IEP}$ has been reported elsewhere³⁸.

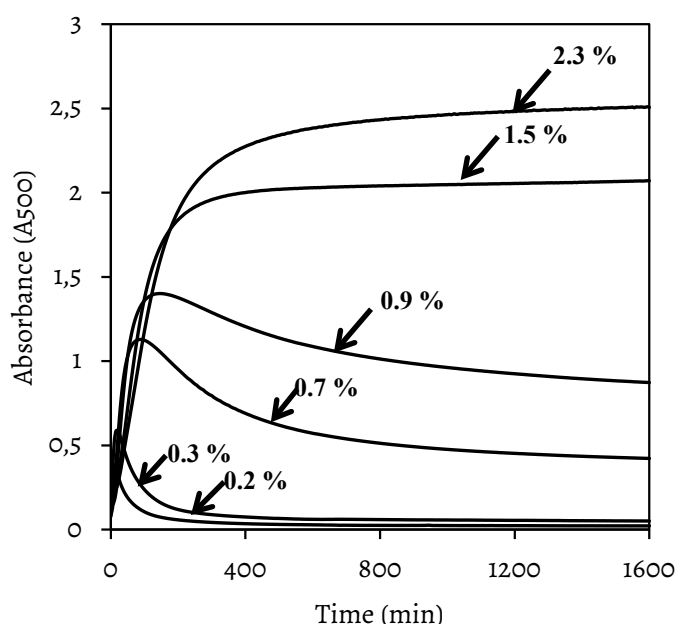


Figure 6: Changes in turbidity over time at A500 nm for various protein concentrations of unmodified WPI fibrils (F) from 0.2 wt %, 0.3 wt %, 0.7 wt %, 0.9 wt %, 1.5 wt %, and 2.3 wt %.

The final turbidity of unmodified WPI fibrils increased with increasing protein concentrations. At low protein concentration (0.2 and 0.3 wt %) the solutions remained transparent. At higher protein concentrations (0.7 and 0.9 wt %), turbidity increased. Persistent turbid gels were only formed at concentrations of 1.5 and 2.3 wt % as the turbidity increased steadily with ongoing gelation and leveled off after 20 h (**Figure 6**).

The development of G' was followed in time as a measure of gelation for different protein concentrations for both fibrillar and spherical aggregates. Gelation was assumed to have occurred when $\tan \delta$ of the solution was less than 1 ($G' > G''$)³⁹.

Fig. 7 shows the G' values attained after 24 h of gelation at 25 °C as a function of protein concentration for WPI fibrillar (**Fig. 7 A**) and spherical aggregates (**Fig. 7 B**).

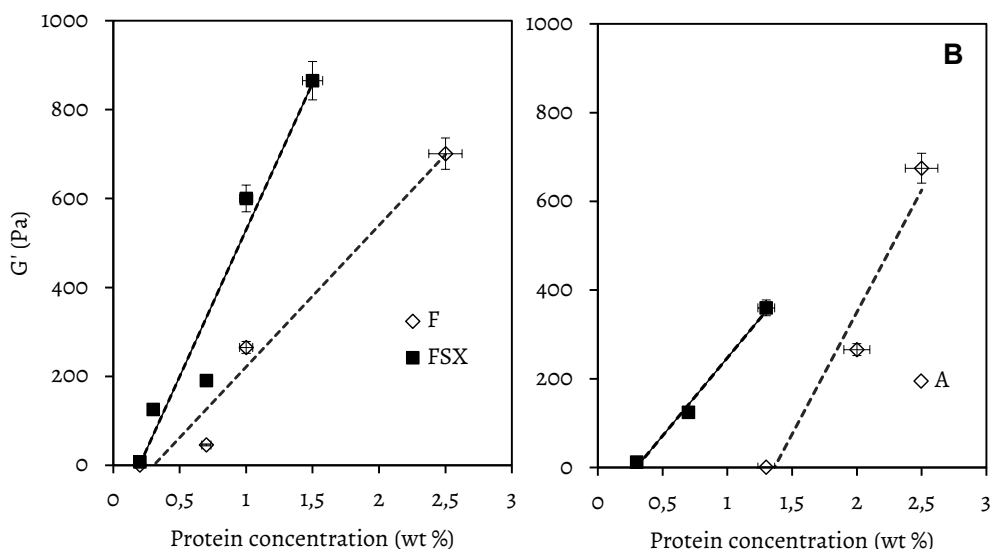


Figure 7: Changes in final G' (Pa) values obtained after 24 h of GDL induced gelation as a function of protein concentration for A) unmodified WPI fibrils (F) and blocked variant of thiolated WPI fibrils (FSX); B) unmodified spherical aggregates (A) and blocked variant of thiolated spherical aggregates (ASX). The error bars represent standard deviation from the mean of duplicate measurements performed on different batches of samples thiolated in a similar way.

With increasing protein concentrations, G' values obtained after 24 h gelation also increased. The increase in G' as a function of concentration was higher for FSX than for F. For example, at a concentration of about 0.9 wt % the G' obtained for FSX was 600 Pa whereas that of F variant was 265 Pa (**Table 3 and Fig. 6**). Deblocking of the thiol groups to FSH did not result in a further increase in G' (**Table 3**). Similar trends were observed for unmodified (A) and modified (ASX) variants of spherical aggregates (**Fig. 7 B**), although the resultant gels were weaker for spherical aggregates compared to fibrillar aggregates at similar protein concentrations.

Thiolation appeared to effectively reduce the critical gel concentration compared to unmodified fibrillar and spherical aggregates, which could be attributed to increased potential of chemical cross-linking between fibrillar and spherical aggregates upon thiolation.

It has been reported that the conversion of peptides to fibrils is not as efficient as the conversion of monomeric proteins to spherical aggregates, as over 95 % of monomeric protein is converted into spherical aggregates following the heating of proteins¹⁴ compared to about 50 % conversion of peptides to fibrils⁹.

To ensure that the observed effects of thiolation on gelation of fibrils had no interference from non-converted peptides, WPI fibrils were ‘purified’ as previously described⁴⁰. The results show that the presence or absence of non-aggregated proteins/peptides in the samples does not interfere with either thiolation or gelation of WPI fibrillar aggregates (see supplementary information).

Comparing fibrils to unmodified and thiolated spherical aggregates, it can be observed that thiolation of spherical aggregates also reduces gelation concentration and increases final gel strength (Figs. 7 B and 8), even though thiol reactivity was not significantly improved (Table 2). At similar protein concentration fibrillar aggregates formed stronger networks than spherical aggregates (Table 3). For example, at a concentration of about 0.9 wt % no gels were formed for A whereas ASX formed gels with a G' of 360 Pa.

Fibrils have been shown to form gels at low protein concentration.¹⁵ It has been reported that fibrils are capable of forming gels with an order of magnitude lower protein concentrations than conventional cold or heat induced gelation of aggregates upon the introduction of an extra attractive interaction¹⁵.

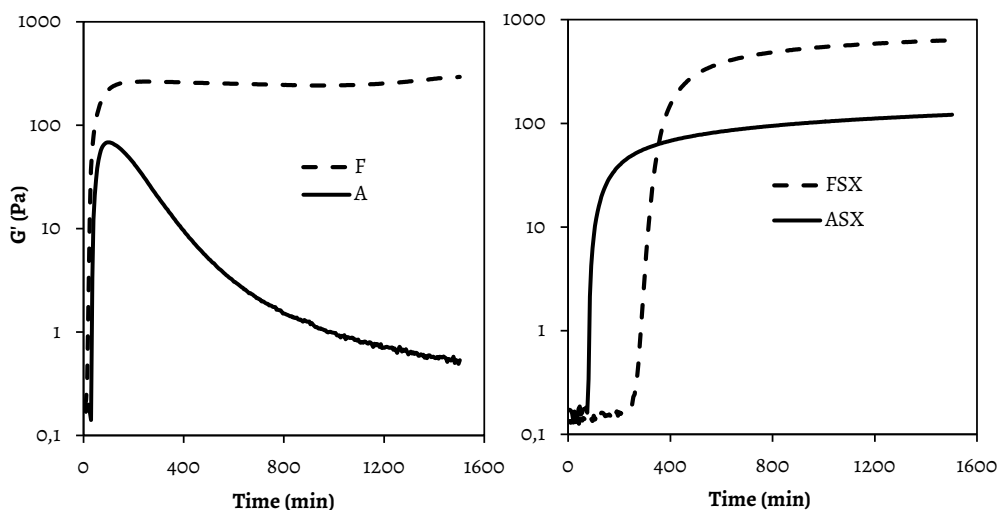


Figure 8: Changes in G' (Pa) over time for GDL-induced gelation of WPI at a protein concentration of 0.9 wt % for A) unmodified spherical aggregates (A) and fibrils (F); B) blocked variants of spherical (ASX) and fibrillar (FSX) aggregates.

Such additional attractive interactions were introduced in this article by means of thiolation. Fibrillar forms of WPI, regardless of whether they were thiolated or not, always formed gels with higher G' values than gels formed from spherical aggregates.

Gelation of ASX and ASH resulted in formation of weaker gels than FSX and FSH, at a similar protein concentration.

The final gel strength for FSX and FSH was higher than ASX and ASH. FSH had comparable gel firmness as FSX whereas ASH gels were weaker than ASX (**Table 3**).

Formation of weaker gels by ASX and ASH can be attributed to the differences in the reactivity of thiol groups as lower chemical reactivity was observed in ASX/ASH as opposed to FSX/FSH (**Table 2**). Additionally, differences in the curvature of spherical aggregates in comparison to linear fibrillar aggregates have been shown to lead to lower gel stiffness in ovalbumin²³.

Table 3: Final G' (Pa) of WPI variants following acidification using GDL and onset gelation time (min) at 0.9 wt % protein concentration.

WPI variant	final G'	onset gelation
	(Pa, after 1600 min)	(min)
F	265±2	120
FSX	600±4	285
FSH	664±3	116
A	1±0.12	25
ASX	360±1	60
ASH	45±3	260

Gelation kinetics between ASX, FSX, ASH, and FSH were different (**Table 3**). Observed differences in gelation kinetics and gel firmness for ASX and ASH could be related to deblocking of the introduced sulfhydryl groups, which could enhance the possibility of reaction of adjacent -SH groups resulting in disulfide bond formation. The permanent nature of disulfide bonds does not provide rotational freedom in the gel network which can result in rearrangement of the hydrophobic interactions to form a structure that can optimize gel strength due to the high disulfide bond energy²³.

Conclusions

In conclusion, it can be stated that SH/SS groups play an important role in determining the strength of GDL induced protein gels. The influence of SH/SS on gel formation was more pronounced in networks made from fibrillar than from spherical aggregates. This study has shown that a combination of thiolation with GDL induced gelation decreases gelation concentration and increases final gel strength of WPI fibrillar and spherical aggregates. The results show that the capacity of WPI as a structuring agent can be increased by thiolation of pre-formed fibrillar and spherical aggregates.

Thus, proteins as food ingredients could be employed more broadly to attain new food structures by increasing their chemical cross-linking potency by means of thiolation. However, thiolated protein aggregates have to be tested on toxicological and organoleptic properties in order to be regarded safe to use in food applications.

Acknowledgements

The authors acknowledge help with transmission electron microscopy by Harry Baptist and the assistance with biochemical assays by Eefjan Timmerman.

References

- (1) Bolder, S. G.; Hendrickx, H.; Sagis, L. M. C.; van der Linden, E., Fibril assemblies in aqueous whey protein mixtures. **J. Agric. Food. Chem** 2006, **54**, 4229-4234.
- (2) Roefs, S. P. F. M.; De Kruif, K. G., A model for the denaturation and aggregation of β -lactoglobulin. **Eur. J. Biochem.** 1994, **226**, 883-889.
- (3) Havea, P.; Singh, H.; Creamer, L. K., Heat-induced aggregation of whey proteins: Comparison of cheese WPC with acid WPC and relevance of mineral composition. **J. Agric. Food. Chem.** 2002, **50**, 4674-4681.
- (4) Hong, Y. H.; Creamer, L. K., Changed protein structures of bovine β -lactoglobulin B and α -lactalbumin as a consequence of heat treatment. **Int. Dairy J.** 2002, **12**, 345-359.
- (5) Qi, P. X.; Onwulata, C. I., Physical properties, molecular structures, and protein quality of texturized whey protein isolate: Effect of extrusion temperature. **J. Agric. Food. Chem** 2011, **59**, 4668-4675.
- (6) Zúñiga, R. N.; Tolkach, A.; Kulozik, U.; Aguilera, J. M., Kinetics of formation and physicochemical characterization of thermally-induced β -Lactoglobulin aggregates. **J. of Food Sci** 2010, **75**, E261-E268.
- (7) Mudgal, P.; Daubert, C. R.; Foegeding, E. A., Cold-set thickening mechanism of β -lactoglobulin at low pH: Concentration effects. **Food Hydrocolloid** 2009, **23**, 1762-1770.
- (8) Cheftel, J. C.; Dumay, E., Microcoagulation of proteins for development of "creaminess". **Food Rev. Int.** 1993, **9**, 473-502.
- (9) Kroes-Nijboer, A.; Sawalha, H.; Venema, P.; Bot, A.; Floter, E.; den Adel, R.; Bouwman, W. G.; van der Linden, E., Stability of aqueous food grade fibrillar systems against pH change. **Faraday Discuss.** 2012, **158**, 125-138.
- (10) Langton, M.; Hermansson, A.-M., Fine-stranded and particulate gels of β -lactoglobulin and whey protein at varying pH. **Food Hydrocolloid** 1992, **5**, 523-539.
- (11) Arnaudov, L. N.; de Vries, R., Thermally induced fibrillar aggregation of hen egg white lysozyme. **Biophys. J.** 2005, **88**, 515-526.
- (12) Akkermans, C.; van, d. G. A. J.; Venema, P.; Gruppen, H.; Vereijken, J. M.; van, d. L. E.; Boom, R. M., Micrometer-sized fibrillar protein aggregates from soy glycinin and soy protein isolate. **J. Agric. Food. Chem.** 2007, **55**, 9877-9882.
- (13) Alting, A. C.; Hamer, R. J.; de Kruif, C. G.; Paques, M.; Visschers, R. W., Number of thiol groups rather than the size of the aggregates determines the hardness of cold set whey protein gels. **Food Hydrocolloid** 2003, **17**, 469-479.
- (14) Alting, A. C.; Hamer, R. J.; De Kruif, C. G.; Visschers, R. W., Cold-set globular protein gels: Interactions, structure and rheology as a function of protein concentration. **J. Agric. Food. Chem.** 2003,

51, 3150-3156.

- (15) Veerman, C.; Sagis, L. M. C.; van der Linden, E., Gels at extremely low weight fractions formed by irreversible self-assembly of proteins. **Macromol. Biosci.** 2003, **3**, 243-247.
- (16) Veerman, C.; Baptist, H.; Sagis, L. M. C.; van der Linden, E., A new multistep Ca²⁺-induced cold gelation process for β -lactoglobulin. **J. Agric. Food. Chem** 2003, **51**, 3880-3885.
- (17) Shimada, K.; Cheftel, J. C., Sulfhydryl group/disulfide bond interchange reactions during heat-induced gelation of whey protein isolate. **J. Agric. Food. Chem** 1989, **37**, 161-168.
- (18) Zhang, H.; Li, L.; Tatsumi, E.; Kotwal, S., Influence of high pressure on conformational changes of soybean glycinin. **Innov. Food Sci. Emerg.** 2003, **4**, 269-275.
- (19) Arzeni, C.; Martínez, K.; Zema, P.; Arias, A.; Pérez, O. E.; Pilosof, A. M. R., Comparative study of high intensity ultrasound effects on food proteins functionality. **J. Food Eng.** 2012, **108**, 463-472.
- (20) Strange, E.; Holsinger, V.; Kleyn, D., Chemical properties of thiolated and succinylated caseins. **J. Agric. Food. Chem** 1993, **41**, 30-36.
- (21) Strange, E. D.; Holsinger, V. H.; Kleyn, D. H., Rheological properties of thiolated and succinylated caseins. **J. Agric. Food. Chem** 1996, **44**, 54-58.
- (22) Klotz, I. M.; Stryker, V. H., Introduction of sulfhydryl groups into macromolecules. **Biochem. Biophys. Res. Commun.** 1959, **1**, 119-123.
- (23) Broersen, K.; Van Teeffelen, A. M. M.; Vries, A.; Voragen, A. G. J.; Hamer, R. J.; De Jongh, H. H. J., Do sulfhydryl groups affect aggregation and gelation properties of ovalbumin? **J. Agric. Food. Chem** 2006, **54**, 5166-5174.
- (24) de Jongh, H. H.; Broersen, K., Application potential of food protein modification.
- (25) Kim, S. C.; Olson, N. F.; Richardson, T., Polymerization and gelation of thiolated β -lactoglobulin at ambient temperature induced by oxidation by potassium iodate. **Milchwissenschaft** 1990, **45**, 627-631.
- (26) Klotz, I. M.; Stellwagen, E. C.; Stryker, V. H., Ionic equilibria in protein conjugates: Comparison on proteins. **BBA - General Subjects** 1964, **86**, 122-129.
- (27) Ellman, G. L., Tissue sulfhydryl groups. **Arch. Biochem. Biophys.** 1959, **82**, 70-77.
- (28) Kosters, H. A.; Broersen, K.; de Groot, J.; Simons, J. W.; Wierenga, P.; de Jongh, H. H., Chemical processing as a tool to generate ovalbumin variants with changed stability. **Biotechnol Bioeng** 2003, **84**, 61-70.
- (29) Owusu-Apenten, R. K.; Chee, C.; Hwee, O. P., Evaluation of a sulphhydryl-disulphide exchange index (SEI) for whey proteins— β -lactoglobulin and bovine serum albumin. **Food Chem.** 2003, **83**, 541-545.

- (30) Wierenga, P. A.; Kusters, H.; Egmond, M. R.; Voragen, A. G. J.; de Jongh, H. H. J., Importance of physical vs. chemical interactions in surface shear rheology. **Adv. Colloid Interface Sci.** 2006, **119**, 131-139.
- (31) Weijers, M.; Velde, F. v. d.; Stijnman, A.; Pijpekamp, A. v. d.; Visschers, R. W., Structure and rheological properties of acid-induced egg white protein gels. **Food Hydrocolloid** 2006, **20**, 146-159.
- (32) Visschers, R. W.; de Jongh, H. H. J., Disulphide bond formation in food protein aggregation and gelation. **Biotechnol. Adv.** 2005, **23**, 75-80.
- (33) Sakai, K.; Sakurai, K.; Sakai, M.; Hoshino, M.; Goto, Y., Conformation and stability of thiol-modified bovine lactoglobulin. **Protein Sci.** 2000, **9**, 1719-1729.
- (34) Pain, R. H., Determining the Fluorescence Spectrum of a Protein. **Curr. Prot. Food Anal. Chem.**
- (35) Chamani, J.; Moosavi-Movahedi, A. A.; Hakimelahi, G. H., Structural changes in β -lactoglobulin by conjugation with three different kinds of carboxymethyl cyclodextrins. **Thermochim. Acta** 2005, **432**, 106-111.
- (36) Shammass, Sarah L.; Knowles, Tuomas P. J.; Baldwin, Andrew J.; MacPhee, Cait E.; Welland, Mark E.; Dobson, Christopher M.; Devlin, Glyn L., Perturbation of the Stability of Amyloid Fibrils through Alteration of Electrostatic Interactions. **Biophys. J.** 2011, **100**, 2783-2791.
- (37) Li, H.; Rahimi, F.; Sinha, S.; Maiti, P.; Bitan, G.; Murakami, K., Amyloids and protein aggregation—analytical methods. In **EAC**, John Wiley & Sons, Ltd: 2006.
- (38) Ju, Z. Y.; Kilara, A., Gelation of pH-aggregated whey protein isolate solution induced by heat, protease, calcium salt, and acidulant. **J. Agric. Food. Chem.** 1998, **46**, 1830-1835.
- (39) Ross-Murphy, S. B., Incipient behaviour of gelatin gels. 1991, **30**, 401-411.
- (40) Jordens, S.; Adamcik, J.; Amar-Yuli, I.; Mezzenga, R., Disassembly and reassembly of amyloid fibrils in water-ethanol mixtures. **Biomacromolecules** 2011, **12**, 187-193.

Chapter 2: Supplementary information

Introduction

To evaluate the effect of thiolation of whey protein isolate (WPI) and its strengthening potential on gels, fibrillar aggregates were prepared from WPI. These fibrillar aggregates were subsequently thiolated. However, it has been reported that the conversion of peptides to fibrils is not as efficient as the conversion of monomeric proteins to spherical aggregates, as about 50 % of peptides are converted into fibrils¹ compared to a 95 % conversion of monomeric proteins to spherical aggregates². Thus, it could be argued that for the fibril variants described, non-converted peptides could interfere with the thiolation process or network efficiency. To study the effect of non-converted peptides on thiolation, separation of the peptides from the fibrils ('purification') was carried out prior to thiolation of the fibrils, now essentially free from non-aggregated peptides or proteins.

Experimental

Fibril preparation was carried out as described in the materials and methods section of the manuscript mentioned above. The formed fibrils were then dialyzed using 100 000 MWCO dialysis membrane to remove non-converted peptides as well as non-reacted materials as previously described³. This yielded the purified fibril fraction denoted as 'PF'.

The PF fraction was then thiolated in a similar way as described in the manuscript resulting in blocked variant ('PFSX'), which could be subsequently deblocked leading to 'PFSH'. A summary of the purified WPI fibrils variants is presented in **Table S1**.

Table S1: Overview of unmodified purified WPI fibrils and thiolated (SX-blocked and SH-deblocked variants) WPI fibrils essentially free from non-aggregated proteins/peptides.

	Blocked/deblocked	Variant abbreviation
WPI fibrils	Unmodified	PF
Thiolated WPI fibrils	Blocked	PFSX
Thiolated WPI fibrils	Deblocked	PFSH

Supplementary results

Table S2 shows that thiol groups were successfully introduced in purified fibrils with an efficiency and reactivity comparable to non-purified fibrils.

The number of detected free –SH groups were comparable in PFSX and FSX, but higher in PFSH than FSH. The apparent chemical reactivity of PFSX and PFSH was however lower than that of FSX and FSH (**Table S2**).

The lower chemical reactivity of PFSX and PFSH compared to FSX and FSH may be related to reduction in the contribution to chemical reactivity of thiol groups attached to non-converted proteins/peptides. **Fig. S1** shows that Th T binding was comparable for unmodified and thiolated purified fibrils. Purification resulted in a higher Th T binding efficiency, as expected, based on the higher fibrillated protein content in the purified samples compared to the non-purified samples.

Table S2: Physicochemical characterization of WPI samples modified with a ratio of 1:8 S-AMSA: amines– degree of substitution (DS) % and thiol reactivity (%).

	Number of thiol groups (mM/mM of protein \pm stdev)	DS (%)	Reactivity (SEI) %
Native	0.20 \pm 0.03	0	0 \pm 0.0
F	0.60 \pm 0.07	n.a	8 \pm 0.30
FSX	1.76 \pm 0.02	65 \pm 3	54 \pm 0.58
FSH	3.10 \pm 0.01	66 \pm 2	96 \pm 1.49
PF	0.50 \pm 0.04	n.a	n.d
PFSX	1.78 \pm 0.28	63 \pm 1	38 \pm 0.01
PFSH	4.00 \pm 1.13	70 \pm 1	84 \pm 0.01

Where n.a=not applicable, F=fibrils, P=purified, and n.d=not determined, DS = % modified amines of the total number of amines available derived from OPA assay; n.a =not applicable. The number of measurements (n) = 2.

Small deformation rheological characterization of the samples indicates that non-converted peptides do not interfere with thiolation nor contribute to the observed storage moduli (G'), as comparable G' (Pa) were obtained for purified (isolated) and non-purified (non-isolated) variants (**Fig. S2**). The results demonstrate that the G' observed is related to the fibrillar network formation and does not reflect non-aggregated protein responses. However, it also implies that the protein concentration is an over-estimation of actual protein incorporated in the networks. It has to be noted that the kinetics of gel formation increased for the purified fibrils. Thiolated samples (PFSX) showed a longer lag time compared to unmodified samples (PF) in the onset of G' . The resultant gels were stronger for PFSX as compared to PF (**Fig. S2**).

Similar trends were observed for non-purified unmodified WPI fibrils (F) and thiolated variants (FSX) prepared from fibrils without isolating non-aggregated peptides/proteins.

Thiolation of PFSX on the other hand resulted in a two-fold decrease in lag time as compared to FSX. The resultant gels prepared from PFSX were however not stronger than FSX gels. The finding suggests that thiolation of purified fibrils effectively reduces time required for gel formation (onset of gelation). Reduction of onset of gelation of PF compared to F may be related to the buffering capacity of the non-converted protein/peptides in F, which results in longer time required for initiation of gel formation in F compared to PF.

In conclusion, these data show that thiolation of fibrils prepared from WPI in itself is responsible for formation of stronger gels and that the presence or absence of non-aggregated proteins/peptides in the samples does not interfere with either thiolation or gelation of WPI fibrillar aggregates.

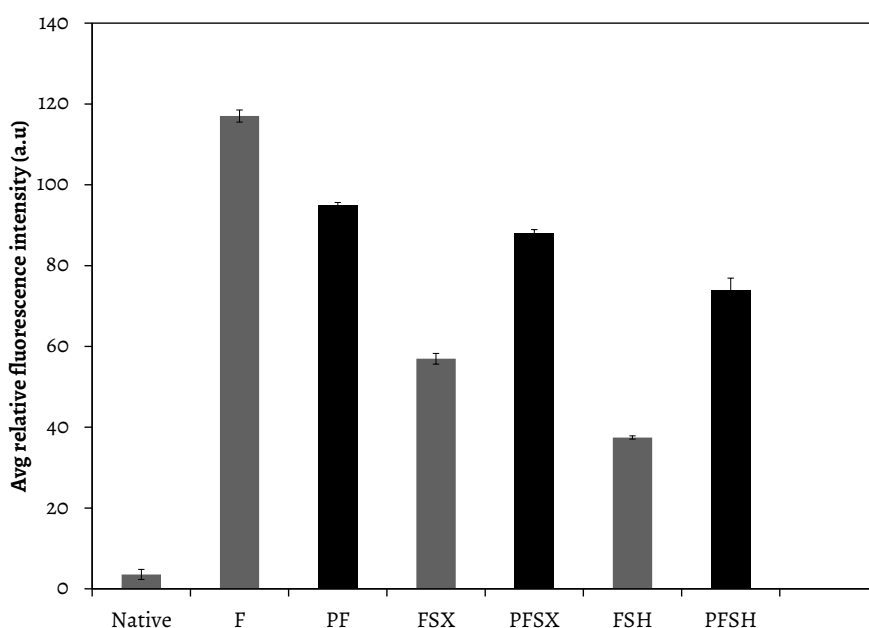


Figure S1: Average relative fluorescence intensities probed by Th T fluorescence at 485 nm wavelength for unmodified (F), thiolated blocked (FSX) and deblocked (FSH) variants of non-purified WPI fibrils and unmodified (PF), thiolated blocked (PFSX) and deblocked (PFSH) variants of purified WPI fibrils.

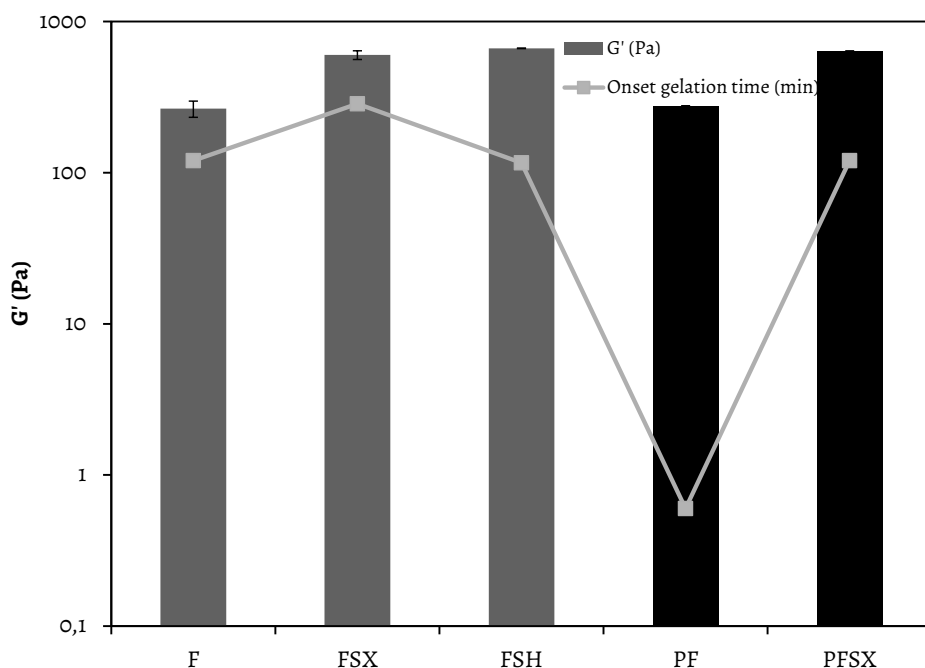


Figure S2: Final G' (Pa) of WPI variants following acidification using GDL and onset gelation time (min) for 0.9 wt % protein concentration for unmodified non-purified WPI fibrils (F), unmodified purified WPI fibrils (PF), blocked variant of thiolated non-purified WPI fibrils (FSX), blocked variant of thiolated purified WPI fibrils (PFSX), and deblocked variant of thiolated non-purified WPI fibrils (FSH). The error bars represent standard deviation from the mean of duplicate measurements performed on different batches of samples thiolated in a similar way.

References

- (1) Kroes-Nijboer, A.; Sawalha, H.; Venema, P.; Bot, A.; Floter, E.; den Adel, R.; Bouwman, W. G.; van der Linden, E., Stability of aqueous food grade fibrillar systems against pH change. **Faraday Discuss.** 2012, **158**, 125-138.
- (2) Alting, A. C.; Hamer, R. J.; de Kruif, C. G.; Visschers, R. W., Cold-Set Globular Protein Gels: Interactions, Structure and Rheology as a Function of Protein Concentration. **J. Agric. Food. Chem** 2003, **51**, 3150-3156.
- (3) Jordens, S.; Adamcik, J.; Amar-Yuli, I.; Mezzenga, R., Disassembly and Reassembly of Amyloid Fibrils in Water–Ethanol Mixtures. **Biomacromolecules** 2010, **12**, 187-193.

Chapter 3

Fibril formation from pea protein and subsequent gel formation

Micrometer-long and a few nm thick fibrillar aggregates were observed after heating pea protein solutions for 20 h at pH 2.0. The proteins were hydrolyzed into peptides of which 50 % assembled into fibrils. Structural changes in pea proteins were evaluated by the use of circular dichroism, transmission electron microscopy, and particle size analysis. An increase in aggregate size was observed upon the formation of fibrils which coincided with an increase in thioflavin T binding, an indication of the presence of β -sheet aggregates. The formed fibrils appeared to be branched and curly. Formation of gels using fibrils made from pea proteins was induced by slow acidification using glucono- δ -lactone from a pH 7.0 to a final pH of around pH 5.0. Pea protein-based fibrillar gels fractured at comparable strains during an amplitude sweep as soy protein and whey protein-based fibrillar gels, although gels prepared from fibrils made using pea protein and soy protein were weaker than those of whey protein. The results show that fibrils can be prepared from pea protein which can be incorporated into protein-based fibrillar gels.

This chapter is published as:

Munialo, C.D.; Martin, A.H.; van der Linden, E.; de Jongh, H. H. J. Fibril formation from pea protein and subsequent gel formation. ***Journal of Agricultural and Food Chemistry*** 2014, 62, (11), 2418-2427.

Introduction

Animal proteins have been used in the past for food production. In view of sustainability, availability, and cost, plant storage proteins become more important in contributing to larger supplies of proteins for nutrition, as a robust alternative to animal proteins¹. Legumes such as lentils, beans, and peas have been used in the diets of people from many cultures, especially where animal proteins are expensive or scarce¹. However, in order to make plant proteins from sources like legumes more attractive as a food ingredient, the study of their structure and functional characteristics, such as foaming, aggregation, and gelling behavior is important².

Storage proteins of peas (*Pisum sativum* L.) can be used in the food industry for new food products formulation because of their high nutritive value and are not in the list of common allergens³. Pea proteins which are composed of legumin, vicilin and a minor protein convicilin⁴ were in the late 20th century (1960's and 70's) identified as a potential alternative to soy bean proteins. Pea legumin is described as being a hexamer of six subunit pairs, each consisting of a basic subunit of ~20 kDa, and an acidic subunit of ~40 kDa⁴. Vicilin consists mainly of ~30 kDa, ~34 kDa, ~47 kDa, and ~50 kDa subunits⁵, whereas convicilin is denoted as α -subunits of vicilin.⁶ Some reports have been presented on the rheological behavior⁷ and the functional properties of pea globulin fractions⁸. Studies on thermal behavior of pea proteins have also been carried out⁹.

Aggregation in proteins has been shown to occur following the heating of proteins¹⁰. During heat treatment at a pH away from the isoelectric point (IEP) of the protein, aggregation occurs resulting in the formation of fibrillar aggregates (fibrils)¹¹. Fibrils can be used in low-caloric products because of their functionality that ranges from gelling agents to stabilizers of foams and emulsions¹². Additionally, fibrils have been reported to have the ability to form entanglement networks that could increase bulk viscosity with relatively little protein, making them potentially economical ingredients for modifying texture in food and biomedical products¹³.

Many proteins of animal origin such as whey proteins and ovalbumin have been assembled into fibrils¹⁴⁻¹⁷. Fibrils prepared using whey proteins have been described as being 1 μm long and a few nm thick.¹⁸ Fibrils have also been prepared from plant storage proteins, namely kidney bean phaseolin¹⁹, vicilin²⁰, and soy proteins^{21, 22}. Fibrils made using soy proteins were shown to exhibit different characteristics such as being more branched and curly than those made using whey proteins²¹.

Past research on fibrillar aggregates has described the assembly process¹⁸. Fibril formation process in β -lactoglobulin has been reported to be initiated following the hydrolysis of proteins at pH 2 into peptides, some of which assemble into fibrils²³. Soy glycinin was found to follow a similar aggregation pattern²³ but this has not been investigated so far for other plant proteins such as pea proteins.

Gelation of preformed fibrils has been previously carried out. Cold gelation of whey protein fibrils prepared at a low pH, induced by CaCl_2 ²⁴, NaCl ²⁵, and glucono- δ -lactone (GDL)²⁶, has been reported. However, information on the preparation, characterization, and subsequent gelation of fibrils made using pea proteins has not been reported.

The objective of this study was to characterize fibrillar aggregates made using pea proteins, and to assemble formed fibrils into protein-based gels in order to study the rheological behavior of these gels. The results described in this paper include the characterization of fibrils made using pea proteins with the use of thioflavin T (Th T) assay, circular dichroism (CD), transmission electron microscopy (TEM), and the rheological evaluation of protein-based fibrillar gels. To the best of our knowledge, this is the first report addressing the assembly of pea proteins into fibrils at low pH, the subsequent assembly of fibrils in spatial networks, and the mechanical characterization of formed gels.

Experimental

Materials

Pre-dried dehulled commercial green pea seeds with a protein content of 22 g/100 g (dry weight basis) were purchased from a local supermarket. Whey protein isolate (WPI) BiproTM was obtained from Davisco Food International, Inc. (Le Sueur, MN, USA). Soy protein isolate was extracted from defatted soy protein flour provided by Cargill BV (Amsterdam, the Netherlands). Soy protein extraction was carried out according to a previously described protocol²¹ with slight modifications, in which acid precipitation was carried out at pH 4.5 instead of pH 4.8, and the final soy protein isolate was not freeze dried. Glucono- δ -lactone (GDL), ortho-phthaldialdehyde (OPA), N, N-dimethyl-2-mercaptoethyl-ammoniumchloride (DMA), di-sodiumtetraborate decahydrate (Borax), sodiumdodecylsulfate (SDS), urea, dithiothreitol (DTT), trifluoroacetic acid (TFA), acetonitrile, and uranyl acetate were purchased from Sigma-Aldrich (Steinheim, Germany). Thioflavin T (Th T) was obtained from Acros organics (Geel, Belgium). All reagents were of analytical grade and used without further purification.

Pea protein extraction and characterization

Pea protein isolate was extracted from commercial green peas by isoelectric precipitation. Extraction of pea protein was based on a previously described procedure⁶, with modifications. Pea protein flour was milled from dried peas in a Waring commercial blender (New Hartford, Connecticut, USA). Milling was performed in the presence of liquid nitrogen to prevent excessive heating that may lead to heat denaturation of the proteins. Milled pea flour was dispersed in MilliQ water in the ratio of 1:10 (g/mL) to make protein slurry. The pH of the slurry was adjusted to pH 8.0 with 1 M NaOH, and incubated at room temperature ($20\text{ }^{\circ}\text{C} \pm 2\text{ }^{\circ}\text{C}$) for 1 h. The slurry was then centrifuged at $10000 \times g$ ($20\text{ }^{\circ}\text{C}$, 25 min) to remove insoluble materials. The supernatant was collected and the pH readjusted to pH 4.8 using 1 M HCl.

The supernatant was then incubated at 20 °C for 2 h under continuous stirring, and subsequently centrifuged at 10000 × *g* (20 °C, 25 min). Following this, the supernatant containing albumins and sugars was discarded. The pellet was collected and re-dispersed in MilliQ water in the ratio of 1:10 (g/mL). The re-dispersed suspension at a pH of 4.8 was centrifuged at 10000 × *g* (20 °C, 25 min) and the pellet resuspended in MilliQ water in the ratio of 1:3 (g/mL) to remove remaining sugars and albumins. The pH of the resuspended pellet was set to pH 8.0 using 2 M NaOH and the solution was incubated at room temperature (20 °C ± 2 °C) for 1 h, followed by centrifugation at 10000 × *g* (20 °C, 25 min) to remove remaining traces of insoluble materials. The supernatant was collected, the pH measured, and adjusted to a final pH of 8.0 using 2 M NaOH if necessary. The pea protein isolate was then stored at 4 °C in the presence of 0.02 % sodium azide to prevent microbial growth. The pea protein solution extracted in this way will be referred to as 'native' pea protein. The protein content of native pea protein was determined using Dumas (NA 2100 Protein, CE instruments, Milan, Italy) using a factor of 5.52²⁷ and was found to be about 87 ± 0.1 mg/mL. The dry matter content of native pea protein was 94 mg/mL and the purity of pea protein extract was 92 ± 1 %. Pea proteins showed a typical denaturation temperature around 77 °C as demonstrated by calorimetric measurements at a heating rate of 2 °C/min for 87 mg/mL pea protein solution (results not shown).

The protein composition of native, unheated, and heated pea protein solutions at an approximate concentration of 10 mg/mL was analyzed using sodium dodecylsulphate polyacrylamide gel electrophoresis (SDS-PAGE) under reducing conditions. A MOPS-SDS (20 ×) buffer was used as a running buffer. Electrophoresis conditions were 200 V, 10 mA throughout at 25 °C and 50 min running time. Following separation, the proteins were fixed and stained using the Simply Blue Safe stain and developed to obtain a suitable background color.

The apparent molecular weights of the present proteins were determined by comparison to the molecular weight standard (Sigma wide range molecular weight markers, 6 -200 kDa) applied into a separate lane. The gels were scanned and the acquired images were analyzed by Image Master® software. SDS-PAGE was also carried out on pea protein solutions heated for different periods at pH 2.0.

Pea protein solutions preparation and fibril formation

Native pea protein solutions were diluted to 40 mg/mL in MilliQ water adjusted to pH 2.0 using HCl. The obtained solutions were then centrifuged at 15000 × *g* for 30 min at 4 °C to remove any traces of insoluble material that could arise following pH readjustments. The supernatant was collected and filtered through a 1.2 µm (Millex-SV, Millipore Corp., Bedford, MA) filter. The final pH of the sample was adjusted to pH 2.0 using 6 M HCl. Determined protein concentrations after centrifugation and filtration showed that negligible protein losses occurred during these processes.

Fibril preparation using pea protein was carried out according to a previously described protocol²¹.

In summary, aliquots of 20 mL protein solutions prepared as described above were incubated at 85 °C for 20 h in a temperature-controlled water bath equipped with a stirring device, and continuously stirred with a magnetic stirring bar at 300 rpm. After the heat treatment, samples were cooled in an ice bath and stored at 4 °C until further use, typically within two weeks.

Fibrils made using 40 mg/mL soy protein were prepared in a similar way as previously described²¹ except for soy protein being heated in a water bath equipped with a stirring device, and continuously stirred with a magnetic stirring bar at 300 rpm, instead of being heated using a shearing device, whereas fibrils made using whey protein were prepared according to a previously described protocol²⁶.

Characterization of fibrils made using pea protein

Determination of the number of primary amines present following the hydrolysis of pea proteins into peptides was carried out using chromogenic OPA assay as previously outlined²⁸. Reversed phase high performance liquid chromatography (RP-HPLC) (Shimadzu, Kyoto, Japan) was used according to a method adapted from a previously described procedure²⁹, to determine how much of the protein was hydrolyzed into peptides. All samples were analyzed in aqueous solutions containing 4 M urea and 0.3 % DTT. RP-HPLC was carried out using 2 M 6000A pumps in combination with a high sensitivity accessory block (Waters), an ISS-100 injector (Perkine Elmer, Uberlingen, Germany), a Waters Model 680 gradient controller, and a Kratos 783 detector (Kratos Analytical, Ramsey, NJ, USA). A 250 x 4.6 mm Aeris wide pore C18 column (Phenomex, The Netherlands) was used with a KrudKatcher Ultra HPLC Column In-Line Filter (Phenomex) as a guard column. A 10 µL pea protein sample was injected on to a wide-pore C18 analytical column thermostated at 40 °C. Samples were eluted at a flow rate of 0.40 mL/min with a linear gradient of 0.10 v/v % trifluoroacetic acid (TFA) in 98 v/v % water and 2 v/v % acetonitrile to 0.10 v/v % TFA in 10 v/v % water and 90 v/v % acetonitrile. The equipment was linked to a data acquisition and processing system (Turbochrom, PerkineElmer). Data analysis was done with Chromeleon software version 7.1 (ThermoFisher Scientific).

Determination of the degree of conversion of peptides into fibrils was carried out on heated samples according to the previously described procedure²¹. In summary, heated pea protein solutions at pH 2.0 were diluted to 2 mg/mL. The solutions were divided into 6 centrifugal tubes containing filters with a molecular weight cut off (MWCO) of 100 kDa and centrifuged in four consecutive steps (3000 × g, 30 min, 15 °C) yielding four filtrates (F1 to F4). The obtained volumes were in this way sufficient to determine the protein content of each centrifugation step as determined by Dumas (NA 2100 Protein, CE instruments, Milan, Italy) with a protein factor of 5.52²⁷. The degree of conversion of monomers to fibrils was determined using the equation 1

$$C = \frac{P - (F_1 + F_2 + F_3 + F_4) \times 100}{P} \% \quad (1)$$

where **C** is the conversion factor (%), **P** is the initial protein content (g) in the solution, **F₁** is the protein content (g) in filtrate 1, **F₂** is the protein content (g) in filtrate 2, **F₃** is the protein content (g) in filtrate 3, **F₄** is the protein content (g) in filtrate 4.

Th T fluorescence assay was used to evaluate the formation of β -sheet structures based on a previously described principle³⁰. After fibril preparation, a volume of 48 μ L of heated pea protein samples was mixed with 4 mL of filtered (0.2 μ m, Schleicher and Schuell) 60 μ M Th T solution in a phosphate buffer (10 mM phosphate, 150 mM NaCl at pH 7.0), and incubated for 10 min at 25 °C. Fluorescence intensity was measured using a fluorescence spectrophotometer (Perkin-Elmer LS 50 B) at an excitation wavelength of 460 nm (slit width 2.5 nm), and emission wavelength from 465 to 550 nm (slit width 2.5 nm). Controls included the fluorescence intensity of Th T solution without the addition of protein solution and unheated pea protein solutions.

Spectroscopic and microscopic analyses

Determination of the hydrodynamic diameters of the protein aggregates was carried out using dynamic light scattering (DLS) (Zetasizer Nano ZS, Malvern Instruments, Worcestershire, UK). Changes in aggregate size during the heating of 5 mg/mL pea protein solutions at 85 °C for 20 h were recorded as a function of time at pH 2.0. Reported values are the average hydrodynamic diameters of the largest intensity peak, as found in the distribution analysis using Malvern DTS 5.03 software. The particle size distribution from DLS was derived from a deconvolution of the measured intensity autocorrelation function of the samples using a non-negatively constrained least squares (NNLS) fitting algorithm. Duplicate measurements were performed for this analysis.

Far-UV circular dichroism (CD) was used to investigate the secondary structure of native and fibrillar pea protein solutions. Far-UV CD spectra of ~0.2 mg/mL native and fibrillar pea protein solutions were obtained and recorded at 25 °C in the spectral range from 190 to 260 nm with a Jasco J-715 spectropolarimeter (Jasco Corporation, Japan), using a quartz cuvette with an optical path of 0.1 cm. The spectral resolution was 0.5 nm, the scan speed was 100 nm/min, with a response time of 0.125 sec at a bandwidth of 1 nm. Twenty scans were accumulated and averaged and the spectra were corrected for that of a protein free sample.

Near-UV circular dichroism (CD) was used to investigate the tertiary and/or quaternary structure of native and pea protein fibrillar solutions. Near-UV spectra of ~2 mg/mL native and fibrillar pea protein solutions were obtained and recorded at 25 °C in the spectral range from 250 to 350 nm with a Jasco J-715 spectropolarimeter (Jasco Corporation, Japan), using a quartz cuvette with an optical path of 1 cm. The spectral resolution was 0.5 nm, the scan speed was 100 nm/min, with a response time of 0.125 sec at a bandwidth of 1 nm. Twenty scans were accumulated and averaged and the spectra were corrected for that of a protein free sample.

Fibrillar solutions made using pea protein were prepared for transmission electron microscopy (TEM) by negative staining according to a previously described protocol²⁶. A 10 µL aliquot of 0.25 mg/mL fibrillar solutions made using pea protein was deposited onto a carbon support film on a copper grid (Aurion-Immuno Gold Reagents & Accessories, Wageningen, The Netherlands). The excess fibrillar solution was removed after 30 s using a filter paper (Whatman No. 1, 512-1002, VWR International Europe BVBA, Leuven, 3001, Belgium). A droplet of 2 % uranyl acetate at pH 3.8 was added for 30 s to improve the contrast. Excess uranyl acetate was removed by use of a filter paper. Electron micrographs were obtained using a Jeol JEM1011 transmission electron microscope (Tokyo, Japan) operating at 80 kV.

Rheological characterization of protein-based fibrillar gels

Gelation of fibrillar aggregates made using pea protein was carried out by acid-induced cold gelation using glucono-δ-lactone (GDL). Before gelation was initiated, the pH of the fibrillar solutions made using pea protein at pH 2 was adjusted to pH 7. The concentrations of GDL added to the samples to induce gelation were determined using the empirical relation (% GDL (wt/wt) = $0.0065 \times C_{\text{protein}} \text{ (g/L)} + 0.045$)³¹. GDL was added to fibrillar solutions made using pea protein with a protein concentration ranging from 40 – 160 mg/mL to induce gelation at 25 °C. For gelation at a protein concentration as high as 160 mg/mL, pea protein fibrillar solutions prepared at 40 mg/mL were concentrated by ultrafiltration using Merck Millipore Amicon stirred cell fitted with 30 kDa MWCO membrane (Darmstadt, Germany). Several trials were carried out using calculated GDL concentrations and a final GDL concentration range of 0.3 - 1 % was chosen in order to get to a final pH of about pH 5 at the end of gelation time. The pH of all the samples was determined as a function of time during 15 h of incubation at 25 °C. A stress-controlled rheometer (ARG2, TA Instruments, Leatherhead, UK) with a concentric cylinder geometry (C14: cup diameter, 15.4 mm; bob diameter, 14.04 mm) was used to determine storage modulus (G') and loss modulus (G'') as a function of time (frequency, 1 Hz; temperature, 25 °C; % strain, 0.05, 15 h). After 15 h of incubation, an oscillation amplitude sweep was performed (frequency, 1 Hz; temperature, 25 °C; % strain, 0.001 - 100). Duplicate measurements were carried out for each protein concentration within the linear region which was between a % strain of 0.001 and 10.

Results and Discussion

Characterisation of fibrils using pea protein

Hydrolysis of pea protein into peptides

It has been reported that the fibril formation process in β-lactoglobulin is initiated following the hydrolysis of proteins at pH 2 into peptides, some of which assemble into fibrils³². Heat induced hydrolysis of protein at pH 2 has been shown to play a significant role in fibril assembly of soy 7S/11S globulin²².

To study whether this phenomenon plays a role in fibril assembly using pea protein, the degree of hydrolysis as quantified by the number of primary amine groups available following heating of pea protein was determined by chromogenic OPA assay. The chromogenic OPA assay results showed that about 30 % of primary amines could be detected after heating 40 mg/mL pea protein at pH 2.0, 85 °C for 20 h. Assuming an average lysine content of about 8 % per protein, this would correspond to an ensemble-averaged degree of hydrolysis of about 3 fragments generated from every protein.

SDS-PAGE was carried out on pea protein solutions to study the molecular weight degradation (**Fig. 1**).

Fig. 1 A (lane **B**) shows that the isolated pea protein used in this study contains both legumin (less dominant bands at ~40, ~20 kDa) and vicilin/convicilin (dominant bands at ~70, ~50, ~33-14 kDa). Native pea protein solutions at pH 8.0 (**Fig. 1 A**, lane **B**) showed similar bands as pea protein solutions at pH 2.0 before heating (**Fig. 1 A**, lane **C**; and **1 B**, lane **o h**). This shows that both vicillin/convicilin and legumin fractions were still present in the samples before heating. SDS-PAGE was also carried out on pH 2.0 samples as a function of heating time (h) as shown in **Fig. 1 B**.

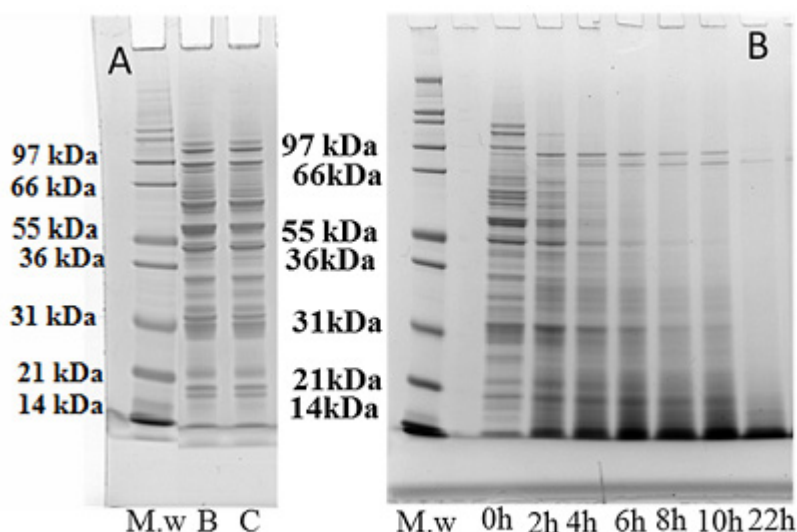


Figure 1 A: SDS-PAGE electrophoretograms for standard marker (M.w), native pea protein solutions at pH 8 (B), and pea protein solutions at pH 2 prepared for fibril formation but not heated (C). **Figure 1 B:** SDS-PAGE electrophoretograms for time-dependence heating of pea protein solutions at pH 2.0 for up to 22 h. The band marked M.w is the standard marker, 0 h, 2 h, 4 h, 6 h, 8 h, 10 h, and 22 h represents heating of the samples for up to 22 h. The dominant bands at ~70, 50, 33-14 kDa are vicilin/convicilin fraction subunits whereas the less dominant bands at ~40, 20 kDa represent the legumin fraction subunits.

The results show that with heating of the samples for 2 h, bands of molecular weights above 97 kDa disappear.

Heating the sample for longer than 10 h causes the bands above 21 kDa to disappear (**Fig. 1 B**), suggesting that progressive hydrolysis occurs during prolonged heating of pea protein solutions at pH 2.0. There were persistent bands of between 66 and 97 kDa that remained dominant over all the heating times at 85 °C (**Fig. 1 B**). The bands at around 70 kDa are convicilin polypeptides whereas the bands around 97 kDa that seem to fade off at heating times exceeding 10 h could be traces of lipoxygenase⁴.

RP-HPLC analysis of the protein solutions following heating at pH 2.0 in comparison to native pea protein (**Fig. 2**) showed that all proteins were degraded to different degrees from the native form.

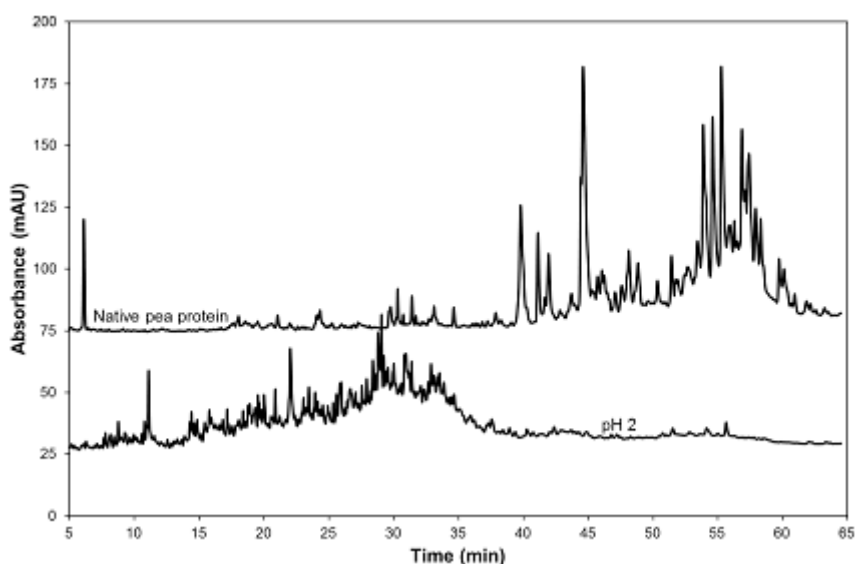


Figure 2: Reversed phase high performance liquid chromatography (RP-HPLC) chromatograms for native pea protein and heated pea protein solutions at pH 2.0.

This confirms that hydrolysis of all proteins present occurs following the heating of pea proteins at pH 2.0 (**Fig. 2**).

The findings on the study of molecular weight degradation of pea protein suggest that: (i) hydrolysis of pea protein into peptides which can assemble into fibrils is a process that requires prolonged heating of the samples at a pH away from the IEP, at low ionic strength, combined with heating temperatures above the denaturation temperature of the protein, (ii); gradual degradation of pea proteins occurs over incubation time (h); and that

(iii) hydrolysis of pea protein to peptides which assemble into fibrils follows the generic fibrillization mechanism similar to that of other globular proteins like whey proteins²³, soy proteins²¹, and lysozyme³³.

Degree of conversion of peptides into fibrils made using pea protein

To determine the degree of conversion of peptides into fibrils, a centrifugal filtration method was used as described before¹². No protein was found by the Dumas method in the 4th washing step, which indicates that at this stage of the procedure, the obtained fibril solution was free from non-aggregated peptides. It was found that about 50 % of the initial protein was present in the form of fibrils in pea proteins.

Th T fluorescence assay

Heated pea protein solutions were checked for the presence of β -sheet aggregates as a typical characteristic for fibril assembly. **Fig. 3** and **Table 1** shows the results of thioflavin T (Th T) assay as a function of heating time (**Fig.3**) and pH (**Table 1**).

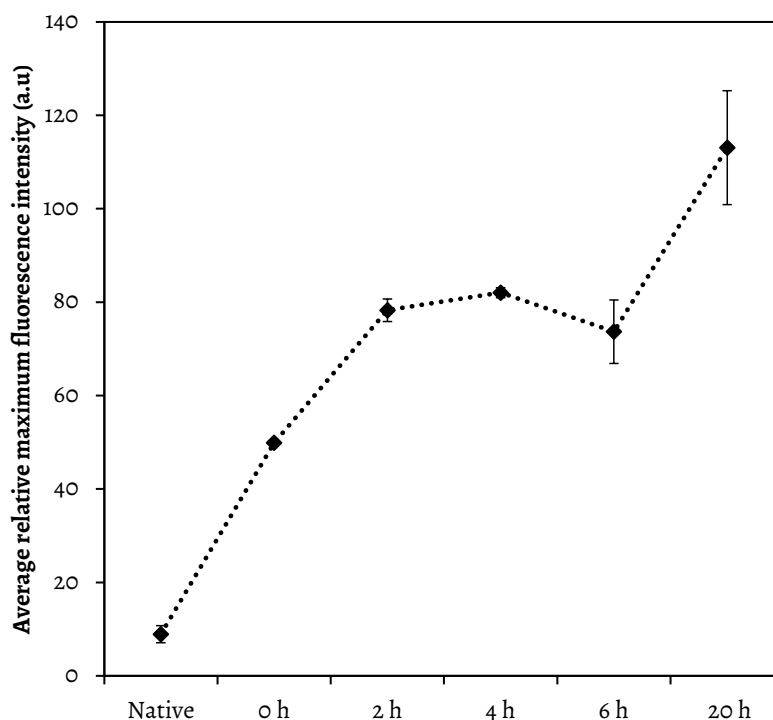


Figure 3: Average relative maximum fluorescence intensities as a function of heating time at a protein concentration of 40 mg/mL.

The use of Th T to evaluate the formation of β -sheets in proteins following the heating of protein solutions at low ionic strength and pH 2.0 for a prolonged time has been described in detail elsewhere.³⁰ Native pea protein solutions had the lowest fluorescence intensity (**Table 1**). Following the incubation of pea protein solutions at pH 2.0, an increase in maximum fluorescence intensity was observed within the first 2 h of incubation (**Fig. 3**).

After 2 h of incubation, an initial gradual reduction in maximum fluorescence intensity was observed, suggesting that fibrils were formed during heating.¹¹ The gradual reduction in maximum fluorescence intensity after 2 h of heating coincided with the disappearance of bands of molecular weights above 66 kDa as observed in SDS-PAGE electrophoretograms (**Fig. 1 B**). A further slight decrease in maximum fluorescence intensity was observed at an incubation time of between 5-6 h followed by a steady increase in maximum fluorescence intensity.

Table 1: Comparison of maximum relative fluorescence intensity (a.u) for native pea protein solutions, heated pea protein solutions at pH 2.0 during the study of aggregate assembly kinetics, heated pea protein solutions at pH 2 prepared following heating of 40 mg/mL of pea protein solutions at 85 °C for 20 h, heated pea protein solutions at pH 7, heated soy protein solutions at pH 2 and heated whey protein solutions at pH 2.0.

Protein sample	pH	Maximum relative fluorescence intensity (a.u) \pm stdev
Native	8	9 \pm 0.1
Pea protein	2 ^a (Aggregate assembly kinetics)	10 \pm 0.5
Pea protein	2 ^b	113 \pm 1
Pea protein	7	62 \pm 0.5
Soy protein	2	121 \pm 3
Whey protein	2	349 \pm 5

Where 2^a represents samples used in study of fibril assembly kinetics that were followed over time using dynamic light scattering (aggregate size results are shown in Fig. 4) whereas 2^b represents heated pea solutions at (40 mg/mL, pH 2.0) after which the pH of the samples was adjusted to pH 7.0 for gelation to be induced using GDL.

Such a reduction in fluorescence intensity has been attributed to the partial disruption of the highly ordered structure by further polypeptide hydrolysis¹¹.

Progressive increase in fluorescence intensity was observed following heating of the samples for more than 6 h of incubation (**Fig. 3**), whereas following heating of the sample for more than 10 h, bands of molecular weights above 21 kDa disappeared as observed in SDS-PAGE electrophoretograms (**Fig. 1 B**). An increase in the fluorescence intensity in heated samples at pH 2.0 for incubation periods above 6 h confirms the presence of β -sheets to which Th T reagent could bind. Following subsequent readjustment of the pH from pH 2.0 to pH 7.0, the fluorescence intensity of the pea protein sample was shown to decrease to almost half (**Table 1**).

The decrease in fluorescence intensity could be as a result of partial disruption of the β -sheet fibrillar structure as previously reported for other type of fibrils³⁴. The pH adjustment to pH 7.0 is essential to enable acid-induced gelation as described under rheological characterization of protein-based fibrillar gels. The findings show that thioflavin T can also bind to the β -sheets present in fibrils made using pea protein.

Changes in structural properties during fibril assembly

Aggregate assembly kinetics

Typical particle size distribution profiles of up to 12 h (by intensity) of heating of pea protein solutions are presented in **Fig. 4**.

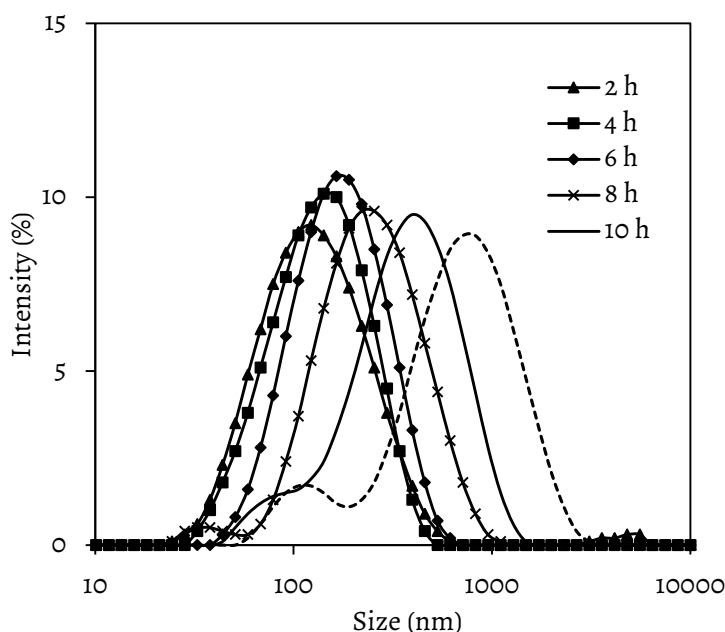


Figure 4: Changes in aggregate size over time for 5 mg/mL pea protein solutions heated at pH 2, and 85 °C monitored by the use of dynamic light scattering.

A concurrent increase in particle size was observed over time. This increase in particle size is associated with thermal denaturation of the protein and subsequent aggregation. For heating periods below 6 h, predominant monomodal contributions were observed. When the heating period exceeded 6 h, the contributions became bimodal, and the distribution peaks shifted towards much higher aggregate sizes above 150 nm (**Fig. 4**). The shift in the distribution peaks towards higher sizes coincided with a further increase in Th T binding after 6 h of incubation (see **Fig. 3**).

Bimodal contributions indicate that the fibril assembly (especially elongation of fibrils) occurred only after heating with enough incubation periods. The results show that the formation of pea protein β -sheet aggregates occurred following heating over incubation periods longer than 6 h. The Th T assay performed on this sample following heating also showed the presence of some β -sheet aggregates (**Table 1**).

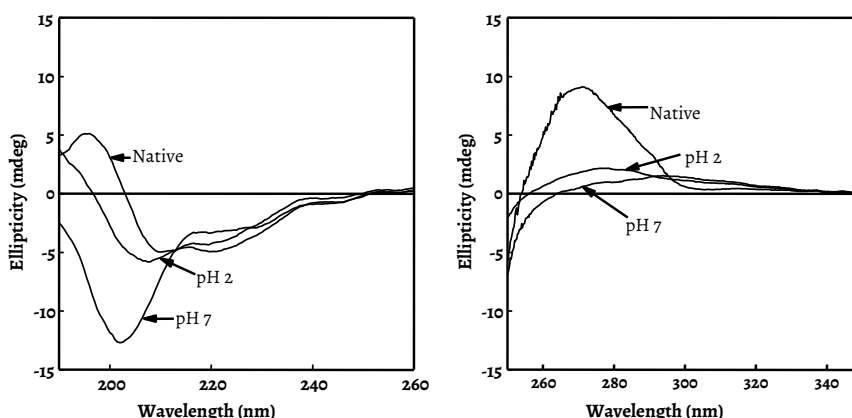


Figure 5: Analysis of secondary structural elements by far UV-CD of native pea protein solutions, heated pea protein solutions at pH 2.0, and heated pea protein solutions at pH 7.0 are shown in **Figure 5 A**. Near UV-CD spectra of these samples are shown in **Figure 5 B**.

Secondary structure

To probe the secondary conformational changes, Far-UV CD spectra were recorded of native pea protein, heated pea protein at pH 2.0, and the heated protein at pH 7.0 as shown in **Fig. 5 A**.

The spectrum of native pea protein show two minima around 222 nm and 208 nm and a zero crossing at 204 nm, indicative of a secondary structure that is highly predominated by α -helical and some β -sheet contributions³⁵. Upon heating of pea protein solutions at pH 2.0, a shift at the zero crossing to 197 nm was observed, illustrating a considerable loss of β -sheet strands. Substantial amounts (about 20 %) of β -sheet were however still present in pea protein heated at pH 2.0 when the far-UV CD spectra were analyzed by the method previously described³⁶. Following adjustment of the sample pH from pH 2.0 to pH 7.0, the CD spectrum showed a predominance of random coil elements.

The predominance of random coil gives an indication of a further unfolding of the polypeptides upon adjustment of the pH of fibrillar solutions formed using pea protein at pH 2.0 to pH 7.0.

Far-UV CD results were in agreement with the Th T assay as a reduction in Th T intensity occurred when the pH was adjusted from pH 2.0 to pH 7.0 (**Table 1**). Similarly, conformational changes to random coil from β -sheet structures occurred with pH adjustment (**Fig. 5 A**).

Tertiary and/ or quaternary structure

To probe the tertiary and to some extent quaternary conformational changes, near UV-CD spectra were recorded of native pea protein solutions, heated pea protein solutions at pH 2.0, and heated pea protein solutions readjusted to pH 7.0 (**Fig. 5 B**). The actual shape and magnitude of the near-UV CD spectrum of proteins depends on the number of aromatic amino acids restrained in their mobility, typically caused by spatial packing of the polypeptide³⁷. Unheated native pea protein was shown to exhibit a prominent positive dichroic band at 270 nm, which is a typical contribution of tyrosine residues³⁸. The magnitude of this contribution decreased substantially following heating, illustrating that the protein loses its tertiary packing constraints, resulting in the formation of a less well-defined structure. The decrease in the dichroic intensity may also reflect progressive exposure of tyrosine residue to the aqueous phase, as a result of heat-induced protein structural unfolding as well as polypeptide hydrolysis¹¹. Readjustment of the pH from pH 2.0 to pH 7.0 did not result in major changes in tyrosine residues, implying that the protein tertiary structure remains unfolded.

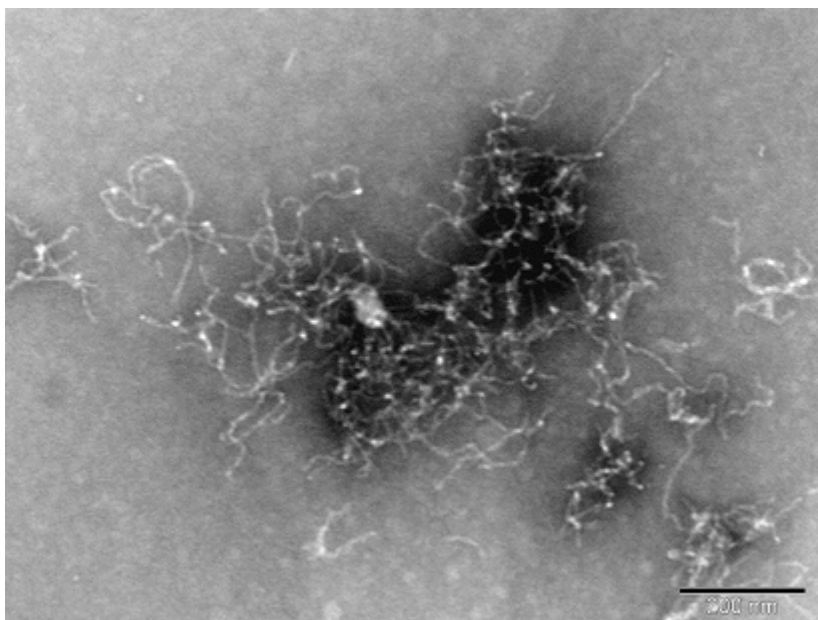


Figure 6: Transmission electron micrographs (TEM) of 0.25 mg/mL pea protein fibrils prepared at pH 2.0 following prolonged heating at 85 °C. Scale bars represent 200 nm.

The results suggests that adjustment of the pH from pH 2.0 to pH 7.0 following heating of the protein solutions at low pH destabilizes the secondary structure of the protein/peptides, whilst changes in tertiary structure could not be observed.

Transmission electron microscopy (TEM)

To analyze the formed pea protein fibrils on a microscopic scale, TEM pictures of the samples were taken (**Fig. 6**). Differences in the morphology of pea protein and whey protein fibrils could be attributed to inherent differences between plant storage and animal proteins as well as differences in the quaternary structure of the protein and its solubility, which may have a considerable influence on the aggregation behavior of the proteins.

Comparison between fibrils made using pea proteins and soy proteins

Past research has shown that fibrils can be obtained using other plant storage proteins^{11, 22}. To compare fibrils made using pea proteins and soy proteins, characterization of fibrils prepared using soy proteins was carried out. Fibrils made using pea proteins showed a comparable ability to bind to Th T fluorescent dye as those made using soy protein (**Table 1**). Moreover, the characterization of fibrils assembled using pea proteins as a function of heating time also showed a similar increase in size compared to soy β -conglycinin¹¹.

During the assembly of peptides from soy β -conglycinin to fibrils, an initial increase in maximum relative fluorescence intensity was observed as a function of time. A gradual decrease in the maximum fluorescence intensity following incubation periods of about 8 h was observed¹¹. A similar observation was recorded for fibrils made using pea protein although the decrease in maximum fluorescence intensity occurred 2 h earlier in pea protein than in soy β -conglycinin. Fibrils formed from soy protein were found to have an approximate contour length of 1 μm , the persistence length of 2.3 μm , and the thickness of a few nanometers²¹. Fibrils made using soy protein were described as being more branched and curly than those made using whey protein²¹, and also confirmed in our lab (Results not shown). Comparisons of TEM micrographs of fibrils made using pea protein and soy protein showed that fibrils made using both pea proteins and soy proteins exhibited similar characteristics of being highly flexible, worm-like, and curly.

Progressive and remarkable changes in the secondary conformation as a result of fibril formation using pea proteins were observed in this study, similar to that reported for soy β -conglycinin and glycinin²². An increase in particle size during fibril assembly in pea proteins was also observed in this study, similar to that reported for soy proteins²². The results show that (i) pea proteins can be assembled into fibrils that have comparable structural characteristics to soy proteins, and that (ii) plant proteins show similar characteristics in fibril formation, and hence pea proteins can effectively be used as a potential substitute for other plant proteins such as soy proteins.

Comparison between fibrils made using pea proteins and whey proteins

The characterization of fibrils prepared using whey protein has been extensively carried out in the past^{14, 18, 39}, and also confirmed in our lab²⁶. Considering the inherent differences in the structure and composition of pea proteins and whey proteins, it was expected that the characteristics of fibrils made using pea proteins would vary from those made using whey protein. β -lactoglobulin (β -lg), the major fraction of WPI, has been reported to have a typical conversion factor of about 50 %¹². In this study, fibrils made using pea proteins also had a conversion factor of about 50 %.

The use of thioflavin T assay to compare the formation of β -sheet aggregates in pea proteins and whey proteins was also carried out. The results showed that thioflavin T can bind to the β -sheets present in both pea proteins and whey proteins, although β -sheets in whey proteins exhibited a higher maximum relative fluorescence intensity compared to those of pea proteins (**Table 1**). This could give an indication of the presence of less β -sheet aggregates in pea proteins compared to whey proteins, with a similar incorporation in fibrillar aggregates.

Using TEM to analyze the microstructure, fibrils made using whey proteins were found to be longer, and to have a thickness of few nm and a length of 1 μm ⁴⁰. Fibrils prepared using whey proteins were also described as being semiflexible³⁹. The characterization of fibrils made using pea protein on the other hand showed that the fibrils were highly flexible, more branched, and curly (**Fig. 6**). However, depending on several conditions such as ionic strength, pH, protein concentration, and whether the protein solutions were stirred during heating or not, whey protein has been reported to be capable of forming curly fibrils that are as flexible³⁹ as fibrils made using pea proteins.

Rheological characterization of protein-based fibrillar gels

Fibrils have been shown to form gels at relatively low protein concentration⁴¹.

Table 2: The final G' (Pa) and $\tan \delta$ values for different fibrillar solutions made using concentrations of pea protein, 40 mg/mL soy protein, and 25 mg/mL whey protein. The values were obtained after 15 hours of gelation following addition of GDL to the fibrillar solutions at 25 °C.

Protein sample	Final G' (Pa) \pm stdev	Final $\tan \delta \pm$ stdev
40 mg/mL pea	22 \pm 2.3	0.18 \pm 0.01
80 mg/mL pea	70 \pm 5.01	0.22 \pm 0.001
160 mg/mL pea	2058 \pm 3.4	0.20 \pm 0.02
40 mg/mL soy	31 \pm 4.0	0.17 \pm 0.01
25 mg/mL whey	5845 \pm 22.0	0.07 \pm 0.002

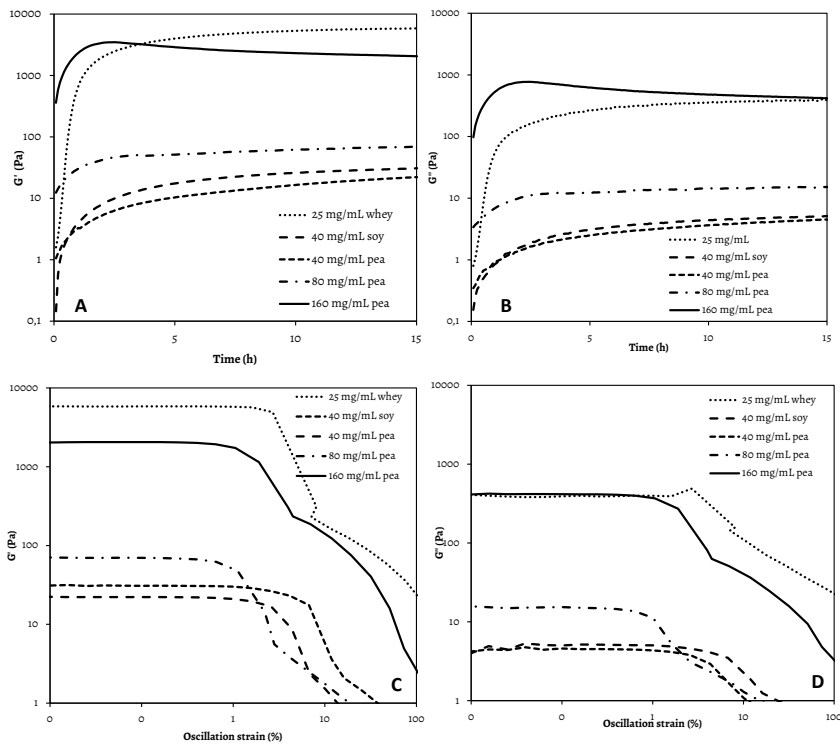


Figure 7: Changes in G' (Pa) (A) and G'' (Pa) (B) over time for 40, 80 and 160 mg/mL pea protein fibril solutions prepared at pH 2.0 and pH adjusted to pH 7.0 before initiation of gelation using GDL. The gelation was compared with 40 mg/mL of soy protein prepared at pH 2.0, 85 °C for 20 h, and 25 mg/mL of whey protein fibrils prepared at pH 2.0, 80 °C for 20 h. **Figures 7 C and D** shows changes in oscillation strain (%) as a function of G' (Pa) (C) and G'' (Pa) (D) for 40, 80 and 160 mg/mL pea protein, 40 mg/mL of soy protein and 25 mg/mL of whey protein-based fibrillar gels following slow acidification towards the isoelectric point using GDL.

To study the ability of fibrils made using pea protein to form gels at low protein concentrations compared to conventional cold or heat induced gelation of pea protein¹⁰, gel formation in fibril solutions made using pea protein was initiated using glucono- δ -lactone (GDL), after fibrillar solution pH was adjusted to pH 7.0. During the adjustment of pH from pH 2.0 to pH 7.0, gelation of the fibrillar solutions did not occur although the samples became increasingly turbid at pH 5.

GDL was added to the samples at pH 7.0 to allow for slow acidification towards the isoelectric point of the sample (around pH 5). Changes in the storage modulus (G') and loss modulus (G'') were followed as a function of time after the addition of GDL (**Fig. 7 A and B**).

Gelation was assumed to have occurred when $\tan \delta$ of the solution was less than 1 ($G' > G''$)⁴².

In all gelation experiments G' values were higher than G'' at the beginning of all the measurements (**Fig. 7 A** and **B**), whereas $\tan \delta$ values were less than 1 at the end of all gelation experiments (**Table 2**). With increasing protein concentrations, G' values obtained after 15 h gelation increased. Increasing the protein concentration to 160 mg/mL resulted in an increase in the G' with a high G' (350 Pa) being observed even at time 0 h, although self-supportive gels (gels that are firm and can retain their shape without support) could not be formed by the fibrils even at protein concentrations as high as 160 mg/mL.

The inability of fibrils made using pea protein to form self-supportive gels even at relatively high protein concentrations may be related to the flexibility of the fibril rods as seen in **Fig. 6**. The flexibility of the fibril rods could have an influence on the ability to form stronger gels at higher protein concentrations. Furthermore, an increase in protein concentration at a low ionic strength could result in a high electrostatic interaction making it difficult to form cross-links between fibrils resulting in high percolation concentrations⁴³ that could influence the strength of the gels. Additionally, the analysis of steady-state birefringence by use of rheo-optic measurements as previously described⁴⁴ in fibrillar solutions made using pea protein did not show typical decay curves and no birefringence domains were observed (results not shown). This suggests that short and/or flexible aggregates are formed using pea proteins which do not easily form strong gels.

The final pH of the samples upon the addition of GDL in this study was \sim pH 5, which is close to the reported iso-electric point (IEP) of 4.8 for the legumin pea fraction but below the IEP of 5.5 for the vicillin fraction⁴⁵. The resultant gels at pH 5 were turbid due to the final pH being close to the IEP, as opposed to the transparent gels that were prepared from pea protein isolated using ammonium sulphate, at a more acidic pH using citric acid⁴⁵.

For comparison, gels were also prepared from fibrils made using soy protein and whey protein as indicated by the dashed lines in **Fig. 7 A** (G') and **7 B** (G''). Gels prepared from fibrils made using pea protein were comparable in strength to gels prepared from fibrils made using soy protein at the same protein concentration (**Fig. 7 A**). This may be attributed to similarities in flexibility of the rods. Pea protein-based fibrillar gels were however weaker than whey protein-based fibrillar gels as about 6 times more pea protein fibrils were needed to derive a comparable G' to whey protein-based fibrillar gels. The differences in gel strength between pea protein and whey protein may be attributed to the fact that fibrils made using whey protein may have the ability to form networks with higher efficiency compared to those made using pea protein, due to differences in the flexibility of the fibril rods.

To analyze the deformability of the gels prepared from fibrils made using pea protein, soy protein, and whey protein, an amplitude sweep was performed on protein-based fibrillar gels as a function of applied strain. Pea protein, soy protein, and whey protein-based fibrillar gels were all still within the linear region of % strain between 0.001 and 10, at a frequency of 1 Hz, following deformation as a function of applied strain (**Fig. 7 C** and **D**).

With an increase in oscillation strain above 10 %, pea protein-based fibrillar gels prepared at a lower protein concentration (40 mg/mL and 80 mg/mL) fractured earlier compared to pea protein-based fibrillar gels at a higher concentration (160 mg/mL), soy protein-based fibrillar gels (40 mg/mL), and whey protein-based fibrillar gels (25 mg/mL) (**Fig. 7 C**). The findings suggest that the fracture properties of pea protein-based fibrillar gels at a high concentration were comparable to soy protein and whey protein-based fibrillar gels, although pea protein and soy protein-based fibrillar gels were generally weaker compared to whey protein-based fibrillar gels.

Conclusions

In conclusion, it can be stated that fibril assembly using pea protein was successfully carried out at pH 2.0. Fibrils made using pea protein were more flexible, branched, and curly compared to fibrils made using whey protein, but comparable to fibrils made using soy protein. Fibrils made using pea protein were assembled into gels that had a comparable strength to soy protein-based fibrillar gels but were weaker than whey protein-based fibrillar gels. The findings show that the fibril formation mechanism in plant storage proteins seems to be generic as pea protein fibrils were comparable to soy protein fibrils. Thus, pea protein can effectively be used as a possible replacement for other globular proteins such as soy protein as a structural food ingredient in protein-based fibrillar gels. These findings contribute to the existing knowledge on fibril assembly in globular protein, and the information on the rheological behavior of protein fibrils enhances the understanding of rheological behavior of pea protein-based fibrillar gels.

Acknowledgements

The authors acknowledge help with transmission electron microscopy by Harry Baptist, Jolan de Groot for performing HPLC analyses, and the assistance with pea protein extraction by Eefjan Timmerman. Laurice Pouvreau is also appreciated for useful discussions.

References

- (1) Pimentel, D.; Pimentel, M., Sustainability of meat-based and plant-based diets and the environment. **Am. J. Clin. Nutr.** 2003, **78**, 660S-663S.
- (2) Johnson, E. A.; Brekke, C. J., Functional properties of acylated pea protein isolates. **J. Food Sci.** 1983, **48**, 722-725.
- (3) Gharsallaoui, A.; Saurel, R.; Chambin, O.; Voilley, A., Pea (*Pisum sativum*, L.) Protein Isolate Stabilized Emulsions: A Novel System for Microencapsulation of Lipophilic Ingredients by Spray Drying. **Food Bioprocess Technol.** 2012, **5**, 2211-2221.
- (4) Barac, M.; Cabrilo, S.; Pesic, M.; Stanojevic, S.; Zilic, S.; Macej, O.; Ristic, N., Profile and functional properties of seed proteins from six pea (*Pisum sativum*) genotypes. **Int. J. Mol. Sci.** 2010, **11**, 4973-4990.
- (5) Croy, R.; Gatehouse, J. A.; Tyler, M.; Boulter, D., The purification and characterization of a third storage protein (convicilin) from the seeds of pea (*Pisum sativum* L.). **Biochem. J** 1980, **191**, 509-516.
- (6) O’Kane, F. E.; Happe, R. P.; Vereijken, J. M.; Gruppen, H.; van Boekel, M. A. J. S., Characterization of Pea Vicilin. 1. Denoting Convicilin as the α -Subunit of the *Pisum* Vicilin Family. **J. Agric. Food Chem.** 2004, **52**, 3141-3148.
- (7) Nunes, M. C.; Raymundo, A.; Sousa, I., Rheological behaviour and microstructure of pea protein/kappa-carrageenan/starch gels with different setting conditions. **Food hydrocolloids.** 2006, **20**, 106-113.
- (8) Koyoro, H., **Functional Properties of Pea Globulins**. Washington State University: 1984.
- (9) Bacon, J. R.; Noel, T. R.; Wright, D. J., Studies on the thermal behaviour of pea (*Pisum sativum*) vicilin. **J. Sci. Food Agric.** 1989, **49**, 335-345.
- (10) Shand, P. J.; Ya, H.; Pietrasik, Z.; Wanasundara, P. K. J. P. D., Physicochemical and textural properties of heat-induced pea protein isolate gels. **Food Chem.** 2007, **102**, 1119-1130.
- (11) Tang, C.-H.; Wang, S.-S.; Huang, Q., Improvement of heat-induced fibril assembly of soy β -conglycinin (7S Globulins) at pH 2.0 through electrostatic screening. **Food Res. Int.** 2012, **46**, 229-236.
- (12) Kroes-Nijboer, A.; Sawalha, H.; Venema, P.; Bot, A.; Floter, E.; den Adel, R.; Bouwman, W. G.; van der Linden, E., Stability of aqueous food grade fibrillar systems against pH change. **Faraday Discuss.** 2012, **158**, 125-138.
- (13) Loveday, S. M.; Su, J.; Rao, M. A.; Anema, S. G.; Singh, H., Whey protein nanofibrils: Kinetic, rheological and morphological effects of group IA and IIA cations. **Int Dairy J.** 2012, **26**, 133-140.
- (14) Durand, D.; Gimel, J. C.; Nicolai, T., Aggregation, gelation and phase separation of heat de-

natured globular proteins. **Phys. A** 2002, **304**, 253-265.

(15) Kavanagh, G. M.; Clark, A. H.; Ross-Murphy, S. B., Heat-induced gelation of globular proteins: part 3. Molecular studies on low pH β -lactoglobulin gels. **Int. J. Biol. Macromol.** 2000, **28**, 41-50.

(16) Veerman, C.; de Schifart, G.; Sagis, L. M. C.; van der Linden, E., Irreversible self-assembly of ovalbumin into fibrils and the resulting network rheology. **Int. J. Biol. Macromol.** 2003, **33**, 121-127.

(17) Veerman, C.; Sagis, L. M. C.; Heck, J.; van der Linden, E., Mesostructure of fibrillar bovine serum albumin gels. **Int. J. Biol. Macromol.** 2003, **31**, 139-146.

(18) Bolder, S. G.; Hendrickx, H.; Sagis, L. M. C.; van der Linden, E., Fibril assemblies in aqueous whey protein mixtures. **J. Agric. Food. Chem.** 2006, **54**, 4229-4234.

(19) Tang, C.-H.; Zhang, Y.-H.; Wen, Q.-B.; Huang, Q., Formation of amyloid fibrils from kidney bean 7S globulin (Phaseolin) at pH 2.0. **J. Agric. Food. Chem.** 2010, **58**, 8061-8068.

(20) Liu, J.; Tang, C.-H., Heat-induced fibril assembly of vicilin at pH 2.0: Reaction kinetics, influence of ionic strength and protein concentration, and molecular mechanism. **Food Res. Int.** 2013, **51**, 621-632.

(21) Akkermans, C.; van der Goot, A. J.; Venema, P.; Gruppen, H.; Vereijken, J. M.; van der Linden, E.; Boom, R. M., Micrometer-sized fibrillar protein aggregates from soy glycinin and soy protein isolate. **J. Agric. Food. Chem.** 2007, **55**, 9877-9882.

(22) Tang, C.-H.; Wang, C.-S., Formation and characterization of amyloid-like fibrils from soy β -conglycinin and glycinin. **J. Agric. Food. Chem.** 2010, **58**, 11058-11066.

(23) Akkermans, C.; Venema, P.; van der Goot, A. J.; Gruppen, H.; Bakx, E. J.; Boom, R. M.; van der Linden, E., Peptides are building blocks of heat-induced fibrillar protein aggregates of β -lactoglobulin formed at pH 2. **Biomacromolecules** 2008, **9**, 1474-1479.

(24) Bolder, S. G.; Hendrickx, H.; Sagis, L. M. C.; van der Linden, E., Ca²⁺-induced cold-set gelation of whey protein isolate fibrils. **Appl. Rheol.** 2006, **16**, 258-264.

(25) Bolisetty, S.; Harnau, L.; Jung, J.-m.; Mezzenga, R., Gelation, phase behavior, and dynamics of β -lactoglobulin amyloid fibrils at varying concentrations and ionic strengths. **Biomacromolecules** 2012, **13**, 3241-3252.

(26) Munialo, C. D.; de Jongh, H. H. J.; Broersen, K.; Van Der Linden, E.; Martin, A. H., Modulation of the gelation efficiency of fibrillar and spherical aggregates by means of thiolation. **J. Agric. Food. Chem.** 2013, **61**, 11628-11635

(27) Holt, N. W.; Sosulski, F. W., Amino acid composition and protein quality of field peas. **Can. J. Plant Sci.** 1979, **59**, 653-660.

(28) Kusters, H. A.; Broersen, K.; de Groot, J.; Simons, J. W.; Wierenga, P.; de Jongh, H. H., Chemical processing as a tool to generate ovalbumin variants with changed stability. **Biotechnol. Bioeng.** 2003, **84**, 61-70.

- (29) Visser, S.; Slangen, C. J.; Rollema, H. S., Phenotyping of bovine milk proteins by reversed-phase high-performance liquid chromatography. **J. Chromatogr. A** 1991, **548**, 361-370.
- (30) Naiki, H.; Higuchi, K.; Hosokawa, M.; Takeda, T., Fluorometric determination of amyloid fibrils invitro using the fluorescent dye, thioflavine T. **Anal. Biochem.** 1989, **177**, 244-249.
- (31) Weijers, M.; Van De Velde, F.; Stijnman, A.; Van De Pijpekamp, A.; Visschers, R. W., Structure and rheological properties of acid-induced egg white protein gels. **Food Hydrocolloids** 2006, **20**, 146-159.
- (32) Akkermans, C.; van der Goot, A. J.; Venema, P.; van der Linden, E.; Boom, R. M., Formation of fibrillar whey protein aggregates: Influence of heat and shear treatment, and resulting rheology. **Food Hydrocolloids** 2008, **22**, 1315-1325.
- (33) Mishra, R.; Sörgjerd, K.; Nyström, S.; Nordigården, A.; Yu, Y.-C.; Hammarström, P., Lysozyme Amyloidogenesis Is Accelerated by Specific Nicking and Fragmentation but Decelerated by Intact Protein Binding and Conversion. **J. Mol. Biol.** 2007, **366**, 1029-1044.
- (34) Shammass, S. L.; Knowles, T. P. J.; Baldwin, A. J.; MacPhee, C. E.; Welland, M. E.; Dobson, C. M.; Devlin, G. L., Perturbation of the stability of amyloid fibrils through alteration of electrostatic interactions. **Biophys. J.** 2011, **100**, 2783-2791.
- (35) de Jongh, H. H. J.; Robles, C. L.; Timmerman, E.; Nordlee, J. A.; Lee, P.-W.; Baumert, J. L.; Hamilton, R. G.; Taylor, S. L.; Koppelman, S. J., Digestibility and IgE-Binding of Glycosylated Codfish Parvalbumin. **BioMed Res. Int.** 2013, **2013**, 10.
- (36) de Jongh, H. H. J.; Goormaghtigh, E.; Killian, J. A., Analysis of circular dichroism spectra of oriented protein-lipid complexes: Toward a general application. **Biochemistry** 1994, **33**, 14521-14528.
- (37) Purdie, N., Circular dichroism and the conformational analysis of biomolecules edited by Gerald D. Fasman (Brandeis University). Plenum Press: New York. 1996. x+ 738 pp. \$125.00. ISBN 0-306-45142-5. **J. Am. Chem. Soc.** 1996, **118**, 12871-12871.
- (38) Yang, J. T.; Wu, C.-S. C.; Martinez, H. M., Calculation of protein conformation from circular dichroism. In **Methods Enzymol.**, Academic Press: 1986; Vol. Volume 130, pp 208-269.
- (39) Loveday, S. M.; Su, J.; Rao, M. A.; Anema, S. G.; Singh, H., Whey protein nanofibrils: The environment-morphology-functionality relationship in lyophilization, rehydration, and seeding. **J. Agric. Food. Chem.** 2012, **60**, 5229-5236.
- (40) Bolder, S. G.; Sagis, L. M. C.; Venema, P.; van der Linden, E., Thioflavin T and birefringence assays to determine the conversion of proteins into fibrils. **Langmuir** 2007, **23**, 4144-4147.
- (41) Veerman, C.; Baptist, H.; Sagis, L. M. C.; van der Linden, E., A new multistep Ca²⁺-induced cold gelation process for β -lactoglobulin. **J. Agric. Food. Chem.** 2003, **51**, 3880-3885.
- (42) Ross-Murphy, S. B., Incipient behaviour of gelatin gels. **Rheol. Acta** 1991, **30**, 401-411.
- (43) Veerman, C.; Ruis, H.; Sagis, L. M. C.; van der Linden, E., Effect of Electrostatic Interactions

on the Percolation Concentration of Fibrillar β -Lactoglobulin Gels. **Biomacromolecules** 2002, **3**, 869-873.

(44) Rogers, S. S.; Venema, P.; van der Ploeg, J. P. M.; Sagis, L. M. C.; Donald, A. M.; van der Linden, E., Electric birefringence study of an amyloid fibril system: The short end of the length distribution. **Eur. Phys. J. E** 2005, **18**, 207-217.

(45) Bacon, J. R.; Noel, T. R.; Lambert, N., Preparation of transparent pea protein gels: a comparison of isolation procedures. **Int. J. Food Sci. Technol.** 1990, **25**, 527-537.

Chapter 4

The ability to store energy in pea protein gels is set by network dimensions smaller than fifty nanometers

In this chapter, various network structures were generated from pea proteins by varying the pH and salt conditions during gel formation. The coarseness of these network structures was visualized by the use of confocal laser scanning microscopy (CLSM) and scanning electron microscopy (SEM) and subsequently ranked from least coarse to most coarse networks. Mechanical deformation properties of the gels were measured by the use of a texture analyzer and correlated to the coarseness of the networks structure. The influence of coarseness on the networks ability to elastically store energy was observed for length scales below 50 nm. The findings show that elastically stored energy of pea protein gels can be modulated via the creation of different network structures that are below 50 nm length scales.

This chapter is published as:

Munialo, C.D.; van der Linden, E.; de Jongh, H. H. J. The ability to store energy in pea protein gels is set by network dimensions smaller than 50 nm. ***Food Research International*** 2014, 64, 482-491.

Introduction

In recent years plant storage proteins, such as pea proteins, have been shown to have a considerable potential to contribute to food supplies as a more sustainable, better accessible, and cheaper alternative to animal proteins¹. However, to make plant proteins more versatile as a food ingredient, an understanding of the relationship between the structure and functional properties, such as gelling behavior of these proteins is important².

Gel formation by proteins such as pea protein is of great importance in the generation of texture in food. Heat induced gelation of globular proteins is a multi-step process that requires thermally-induced (partial) unfolding of the native protein³. Partial unfolding of native proteins exposes interaction sites leading to intermolecular interactions, eventually resulting in clustering of aggregates to form a gel network³. At sufficiently high protein concentrations, self-supporting spatial gel networks can be formed, and large deformation and fracture behavior can be studied. Large deformation and fracture properties are important quality characteristics determining functional properties of gels such as handling and cutting⁴. Additionally, oral processing and sensory/mouthfeel perception of foods involves large deformation mechanics⁵.

In linear elastic fracture mechanics, all deformation energy applied to materials is initially stored and can be used to propagate fracture⁴. However, in many gels only part of the deformation energy supplied is stored elastically, whereas the other part is dissipated during deformation (primarily due to viscous flow or friction process between different components of the gels) or directed towards fracture⁶. The recoverable energy which represents the energy that is elastically stored during deformation is one of the main characteristics that defines the fracture mechanisms of gels by controlling the energy balance within the gel structure during deformation⁷. Recoverable energy has been shown to be correlated to sensory properties, such as crumbly effect of gels⁵.

Storage proteins of pea (*Pisum sativum* L.) have the potential of being used in the food industry for the formulation of new food products because of their high nutritive value and non-allergenic character⁸. Pea proteins were in the 1960's and 70's identified as a potential alternative to soy bean proteins. Pea proteins consist predominantly of legumin (11S), and vicilin (7S). Pea legumin is described as a hexamer of subunit pairs, each consisting of a basic subunit of ~20 kDa, and an acidic subunit of ~40 kDa⁹. Vicilin consists mainly of ~30 kDa, ~34 kDa, ~47 kDa, and ~50 kDa subunits¹⁰.

Studies on pea protein gelation and the effect of processing conditions on thermal and textural properties of heat-induced gels have been reported^{11, 12}. Shand and coworkers investigated the effect of pH and NaCl on commercial pea protein isolate gel formation¹¹, whereas Sun and Arntfield investigated these effects for salt extracted pea protein isolate¹².

However, an investigation into the effect of the combination of the pH and salt concentration on the large deformation properties and the elastically stored energy of pea protein has not been reported.

In most of the reports on pea protein gelation, the study of the microstructure of gels made at varying pH, and/or ionic strength was not included. Heating of pea proteins at varying pH and ionic strength can result in the formation of fine or coarse stranded networks. Fine-stranded gels are formed when electrostatic repulsion between the protein molecules is large such as at a pH away from isoelectric point (IEP) or at low ionic strength (**I**)¹³. The thicknesses of fine-stranded networks can be in the order of nanometer in size¹⁴. With decreasing intermolecular repulsion either by changing the pH of samples toward the isoelectric point (IEP), or by increasing the ionic strength, the gel networks become coarser, being composed of more particulate aggregates. The thickness of coarse stranded networks could be as large as micrometers¹⁴. Structural characterization of these networks should therefore be above the mentioned length scales.

To be able to classify network structures into fine or coarse stranded, and to determine the relationship between the network structures, mechanical deformation properties, and elastically stored energy of pea protein gels, various microstructures were generated in this study by varying the pH and ionic strength during pea protein gel formation. The objective of this study was to identify which length scales set the ability to elastically store energy (by means of recoverable energy) in pea protein network structures. An understanding of the ability of pea proteins to store energy is important as this can enable the food industry to better tailor products for consumers; given that the recoverable energy of food gels has been shown influence the sensorial properties of foods⁵.

Experimental

Materials

Predried dehulled commercial green pea seeds with a protein content of 22 g/100 g (dry weight basis) were purchased from a local supermarket. Dimethyl sulfoxide (DMSO), Rhodamine B, acetone, glutaraldehyde, NaOH pellets, HCl, NaCl, and CaCl₂ were all purchased from Sigma-Aldrich (Steinheim, Germany). Paraffin oil was purchased from Merck (Darmstadt, Germany). Omnifix® syringes were obtained from Braun (Melsungen, Germany). All materials were of analytical grade and used without further purification. All solutions were prepared with MilliQ water.

Pea protein extraction and characterization

Pea protein isolate was extracted from commercial green peas by isoelectric precipitation. Extraction of pea protein was based on a previously described procedure¹⁶, with slight modifications.

Milled pea flour with a protein content of 186 mg/mL ($N \times 6.25$), and a dry matter content of 86 ± 1.1 % was dispersed in 0.2 M NaCl solutions in the ratio of 1:10 (g/mL) to make a protein slurry instead of being dispersed in MilliQ water, and the pH of the slurry was not adjusted to pH 8 as previously described¹⁶. Additionally, following the washing steps, the supernatant (pea protein isolate) was collected, the final pH was adjusted to pH 7.0 using 2 M NaOH. The pea protein isolate was stored at 4 °C in the presence of 0.02 % sodium azide to prevent microbial growth. The pea protein isolate extracted in this way will be referred to as 'native' pea protein. The protein content of native pea protein was determined using Kjeldahl method with a protein factor of 6.25, and found to be about 115.5 ± 1.3 mg/mL. The dry matter content of native pea protein was 11.5 ± 1.2 %. Stock solutions of pea protein were prepared by concentrating native pea protein to a final 150 mg/mL by ultrafiltration using Merck Millipore Amicon stirred cell fitted with a 30 kDa MWCO membrane (Darmstadt, Germany).

Thermal denaturation of the proteins in pea flour and native pea protein solutions was evaluated by a TA Q100- Tzero™ differential scanning calorimetry (DSC) thermal analyzer (TA Instruments, New Castle, DE, USA). Aliquots of about 20 mg of the samples were added into aluminum sample pans, and the pans were hermetically sealed. A sealed empty pan was used as a reference. The samples in the pans were heated in the calorimeter from 20 to 120 °C at a heating rate of 2.5 °C/min. The on-set temperature of denaturation (T_m), peak denaturation temperature (T_d), and the enthalpy change of the major endotherm (ΔH), were deducted from the thermograms by a Universal Analysis 2000 software, Version 4.3A (TA Instruments-Waters LLC, New Castle, DE). All measurements were performed in duplicate. Protein aggregation was followed by measuring the turbidity of the samples over time. Changes in turbidity at 600 nm were recorded as a function of time for up to 60 min at a protein concentration of 2 mg/mL in a Cary 4000 UV-vis spectrophotometer (Varian, Nederland BV) equipped with a temperature controller. The measurements were carried out before and after heating of pea protein solutions (95 °C, 30 min), with and without the adjustment of the ionic strength of the protein solutions. The absorbance was measured using quartz cuvettes with a 10 mm path length. The turbidity was obtained by dividing the absorbance at 600 nm by the optical path length of 10 mm. Duplicate measurements were carried out for each sample.

Determination of the hydrodynamic diameter of pea protein aggregates was carried out using dynamic light scattering (DLS) (Zetasizer Nano ZS, Malvern Instruments, Worcestershire, UK). Changes in aggregate size for 2 mg/mL were recorded at 20 °C following heating of pea protein solutions (95 °C, 30 min), with and without the adjustment of the ionic strength. Reported values are the average hydrodynamic diameters of the largest intensity peak, as found in the distribution analysis using Malvern DTS 5.03 software. The particle size distribution from DLS was derived from a deconvolution of the measured intensity autocorrelation function of the samples using a non-negatively constrained least-squares (NNLS) general purpose fitting algorithm. Duplicate measurements were performed for this analysis.

Preparation of pea protein gels

The apparent ionic strength, as deduced from the conductivity measurements, showed that the stock solution of native pea protein, following the washing steps during protein extraction, had an ionic strength comparable to that of about 0.02 M NaCl. For all gelation experiments, where no additional salts were added to the samples, the salt concentration (ionic strength) will be referred to as 0 M salt. From preliminary experiments, the minimal concentration needed to obtain self-supporting gels was established to be about 140 – 150 mg/mL. A final protein content of 150 mg/mL was selected and kept constant for all subsequent gelation experiments. The pH of the stock solution at pH 7 was adjusted to pH 3, pH 5, and, pH 9 (± 0.05) using 2 M NaOH or HCl. For samples prepared at pH 7, the pH was not adjusted. The ionic strength was adjusted to 0.01 M CaCl_2 , 0.1 M CaCl_2 , and 0.3 M NaCl followed by degassing of the protein solutions. Degassed pea protein solutions were then poured into 20 mL Omnifix[®] syringes with an internal diameter of 19.7 mm, which were coated with paraffin oil, and closed at the bottom with sterile luer lock closures. The solutions were heated at 95 °C in a water bath for 30 min, followed by cooling at room temperature (20 ± 2 °C) overnight prior to testing. Each sample was prepared in triplicate.

Characterization of the microstructure

Visualization of the microstructure was performed using a Leica TCS SP confocal laser scanning microscope (CLSM) configured with an inverted microscope using an Ar/Kr laser for excitation in the fluorescence single-photon mode as previously described⁵. The gels were stained with 20 $\mu\text{L/mL}$ of sample aqueous solution of Rhodamine B (0.2 % w/w) which binds non-covalently to the protein network. The excitation was performed at 561 nm, and the emission of Rhodamine was recorded between 570, and 725 nm. Pictures were taken with a water-immersed 63 \times objective at a scan depth of 20 μm .

Gels for scanning electron microscopy (SEM) were prepared in cut pipette tips. After gelation, the gels in pipette tips were cross-linked in 1 % glutaraldehyde solution for 8 h. Subsequently, excess of glutaraldehyde was removed (after the crosslinking step) by placing the tips overnight into MilliQ water. The MilliQ water was replaced by 50 % dimethyl Sulfoxide (DMSO) in 3 steps - 10, 20, and 50 % DMSO in water solutions. The samples were subsequently slowly frozen in liquid nitrogen followed by peeling the tips away from the gels and the remaining gels being cut into slices. The slices from the middle of the gels were thawed in the 50 % DMSO in water solution. The DMSO was replaced with MilliQ water in several steps by gently pipetting away DMSO and replacing the volume of removed DMSO with MilliQ water, and subsequently the MilliQ water was replaced with acetone in a few stages. The samples in acetone were dried by critical point drying (CPD 030 Baltec, Liechtenstein) in which the acetone was replaced with liquid carbon dioxide under pressure in five steps to ensure complete replacement. The samples were glued onto a SEM sample holder using carbon glue (Leit-C, Neubauer Chemicalien, Germany), and subsequently stored overnight under vacuum.

After drying of the carbon cement, the samples were sputter coated with 10 nm iridium in SCD 500 (Leica EM VCT 100, Leica, Vienna, Austria) prior to imaging. All samples were analyzed with a field emission scanning electron microscope (Magellan XHR 400L FE-SEM, FEI, Eindhoven, the Netherlands) at room temperature at a working distance of 4 mm with SE detection at 2 kV. Images were digitally recorded.

Following imaging, the microstructure of samples was ranked from 1 to 16 based on CLSM and SEM micrographs in the order of the apparent coarseness of the network structure, where 1 is the least and 16 the most coarse network. The apparent coarseness was related to strand thickness of the network structures which was measured by use of the public domain ImageJ® software (National Institutes of Health, Bethesda, MD)¹⁷.

Rheological characterization

Uniaxial compression

To determine the fracture properties of pea protein gels, compression tests were performed on cylindrical gel samples (19.7 mm in diameter and 20 mm in height) compressed by a texture analyzer fitted with a 5 kg load cell and P/75 probe (TA.XTPlus, Stable Micro Systems, Surrey, UK). The fracture properties were studied by uniaxial compression test up to a 90 % deformation at a rate of 1 mm/s. The determined fracture properties included the true fracture stress (σ_f) and the true fracture (**Hencky**) strain (ϵ_H). The true fracture stress and true fracture strain will be designated as the fracture stress and fracture strain throughout this paper. The fracture stress and fracture strain were calculated at each point from time at zero to time of final deformation as follows:

$$\text{Fracture stress: } \sigma_f = \frac{F}{A_f} \times \left(\frac{L_i - \Delta L}{L_i} \right) \quad (1)$$

$$\text{Fracture strain: } \epsilon_H = \ln \left(\frac{L_i}{L_i - \Delta L} \right) \quad (2)$$

where F is the force measured during compression (N), A_i is the initial contact area of the specimen (m^2), L_i = initial specimen height (m), and ΔL is the absolute deformation (m)⁷. The Young's modulus was calculated from the slope of the linear region of the stress-strain curve as previously described⁷.

Recoverable energy

In a compression-decompression cycle, the recoverable work represents the stored (recoverable) energy¹⁸. The recoverable energy measurements were carried out on a cylindrically cut sample as described above. Compression and decompression of the specimen was then analyzed on the above described Texture Analyzer. Fifty percent of the maximum strain before fracture was applied to determine the energy release during relaxation at a deformation speed of 1 mm/s.

The percentage of recoverable energy of the gel was calculated from the area under the force-deformation curve as being the ratio of the amount of energy that was recovered after applying the stress over the amount of energy that was applied during the compression and decompression of the gels⁵.

Statistical evaluations

The averages, standard deviations, and the standard errors were all calculated using Microsoft Excel software (Microsoft Corporation, Redmond, USA) where applicable.

Results and discussion

To be able to identify which length scales set the ability to elastically store energy in pea protein gels, a range of network structures were prepared by varying the pH and salt conditions during gel formation. To have a better control of the purity and solubility of the pea protein as well as reproducibility of the results, pea proteins were isolated as previously described under section 2.2, and used in subsequent gelation experiments.

Table 1: The thermal transitions of pea proteins including the on-set temperature of denaturation (T_m), peak denaturation temperature (T_d), and the enthalpy change of the major endotherm (ΔH) at varying pH and ionic strength.

Pea proteins				
pH	NaCl (M)	T_m (°C) \pm stdev	T_d (°C) \pm stdev	ΔH (J/g) \pm stdev
3	0	n.d*	n.d*	n.d*
	0.3	n.d*	n.d*	n.d*
5	0	78.8 \pm 1.0	88.5 \pm 0.5	1.88 \pm 0.5
	0.3	82.2 \pm 2.0	91.6 \pm 0.1	3.90 \pm 0.3
7	0	74.3 \pm 2.1	84.9 \pm 1.6	9.43 \pm 0.8
	0.3	80.2 \pm 1.1	90.5 \pm 1.0	6.64 \pm 0.1
9	0	73.5 \pm 0.1	83.6 \pm 1.1	4.90 \pm 0.5
	0.3	78.5 \pm 1.2	89.4 \pm 1.5	5.98 \pm 0.6

Where n.d* is not detected

Characterization of pea proteins

The results of calorimetric analysis of pea proteins by DSC at varying pH and ionic strength are shown in **Table 1**. All the pea protein samples show a single endothermic peak, in contrast Shand and coworkers, who found an additional peak at around 67 °C, caused by presence of non-globulin fraction components 11.

The presence of only one endothermic peak illustrates that the isolated pea protein used here lacks contaminants such as fibers or starch.

The observed single endothermic transitions were assumed to represent denaturation of both vicilins and legumins as these proteins denature at the same point¹⁹

The T_d of native pea protein at pH 7 was about 84.9 ± 1.6 °C, the ΔH was 9.4 ± 2.8 J/g protein, and the T_m was 74.3 ± 2.1 °C. The observed T_d from the endothermic peak obtained at pH 7 was comparable to that of the peak observed by Shand and coworkers for laboratory prepared pea protein¹¹ and in the same range as the previously found value of 86.2 °C for salt-extracted pea protein isolate¹². No distinct endothermic peaks were observed at pH 3, 0 M salt and pH 3, 0.3 M NaCl. A lack of an endothermic peak for pea proteins at pH 3 is suggested to be related to the dissociation of the protein at this pH²⁰.

The highest T_d of 88.5 °C was found at pH 5. As the pH increased to pH 7, the T_d decreased to about 85 °C, whereas at pH 9, the T_d was 83.6 °C. With the addition of 0.3 M NaCl, an increase in T_d was observed (**Table 1**). The increase in T_d may be a result of stabilization of the proteins' native, quaternary structure, by reducing intramolecular repulsion^{12, 21, 22}. Similar effects of salts on T_d were found by Shand and co-workers (Shand, Ya, Pietrasik, & Wanasundara, 2007). The DSC results show that native pea protein used here can thermally denature at varying pH ranges (pH 3 to pH 9) and ionic strength.

To study aggregation behavior of pea proteins, the changes in turbidity were monitored over time following heating of the proteins at various pH and ionic strength. We only discuss the changes in aggregate size results for 0 M salt (without salt), and the addition of NaCl to the protein solutions as CaCl_2 results showed a similar trend. Changes in turbidity (**Fig. 1**) were related to an increase in aggregate size in heated samples compared to unheated samples, with the highest turbidity being recorded for both unheated and heated samples at pH 5, 0 M salt (**Fig. 1 A**). The observed high turbidity values at pH 5 indicate the formation of larger aggregates as a result of aggregation close to the IEP. At a pH away from IEP (pH 3, pH 7, and pH 9), the aggregate sizes were smaller than those at pH 5 with the aggregates at pH 3 being the smallest as observed from the lowest turbidity values (**Fig. 1 A**). The low turbidity at pH 3 and pH 9 could be attributed to dissociation of legumin²¹. The dissociation of pea protein at pH 3 was also confirmed by the lack of distinct endothermic peak from calorimetric analysis as seen in **Table 1**. Following the addition of 4 mM NaCl to 2 mg/mL pea protein solutions (equivalent to 0.3 M NaCl in 150 mg/mL pea protein solutions), no significant changes in turbidity were observed for both heated and unheated pea protein solutions (**Fig. 1 B**).

Variations in aggregate sizes as determined by DLS measurements were observed in 2 mg/mL of unheated pea proteins (**Fig. 2**). The average aggregate sizes varied from about 122-190 nm for pea protein samples at different pH (**Fig. 2 A**).

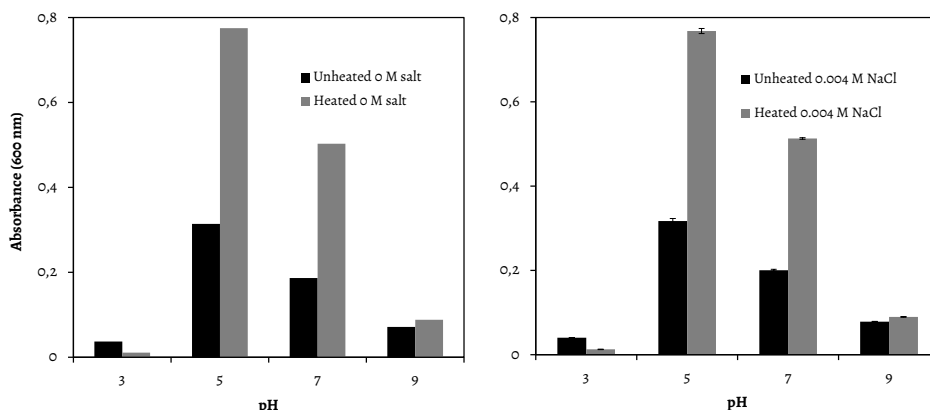


Figure 1: Changes in turbidity of 2 mg/mL of unheated and heated pea protein samples in the absence (**Fig. 1 A**), and in the presence of salt (**Fig. 1 B**). Reported values are the average absorbance values after 60 min measuring time. In the case of heated samples, pea proteins solutions in the presence and absence of NaCl were heated at 95 °C for 30 min before the measurements were carried out.

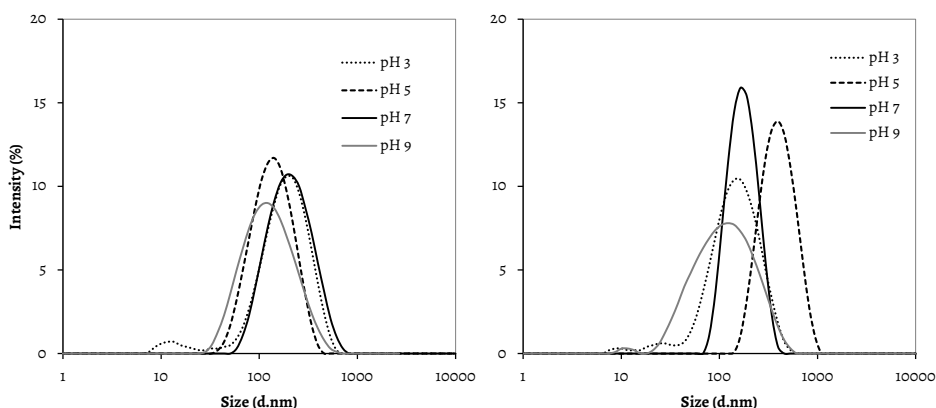


Figure 2: Changes in aggregate size for 2 mg/mL of unheated (**Fig. 2 A**) and heated (**Fig. 2 B**) pea proteins solutions. This measurement was carried out to study the effect of the pH, ionic strength, and heating, on pea proteins aggregate sizes.

Upon heating of the samples, a shift in aggregate size distribution towards much higher sizes was observed at pH 5 (**Fig. 2 B**) as there was more than 2 fold increase in aggregate size upon heating, which coincided with higher turbidity values at this pH (see **Fig. 1**).

At pH 3, a major aggregate size peak was observed at around 190 nm. Upon heating of the samples at pH 3, the aggregate size decreased from about 190 nm to about 140 nm.

Table 2: The conditions (pH and ionic strength) under which gels were formed from pea proteins. Following visualization of the microstructure by use of CLSM and SEM, the network structures were ranked according to their coarseness from number 1 to 16, where number 1 is the least coarse and 16 the most coarse network structure. The coarseness was measured by the use of ImageJ and is given as a range due to heterogeneity in the thickness of the strands that were obtained under the varying pH and ionic strength conditions. The coarseness was related to large deformation properties and energy storage of pea protein gels as shown in Table 3.

pH	NaCl (M)	CaCl ₂ (M)	CLSM rank	SEM rank	Coarseness range (nm)
3	0	-	1	2	20 - 40
3	-	0.01	2	1	15 - 20
7	0	-	3	11	60 - 100
9	-	0.01	4	4	28 - 60
9	0.3	-	5	9	60 - 77
9	0	-	6	7	41 - 55
7	0.3	-	7	6	39-50
7	-	0.01	8	5	30-40
3	-	0.1	9	3	23 - 46
3	0.3	-	10	12	n.d**
5	0	-	11	13	110 - 250
7	-	0.1	12	10	n.d**
9	-	0.1	13	16	500 - 1000
5	-	0.1	14	8	50-60
5	0.3	-	15	15	470 - 650
5	-	0.01	16	14	400 - 620

Where n.d** is not determined. For networks ranked number 10 and 12 strands could not be clearly distinguished and hence the thickness of the strands was not measured.

The decrease in aggregate size could be an indication of further disassociation of the protein resulting in smaller protein forms also confirmed by lower turbidity values (**Fig. 1**) and the lack of distinct endothermic peaks at this pH (**Table 1**). Although no remarkable changes were observed in aggregate size at pH 9, the aggregate size distribution broadened following heating of the samples. For pH 7, a decrease in aggregate size was observed similar to pH 3, although the decrease in aggregate size was less pronounced.

Table 3: Fracture stress, fracture strain, Young's moduli, and recoverable energy for 16 pea protein gels ranked according to coarseness obtained from CLSM and SEM micrographs at varying pH and ionic strength (I). Mean values (5-6 samples) and standard deviations are given.

CLSM rank	SEM rank	pH and I	Fracture stress, σ_f (kPa)	Fracture strain, ϵ_f (-)	Young's modulus (kPa)	Recoverable energy (%)
1	2	3, 0 M	2.89 \pm 0.33	0.45 \pm 0.01	4.83 \pm 0.63	65 \pm 1.95
2	1	3, 0.01 M CaCl ₂	14.10 \pm 0.82	0.31 \pm 0.03	48.80 \pm 0.89	86 \pm 1.14
3	11	7, 0 M	1.03 \pm 0.21	1.11 \pm 0.06	7.70 \pm 0.42	34 \pm 5.89
4	4	9, 0.01 M CaCl ₂	syneresis	syneresis	syneresis	syneresis
5	9	9, 0.3 M	syneresis	syneresis	syneresis	syneresis
6	7	9, 0 M	syneresis	syneresis	syneresis	syneresis
7	6	7, 0.3 M	syneresis	syneresis	syneresis	syneresis
8	5	7, 0.01 M CaCl ₂	1.96 \pm 0.15	0.41 \pm 0.02	4.72 \pm 0.58	40 \pm 5.19
9	3	3, 0.1 M CaCl ₂	6.01 \pm 0.08	0.31 \pm 0.01	18.44 \pm 1.04	58 \pm 0.78
10	12	3, 0.3 M	5.23 \pm 0.26	0.17 \pm 0.01	25.14 \pm 2.88	48 \pm 3.39
11	13	5, 0 M	2.78 \pm 0.75	0.35 \pm 0.03	8.81 \pm 2.47	36 \pm 2.56
12	10	7, 0.1 M CaCl ₂	4.01 \pm 0.59	0.43 \pm 0.03	8.45 \pm 1.36	38 \pm 1.10
13	16	9, 0.1 M CaCl ₂	1.68 \pm 0.14	0.30 \pm 0.01	5.62 \pm 0.51	38 \pm 1.20
14	8	5, 0.1 M CaCl ₂	2.54 \pm 0.11	0.20 \pm 0.01	13.18 \pm 0.45	35 \pm 0.78
15	15	5, 0.3 M	3.53 \pm 0.66	0.33 \pm 0.04	10.56 \pm 1.43	48 \pm 2.73
16	14	5, 0.01 M CaCl ₂	1.86 \pm 0.24	0.28 \pm 0.05	6.92 \pm 2.04	35 \pm 0.10

Differences in aggregate sizes in pea proteins at varying pH and ionic strength gives the indication of formation of protein aggregates with differences in sizes that are the building blocks for pea proteins network structure formation.

Gel microstructure

Following heating of 150 mg/mL pea protein solutions at varying pH and ionic strength (95 °C, 30 min), self-supporting gels were formed although syneresis was observed at pH 9 (0 M salt, 0.3 M NaCl, and 0.01 M CaCl_2), and at pH 7, 0.3 M NaCl (**Table 3**). The microstructure of these gels was visualized using CLSM and SEM, and subsequently, the network structures were ranked based on apparent coarseness as shown in **Table 2**. Visually, transparent gels were obtained at lower coarseness ranking whereas turbid (opaque) gels were obtained at higher coarseness ranking.

Confocal laser scanning microscopy (CLSM)

CLSM was used to obtain structural information of pea protein gels within the sub-micron range. Confocal laser scanning micrographs (**Fig. 3**) (scale bar of 250 μm) were obtained from pea protein gels at different pH and ionic strength.

The protein networks are depicted as bright areas whereas the serum phase is depicted by the dark areas. Different gel microstructures observed at various conditions were ranked based on apparent coarseness, defined as inhomogeneity of gel networks as related to the interplay between the network and the enclosed serum phase. At lower ranks, least coarse network structures were observed whereas at higher ranks more coarse networks were observed (ranking is shown in **Table 2**). For least coarse networks (number 1), the inhomogeneity of the samples could be characterized as being below 0.5 μm , whereas at the most coarse evaluated samples (number 16), the inhomogeneity could be characterized at about 100 - 300 μm (measured using ImageJ software, Results not shown). The network structures ranked as number 1 (obtained at pH 3, 0 M salt) were < 0.5 μm which is outside the resolution range of CLSM (< 1 μm) and thus they could not be clearly distinguished by this technique. At relatively high salt concentrations (such as 0.3 M NaCl and 0.1 M CaCl_2), and pH values closer to the IEP (pH 5), coarser network structures were observed (**Table 2**). Least coarse network structures were composed of smaller aggregates sizes whereas coarser networks were composed of larger aggregates sizes as observed from turbidity and aggregate size measurement results (**Figs. 1 and 2**). Evaluating **Table 2** shows that gels prepared close to IEP appear most coarse as expected. Away from IEP one can observe that different salt concentrations and pH provide a wide scope of coarseness.

Scanning electron microscopy (SEM)

To obtain more detailed information on the network structure, SEM was used allowing structural information to be obtained within the nm range.

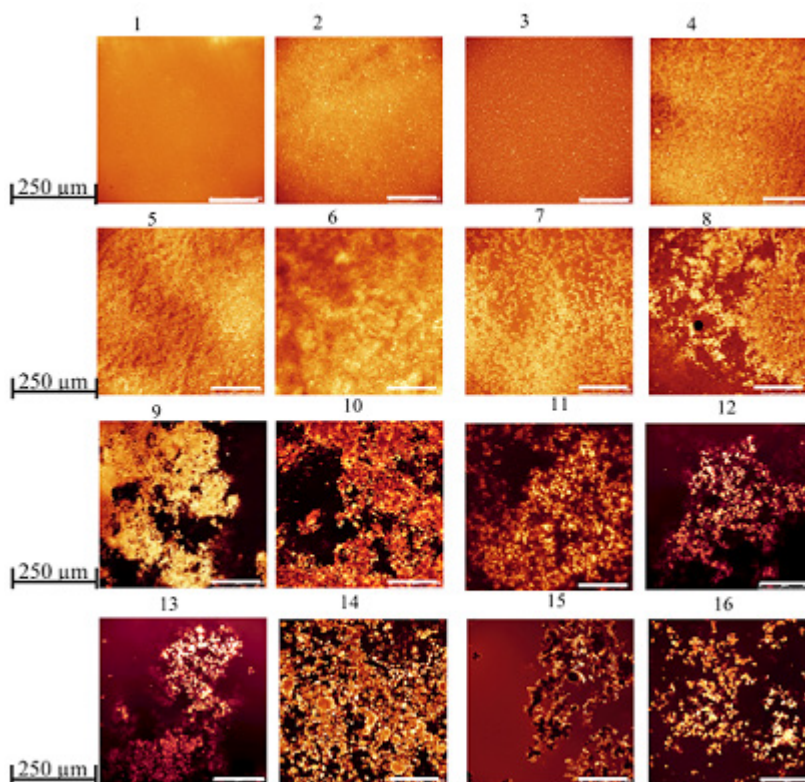


Figure 3: Confocal laser scanning micrographs showing the differences in the microstructure of pea protein gels. The micrographs were arranged based on coarseness from 1 (finest microstructure) to 16 (coarsest microstructure). The scale bars indicate 250 μm . The conditions (pH and ionic strength) at which the gels were formed are shown in **Table 2**.

Scanning electron micrographs (scale bars 500 nm) were obtained from pea protein gels (**Fig. 4**) and ranked based (**Table 2**) on the apparent coarseness defined as the inhomogeneity of gel networks as related to the thickness of strands that span the networks. At a pH away from IEP (pH 3) and at a low ionic strength (0 M), least coarse network structures (coarseness rank number 1) were observed.

From **Fig. 4**, it can be observed that the coarseness increases with an increase in smallest filament thickness which typically ranges from least coarse networks with filament sizes in the order of about 15 - 20 nm (coarseness rank number 1), to the most coarse networks which show filaments with thickness in the order of about 500 - 1000 nm (coarseness rank number 16) as measured by the use of ImageJ software (**Table 2**). The networks ranked number 1 can be described as being highly branched, linear, long, and 'fibrillar-like', whereas network structures ranked as number 2 are denser and composed of small spherical aggregates connected with thread-like strands with a short distance between the junctions.

Least coarse network structures were composed of smaller aggregates sizes (see **Figs. 1** and **2**). At higher ionic strength and at pH closer to IEP, more coarse network structures with non-specific branching were observed with higher coarseness ranks composed of larger aggregates sizes (see **Figs. 1** and **2**). Evaluating **Table 2**, it can observe that gels prepared at higher (0.1 M) CaCl_2 concentration were the coarsest with the exception of pH 5, 0.01 M CaCl_2 . The formation of more coarse structures at higher CaCl_2 concentration can be related to excessive bridging between calcium and the negatively charged groups present on adjacent unfolded protein molecules, resulting in the aggregation of the proteins, leading to the collapse of the protein matrix and formation of large dense non continuous aggregates²³.

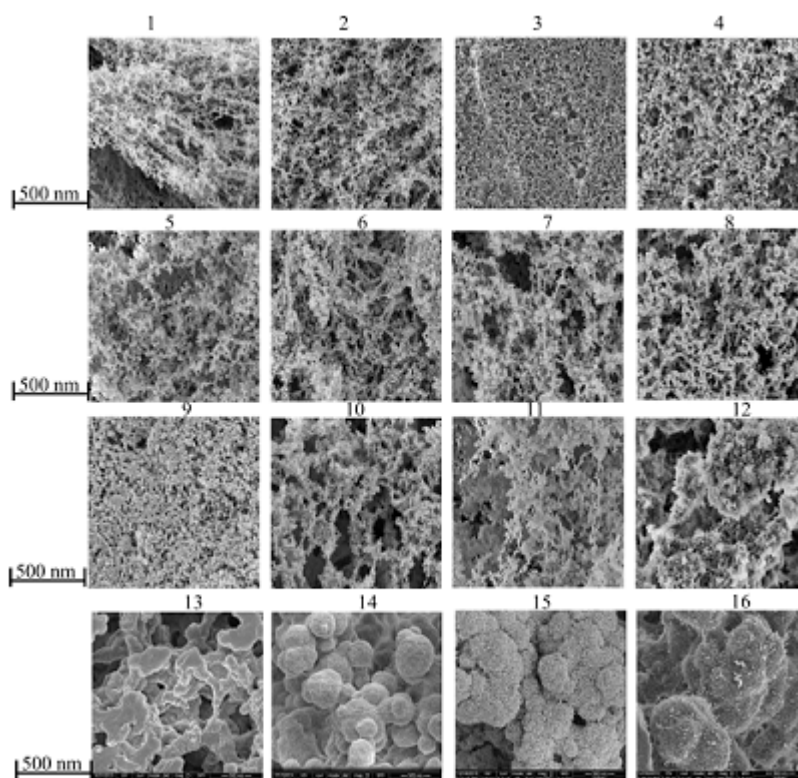


Figure 4: Scanning electron micrographs showing the differences in the microstructure of pea protein gels. The micrographs were arranged based on coarseness from 1 (finest microstructure) to 16 (coarsest microstructure). The scale bars indicate 500 nm. The conditions (pH and ionic strength) at which the gels were formed are shown in **Table 2**.

Large deformation properties of pea protein gels

To better pinpoint the structural basis of storing energy in networks, it is relevant to define the large deformation properties of gels such as the fracture stress, fracture strain, and Young's moduli. **Table 3** presents these properties for pea protein gels obtained under varying pH and salt conditions.

Fracture stress gives an indication of gel strength ²⁴. Network structure and coarseness can have an effect on the fracture stress of the gels. Coarser gels may have lower fracture stress due to larger defects in the gels²⁵. The fracture stress was highest for least coarse gels prepared at pH away from IEP and at low ionic strength (CLSM coarseness rank number 2 and SEM coarseness rank number 1). Coarsest network structures prepared at pH close to IEP (CLSM coarseness rank number 16 and SEM coarseness rank number 14) had lower fracture stress (**Table 3** and **Fig. 5 A** and **6 A**).

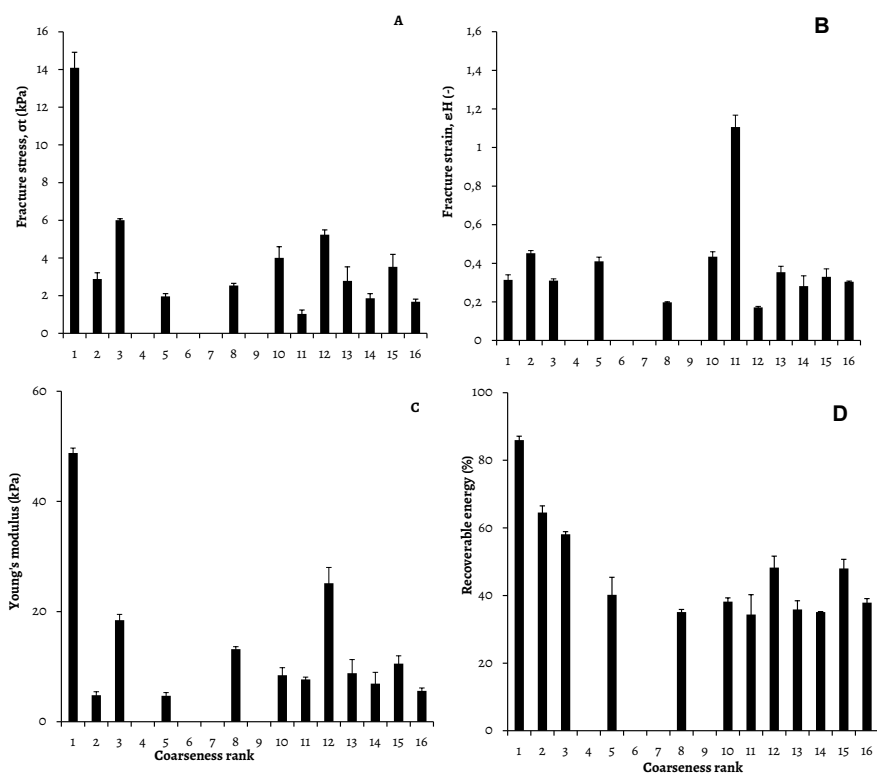


Figure 5: Fracture stress (A), fracture strain (B), Young's modulus (C), and recoverable energy (D) related to the coarseness of pea protein gels ranked from 1 (least coarse) to 16 (most coarse) based on scanning electron micrographs. The 4 gels that showed syneresis are excluded.

Lower fracture stress observed in coarsest network structures could be related to differences in the connectivity of the network structures. When the gel network shifts from least coarse to coarser, the network structures become less dense (**Figs. 3 and 4**). Less dense β -lactoglobulin have been reported to have lower fracture stress²⁶. Particulate whey protein isolate gels were also reported to show discontinuous crack propagation during tensile fracture as visualized by CLSM²⁷. Additionally, the porous nature of coarser pea protein network structures could cause a step-wise crack growth due to micro-scale inhomogeneities between protein clusters in the form of pores, flaws, cracks, or weak regions resulting in lower fracture stress. From **Fig. 5 A**, where fracture stress is plotted as a function of coarseness based on SEM micrographs, and **Fig. 6 A** where fracture stress is plotted as a function of coarseness based on CLSM micrographs, it follows that there is no correlation between coarseness and fracture stress except for rank number 1 and 2 networks structures that show higher stress values. Fracture strain gives an indication of the brittleness of gels²⁴.

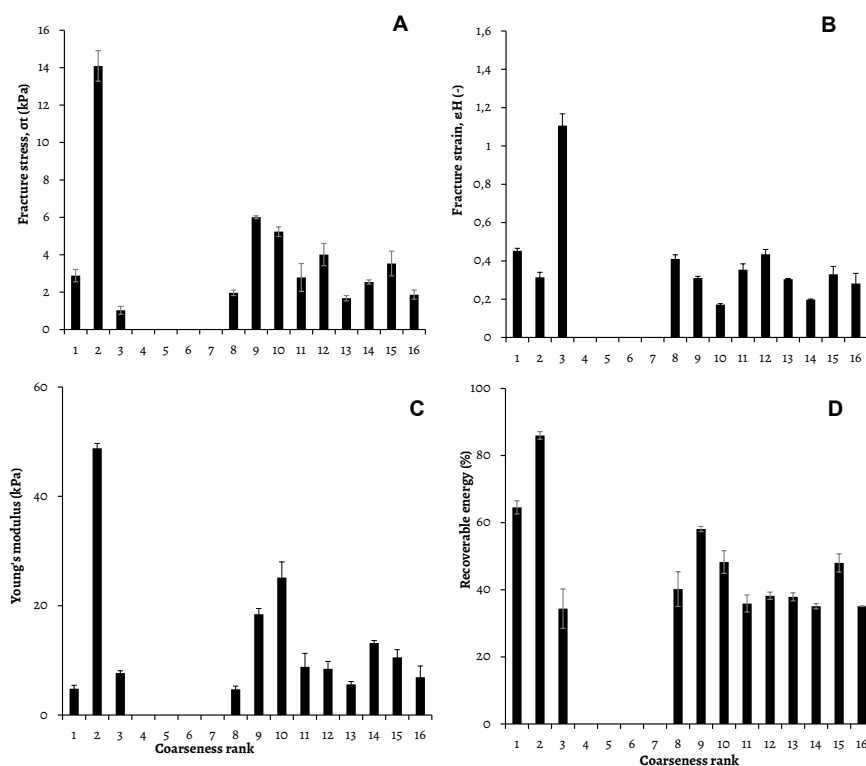


Figure 6: Fracture stress (A), fracture strain (B), Young's modulus (C), and recoverable energy (D) related to the coarseness of pea protein gels ranked from 1 (least coarse) to 16 (most coarse) based on confocal laser scanning electron micrographs. The 4 gels that showed syneresis are excluded.

From the fracture strain results (**Table 3**), coarse stranded network structures (SEM rank number 11) had the highest fracture strain, an indication that the gels were rubber-like. Network structure ranked number 10 (based on CSLM) and 12 (based on SEM) had the lowest fracture strain, an indication that the gels were brittle. The fracture strain of pea protein gels was studied in relation to the coarseness of network structures based on SEM (**Fig. 5 B**) and CLSM micrographs (**Fig. 6 B**). From the results in these figures, it follows that there was no unequivocal relation between coarseness and fracture strain of pea protein gels. The almost similar fracture strains suggest that the gel networks are equally brittle with the exception of sample number 11 (based on SEM ranking) and 3 (based on CLSM ranking) which show higher fracture strains (rubber-like behavior).

Young's (elasticity) modulus, which is the measure of the stiffness of a material⁷ was determined as listed in **Table 3** and plotted as a function of coarseness based on SEM (**Fig. 5 C**) and CLSM (**Fig. 6 C**) micrographs. The apparent Young's modulus was measured at a single compression rate and hence is not considered an absolute material property for pea protein gels. Pea protein gels with seemingly lowest coarseness (rank number 1 based on SEM and 2 based on CLSM) showed highest stiffness (**Table 3**). With increasing coarseness, the stiffness of gels decreased, although an increase in stiffness was observed at coarseness ranked as number 8 and 12 based on SEM coarseness ranking (**Fig. 5 C**), and coarseness ranked as number 9 and 10 based on CLSM (**Fig. 6 C**). The high Young's modulus for coarseness rank number 12 (based on SEM micrographs) could be related to higher ionic strength due to addition of relatively high salt (0.3 M NaCl) concentration to the samples (**Table 2**), as the moduli of gels have been reported to increase on the addition of salt⁴. Higher Young's modulus for coarseness rank number 12 could also be related to the thickness of the strands as coarser networks (thicker strands) are difficult to bend than thin strands as the bending load of a cylinder scales with the diameter²⁸.

At higher coarseness ranks, the Young's modulus was shown reach to a kind of an optimum. A gradual decrease followed by an increase and then a subsequent decrease in Young modulus as the coarseness increased as seen in **Fig. 5 C** suggest that there may be an additional contribution which sets the Young's moduli of protein gels at larger length scales. From the study of the elasticity of pea protein gels, it follows that there was also no unequivocal relation between coarseness of the network structure of pea protein gels and the stiffness of the gels. A lack of correlation between coarseness of network structure and Young's moduli has also been reported in soy protein gels²⁹.

Elastically stored energy of pea protein gels in relation to network structure

The recoverable energy of the protein gels was determined as listed in **Table 3** and plotted as a function of coarseness based on SEM (**Fig. 5 D**) and CLSM (**Fig. 6 D**). At low ionic strength and at a pH away from the IEP, network structures with the least turbidity values (**Fig. 1**), smaller aggregate size (**Fig. 2**), and least coarseness (**Figs. 3 and 4**), were formed. These network structures showed a higher ability to elastically store energy compared to coarser networks formed at high ionic strength or at a pH close to IEP of pea protein.

The lower recoverable (stored) energy in coarser networks may be related to coarse networks having a less dense structure with large pore sizes (**Figs. 3 and 4**). The higher recoverable energy in least coarse (fine-stranded) networks shows that the gels are more elastic than coarse networks. Elasticity in gels is higher, when more water is held inside the gel network. Least coarse (fine-stranded) gels are known to hold more water than coarser gels ⁷. From visual observations, less dense structures showed higher water (serum) release/flow during compression which could result in higher energy being lost via dissipation, thus lower recoverable energy in coarser networks.

From the correlation of coarseness and the recoverable energy, least coarse networks were shown to have a higher sensitivity to recoverable energy based on SEM correlations (**Fig. 5 D**). For coarser networks, there was no specific impact on the recoverable energy as the recoverable energy was almost the same with the exception of network structures ranked 12 and 15 (based on SEM). There was a much more clear tendency that recoverable energy is detected by filament thickness (based on SEM ranking) but only up to the length scales of coarseness ranks between 5 and 8 which correlates to typical filament thickness in the order of about 30 - 40 nm (rank number 5) and about 50 - 60 nm (rank number 8) as measured by the use of ImageJ software (**Table 2**). This suggests that smaller strands contribute to the ability of the networks to store energy. There was no correlation between coarseness ranked on inhomogeneities of the gel networks as related to the interplay between the network and the enclosed serum phase and the recoverable energy (**Fig. 6 D**). A higher sensitivity to recoverable energy at CLSM level was observed only for finest structures (samples ranked lowest in coarseness). From the CLSM results, it follows that below the resolution range of the microscope, differentiation in recoverable energy based on coarseness matters. Correlation between recoverable energy and coarseness based on SEM shows that recoverable energy of pea protein gels is reflected at nanometer length scales of network structure as opposed to a micron length scale.

Conclusions

A broad variety of network structures with different coarseness were created from pea proteins by varying the pH, ionic strength, and ionic species. Network structures showed a correlation between coarseness and the recoverable energy at typical nanometer length scales (reflected at SEM level) as opposed to micron length scales (reflected at CLSM level). The ability of the network structures elastically store energy was higher in least coarse than more coarse network. The results show that (i) the ability to store energy in pea protein gels is set by length scales below 50 nm and that (ii) to be able to link the storing of energy to the microstructure of pea protein networks structures based on CLSM, additional characterization of the networks structures is important as relying on the coarseness alone may not be adequate, given that the length scales that matter for storing of energy are below CLSM detection limits. This study provides an understanding of the parameters that are necessary in the setting and modulation of the storing of energy in pea protein networks.

An understanding of the parameters that set the ability of pea protein gels to store energy offers possibilities to optimize the quality of pea protein gels and to fine tune the gel characteristics to the demands of the food industry.

Acknowledgements

Maike Nieuwland and Tiny Franssen-Verheijen are appreciated for the help with SEM sample preparation and analysis. Claudia Choi is acknowledged for her contributions towards the large deformation measurements. Anneke Martin is appreciated for meaningful discussions and Eefjan Timmerman for the help with pea protein extraction.

References

- (1) Pimentel, D.; Pimentel, M., Sustainability of meat-based and plant-based diets and the environment. **Am. J. Clin. Nutr.** 2003, **78**, 660S-663S.
- (2) Subirade, M.; Gueguen, J.; Pézolet, M., Conformational changes upon dissociation of a globular protein from pea: a Fourier transform infrared spectroscopy study. **Biochim. Biophys. Acta** 1994, **1205**, 239-247.
- (3) Clark, A. H.; Kavanagh, G. M.; Ross-Murphy, S. B., Globular protein gelation—theory and experiment. **Food Hydrocolloid** 2001, **15**, 383-400.
- (4) van Vliet, T., Large deformation and fracture behaviour of gels. **Curr. Opin. Colloid Interface Sci.** 1996, **1**, 740-745.
- (5) van den Berg, L.; Carolas, A. L.; van Vliet, T.; van der Linden, E.; van Boekel, M. A. J. S.; van de Velde, F., Energy storage controls crumbly perception in whey proteins/polysaccharide mixed gels. **Food Hydrocolloid** 2008, **22**, 1404-1417.
- (6) van Vliet, T.; Luyten, H.; Walstra, P., **Fracture and yielding of gels**. 1991; p 392-403.
- (7) Çakir, E.; Daubert, C. R.; Drake, M. A.; Vinyard, C. J.; Essick, G.; Foegeding, E. A., The effect of microstructure on the sensory perception and textural characteristics of whey protein/κ-carrageenan mixed gels. **Food Hydrocolloid** 2012, **26**, 33-43.
- (8) Gharsallaoui, A.; Saurel, R.; Chambin, O.; Voilley, A., Pea (*Pisum sativum*, L.) Protein isolate stabilized emulsions: A novel system for microencapsulation of lipophilic ingredients by spray drying. **Food Bioprocess Technol.** 2012, **5**, 2211-2221.
- (9) Barac, M.; Cabrilo, S.; Pesic, M.; Stanojevic, S.; Zilic, S.; Macej, O.; Ristic, N., Profile and functional properties of seed proteins from six pea (*Pisum sativum*) genotypes. **Int. J. Mol. Sci.** 2010, **11**, 4973-4990.
- (10) Croy, R.; Gatehouse, J. A.; Tyler, M.; Boulter, D., The purification and characterization of a third storage protein (convicilin) from the seeds of pea (*Pisum sativum* L.). **Biochem. J.** 1980, **191**, 509-516.
- (11) Shand, P. J.; Ya, H.; Pietrasik, Z.; Wanasundara, P. K. J. P. D., Physicochemical and textural properties of heat-induced pea protein isolate gels. **Food Chem.** 2007, **102**, 1119-1130.
- (12) Sun, X. D.; Arntfield, S. D., Gelation properties of salt-extracted pea protein induced by heat treatment. **Food Res. Int.** 2010, **43**, 509-515.
- (13) Langton, M.; Hermansson, A. M., Fine-stranded and particulate gels of beta-lactoglobulin and whey protein at varying pH. **Food Hydrocolloid** 1992, **5**, 523-539.
- (14) Clark, A. H.; Judge, F. J.; Richards, J. B.; Stubbs, J. M.; Suggett, A., Electron microscopy of network structures in thermally-induced globular protein gels. **Int. J. Pept. Protein Res.** 1981, **17**, 380-

392.

- (15) Ikeda, S.; Morris, V. J., Fine-stranded and particulate aggregates of heat-denatured whey proteins visualized by atomic force microscopy. **Biomacromolecules** 2002, **3**, 382-389.
- (16) Munialo, C. D.; Martin, A. H.; van der Linden, E.; de Jongh, H. H. J., Fibril formation from pea protein and subsequent gel formation. **J. Agric. Food Chem.** 2014, **62**, 2418-2427.
- (17) Rasband, W. 2009. ImageJ, U.S National Institutes of Health, Bethesda, Maryland, USA. <http://rsb.info.nih.gov/ij/>
- (18) Nussinovitch, A.; Kaletunc, G.; Normand, M. D.; Peleg, M., Recoverable work versus asymptotic relaxation modulus in agar, carrageenan and gellan gels. **J. Texture Stud.** 1990, **21**, 427-438.
- (19) O'Kane, F. E.; Happe, R. P.; Vereijken, J. M.; Gruppen, H.; van Boekel, M. A. J. S., Characterization of pea vicilin. 2. Consequences of compositional heterogeneity on heat-induced gelation behavior. **J. Agric. Food Chem.** 2004, **52**, 3149-3154.
- (20) Arntfield, S. D.; Murray, E. D., The Influence of processing parameters on food protein functionality I. Differential scanning calorimetry as an indicator of protein denaturation. **Can. Inst. Food Sci. Technol. J.** 1981, **14**, 289-294.
- (21) Gueguen, J.; Chevalier, M.; And, J. B.; Schaeffer, F., Dissociation and aggregation of pea legumin induced by pH and ionic strength. **J. Sci. Food Agric.** 1988, **44**, 167-182.
- (22) Chronakis, I. S., Network formation and viscoelastic properties of commercial soy protein dispersions: effect of heat treatment, pH and calcium ions. **Food Res. Int.** 1996, **29**, 123-134.
- (23) Mulvihill, D. M.; Kinsella, J. E., Gelation of β -lactoglobulin: Effects of sodium chloride and calcium chloride on the rheological and structural properties of gels. **J. Food Sci.** 1988, **53**, 231-236.
- (24) Walstra, P., **Physical chemistry of foods**. CRC Press: 2002; Vol. 121.
- (25) van Vliet, T.; Luyten, H., Fracture mechanics of solid foods. In **In: New physico-chemical techniques for the characterization of complex food systems**, E. Dickinson (ed.). Blackie Acad. & Professional, Glasgow (1995) 157-176., 1995.
- (26) Öhgren, C.; Langton, M.; Hermansson, A. M., Structure-fracture measurements of particulate gels. **J. Mater. Sci.** 2004, **39**, 6473-6482.
- (27) Brink, J.; Langton, M.; Stading, M.; Hermansson, A.-M., Simultaneous analysis of the structural and mechanical changes during large deformation of whey protein isolate/gelatin gels at the macro and micro levels. **Food Hydrocolloid** 2007, **21**, 409-419.
- (28) Young, W. C.; Budynas, R. G., **Roark's formulas for stress and strain**. McGraw-Hill New York: 2002; Vol. 7.
- (29) Renkema, J. M. S., Relations between rheological properties and network structure of soy protein gels. **Food Hydrocolloid** 2004, **18**, 39-47.

Chapter 5

Quantitative analysis of the network structure that underlines the transitioning in mechanical responses of pea protein gels

In this chapter, various network structures were generated from pea proteins by varying the pH and protein concentration during gel formation. The network structures were visualized by the use of confocal laser scanning microscopy (CLSM) and scanning electron microscopy (SEM) and the typical length scales of the formed networks were quantitatively analyzed by the use of the pair correlation function. The transitioning from fine to coarse stranded networks was shown to occur at around pH 3.7 based on the string sizes and this corresponded to a correlation length of about 100 nm. The transition in the network structure was also shown to result in transitioning in various rheological responses including the ability of the networks to elastically store energy as obtained from the recoverable energy measurements.

This chapter is published as:

Munialo, C.D.; van der Linden, E.; Ako, K.; de Jongh, H. H. J. Quantitative analysis of the network structure that underlines the transitioning in mechanical responses of pea protein gels. **Food Hydrocolloids** 2015, 49, 104-117.

Introduction

Storage proteins of pea (*Pisum sativum* L.) have a considerable potential to be used in the food industry for the formulation of new food products as a better accessible and sustainable alternative to animal proteins supplies^{1,2}. However, the inability to structure plant proteins such as from pea into desirable textures can limit their application³.

Gel formation by globular proteins such as pea proteins is of great importance in the generation of texture in food. Heating globular proteins above their denaturation temperature results in partial unfolding of the proteins. This exposes interaction sites, giving rise to intermolecular interactions, eventually resulting in clustering of protein aggregates to form a spatial gel network⁴. At sufficiently high protein concentrations, these gels can be self-supporting, and large deformation and fracture behavior can be studied⁵. Large deformation and fracture properties are important quality characteristics that determine the functional properties of gels, such as cutting, handling, oral processing, and sensory/mouthfeel perception^{6,7}.

The fracture and macroscopic breakdown properties of gels can be explained by the energy balance in materials⁸. When gels are subjected to deformation, all supplied energy is either stored⁶ or dissipated during deformation⁹. Some of the processes that lead to dissipation of energy are via fracturing events at length scales larger than that of microstructures that make up the spatial network, the de-bonding of physical contacts that form the network, friction between microstructural elements during applied deformation, viscous serum flow of the liquid that is entrapped by the network, plastic deformation, and the relaxation of the structure elements. The detailed explanation of how these dissipation modes contribute to energy loss can be found elsewhere¹⁰. The energy that is stored elastically during deformation is referred to as the recoverable energy. The recoverable energy is one of the main characteristics that define the fracture characteristics of food gels by controlling energy balance within the gel structure during deformation^{5,8}. The recoverable energy has been correlated to perceived crumbliness of food gels⁷.

The properties of protein gels are influenced by a number of interrelated factors such as: protein concentration, pH, and ionic strength during gel formation¹¹. The strength of protein gels has been shown to increase with an increase in protein or solid matter content¹². Whereas, depending on the gelling conditions, globular proteins such as pea proteins form gels varying in appearance from transparent to opaque⁵. With increasing the pH towards the isoelectric point (IEP) of the protein, the formation of gels with coarse-strands is promoted. Coarse-stranded gels are composed of particulate aggregates¹³, and have an opaque appearance⁵. Contrarily, gels formed at a low ionic strength, and at pH away from IEP are fine-stranded with transparent appearance¹⁴.

The mechanical deformation properties of protein gels at varying conditions have been reported before.

A significant increase in stiffness of gels made from whey protein was reported with an increase in protein concentration from 60 to 100 g/L (w/v)¹⁵. Changes in fracture properties of protein gels with changes in pH have also been reported. At pH < 4.5, whey proteins were shown to form particulate gels that had a rather adhesive texture¹⁶. Whey protein gels prepared at pHs 2 - 4 were reported as being weak, and brittle, whereas gels that were formed around neutral pH were described as being strong and elastic¹⁷. Pea protein gels formed at varying pH and ionic strength that showed differences in the rheological behavior have also been reported^{5, 18-21}. However, the precise pH range at which structural transitioning of pea protein gels occurs, and the effect of varying pH and protein concentration on the resultant rheological responses of the formed gels has not yet been reported.

The structural changes between fine and coarse-stranded gels have been reported to occur over a range of pH and ionic strength in systems containing globular proteins such as whey proteins^{22, 23}. A sharp transition from transparent to opaque gels was observed in 10 % w/v β -lg, when pH was increased from pH 4.1 to 4.3 or decreased from 5.7 to 5.3²³. However, studies on the structural transitioning of pea protein gels over a narrow range of pH, and at varying protein concentrations have not yet been reported.

To be able to determine the transitioning in mechanical responses of pea protein gels as a result of changes in the network structure, various microstructures were generated in this study. The aim of this study was to quantitatively characterize the network structure that underlines the transitioning in the mechanical responses of pea protein gels. To realize the structural changes, two approaches were chosen to affect the morphology, (i) via pH variations from pH 3.0 – pH 4.2 at a fixed protein concentration (100 mg/mL) (where electrostatic interactions are changed as a result of changes in the pH), and (ii) via changes in the protein concentration from 100 to 150 mg/mL at a fixed pH 3.0 (where kinetics of gel formation may be altered due to changes in protein content). Subsequently, the rheological and structural properties of the formed gels were evaluated.

Experimental

Materials

Pre-dried de-hulled commercial green pea seeds with a protein content of 22 g/100 g (dry weight basis) were purchased from a local supermarket. Rhodamine B, acetone, dimethyl sulfoxide (DMSO), glutaraldehyde, NaOH pellets, HCl, and NaCl were all purchased from Sigma-Aldrich (Steinheim, Germany). Paraffin oil was purchased from Merck (Darmstadt, Germany). Omnifix® syringes were obtained from Braun (Melsungen, Germany). All materials were of analytical grade and used without further purification. All solutions were prepared with MilliQ water.

Pea protein extraction

Pea protein isolate was extracted from commercial green peas by isoelectric precipitation according to a previously described procedure^{5, 24}. The pea protein isolate extracted in this way will be referred to as 'native' pea protein. The protein content of native pea protein was determined using the Kjeldahl method with a nitrogen-to-protein conversion factor of 6.25, and found to be 123.9 ± 1.3 mg/mL. The dry matter content of native pea protein was 12.6 ± 1.2 %. Conductivity measurements showed that native pea protein isolate at pH 7.0, following the washing steps during protein extraction had an ionic strength comparable to that of about 0.02 M NaCl. Stock solutions of pea protein were prepared by concentrating native pea protein isolate to a final concentration of 150 mg/mL by ultrafiltration using a Merck Millipore Amicon stirred cell fitted with a 30 kDa MWCO membrane (Darmstadt, Germany).

Characterization of pea proteins

The thermal denaturation of the proteins in native pea protein solutions was evaluated by a TA Q100-Tzero™ differential scanning calorimetry thermal analyzer (TA Instruments, New Castle, DE, USA) according to a previously described procedure 5. The calorimetric analysis of native pea proteins showed a single peak denaturation temperature (T_d) of 84.9 ± 1.6 °C, on-set temperature of denaturation (T_m) of 74.3 ± 2.1 , and the enthalpy change of the major endotherm (ΔH) of 9.4 ± 2.8 J/g protein (thermograms not shown).

Protein aggregation was followed by measuring the turbidity of the samples in a Cary 4000 UV-vis spectrophotometer (Varian, Nederland BV, the Netherlands), accordingly to a previously described procedure 5. The intensity of the transmitted light was measured using quartz cuvettes with a 10 nm path length at 20 °C following heating of 2 mg/mL pea protein solutions at varying pHs from pH 3.0 - pH 4.2, at 95 °C for 30 min and the absorbance calculated. The turbidity of the samples was obtained by dividing the absorbance at 500 nm by the optical path length of 10 nm. Typically, three measurements were carried out on each sample and averaged.

Preparation of pea protein gels

All gelation experiments were carried out without further adjustment of the ionic strength of the protein solutions. Prior to gelation, the pH of the native pea protein solutions was adjusted using 2 M HCl to pHs 3.0 to 4.2 ± 0.01 in steps of 0.2 at a fixed protein concentration of 100 mg/mL, as well as the protein concentration was varied from 100–150 mg/mL at a fixed pH 3.0 ± 0.01 . Following adjustment of the pH and the concentration of the pea protein solutions, the samples were degassed and subsequently poured into 20 mL Omnifix® syringes with an internal diameter of 19.7 mm, which were coated with paraffin oil, and closed at the bottom. The solutions were heated at 95 °C in a water bath for 30 min, followed by cooling at room temperature (20 ± 2 °C) overnight.

Each sample was prepared in triplicate.

Rheological characterization of pea protein gels

Dynamic rheological measurements

Rheological characterization of pea protein gels was carried out according to the previously described procedure²⁵. An Anton Paar MCR 502 rheometer (Anton Paar, Graz, Austria) was used to determine rheological changes which occurred during in situ thermal processing of pea protein solutions. The Anton Paar C-CC17/T200/TI concentric cylinder measuring system was used in all experiments. The measuring system consisted of an oscillating cup and a fixed bob attached to a 13.2 torque bar. The pea protein solutions were carefully poured into the cup at 20 °C, and covered with a thin layer of paraffin oil to prevent water evaporation during experiments. Gels were formed by heating the samples from 20 °C to 95 °C at a constant rate of 5 °C/min, holding at 95°C for 30 min, cooling down to 20 °C at a constant rate of 1 °C/min, and then holding at 20 °C for 30 min. An angular frequency of 6.28 rad/s and a maximum strain of 0.5 were used to measure the storage modulus (G') and loss modulus (G'') of the samples during the entire thermal treatment. The experiments were performed in triplicate and the obtained results were averaged. Testing frequency and strain during gelation process was selected based on preliminary experimental results from strain and frequency sweeps of thermally induced gels to minimize damage to the gel network and to ensure that the linear visco-elastic behavior of the samples was retained.

Uniaxial compression

To determine the fracture properties of pea protein gels, compression tests were performed on cylindrical gel samples (19.7 mm in diameter and 20 mm in height) using a Texture Analyzer fitted with a 5 kg load cell and P/75 probe (TA.XTPlus, Stable Micro Systems, Surrey, UK). The fracture properties were studied by a uniaxial compression test up to a 90 % deformation of the specimen height at a rate of 1 mm/s according to the previously described procedure 5. The true fracture stress and strain which will be designated as the fracture stress and fracture strain throughout this paper were calculated according to a previously described procedure 5. The Young's modulus was calculated from the slope of the linear region of the stress-strain curve as previously described⁸.

The recoverable energy measurements were carried out on the specimen described above according to the previously described procedure⁵. Compression and decompression of the specimen was analyzed on the above described Texture Analyzer. Fifty percent of the strain before fracture was applied to determine the energy release during decompression at a deformation speed of 1 mm/s. The percentage of recoverable energy of the gels was calculated from the area under the force-deformation curve as being the ratio of the amount of energy that was recovered after applying the stress over the amount of energy that was applied during the compression and decompression of the gels⁷.

Characterization of the microstructure

Confocal laser scanning microscopy (CLSM)

CLSM was used to visualize the microstructure of pea protein gels according to a previously described procedure⁵ with modifications. Pea protein solutions were labeled with 20 μL /mL of sample aqueous solution of the fluorochrome Rhodamine B (0.2 % w/w) prior to heat treatment. Solutions of pea protein + Rhodamine B were then inserted between a concave slide and a coverslip and hermetically sealed. Subsequently, the samples were heated at 95 °C for 30 min. Visualization of the microstructure was performed using a Leica TCS SP5 microscope (Leica Microsystems (CMS) GmbH, Mannheim, Germany) configured with an inverted microscope using an Ar/Kr laser for excitation in the fluorescence single-photon mode. Pictures were taken with two different objective lenses: HCx PL APO 63 \times NA = 1.2 and 20 \times NA = 0.7, at a scan depth of 20 μm . The incident light was emitted by a laser beam at 561 nm, and the emission of Rhodamine was recorded between 570 and 725 nm.

Scanning electron microscopy (SEM)

Gels for SEM were prepared in cut pipette tips according to a previously described procedure⁵. In summary, the solvent exchange was performed following gelation of the samples as previously outlined⁵ after which, the samples were dried by critical point drying (CPD 030 BalTec, Liechtenstein) and glued onto a SEM sample holder using carbon glue (Leit-C, Neubauer Chemicalien, Germany), and subsequently stored overnight under vacuum. After drying of the carbon cement, the samples were sputter coated with 10 nm iridium in SCD 500 (Leica EM VCT 100, Leica, Vienna, Austria) prior to imaging. All samples were analyzed with a field emission scanning electron microscope (Magellan XHR 400L FE-SEM, FEI, Eindhoven, the Netherlands) at room temperature (20 ± 2 °C) at a working distance of 4 mm with SE detection at 2 kV.

Image analysis

To determine the characteristic length scales at which structural transitioning from fine to coarse-stranded networks occur in pea proteins, quantitative analyses in terms of the pair correlation function ($g(r)$) of both CLSM and SEM images of heat-set pea protein gels was carried out as previously described²⁶. Six images were used for CLSM analysis and 3 images for SEM analysis, over pairs of 1024×1024 pixels representing one CLSM image and 874×874 pixels representing one SEM image. The $g(r)$ presented is an average of these images. It is however important to note that a dimensional or shadowing effect on an image can result in high density images and thus decreasing the true contrast of the 2D SEM images given that out-of-focus beam is not eliminated during the imaging of SEM samples, which is basically suppressed in CLSM²⁷. In order to reduce the dimensional effect, an average of the dark intensity from the raw images (RI) represented by the threshold level (TL) was measured and subtracted from the images as previously described²⁸.

An example of the intensity distribution of the raw images and the threshold image (TI) from SEM micrographs is shown in **Fig. 1**.

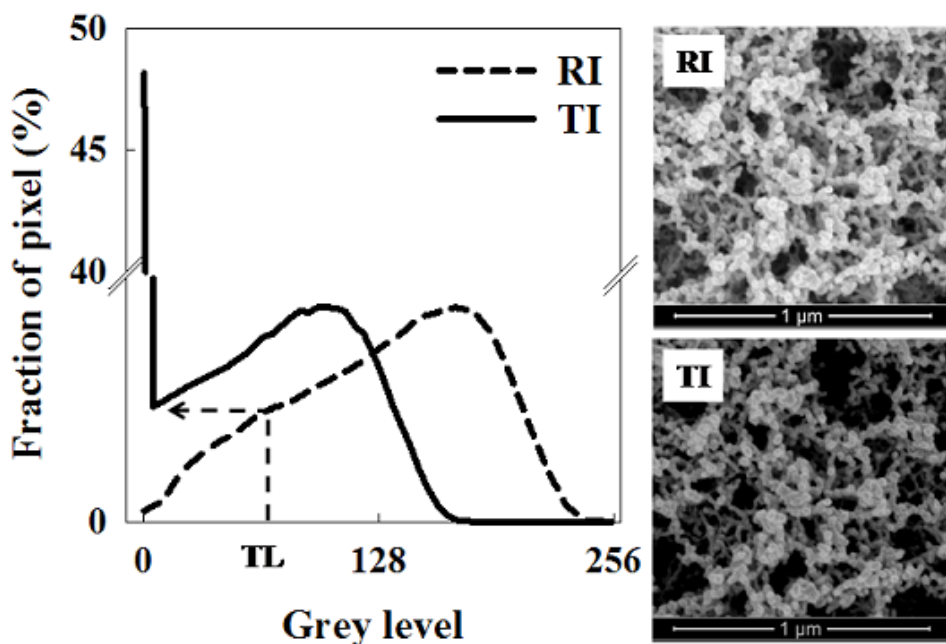


Figure 1: An example of grey level distribution of the raw image (RI) and the threshold image (TI) for SEM images. The threshold level (TL) is an average of the intensity of the RI dark domain.

Statistical analysis

Data are reported as mean values with standard deviations (SD) for all data points. The significance of the differences in mechanical properties were evaluated by determining the correlation between experimental data using paired sample test with minimum significance set at the 5 % level ($P < 0.05$) using SPSS (version 19, International Business Machines, Armonk, NY, USA).

Results and Discussion

The aim of this study was to quantitatively characterize the network structure that underlines the transitioning in the mechanical responses of pea protein gels. To this end, various microstructures were generated from pea proteins by varying the pH of pea proteins solutions prior to gelation from pH 3.0 to pH 4.2 at a fixed protein concentration of 100 mg/mL, as well as varying the protein concentration from 100 – 150 mg/mL at a fixed pH of 3.0.

The variation of the pH prior to gelation was chosen based on a preceding study where gels prepared at pH 3.0 were reported to be translucent, and to have somewhat low fracture stress, high fracture strain values, and high recoverable energy, characteristics of a fine-stranded network⁵. Therefore, to quantitatively analyze the network structure that underlines the transitioning in the mechanical responses of pea protein gels, gels at varying pH from pH 3.0 – pH 4.2 and protein concentration were prepared, because they gave essentially fine to coarse-stranded networks, and hence offers a possibility to relate structural changes of pea protein networks to the transitioning in mechanical responses of pea protein gels.

Characterization of pea protein at varying pHs

To study the aggregation behavior of pea proteins, the changes in turbidity for pea proteins at varying pHs were determined from the absorbance values recorded following heating of the pea protein solutions at 95 °C for 30 min as presented in **Fig. 2**.

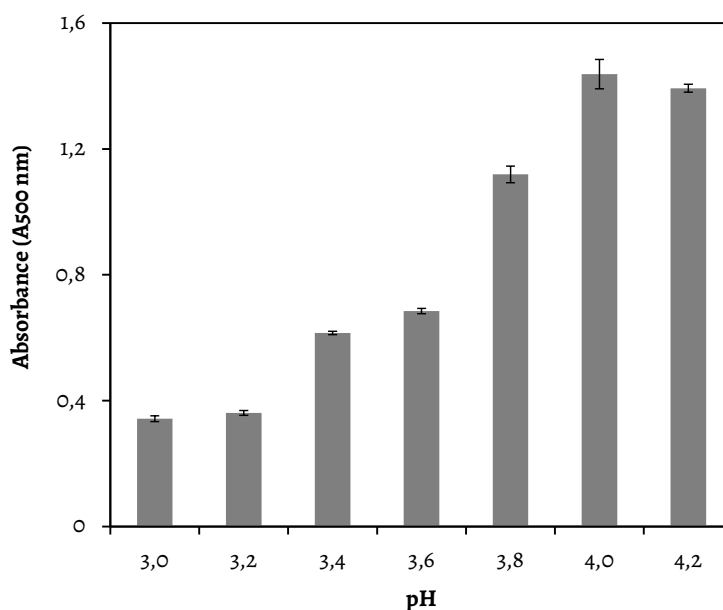


Figure 2: Changes in absorbance in pea protein solutions at pHs 3.0 - 4.2 at a protein concentration of 2 mg/mL. The measurements were carried out at 20 °C following the heating of the samples at 95 °C for 30 min.

It is however not sensible to measure the changes in absorbance as a function of protein concentration at a fixed pH given that these measurements were carried out in diluted system.

Changes in absorbance after heat treatment of pea protein solutions at different pHs at the same protein concentration can be related to aggregate size.

No differences in absorbance were observed at pH 3.0 and pH 3.2 which shows that the size of aggregates at these pHs is comparable. The absorbance increased with an increase in pH towards the IEP (**Fig. 2**). The higher absorbance values at higher pHs shows the predominance of coarser structures in comparison to lower pHs. Higher pHs are closer to the isoelectric point (IEP) of pea protein, which is in the range of 4.8 - 5.5²⁹, where more coarser structures are expected to be formed. At lower pHs, one expects finer structures, resulting in lower absorbance values.

Dynamic visco-elastic properties of pea protein gels

To study the visco-elastic properties of pea protein gels, the small deformation rheological responses of pea protein gels were determined as a function of varying protein concentration at a fixed pH 3.0, and at varying pHs at a fixed 100 mg/mL protein concentration. During the thermal treatment of pea protein solutions at these conditions, the storage modulus (G' , Pa), and loss modulus (G'' , Pa) were recorded as a function of pH and protein concentration. For all samples, the G' values were considerably greater in magnitude than G'' , suggesting that predominantly elastic gels were formed. Only G' values are discussed hereafter.

The G' (Pa) development of pea protein for various protein concentrations at a fixed pH was monitored over time (**Fig. 3 A**). The G' values increased with an increase in protein concentration. In all conditions G' values became higher and continued to increase while maintaining the samples at 95 °C. A subsequent increase in the G' was observed during cooling of the samples to 20 °C. Holding the samples at 20 °C resulted in a further increase in the G' at all protein concentrations.

The G' development of pea protein at varying pH at a fixed protein concentration of 100 mg/mL was monitored over time as shown in **Fig. 3 B**. As in the case of varying protein concentration at a fixed pH 3.0, the G' values became higher and continued to increase during the holding of the samples at 95 °C. A subsequent increase in the G' was observed during cooling of the samples to 20 °C but holding the samples at 20 °C did not result in remarkable changes in the final G' (**Fig. 3 B**). The G' values increased with an increase in pH. The higher G' at pH 4.2 could be related to an earlier onset of gelation (see **Fig. 3 B**), as well as the structural influence of the coarse networks on the stiffness of the gels. Coarse-stranded networks can be formed at higher pHs closer to IEP and are composed of thicker strands and thicker strands are more difficult to bend than thin (finer) strands which imply higher G' values for coarser networks than more fine networks³⁰.

The fact that G' values for pH 4.2 are higher than pH 3.0 suggests that variation in aggregation behavior plays an important role in the determination of the type of network that is formed, which in turn influences the stiffness of the gels. Thus, it can be hypothesized that for gels prepared at pH 4.2, the various subunits that precipitate, participate in the network formation than for pH 3.0, possibly due to more electrostatic repulsion and thus a less efficient incorporation of the protein in the network at pH 3.0 than for pH 4.2.

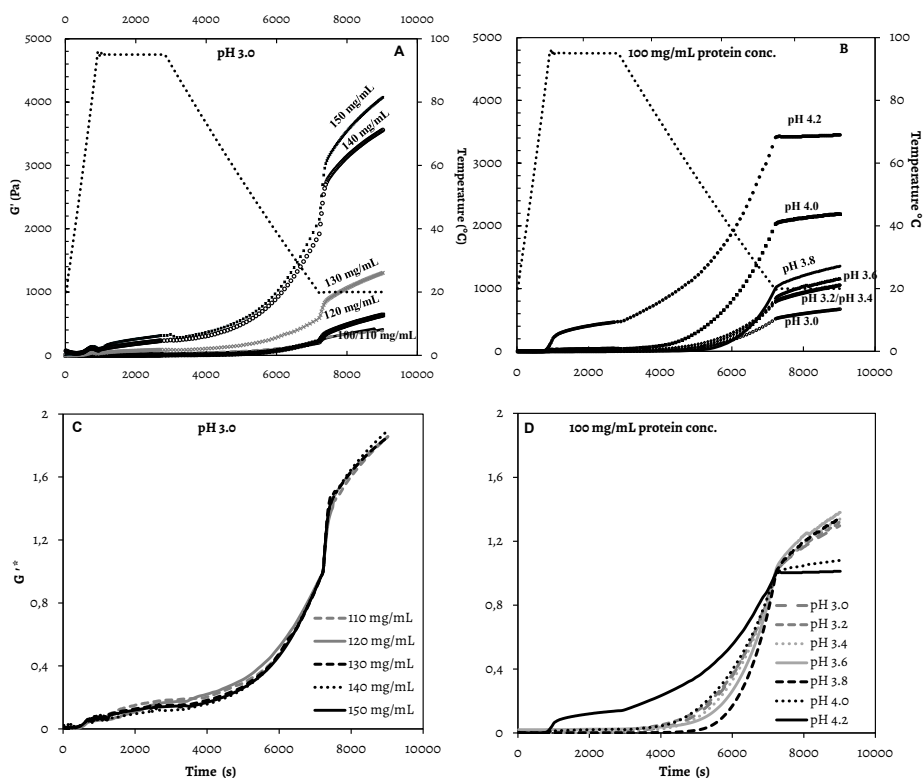


Figure 3 A: G' (Pa) development in 100 mg/mL (\blacktriangle), 110 mg/mL (\longrightarrow), 120mg/mL (\blacksquare), 130 mg/mL(\times), 140 mg/mL (\circ), and 150 mg/mL (\bullet) pea protein samples at constant pH 3.0. **Figure 3 B:** G' (Pa) development in pea protein at pH 3.0 (\circ), pH 3.2 (\bullet), pH 3.4 (Δ), pH 3.6 (\times), pH 3.8 (\longrightarrow), 4.0 (\blacksquare), and pH 4.2 (\bullet) at constant protein concentration of 100 mg/mL. The dotted lines in Figs. 3 A and B represents the temperature history. changes in G'^* versus gelation time for pea protein gels formed at pH 3.0, varying protein concentration from 110 – 150 mg/mL (**Fig. 3 C**) and at pHs 3.0 to 4.2 at 100 mg/mL protein concentration (**Fig. 3 D**). These values were obtained from fitting of the G' data plotted in **Fig. 3 C** and **D** to Eq. (1)

To study the kinetics of gel formation in order to establish the structural transitions, the small deformation data based on variation of protein concentration at a fixed pH 3.0, and variation of pH variations at a fixed 100 mg/mL protein concentration shown in **Fig. 3 A** and **B**, were fitted on to a master curve using the Eq. (1):

$$G'^*(t) = \frac{G'(t)}{G(t=t^*)} \quad (1)$$

Where t^* is the time at which the G' does not change any more which is set here at 7,220 s. This time corresponds to the temperature when cooling was initiated at the end of the gelation profile (20 °C).

Figs. 3 C and D shows the G'' as a function of time for pea protein gels. The results show that gels prepared at varying protein concentration at a fixed pH can be superimposed to a master curve within experimental error by a scaling factor (**Fig. 3 C**). The gels prepared at pHs 3.0 - 3.4 can also be superimposed to the master curve within experimental error by a scaling factor, which show that the kinetics and mechanism of gel formation at these pHs are also similar (**Fig. 3 D**). Although the pH 4.0 curve fits on the master curve, beyond t^* , the G'' value is lower than that of pHs 3.0 to 3.8. Whereas, for pH 4.2 data, a good superposition could not be obtained as the shape of the master curve varied to some extent compared to the other pHs. This shows that with an increase in the pH towards the IEP, gelation kinetics and the mechanism of gel assembly/formation differ due to differences in the aggregates that participate in the network formation.

Changes in G' during heating and cooling were derived from data in **Fig. 3 A and B** for pea proteins as a function of protein concentration (**Fig. 4 A**).

The ratio of the increase in G' during heating ($\Delta G'_{\text{heat}}$) to that during cooling ($\Delta G'_{\text{cool}}$), has been reported to reflect relative contributions of the intermolecular interactions to the final value of G' ^{31, 32}. Gels prepared at 100 mg/mL (pH 3.0) exhibited lower values of $\Delta G'_{\text{heat}}/\Delta G'_{\text{cool}}$ whereas gels prepared at 120 mg/mL pea protein concentration (pH 3.0) exhibited higher values. An increase in protein concentration leads to acceleration of gelation. At protein concentrations beyond 120 mg/mL, no acceleration is observed (**Fig. 4 A**).

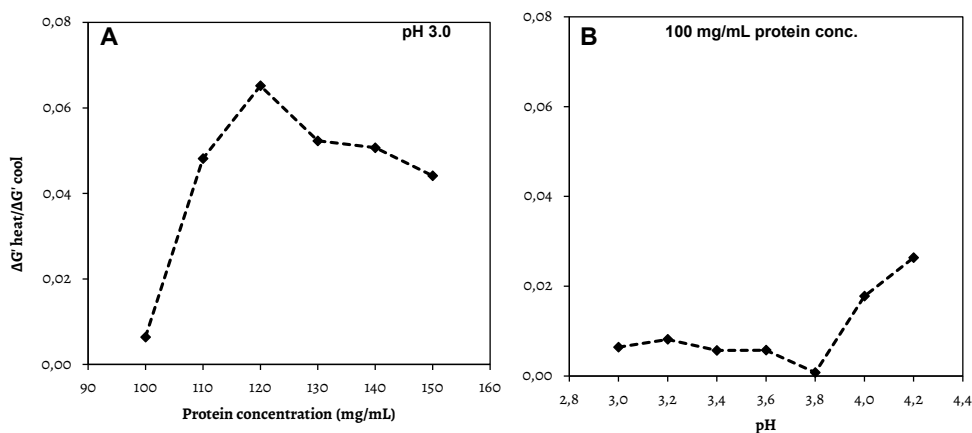


Figure 4: Relationship among pea protein and $\Delta G'_{\text{heat}}/\Delta G'_{\text{cool}}$ values of pea protein at a fixed pH 3.0 at varying protein concentration, and pea protein at fixed protein concentration (100 mg/mL) at varying pH. Three replications were done at each condition and the error bars are derived from the standard error (SE) calculated from the standard deviations (SD) of the variations of 3 replicates.

Changes in G' during heating and cooling as a function of pH are shown in **Fig. 4 B**. The ratio of the increase in G' during heating ($\Delta G'_{\text{heat}}$) to that during cooling ($\Delta G'_{\text{cool}}$) was almost the same for samples prepared at pHs 3.0 to pH 3.6. A slight decrease is observed at pH 3.8. For pH 4.0 and pH 4.2, this ratio increases again. This suggests different intermolecular interactions and consequently different structures are formed going from pH 3.6 to pH 4.2.

Mechanical deformation of pea protein gels

Following heating of pea proteins at varying pHs and protein concentrations, self-supporting gels were formed, and the mechanical deformation (large deformation) properties of these gels were evaluated. The fracture stress, fracture strain and the Young's modulus for the gels were determined as presented in **Fig. 5**.

Fracture stress

The fracture stress, a measure of the gel strength, was determined for pea protein gels at a constant pH 3.0 at varying protein concentrations (**Fig. 5 A**), and at varying pHs at a constant protein concentration (**Fig. 5 B**).

As expected, the fracture stress increases with an increase in protein concentration (**Fig. 5 A**). This is attributed to how much protein participates in the network formation. Increased concentration and enhanced connectivity between protein aggregates lead to increased gel strength³³.

A decrease in the fracture stress with an increase in pH from pH 3.0 to pH 4.2 was observed with samples prepared at pH 4.2 having the lowest fracture stress (**Fig. 5 B**). This may be related to reduction in the connectivity of the network structures with increasing pH. However, given that the structural changes as a result of changes in protein concentration or pH are discussed later on in this paper, the changes in the fracture stress observed here will be explained in relation to previous findings. A shift in the network structure from finer to coarser results in less dense networks with larger and inhomogeneous pore sizes⁵. Less dense β -lg gels have been reported to have lower fracture stress³⁴. Particulate whey protein gels also showed discontinuous crack propagation during tensile fracture as visualized by CLSM³⁵. Additionally, the porous nature of pea protein gels with an increase in pH to pH 4.2 could cause a stepwise crack growth due to micro-scale inhomogeneities between protein clusters in the form of flaws, pores, or weak regions, resulting in lower fracture stress⁵. Moreover, the increased porosity within the protein network reduces the actual fracture surface, resulting in lower fracture stress values³⁶ for pea protein gels with an increase in pH to higher pHs (such as pH 4.0 and pH 4.2).

Fracture strain

An increase in the protein concentration at a fixed pH did not result in significant changes in the fracture strain (**Fig. 5 C**).

Changes in the fracture strain as a function of pH at a fixed 100 mg/mL protein concentration are shown in **Fig. 5 D**.

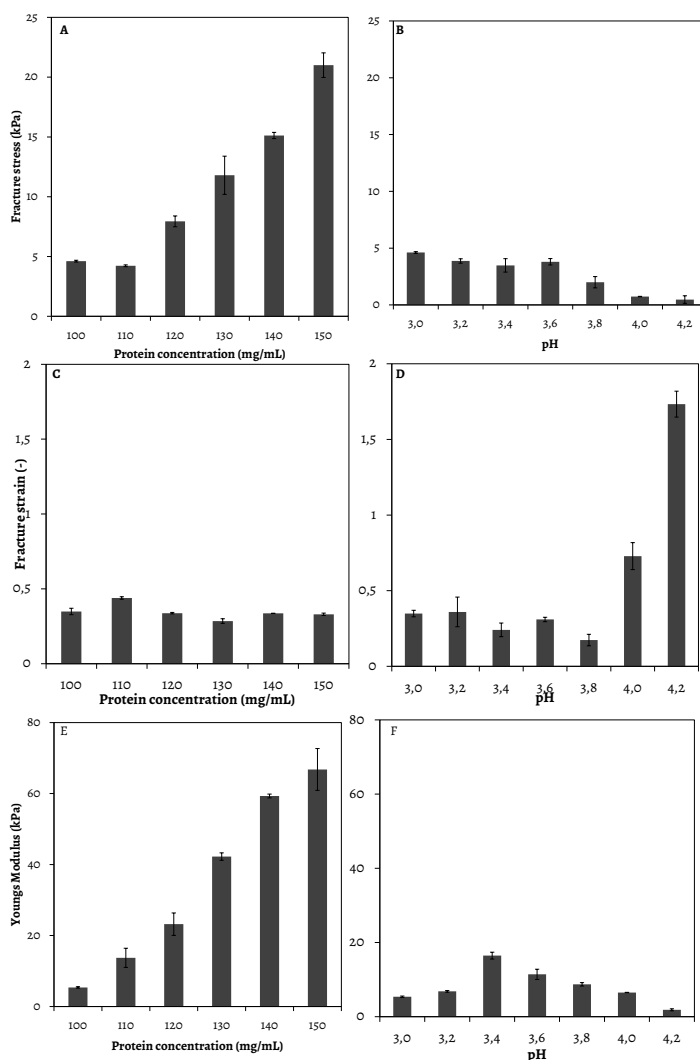


Figure 5: Mechanical deformation properties (fracture stress, fracture strain, and Young's modulus) of pea protein gels. The error bars are derived from the SE calculated from the SD of the variations of 5 – 6 samples.

The fracture strain for pea protein gels prepared at pH 3.0 - pH 3.6 was almost similar. The fracture strain was the lowest at pH 3.8. Changes in the fracture strain can be related to structural changes. As the pH increases, a change in the strand thickness of pea proteins gels can occur, which results in changes in brittleness of the gels.

The influence of strand thickness of protein gels on the fracture strain has been reported for soy protein gels³⁷. The increase in the fracture strain at pHs 4.0 and 4.2 also coincided with an increase in turbidity (**Fig. 2**), and an increase in the $\Delta G'_{\text{heat}}/\Delta G'_{\text{cool}}$ values (**Fig. 4 B**), which all suggest that different structures arise for the pH values around pH 3.8 - pH 4.2.

Young's modulus

An increase in the protein concentration at a fixed pH resulted in an increase in the Young's modulus which is the measure of the stiffness of a material as shown in **Fig. 5 E**. The Young's modulus as a function of pH at fixed protein concentration showed a maximum value around pH 3.4 (**Fig. 5 F**). The maximum in the Young's modulus suggests that there may be several contributions that set the Young's moduli of pea protein gels at different length scales, similar to what has been previously reported⁵.

Elastically stored (recoverable) energy of pea protein gels

The recoverable (stored) energy of the pea protein gels was determined as a function of varying protein concentrations at fixed pH and as a function of varying pH at a fixed protein concentration as shown in **Fig. 6**. There was an initial steady increase in the recoverable energy up to 130 mg/mL, followed by a decrease at higher protein concentrations (**Fig. 6 A**).

The recoverable energy of pea protein gels at a fixed 100 mg/mL protein concentration at varying pHs is shown in **Fig. 6 B**.

The recoverable energy is similar for pHs between 3.0 and 3.8 and decreased with an increase in the pH above pH 3.8. The gels prepared at pH 4.2 had the lowest recoverable energy. The lower ability to elastically store energy is postulated to be related to coarser networks with large and inhomogeneous pore sizes. Coarser networks can result in higher water (serum) release/flow during compression, as water becomes able to move more freely from the network²⁸, and as a result the energy applied is lost more via viscous dissipation (due to serum flow).

The dissipation of energy at the expense of energy storage was confirmed when the recoverable energy obtained for each pH at a fixed 100 mg/mL protein concentration was subtracted from the total applied energy, assumed implicitly to be 100 %. The difference in the energy i.e. 100 % minus measured recoverable energy was taken to represent the relative dissipated energy via the 6 modes described in the introduction. The most probable means by which energy is lost may be via fracture events, relaxation of the structural elements, and the serum flow, as the contribution towards energy dissipation via friction, plastic deformation, and de-bonding of physical contacts between microstructural elements that make up the network (see introduction), are all considered to be small and negligible in this work.

Assuming that during the measurements of recoverable energy the fracture events are avoided, there remain 2 main dissipation modes that contribute substantially to the energy balance. These are the relaxation of the structural elements, and the viscous serum flow. From the stress relaxation measurements carried out according to a previously described procedure¹⁰, the obtained dissipated fraction amounts to around 0.2 at a deformation speed of 1 mm/s deformation speed, which is an equivalent of about 20 % of the applied energy (data not shown). Thus, the remaining proportion of energy loss accounts for the energy dissipated via viscous serum flow. This contribution was observed to increase with an increase in pH (data not shown).

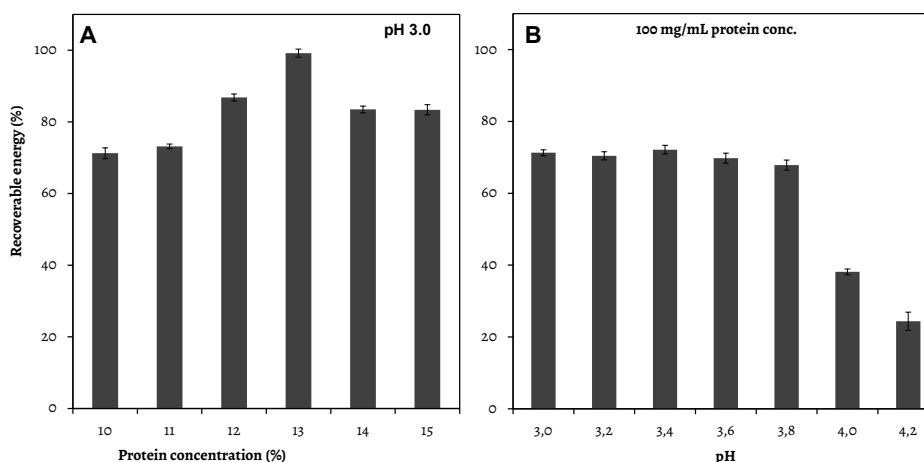


Figure 6: The recoverable energy of pea protein gels prepared at a fixed pH (3.0) at varying protein concentration and at a fixed protein concentration (100 mg/mL) and at varying pHs. The error bars are derived from the SE calculated from the SD of the variations of 5 – 6 samples.

Gel microstructure

To relate the transitioning in the rheological responses of pea protein gels to the changes in the network structure that were formed, the microstructure of pea protein gels was evaluated. Translucent gels were formed at pH 3.0 - pH 3.6 whereas at pH 3.8 - pH 4.2, opaque (white) gels were formed from pea protein at 100 mg/mL protein concentration. There were no visual differences in the appearance of the samples at a fixed pH 3.0 at varying protein concentrations. The microstructure of all gels was visualized by SEM (sub-micron range) and CSLM (μm range) as shown in **Fig. 8**.

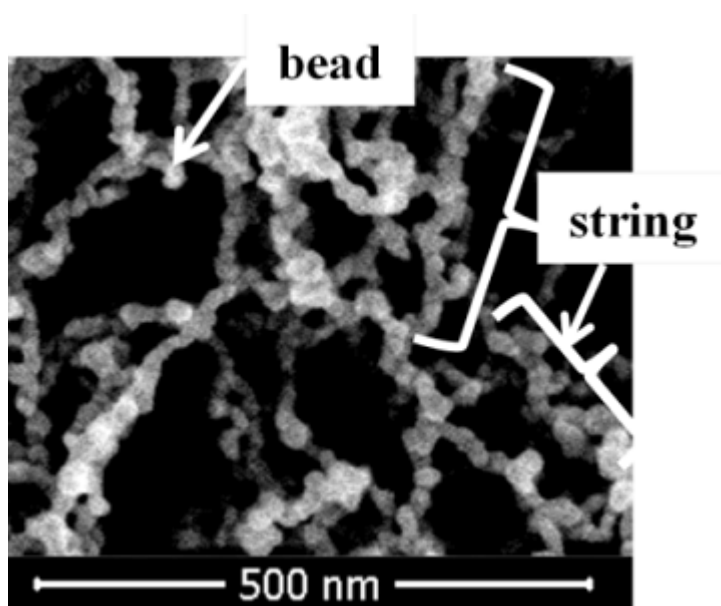


Figure 7: Representation of the local domains (“bead”) and (“string”) that characterize pea protein network structure.

SEM

From SEM micrographs, differences in the coarseness, defined as the heterogeneity of the density of the aggregates that span the network, were observed from samples prepared at varying protein concentration at fixed pH 3.0 (**Fig. 8**). SEM images show that the networks are composed of small spherical aggregates (“bead”) connected with thin thread-like strands/filaments (“string”) as illustrated in **Fig. 7**, with a short distance between the junctions (**Fig. 8**). There are no remarkable changes in thickness of the strings with an increase in protein concentration, although an increase in protein concentration beyond 130 mg/mL results in more dense networks composed of smaller aggregates.

For gels prepared at varying pHs (from pH 3.0 – pH 4.2), at a fixed protein concentration (100 mg/mL) (**Fig. 8**), the SEM images show that the network structures prepared at lower pHs are finer than network structures formed at pHs closer to the IEP. The networks at pH 3.0 are regular and have a dense structure, with relatively small pores connected with thin strings. There is no noticeable difference in thickness of the strands that span the networks for gels prepared at pH 3.0 to pH 3.4, while the distances between the junctions connecting the various aggregates appear larger with an increase in the pH towards pH 3.4. At pHs 3.6 to pH 4.2, there is an increase in number as well as size of the pores which are distinguishable in the images with 100 nm scale bar.

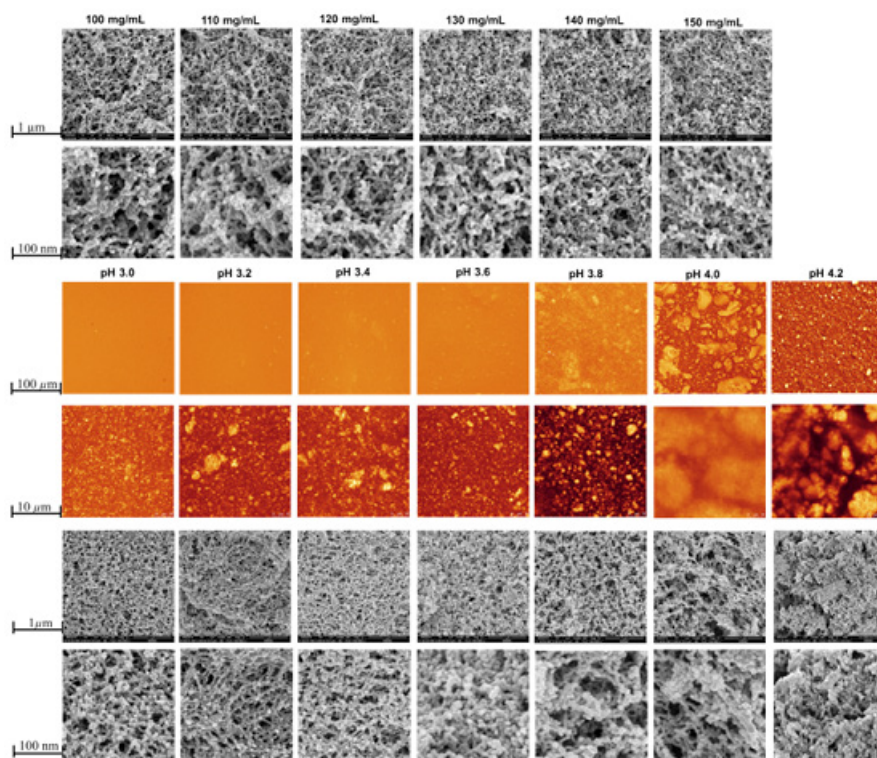


Figure 8: Microstructural changes in pea protein gels at varying pHs from 3.0 - 4.2 at a fixed 100 mg/mL protein concentration and pea protein gels at fixed pH 3.0 at varying protein concentration from 100 - 150 mg/mL as visualized using CLSM and SEM.

The network structures at pH 3.8 and pH 4.0 are more stretched, more open, less dense, and have larger pores. At pH 4.2, rather open, coarser network structures were formed, having relatively large pores sizes, and numerous spherical aggregates which are organized into local clusters (domains) (**Fig. 8**).

CLSM

The appearance of large-scale inhomogeneities was observed by CLSM for gels prepared at varying pHs at a fixed protein concentration of 100 mg/mL (**Fig. 8**). The confocal laser scanning micrographs show variations in the spherical aggregates that are the structural building blocks of pea protein spatial gel networks.

The gels formed at pHs 3.8 to pH 4.2 consist of spherical protein aggregates with a diameter of a few microns. Further away from the IEP (pHs 3.0 – pH 3.6), the gels are homogeneous on lengths scales larger than 0.5 μm , and therefore show no distinguishable features by CLSM.

Some protein aggregates can be observed at objective 63 which increase in size with an increase in the pH. The presence of large aggregates at higher pHs, suggests that the protein aggregates at higher pH's grow to the size of a few microns and subsequently, these aggregates randomly rearrange extensively into large domains that cluster to form a particulate gel structure. Such large aggregates formed at higher pH's were also observed when the changes in the turbidity of pea protein samples at varying pHs were measured following heating of protein solutions in dilute concentrations (see **Fig. 2**).

From the visualization of the network structure by both SEM and CLSM, it was shown that varying pH of pea protein prior to gelation results in the formation of gels that can be ranked as fine to coarse-stranded. There is a remarkable difference between these two types of networks in terms of aggregate size as evaluated from the turbidity measurements (**Fig. 2**). Varying the protein concentration at a fixed pH does not result in major structural differences in pea protein gels whereas varying pH at fixed protein concentration results in structural changes (**Fig. 8**).

Quantitative analysis of CLSM and SEM images

To quantify the networks structures obtained from pea proteins, the characteristic length scales were analyzed (from both CLSM and SEM images) in terms of the pair correlation function ($g(r)$) according to

$$g(r) = g_0 \cdot e^{-(r/\xi)^\beta} + 1 \quad (2)$$

where g is the contrast value at $r \rightarrow 0$, ξ is the correlation length characterizing the size of the domains, and β a stretched exponential factor. The β can show how structural transitions relate to correlation function decay as a result of variation of the pH or protein concentration.

Quantitative analysis of images based on CLSM

From the analysis of CLSM images, variations in the shape of $g(r) - 1$ data (**Fig. 9**) are correlated to the structure of the gels at μm scale. For gels that are homogeneous at length scales larger than the resolution of the CLSM, $g(r)$ is unity at all values of r larger than the resolution²⁶. Examples of such gels are those formed at pH 3.0. Gels prepared at pHs 3.2, 3.4 and 3.6 show a very weak amplitude but the $g(r) - 1$ decreases slowly towards unity at r larger than $3 \mu\text{m}$ (**Fig. 9 a**). This illustrates that pea protein gels are formed with large homogeneous domains at these pHs.

The concentration in the domains at pHs 3.0 – 3.6 is close to the average concentration of the gels (about 5 % more than the average concentration see **Fig. 9 b**).

For gels made at pH 3.8, the amplitude of $g(r) - 1$ shows an increase in the concentration of the domains (about 10 % protein more than the average concentration). The domains at pH 3.8 are about 6 μm , and appear to be bigger and more concentrated than those at pH < 3.6. At pH 4.0 and 4.2, a further increase in the amplitude of $g(r) - 1$ was observed, suggesting a further increase in the concentration of the domains. The results suggest that varying the pH toward IEP leads to the formation of more concentrated domains and bigger domain size at μm scale (**Fig. 9 c** and **d**). The increase in the concentration and size of the domains observed here can be corroborated by the increase of the turbidity when the pH is increased toward the IEP (see **Fig. 2**). The concentration of the domains is proportional to $Cg(r)$ at short distance where C is the average concentration of the protein²⁶.

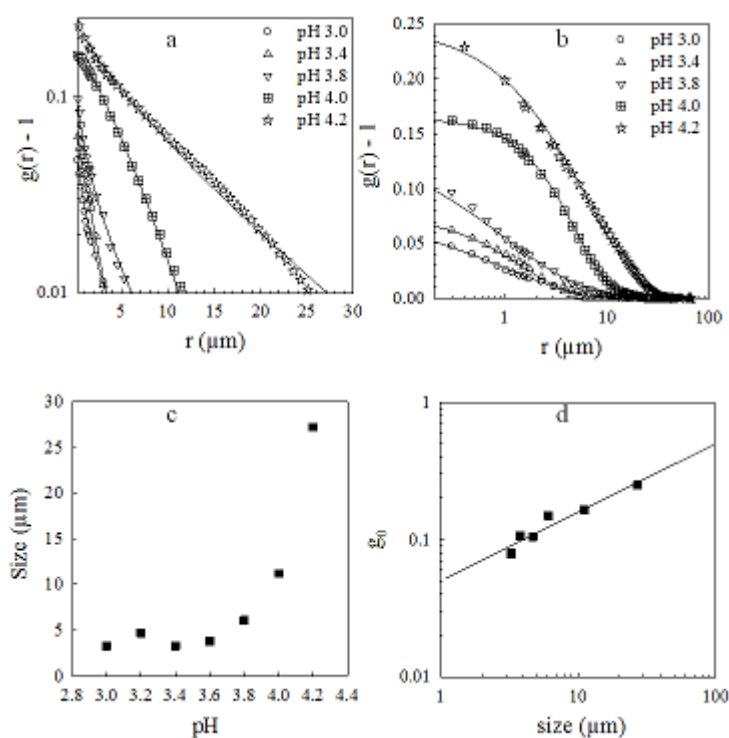


Figure 9: Semi-logarithmic representation of the pair correlation functions ($g(r) - 1$) of pea protein gels formed at pHs 3.0 to pH 4.2 at 100 mg/mL protein concentration plotted in log-linear representation (a), linear-log representation (b). The $g(r) - 1$ shown in **Fig. 9 a** and **b** were obtained from analyzing the microstructure of pea proteins gels based on CLSM micrographs shown in **Fig. 8**. The solid lines in **Fig. 9 a** and **b** represent fits to Eq. (2). Changes in the aggregate size (ξ) as a function of pH are shown in **Fig. 9 c** and the g_0 is plotted as a function of size in **Fig. 9 d**. The solid line in **Fig. 9 d** is a fit to $g_0 = 0.05 (\text{size})^{0.5}$. For clarity pH 3.2 and pH 3.6 are not shown **Fig. 9 a** and **b**.

Thus, the power law variation of g_0 as a function of the domain size from different pHs shown in **Fig. 9 d** can suggest that domains are formed by self-similar aggregation process. The transition between “weak” and “strong” concentration fluctuations occurs between pH 3.6 and pH 3.8 which is thought to correspond to the fine-stranded to coarse-stranded transition.

The changes in the concentration and size of domains that make up the gel networks suggests that the characteristics that determine structural and functional changes of pea protein gels can be characterized at a μm scale. To find out whether the transitioning also occurs at a nm scale, quantitative analysis was also carried out on scanning electron micrographs.

Quantitative analysis of images based on SEM

To analyze typical correlation length at the sub-micron length scale, quantitative analysis in terms of the shape of the $g(r)$ and the size of the domains was carried out based on SEM images. The white domains in the images in **Fig. 8** show the presence of protein aggregates, their shape and sizes, and how these domains are interconnected, which are the parameters that we expected to obtain from the image analysis. These parameters are all well described by the $g(r)$ profile plotted in log-linear plot as function of protein concentration at a fixed pH 3.0 (**Fig. 10 b**), and pH at a fixed 100 mg/mL protein concentration (**Fig. 10 d**), that shows the domain sizes of network structures represented as “string” in **Fig. 7**, at the r values for which $g(r) \rightarrow 1$. The domain sizes of gels at constant pH 3.0 range between 100 nm and 270 nm when the protein concentration is varied, although no clear influence on the domain sizes is observed (**Fig. 10 b**). Whereas, changes in pH at a fixed protein concentration results in a significant change in the domain sizes (**Fig. 10 d**). From **Fig. 10 d**, the domain sizes remain almost constant between pH 3.0 and pH 3.6, after which a sharp increase is observed between pH 3.6 and pH 3.8, which further increases when the pH is increased up to pH 4.2. A sharp increase in ξ with an increase in the pH towards IEP was also reported when quantitative analysis was carried out on CLSM micrographs of gels made from $\beta\text{-Ig}^{23}$.

The insets of **Fig. 10 a** and **Fig. 10 c** show the superimposed plots by vertical and horizontal shift of $g(r) - 1$ data. The vertical dash line in the inset of **Fig. 10 a** and **Fig. 10 c** represents the correlation length scale for pea protein gels at 100 mg/ml at pH 3.0 for which $\xi_b = 1$. The insets are the linear-log representation of the length scale (ξ_b) on which the different gels are correlated for the local domains represented as “bead” in **Fig. 7** and are plotted as function of protein concentration at a fixed pH 3.0 (**Fig. 10 b**) and pH at a fixed 100 mg/mL protein concentration (**Fig. 10 d**). The average of the local domain sizes at which the different gels as function of protein concentration and as function of the pH are correlated to each other is about 60 ± 10 nm (for protein concentration) and 25 ± 10 nm (for pH variation). The correlation length decreased from 60 nm to 25 nm when the pH was increased toward the IEP.

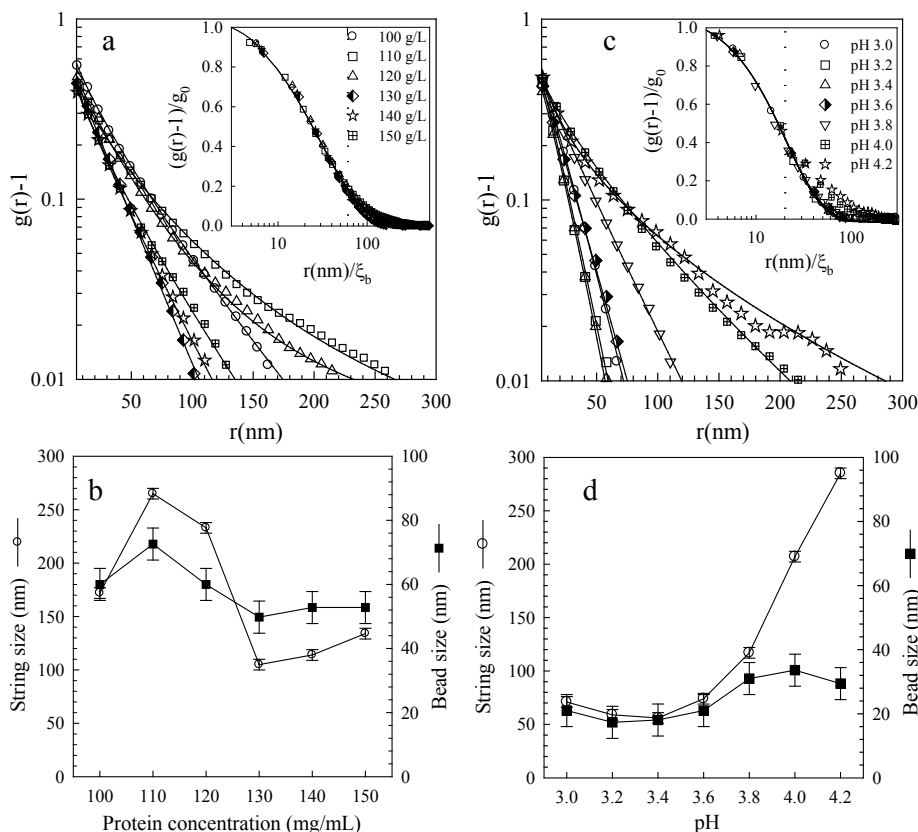


Figure 10: Semi-logarithmic representation of the pair correlation functions of samples at varying protein concentrations at fixed pH (3.0) (**Fig. 10 a**) and varying pHs at a fixed 100 mg/mL protein concentration (**Fig. 10 c**). The inset in Figs. 10 a and c represent the data obtained by normalizing $g(r)-1$ with the amplitude (g_0) and r/ξ_b . The solid lines represent fits to Eq. (2). The pair correlation was calculated based on SEM images presented in **Fig. 8**. Dependence on the concentration at fixed pH 3.0 (**Fig. 10 b**) and pH at a fixed 100 mg/mL protein concentration (**Fig. 10 d**) of local domain “bead” and “string” sizes. The error bars are the size of the nanoparticles (10 nm iridium) used for coating the samples which is not more than ± 5 nm.

Changes in the structure in terms of the β value of pea protein gels

The superposition of the different $g(r)$ will give information about structural change when the pH or the protein concentration is varied. If the length scale on which different $g(r)$ are correlated to each other, i.e. the $g(r)$ from different gels can be superimposed within this length scale, then domain size (both “beads” and “string”) of the gel structures are similar to each other. A similar β value for different gels means that $g(r)-1$ could be superimposed within the experimental error by horizontal and vertical shifts of the domain size.

The value of β used to fit the $g(r)$ with acceptable experimental error of ± 0.05 is plotted as a function of the protein concentration and pH (**Fig. 11**). **Fig. 11** shows that changes in protein concentration do not significantly affect the β value given that the average of β value for the variation of the protein concentration is 0.87 ± 0.06 .

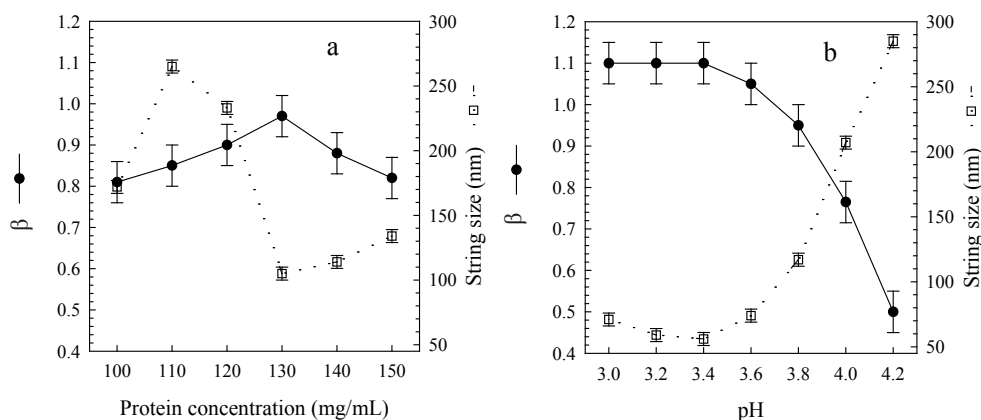


Figure 11: Dependence on the protein concentration at fixed pH 3.0 (**a**) and pH at a 100 mg/mL fixed protein concentration (**b**) of β value and the domain size obtained from the $g(r)$ data. The error bars of β value and the domain size are the acceptable experimental error of the fit to Eq. (2) and the size of the nanoparticles (10 nm iridium) used for coating the samples which is not more than ± 5 nm.

In this case, the standard deviation is close to the experimental error of ± 0.05 and this explains why the gels structure as function of protein concentration at constant pH 3.0 are similar at a larger correlation length (see inset of **Fig 10 a**).

The dependence of β as function of pH is shown in **Fig. 11**. It is clear from **Fig. 11 b** that changes in the structure are correlated to changes in the domain size ($P < 0.05$). From **Fig. 11 b**, the β remains constant between pH 3.0 and pH 3.6 which means that the gels at these pHs have comparable domain sizes. A sharp decrease of β is observed when the pH is increased above pH 3.6, coinciding with an increase in domain size (**Fig. 10**). The pH at which this microstructural transition occurs was found to be around pH 3.7 and this corresponds to a string size about 100 nm. Change in β value (1-1.5) has been observed in the case of β -lg gels when the pH was varied below the IEP²³ which suggest a general behavior in terms of globular protein-protein interaction below the IEP but the pH at which the structural transitioning between fine and coarse-strand/particulate gels occurs will depend on the type of the globular proteins.

From SEM image analysis, it can be concluded that no clear influence on the domain sizes is observed when the protein concentration is varied at a fixed pH, whereas the variation of the pH at a fixed protein concentration results in significant changes in pea protein network structures. Increase of pH from 3.0 to 4.2 promotes self-assembly of beads into strings rather than the growth of beads.

Changes in the network structure of pea protein gels are correlated to changes in the domain sizes as function of pH.

A summary of rheological transitioning in pea proteins gels related to structural changes

The changes in the recoverable energy were related to the changes in the network structure. The changes in the recoverable energy correlate to the changes in the string and bead sizes and the ξ_b observed in the quantitative analysis of the images based on SEM shown in **Figs. 10** and **11**. Beyond ξ_b of 117 nm, the recoverable energy was shown to reduce significantly. The ξ_b is closer to 100 nm, a ξ_b where structural transitioning of the pea protein networks was observed (**Fig 10**).

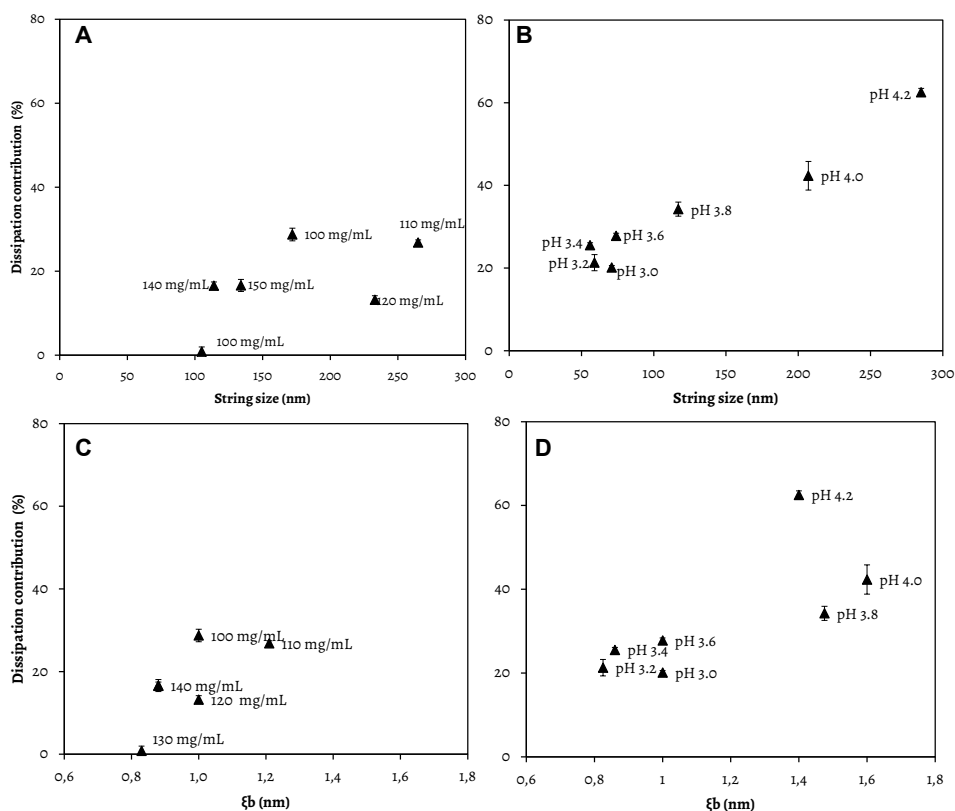


Figure 12: The proportion of energy that is directed towards dissipation as a function of correlation length based on the string sizes (**A**) and for gels prepared at varying protein concentration at a fixed pH and at a fixed 100 mg/mL protein concentration (**B**) and as a function of ξ_b for protein variation at fixed pH (**C**) and pH variation at a fixed concentration (**D**). The measurements were performed at a deformation speed of 1 mm/s. The error bars indicate SE calculated from SD of the variation of $n=5-6$ samples.

The results show that a structural changes from fine to coarse networks results in a lower ability to elastically store energy within pea protein networks. From the recoverable energy measurements, structural differences were shown to result in a significant impact on recoverable energy ($P < 0.05$).

An increase in the total energy directed towards dissipation increased with an increase in string size (**Fig. 12 B**) and ξ_b (**Fig. 12 D**) at a deformation speed of 1 mm/s. There was however, no clear trend in the dissipation contribution for gels prepared at a fixed pH at varying protein concentration as a function of string size (**Fig. 12 A**) and ξ_b (**Fig. 12 C**). The increase in dissipated energy with an increase in pH towards IEP is related to an increase in the pore sizes (**Fig. 8**) and the correlation length (**Fig. 10**) of the network structure.

From the small deformation results, it was shown that structural changes quantified by changes in ξ of pea protein networks as a result of changes in pH coincides with changes in G' , kinetics of gel formation, and $\Delta G'_{\text{heat}}/\Delta G'_{\text{cool}}$ ratios, although the G' is not significantly affected by an increase in the correlation length ($P > 0.05$). An increase in ξ_b up to 233 nm results in stiffer networks, and an increase in $\Delta G'_{\text{heat}}/\Delta G'_{\text{cool}}$ ratios. For the kinetics of gel formation (**Fig. 3 C and D**), a shift in the curves was observed for structures with a ξ_b of 74 and 117 nm, although the structural characterization of network structures that have a ξ_b of 74 nm did not show significant difference with network structures that have a ξ_b between 59 - 71 nm (**Fig. 10**), suggesting a mismatch between microstructural versus mechanistic transitions.

In relating the changes in the large deformation properties to the changes in the network structures, an increase in ξ_b resulted in a concurrent increase in the fracture strain. A decrease in the Young's modulus was observed which coincided with an increase in the coarseness of the gels (**Fig. 8**) and the ξ_b (**Fig. 10**). From the rheological measurements at large deformation, it can be concluded that changes in the coarseness of pea protein gels have an influence on the gel strength (fracture stress) and brittleness (fracture strain) of the gels due to variations in the correlation length of the domain sizes (**Fig. 10**).

Whereas, changes in ξ_b do not have an explicit impact on Young's modulus of the gels. The changes in the gel strength and brittleness as a result of changes in the correlation length of the network structure were also confirmed when paired sample test was performed on correlation length, fracture stress, and fracture strain data giving $P < 0.05$ (for fracture stress) and $P < 0.05$ (for fracture strain). A lack of a correlation between correlation length and the Young's modulus was also observed from the statistical analysis of these data ($P > 0.05$). A summary of the rheological responses that are influenced by structural changes of pea protein gels as a result of variation of protein concentration at a fixed pH, and variation of pH at a fixed protein concentration are shown in **Table 1**.

Table 1: Summary of rheological properties that change with structural changes of pea protein spatial gel networks from fine to coarse-stranded.

Gelling conditions	Modulus (G')	Modulus (E)	Fracture strain (ϵ_R)	Fracture stress (σ_f)	Recoverable energy (%)	SEM structure
pH 3.0, 100 mg/mL	+/-	+/-	+/-	+/-	+/-	Fine
pH 3.0, 110 mg/mL	+/-	+	+/-	+	+	Fine
pH 3.0, 120 mg/mL	+/-	+	+/-	+	+	Fine
pH 3.0, 130 mg/mL	+	+	+/-	+	+	Fine
pH 3.0, 140 mg/mL	++	+	+/-	+	-	Fine
pH 3.0, 150 mg/mL	++	+	+/-	+	-	Fine
pH 3.0, 100 mg/mL	+/-	+/-	+/-	+/-	+/-	Fine
pH 3.2, 100 mg/mL	+/-	+/-	+/-	-	+/-	Fine
pH 3.4, 100 mg/mL	+/-	+	+/-	-	+/-	Fine
pH 3.6, 100 mg/mL	+/-	-	+/-	-	+/-	Fine?*
pH 3.8, 100 mg/mL	++	-	-	-	+/-	Coarse
pH 4.0, 100 mg/mL	++	-	++	-	-	Coarse
pH 4.2, 100 mg/mL	++	-	++	-	-	Coarse

G' = storage modulus, E = Young's modulus, +/- = no effect, - = negative effect, + = positive effect, ++ = strong positive effect, ?* = no clear demarcation into fine or coarse networks. The dashed lines indicate the pHs around which the structural transitioning from fine-stranded to coarse-stranded networks occurs.

Conclusions

The objective of this study was to analyze quantitatively the network structure that underlines the transitioning in the mechanical responses of pea protein gels. The major findings from this study can be summarized as (i) varying the pH during the gel formation of pea proteins results in changes in the aggregate size of the proteins and structural changes in the network. (ii) the visco-elastic properties of pea protein gels are dependent on the protein concentration and on the pH at which pea protein gels are formed, which

correlate to the coarseness of the network structure. (iii), the fracture properties of pea protein correlate well with the structural changes of the protein gels as a result of changes in pH. (iv), structural changes as a result of changes in the pH affect the ability of pea proteins to elastically store energy. Less dense networks show a reduced ability to elastically store energy.

A structural change from finer to coarser pea protein networks occurs at around pH 3.7, at a correlation length of about 100 nm, where an influence on the mechanical deformation properties is clearly observed. Thus, it can be concluded that structural changes of pea protein networks are determined by the interplay between the growth of protein aggregates and the electrostatic interactions between the aggregates, and this has a major impact on resultant rheological responses of pea protein gels.

Acknowledgements

Jos Sewalt is acknowledged for the help with the milling of pea protein into flour. SEM imaging was carried out by Tiny Franssen-Verheijen. Jan Klok is appreciated for his help with CLSM imaging and Carsten Ersch for help with statistical analysis. Laurice Pouvreau is acknowledged for critically reading of the manuscript.

References

- (1) Pimentel, D.; Pimentel, M., Sustainability of meat-based and plant-based diets and the environment. **Am. J. Clin. Nutr.** 2003, **78**, 660S-663S.
- (2) Gharsallaoui, A.; Saurel, R.; Chambin, O.; Voilley, A., Pea (*Pisum sativum*, L.) Protein Isolate Stabilized Emulsions: A Novel System for Microencapsulation of Lipophilic Ingredients by Spray Drying. **Food & Bioprocess Technology** 2012, **5**, 2211-2221.
- (3) Manski, J. M.; van der Goot, A. J.; Boom, R. M., Advances in structure formation of anisotropic protein-rich foods through novel processing concepts. **Trends Food Sci. Technol.** 2007, **18**, 546-557.
- (4) Clark, A. H.; Kavanagh, G. M.; Ross-Murphy, S. B., Globular protein gelation—theory and experiment. **Food Hydrocolloid** 2001, **15**, 383-400.
- (5) Munialo, C. D.; van der Linden, E.; de Jongh, H. H. J., The ability to store energy in pea protein gels is set by network dimensions smaller than 50 nm. **Food Res. Int.** 2014, **64**, 482-491.
- (6) van Vliet, T., Large deformation and fracture behaviour of gels. **Curr. Opin. Colloid Interface Sci.** 1996, **1**, 740-745.
- (7) van den Berg, L.; Carolas, A. L.; van Vliet, T.; van der Linden, E.; van Boekel, M. A. J. S.; van de Velde, F., Energy storage controls crumbly perception in whey proteins/polysaccharide mixed gels. **Food Hydrocolloid** 2008, **22**, 1404-1417.
- (8) Çakir, E.; Daubert, C. R.; Drake, M. A.; Vinyard, C. J.; Essick, G.; Foegeding, E. A., The effect of microstructure on the sensory perception and textural characteristics of whey protein/κ-carrageenan mixed gels. **Food Hydrocolloid** 2012, **26**, 33-43.
- (9) van Vliet, T.; Luyten, H.; Walstra, P., **Fracture and yielding of gels**. 1991; p 392-403.
- (10) de Jong, S.; van Vliet, T.; de Jongh, H. J. H., The contribution of time-dependent stress relaxation in protein gels to the recoverable energy that is used as tool to describe food texture **Mech. Time-Depend. Mater.** 2015, *Submitted*.
- (11) Vardhanabhuti, B.; Foegeding, E. A.; McGuffey, M. K.; Daubert, C. R.; Swaisgood, H. E., Gelation properties of dispersions containing polymerized and native whey protein isolate. **Food Hydrocolloid** 2001, **15**, 165-175.
- (12) Thompson, A.; Boland, M.; Singh, H., **Milk proteins: from expression to food**. Academic Press: 2009.
- (13) Ikeda, S.; Morris, V. J., Fine-stranded and particulate aggregates of heat-denatured whey proteins visualized by atomic force microscopy. **Biomacromolecules** 2002, **3**, 382-389.
- (14) Langton, M.; Hermansson, A. M., Fine-stranded and particulate gels of beta-lactoglobulin and whey protein at varying pH. **Food Hydrocolloid** 1992, **5**, 523-539.
- (15) Hongsprabhas, P.; Barbut, S.; Marangoni, A. G., The Structure of Cold-Set Whey Protein Isolate

Gels Prepared With Ca^{++} . **LWT - Food Science and Technology** 1999, **32**, 196-202.

- (16) Gwartney, E. A.; Larick, D. K.; Foegeding, E. A., Sensory texture and mechanical properties of stranded and particulate whey protein emulsion gels. **J. Food Sci.** 2004, **69**, S333-S339.
- (17) Errington, A. D.; Foegeding, E. A., Factors determining fracture stress and strain of fine-stranded whey protein gels. **J. Agric. Food Chem.** 1998, **46**, 2963-2967.
- (18) Gueguen, J.; Chevalier, M.; And, J. B.; Schaeffer, F., Dissociation and aggregation of pea legumin induced by pH and ionic strength. **J. Sci. Food Agric.** 1988, **44**, 167-182.
- (19) Shand, P. J.; Ya, H.; Pietrasik, Z.; Wanasundara, P. K. J. P. D., Physicochemical and textural properties of heat-induced pea protein isolate gels. **Food Chem.** 2007, **102**, 1119-1130.
- (20) Sun, X. D.; Arntfield, S. D., Gelation properties of salt-extracted pea protein induced by heat treatment. **Food Res. Int.** 2010, **43**, 509-515.
- (21) Sun, X. D.; Arntfield, S. D., Dynamic oscillatory rheological measurement and thermal properties of pea protein extracted by salt method: Effect of pH and NaCl. **J. Food Eng.** 2011, **105**, 577-582.
- (22) Mehalebi, S.; Nicolai, T.; Durand, D., The influence of electrostatic interaction on the structure and the shear modulus of heat-set globular protein gels. **Soft Matter** 2008, **4**, 893-900.
- (23) Ako, K.; Nicolai, T.; Durand, D.; Brotons, G., Micro-phase separation explains the abrupt structural change of denatured globular protein gels on varying the ionic strength or the pH. **Soft Matter** 2009, **5**, 4033-4041.
- (24) Munialo, C. D.; Martin, A. H.; van der Linden, E.; de Jongh, H. H. J., Fibril formation from pea protein and subsequent gel formation. **J. Agric. Food Chem.** 2014, **62**, 2418-2427.
- (25) Munialo, C. D.; de Jongh, H. H. J.; Broersen, K.; van der Linden, E.; Martin, A. H., Modulation of the Gelation Efficiency of Fibrillar and Spherical Aggregates by Means of Thiolation. **J. Agric. Food Chem.** 2013, **61**, 11628-11635.
- (26) Ako, K.; Durand, D.; Nicolai, T.; Becu, L., Quantitative analysis of confocal laser scanning microscopy images of heat-set globular protein gels. **Food Hydrocolloid** 2009, **23**, 1111-1119.
- (27) Fredrich, J. T., 3D imaging of porous media using laser scanning confocal microscopy with application to microscale transport processes. **Physics and Chemistry of the Earth, Part A: Solid Earth and Geodesy** 1999, **24**, 551-561.
- (28) Munialo, C. D.; Ortega, R. G.; van der Linden, E.; de Jongh, H. H. J., Modification of Ovalbumin with Fructooligosaccharides: Consequences for Network Morphology and Mechanical Deformation Responses. **Langmuir** 2014, **30**, 14062-14072.
- (29) Danielsson, C., Seed globulins of the Gramineae and Leguminosae. **Biochem. J.** 1949, **44**, 387.
- (30) Renkema, J. M. S., Relations between rheological properties and network structure of soy protein gels. **Food Hydrocolloid** 2004, **18**, 39-47.

- (31) Bowland, E. L.; Allen Foegeding, E.; Hamann, D. D., Rheological analysis of anion-induced matrix transformations in thermally induced whey protein isolate gels. **Food Hydrocolloid** 1995, **9**, 57-64.
- (32) Ikeda, S.; Foegeding, E. A., Dynamic viscoelastic properties of thermally induced whey protein isolate gels with added lecithin. **Food Hydrocolloid** 1999, **13**, 245-254.
- (33) Weijers, M.; van de Velde, F.; Stijnman, A.; van de Pijpekamp, A.; Visschers, R. W., Structure and rheological properties of acid-induced egg white protein gels. **Food Hydrocolloid** 2006, **20**, 146-159.
- (34) Öhgren, C.; Langton, M.; Hermansson, A. M., Structure-fracture measurements of particulate gels. **J. Mater. Sci.** 2004, **39**, 6473-6482.
- (35) Brink, J.; Langton, M.; Stading, M.; Hermansson, A.-M., Simultaneous analysis of the structural and mechanical changes during large deformation of whey protein isolate/gelatin gels at the macro and micro levels. **Food Hydrocolloid** 2007, **21**, 409-419.
- (36) Walstra, P., **Physical chemistry of foods**. CRC Press: 2002; Vol. 121.
- (37) Renkema, J. M. S.; Gruppen, H.; van Vliet, T., Influence of pH and ionic strength on heat-induced formation and rheological properties of soy protein gels in relation to denaturation and their protein compositions. **J. Agric. Food Chem.** 2002, **50**, 6064-6071.

Chapter 6

Modification of ovalbumin with fructooligosaccharides: consequences for network morphology and mechanical deformation responses

This chapter investigates how the mesh size of ovalbumin variants can be manipulated to result in changes in the rheological responses of protein gels. To change the morphology of the network structure, ovalbumin was modified with fructooligosaccharide (FOS) moieties via the Maillard reaction. Subsequently, gels were formed from FOS-modified ovalbumin variants with non-modified variants being used as control samples, following heating of the samples at 95 °C, 30 min. Differences in the network morphology were visualized by scanning electron microscopy for FOS-modified ovalbumin samples. The large deformation properties of the gels showed that FOS-modified gels had lower fracture stress, lower fracture strain, and lower Young's modulus than non-modified variants. The recoverable energy of the gels decreased with an increase in the degree of modification. The results show that the attachment of FOS to ovalbumin changes the structural and mechanical deformation properties of heat-set protein gels.

This chapter is published as:

Munialo, C.D.; Ortega, R. G.; van der Linden, E., de Jongh, H. H. J. Modification of Ovalbumin with Fructooligosaccharides: Consequences for Network Morphology and Mechanical Deformation Responses. *Langmuir* **2014**, 30, (46), 14062-14072.

Introduction

The increase of the global population has consequences on the demand for food which can result in a constraint on food supply and a reduction in the availability of balanced diets including protein-rich foods. This provides a challenge to the food industry to diversify on the available protein sources. This diversification can be achieved by introducing new ingredients or reformulation of already existing products. This can however result in variations of the product's textural properties which determines an important part of the quality and consumer acceptance of foods¹.

Egg white proteins (albumins) are applied in a wide range of foods because of their functional properties. For most functional applications of egg white proteins, denaturation, and aggregation of the protein is required². At sufficiently high protein concentrations, denaturation and aggregation events can result in the formation of a spatial gel network. The formation of a spatial gel network is the result of thermally-induced (partial) unfolding of the native protein, and as a consequence, aggregation of the protein occurs upon heating, leading to the formation of a gel network³. The ability of egg white proteins, including ovalbumin as the main constituent, to form gels upon heating is important for its textural contribution in foods⁴. Studies on the thermal denaturation, aggregation, and gel network formation of ovalbumin can be found elsewhere^{2, 5}.

From the texture point of view, the determination of the mechanical (large) deformation and fracture properties of protein gels is essential⁶. Large deformation and fracture properties of food gels are important quality characteristics determining the functional properties such as handling and cutting⁷. Additionally, oral processing and mouthfeel/sensory perception of foods are influenced by large deformation mechanics⁸.

The fracture and macroscopic breakdown properties of gels can be explained by the energy balance in the materials⁹. When gels are subjected to deformation, all the energy exerted for deformation is stored elastically unless it dissipates for example due to viscous flow and friction process between different components of the gels, or is directed towards fracture¹⁰. The processes that may lead to dissipation of the energy¹¹ are detailed in equation 1:

$$W_{\text{(dissipated)}} = W_{\text{fr}} + W_{\text{db}} + W_{\text{mf}} + W_{\text{sf}} + W_{\text{pd}} + W_{\text{sr}} \quad (1)$$

where W_{fr} represents the energy that is dissipated via fracturing events, W_{db} is the energy that causes de-bonding of physical contacts that form the network, W_{mf} represents energy that is dissipated via friction, W_{sf} represents the contribution of viscous serum flow, W_{pd} is plastic deformation contribution, and W_{sr} relaxation of the structure elements. The detailed explanation of how these dissipation modes contribute to energy loss can be found elsewhere¹². The energy that is stored elastically during deformation is referred to as recoverable energy⁹. The “recoverable energy” has been related to mouthfeel properties of food gels, such as crumbliness⁸.

In relating the large deformation properties of gels to the network characteristics, the characterization of the structural aspects of the network is important. The structural aspects dominating a gelled network include:- strand thickness^{13, 14}, strand stiffness¹⁵, the interaction energy in the interaction points of the individual strands making up the spatial structure¹⁴, and the mesh size, which is described as the void or distance between filaments, strands or network constituents¹⁶. Obviously, by modulating the network formation one or more of these aspects will be affected.

Modification of various proteins such as ovalbumin has been achieved in the past by several mechanisms such as thiolation¹⁷, and acetylation¹⁸. A number of attempts have been made to improve the functional properties of proteins using a reaction that involves the coupling of sugar moieties to the proteins via Maillard reaction¹⁹. The Maillard reaction of proteins is a spontaneous reaction that can take place during food processing and storage and can result in the formation of a wide variety of end products¹⁹. Maillardation is based on the reaction between a reducing end of a sugar and a free amino group in proteins mainly the ϵ -amino group of lysines as depicted in **Fig. 1**.

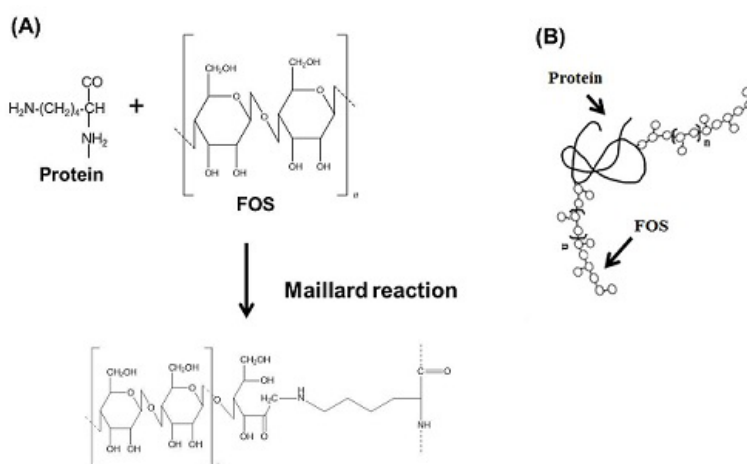


Figure 1: Schematic representation of the condensation of a protein and a FOS through the Maillard reaction (A), and the resulting conjugate (B). Adapted from the work of Kato and co-workers (2002)²⁰. FOS graphic in Fig. 1 was drawn using ChemBioDraw ultra 12.0 (PerkinElmer Inc., Massachusetts, USA).

Maillardation generally results in improved gelling properties²¹ and reduced allergenicity of ovalbumin²². However, the effect of Maillard reaction on the structural aspects of ovalbumin networks, in particular the mesh size, and the mechanical deformation properties of ovalbumin gels, including the ability of the gel networks to elastically store energy has not been reported.

An understanding of how the structural aspects of ovalbumin gels can be modulated from a chemical and material science point of view, to result in the variation in the mechanical deformation properties of the gels is however essential, as this can result in the formulation of products that have desirable physical (textural) and sensorial attributes.

The objective of this study was to evaluate how the conjugation of oligo-sugar moieties onto ovalbumin affects the aggregation, and network morphology, and consequently the large deformation properties of ovalbumin gel networks, including the ability of the networks to elastically store energy. To achieve this, a limited number of bulky sugar moieties (fructooligosaccharides) were covalently linked to some of the primary amine groups of lysine residues of ovalbumin via the Maillard reaction. The linking of the oligo-sugar moieties was used as a tool to modulate the structural aspects of ovalbumin networks, in particular, the mesh size, in order to relate the changes in the network structure to the mechanical deformation properties, and the ability of the networks to elastically store energy. Analytical characterization of non-modified and modified ovalbumin variants was carried out using sodium dodecyl sulfate polyacrylamide gel electrophoresis (SDS-PAGE). Conformational analyses of ovalbumin variants were carried out spectroscopically using circular dichroism (CD), and intrinsic tryptophan fluorescence. Changes in the microstructure were visualized using scanning electron microscopy (SEM), whereas mechanical deformation properties of ovalbumin gels were determined using uniaxial compression.

Experimental

Materials

Albumin (A5503) from chicken egg white (ovalbumin) (grade V, > 98 % pure by agarose electrophoresis, crystallized and lyophilized, Lot # SLBB4340V), ortho-phthaldialdehyde (OPA), acetone, NaOH pellets, HCl, N,N-dimethyl-2-mercaptoethyl-ammonium chloride (DMA), di-sodium tetraborate decahydrate (Borax), sodium dodecyl sulfate (SDS), uranyl acetate, glutaraldehyde, and dimethyl sulfoxide (DMSO) were obtained from Sigma-Aldrich (Steinheim, Germany). Frutafit[®] HD with an average degree of polymerization (DP) of ~10 and a content of fructooligosaccharides (FOS) \geq 92 %, produced by the partial enzymatic hydrolysis of chicory inulin, was provided as a gift by Sensus (Roosendaal, the Netherlands). Sodium nitrite (NaNO_2) and paraffin oil were obtained from Merck (Darmstadt, Germany). All reagents were of analytical grade and used without further purification. All solutions were prepared with MilliQ water.

Preparation of ovalbumin protein solutions

Native ovalbumin solutions were prepared by dispersing 50 mg/mL ovalbumin powder in MilliQ water (Millipore Corp., Billerica, MA), followed by adjusting the solutions to pH 7 using 1 M HCl. The solutions were then stirred at 4 °C, 300 rpm, overnight.

Subsequently, the protein solutions were centrifuged at $20000 \times g$ for 30 min at 4 °C. The supernatant was filtered through a 0.45 µm (Millex-SV, Millipore Corp., Bedford, MA) filter. Determined protein concentrations after centrifugation and filtration using DUMAS (NA 2100 Protein, CE instruments, Milan, Italy) with a conversion factor of 6.25 showed that negligible protein losses occurred during these processes. These protein solutions were used in the Maillardation of ovalbumin with FOS.

Maillardation of ovalbumin with FOS

Maillardation was carried out on ovalbumin as previously described²³. Ovalbumin solutions at pH 7 were mixed with 9 wt % FOS solutions to give a final molar ratio of about 3:1 FOS-reducing ends relative to the number of primary amino groups of the protein (assuming a molecular mass for FOS of 1800 Da from an average DP ~ 10). The pH of the mixture of ovalbumin and FOS was adjusted to pH 8.0 ± 0.1 using 1 M NaOH. The mixed solutions (ovalbumin + FOS) at pH 8 were freeze-dried at 50 mbar at -50 °C for 48 h (Christ Alpha 2-4 LD plus, Shropshire, UK), and the freeze dried powders were incubated at 60 °C in an oven (Fischer Scientific Venticell 111, MMM Medcenter, Belgium) at a relative humidity (RH) of 65 % (exposed to a saturated NaNO₂ solution) for 0, 24, 48, and 72 h. Following the incubation step, dry-powders were resuspended in MilliQ water and subsequently dialyzed (membrane cutoff 12 - 14 kDa) against MilliQ water at 4 °C. Finally, the samples were freeze-dried and stored at -20 °C until use. Prior to each experiment the material was checked for the degree of modification to ensure the stability of the product. Control samples were also prepared by incubation (dry-heating) of the protein solutions without FOS under similar conditions and for the equivalent time intervals as described. Maillardation carried out in this way resulted in the formation of four modified ovalbumin variants. Four control variants were also prepared. Maillard reaction was carried out in dry form as opposed to aqueous dissolved method as the dry method of modification has been reported to have a less damaging effect on the structural integrity of the protein²⁴ and to result in better reproducibility of the modification procedure²⁵ compared to heat treatment in solution.

Analytical methods for characterization of ovalbumin variants

The number of primary amines (lysines and the protein N-terminal amine groups) was determined using chromogenic ortho-phthaldialdehyde (OPA) assay as previously described²⁶. A standard curve was constructed using L-lysine and the number of available amino groups in ovalbumin was calculated as follows:

$$\text{Available amino groups} = \frac{\frac{X}{L_{mw}} \cdot 2}{\frac{1}{P_{mw}}} \quad (2)$$

where x is the value obtained in the equation of the standard curve, L_{mw} , the lysine molecular weight, and P_{mw} , the molecular weight of ovalbumin. Chromogenic OPA assay was carried out in duplicate and the results were used to determine the degree of modification (DM),

defined as the number of moles of FOS attached per mole of monomer of protein.

The molecular weight of ovalbumin variants at an approximate concentration of 10 mg/mL was estimated using sodium dodecyl sulfate polyacrylamide gel electrophoresis (SDS-PAGE) under reducing conditions according to a previously described procedure²⁷. Ready to use homogenous 4 - 12 % NUPAGE® NOVEX® Bis-Tris gels (Invitrogen, France) were used. MOPS-SDS (20 ×) buffer was used as a running buffer. Electrophoresis conditions were 200 V, 10 mA throughout at 20 °C and 50 min running time. Following separation, the proteins were fixed and stained using the Simply Blue™ Safe stain and developed to obtain a suitable background color. The apparent molecular weights of the present proteins were determined by comparison to the molecular weight standard (Sigma wide range molecular weight markers, 6 - 200 kDa) applied into a separate lane.

Conformational analysis of ovalbumin variants

Far-UV circular dichroism (CD) spectra of 0.1 mg/mL ovalbumin samples at pH 7 were recorded at 20 °C in the spectral range from 190 to 260 nm with a spectral resolution of 0.5 nm on a Jasco J-715 spectropolarimeter (Jasco Corporation, Japan) according to a previously described procedure²⁷. Spectra were recorded as averages of twenty scans. The scanning speed was 100 nm/min, and the response time was 0.125 s with a bandwidth of 1 nm. Quartz cuvettes with an optical path of 0.1 cm were used. The spectra were corrected for that of protein-free sample. Noise reduction was applied to the recorded spectra based on the inverse Fourier transformation method using the supplier's software. The far-UV CD spectra of ovalbumin variants were analyzed for the secondary structural elements using non-linear least-squares fitting procedure as previously described²⁸.

Intrinsic tryptophan fluorescence spectra of 50 µg/mL ovalbumin samples in MilliQ water were obtained using a Cary eclipse fluorescence spectrophotometer (Agilent technologies, the Netherlands) according to a previously described procedure²⁹. The spectra of the samples were recorded at the excitation wavelength of 280 nm, and the emission wavelength range from 300 to 400 nm at 20 °C with a resolution of 1 nm. Quartz cuvettes with an optical path of 1 cm were used. The excitation and emission slit widths were 5 nm and a scan speed of 120 nm/min was used. Typically, three spectra were recorded and averaged.

Preparation of ovalbumin protein gels

Preparation of protein gels from ovalbumin variants was carried out as previously described³⁰ with modifications in which solutions of 120 mg/mL protein concentration were prepared by dispersing control and modified freeze-dried ovalbumin variants in MilliQ water. The solutions were adjusted to pH 7, and the samples were degassed, and transferred to 5 mL syringes (Terumo Corporation, Leuven, Belgium) whose walls had been previously coated with paraffin oil for lubrication. The solutions were heated at 95 °C in a water bath for 30 min, followed by cooling at room temperature (20 ± 2 °C) overnight.

Prior to testing, the gels were sliced to cylindrical shapes with an adapted gel slicer. Obtained cylindrical specimen were 10 mm in height and 12.9 mm in diameter with a contact area 130.6 mm². Specimens were prepared in triplicate.

Characterization of the microstructure of ovalbumin protein gels

Gels for scanning electron microscopy (SEM) were prepared in cut pipette tips according to a previously described procedure³⁰. After gelation, the gels in pipette tips were cross-linked in a 1 % glutaraldehyde solution for 8 h. Subsequently, excess glutaraldehyde was removed by placing the tips overnight into MilliQ water. The MilliQ water was replaced by 50 % dimethyl sulfoxide (DMSO) in 3 steps - 10, 20, and 50 % DMSO in water solutions. The samples were subsequently frozen in liquid nitrogen followed by peeling the tips away from the gels and the remaining gels being cut into slices. The slices from the middle of the gels were thawed in the 50 % DMSO in water solution. The DMSO was replaced with MilliQ water in several steps, and subsequently the MilliQ water was replaced with acetone in a few stages. The samples in acetone were dried by critical point drying (CPD 030 BalTec, Liechtenstein) in which the acetone was replaced with liquid carbon dioxide under pressure in five steps to ensure complete replacement. The samples were glued onto a SEM sample holder using carbon glue (Leit-C, Neubauer Chemicalien, Germany), and subsequently stored overnight under vacuum. After drying of the carbon cement, the samples were sputter coated with 10 nm iridium in SCD 500 (Leica EM VCT 100, Leica, Vienna, Austria) prior to imaging. All samples were analyzed with a field emission scanning electron microscope (Magellan XHR 400L FE-SEM, FEI, Eindhoven, the Netherlands) at room temperature (20 ± 2 °C) at a working distance of 4 mm with SE detection at 2 kV. Images were digitally recorded. The apparent aggregate size, the strands thickness, and the distance from one strand (filament) of the network structure to the other was measured by the use of the public domain ImageJ[®] software (National Institutes of Health, Bethesda, MD)³¹ using a custom made macro-instruction (not shown).

Mechanical breakdown of ovalbumin gels

Uniaxial compression

To determine the fracture properties of ovalbumin gels, compression tests were performed on cylindrical gel specimens compressed by a texture analyzer fitted with a 5 kg load cell and P/75 probe (TA.XTPlus, Stable Micro Systems, Surrey, UK). The fracture properties that include the true fracture stress (σ) and the true fracture strain (**Hencky**) (ϵ_H) were studied by uniaxial compression test up to a 90 % deformation at a rate of 1 mm/s. The true fracture stress and true fracture strain, which will be designated as the fracture stress and fracture strain throughout this paper, were calculated at each point from time zero to time of final deformation as follows:

$$\text{Fracture stress: } \sigma_t = \frac{F}{A_i} \times \frac{(L_i - \Delta L)}{L_i} \quad (3)$$

$$\text{Fracture strain: } \epsilon_H = \ln \left(\frac{L_i}{L_i - \Delta L} \right) \quad (4)$$

where F is the force measured during compression (N), A_i is the initial contact area of the specimen (m^2), L_i is the initial specimen height (m), and ΔL is the absolute deformation (m)⁹. The Young's modulus was calculated from the slope of the linear region of the stress-strain curve as previously described⁹.

Recoverable Energy

The recoverable energy measurements were carried out on the specimen using the above described Texture Analyzer according to a previously described procedure³⁰. Fifty percent of the maximum strain before fracture was applied to determine the energy release during relaxation at a deformation speed of 1 mm/s. The percentage of recoverable energy of the gels was calculated from the area under the force-deformation curve as being the ratio of the amount of energy that was recovered after applying the stress and the amount of energy that was applied during the compression of the gels⁸.

Statistical Evaluations

Correlations in experimental data were evaluated with paired sample test using SPSS statistical package (version 19, International Business Machines, Armonk, NY, USA). All tests were carried out at 95 % confidence interval. $P < 0.05$ means that there is a significant difference in the results. Each analysis was performed in triplicate.

Results and Discussion

To be able to evaluate how the attachment of oligo-sugar moieties onto ovalbumin affect its aggregation, and network morphology, and consequently the large deformation properties, ovalbumin was modified by conjugating some of the amino groups with fructooligosaccharide (FOS) sugar moieties via Maillard reaction. Modification of ovalbumin yielded four modified variants. Control variants were also prepared by incubation (dry-heating) of the protein solutions without FOS. The control (non-modified) ovalbumin variants will be referred to as OVA-Co, OVA-C24, OVA-C48, and OVA-C72, whereas the modified variants will be referred to as OVA-Mo, OVA-M24, OVA-M48, and OVA-M72. Where the numbers describe the incubation time during the Maillardation.

Table 1: Chemical characterization of ovalbumin samples modified with a ratio of 3:1 FOS-reducing ends: amines is shown in **Table 1**. The number of free amino groups (%), the DM (%), and the number of FOS linked per ovalbumin molecule (Mean \pm SD) were obtained by OPA assay following the incubation of the samples at 0, 24, 48, and 72 h at 60 °C, and 65 % relative humidity in the presence of FOS. The control sample (OVA-Co) was neither treated by FOS nor incubated.^a

	Dry heating time (h)	Free amino group (%)	DM (%)	FOS linked/OVA (mol/mol)
OVA-Co	0	100 \pm 0.9	0 \pm 0.0	0
OVA-M0	0	98 \pm 0.8	2 \pm 0.8	0
OVA-M24	24	83 \pm 1.8	17 \pm 0.8	3
OVA-M48	48	76 \pm 2.9	24 \pm 3.0	4
OVA-M72	72	70 \pm 1.8	30 \pm 2.0	5

Characterization of ovalbumin variants

The degree of modification (DM) as determined from the number of non-reacted ϵ -amino groups in control and modified ovalbumin variants using the OPA analysis as a function of time (h) are presented in **Table 1**. Longer incubation times were shown to promote the degree of covalent coupling of FOS to ovalbumin. A gradual decrease of free amino groups with increasing dry-heating incubation time was observed for ovalbumin incubated in the presence of FOS. The decrease in free amino groups was higher during the first 24 h (where a decrease in the number of free amino groups from 98 to 83 % was observed), compared to samples incubated for 48 h (where the number of free amino groups decreased from 83 to 76 %), and 72 h (where the number of free amino groups decreased from 76 to 70 %) (**Table 1**). The results show that the number of free amino acids in ovalbumin decreased with an increase in the incubation times. The reason for decrease in the free amino groups with an increase in the incubation period could be that, (i) during the early stages of the Maillard reaction, FOS will first react with the most reactive amino groups available. Upon prolonged incubation the availability of reactive groups decreases, and thereby the reaction rate, and that (ii), given that the N-terminal α -amino group of ovalbumin is acetylated, all the free amino groups of ovalbumin that may become modified originate from the ϵ -amino groups of its 20 lysine residues²² and, as ovalbumin is a globular protein, most of the lysine residues are buried²², which could restrict the amino groups from reacting with FOS for the Maillard reaction to occur.

The total FOS moieties linked per ovalbumin molecule were calculated by dividing the number of modified amino groups with the total number of amino groups present in ovalbumin. The results showed that the modification of ovalbumin with FOS leads to the formation of conjugates with an ensemble-averaged number of three FOS moieties linked per ovalbumin molecule for OVA-M24, four for OVA-M48, and five for OVA-M72 as listed in **Table 1**. The formed conjugates were relatively stable, as prolonged storage (weeks) of the materials in dry form at -20 °C did not result in lower DM (Results not shown).

Covalent linkage of FOS to ovalbumin gave rise to a higher molecular weight as analyzed using gel electrophoresis. The electrophoretogram of ovalbumin variants is shown in **Fig. 2**. Monomers present in native ovalbumin are shown in the band that appears at around 45 kDa, although a small contribution of dimers was also observed at around 90 kDa in lane 2 for OVA-Co.

From **Fig. 2**, it can be observed that with an increase in incubation times, dimer bands gradually increased in intensity for both control samples not treated with FOS but incubated for up to 48 h (lane 3) and 72 h (lane 4); and Maillardated ovalbumin variants OVA-M48 (lane 7) and OVA-M72 (lane 8). This gives an indication of the formation of dimers during processing at moderately elevated temperatures.

Analysis of the structural integrity of ovalbumin variants

To study whether modification had an impact on the conformation of the protein, and thereby possibly on the aggregation propensity, the secondary and tertiary structural levels of ovalbumin were evaluated.

The changes in secondary structure of control (non-modified) and modified ovalbumin variants were assessed using far-UV CD (**Fig. 3 A**). The spectrum of control ovalbumin incubated for 0 h without FOS (OVA-Co) showed a positive extreme around 195 nm, two minima around 222 and 208 nm, and a zero crossing at 204 nm, indicative of a secondary structure that is dominated by β -sheets, with a substantial amount of α -helices. This was corroborated by the analysis of the secondary structure using non-linear least-squares fitting²⁸, (giving estimates of about 60 % and 30 % for β -sheet and α -helix respectively).

There were no significant changes in far-UV CD spectra of control samples incubated for up to 48 h without the addition of FOS (Results not shown) as well as control samples incubated for 72 h as shown in **Fig. 3 A**. Incubating ovalbumin variants with the addition of FOS did not result in significant changes in the far UV-CD spectra (**Fig. 3 A**). The results show that the applied treatments, either in the absence or presence of FOS do not affect the secondary structure of the protein.

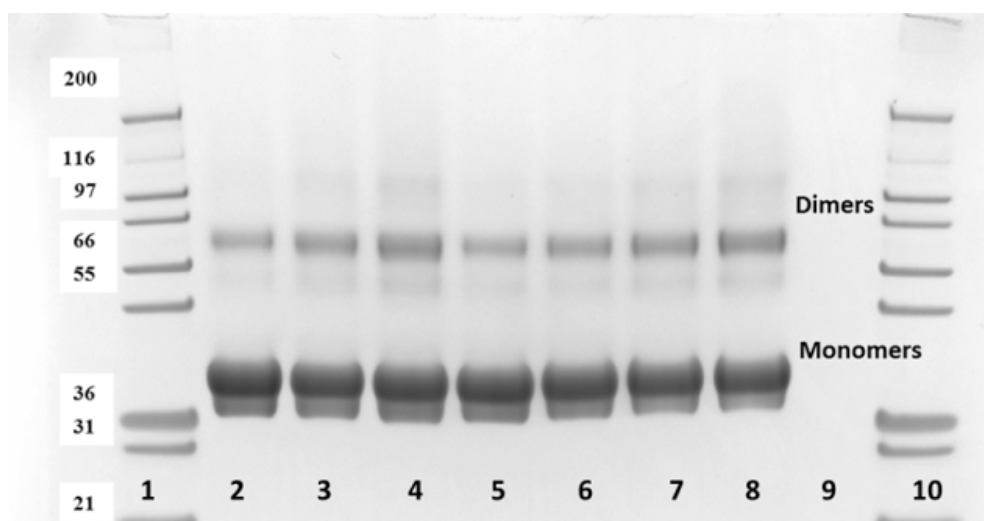


Figure 2: SDS-PAGE electrophoretograms are shown in Fig. 2 for the standard marker (lanes 1 and 10), OVA-Co (lane 2), OVA-C48 (lane 3), OVA-C72 (lane 4), OVA-Mo (lane 5), OVA-M24 (lane 6), OVA-M48, (lane 7), and OVA-M72 (lane 8).

To obtain information on the possible unfolding of ovalbumin upon modification, changes at the tertiary folding level were assessed by monitoring the microenvironmental changes of tryptophans within the protein using intrinsic tryptophan fluorescence. The spectra of ovalbumin variants are shown in **Fig. 3 B**. A fluorescence emission maximum was found at 334 nm in the native ovalbumin molecule (OVA-Co) as well as in the sample in which FOS was added but was not incubated (OVA-Mo) (**Fig. 3 B**). There were also no significant changes in the maximum fluorescence spectra for samples incubated without the addition of FOS (control samples) and incubated for up to 48 h (Results not shown) as well as in OVA-C72 as shown in **Fig. 3 B**. Additionally, no significant shift in the spectra was observed following the incubation of ovalbumin for up to 48 h without the addition of FOS (Results not shown) as well for 72 h (OVA-C72) control (**Fig. 3 B**). Upon modification of ovalbumin to various degrees, no significant shift in the shape and position of the maximum fluorescence spectra was observed, as the modified ovalbumin variants possessed the same emission maximum of 334 nm (**Fig. 3 B**). A decrease in the relative fluorescence intensity of ovalbumin variants was however observed upon modification of the samples (**Fig. 3 B**).

The decrease in the fluorescence intensity upon oligofructosylation could be related to the shielding effect of the FOS chains attached to ovalbumin variants, resulting in lower energy transfer efficiency between tyrosines and tryptophans. A similar decrease in fluorescence intensity was observed upon modification of β -lactoglobulin (β -lg) with cyclodextrins³².

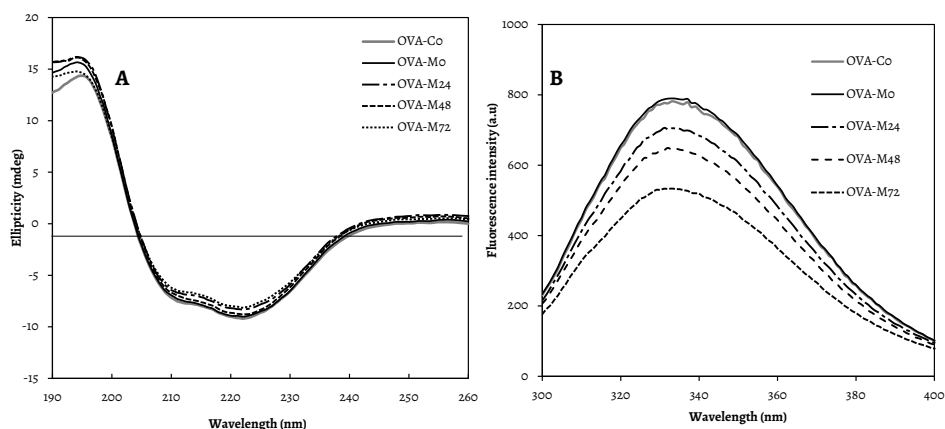


Figure 3 A shows that analysis of the secondary structural elements by far UV-CD of OVA-Co, OVA-Mo, OVA-M24, OVA-M48, and OVA-M72. Analysis of tertiary structural elements by intrinsic tryptophan fluorescence of OVA-Co, OVA-Mo, OVA-M24, OVA-M48, and OVA-M72 as obtained by intrinsic tryptophan fluorescence are shown in **Fig. 3 B**. The far-UV and intrinsic tryptophan fluorescence spectra of OVA-Co, and OVA-C72 are included in both **Fig. 3 A** and **B**.

From the results of the analysis of the structural integrity of ovalbumin variants, it can be concluded that the secondary and tertiary structure of ovalbumin is not affected by modification, and that there are no indications that the different ovalbumin variants will act differently in a heat-induced aggregation process to result in the formation of spatial gel networks.

Effect of modification on the microstructure of ovalbumin gels

Following heating of 120 mg/mL ovalbumin solutions at pH 7.0 (95 °C, 30 min), self-supporting gels were formed from ovalbumin variants. Visually, gels prepared from both control and modified ovalbumin variants were transparent, although the modified ovalbumin variants were brown to brown-yellowish in color compared to non-modified variants (Results not shown).

The microstructure of the gels obtained from the different ovalbumin variants was visualized by use of SEM (**Fig. 4**).

The network structures prepared from control ovalbumin variants were different from network structures prepared from modified ovalbumin variants.

The aggregates constituting the network structures from native ovalbumin (OVA-Co) were denser than the modified ovalbumin variants, and had shorter distances between the junctions connecting each strands.

Similarly, the aggregates constituting the network structures of OVA-C72, and OVA-M24 were denser and had shorter distances between the junction zones connecting each strand than the highly modified variants (**Fig. 4 b**). With higher DM (OVA-M48 and OVA-M72), more open network structures with finer (thinner) strands, and longer (larger) distance between the junctions connecting the strands are formed compared to the network structures of the OVA-Co, OVA-C72, and OVA-M24 ovalbumin variants (**Fig. 4 a and b**). The apparent aggregate size, and strand thickness, as determined by ImageJ analysis decreased with an increase in the DM (**Table 2**), whereas, the distance between the junctions connecting strands, i.e. the apparent mesh size, increased with an increase in the DM (**Fig. 4 b**). The microstructural characterization of ovalbumin variants shows that increasing modification of ovalbumin causes an increase in apparent mesh size and a reduction in apparent strand thickness.

To characterize the local sizes of the aggregates that constitute the networks, analysis of the images obtained from ovalbumin variants was carried out on the SEM samples by calculating the pair correlation function ($g(r)$) of 3 images per sample using Eq. (5) as described in detail³³ on 874×874 pixels images. To reduce the dimensional effect, an average of the dark intensity from the raw images represented by the threshold level was measured and subtracted from the images.

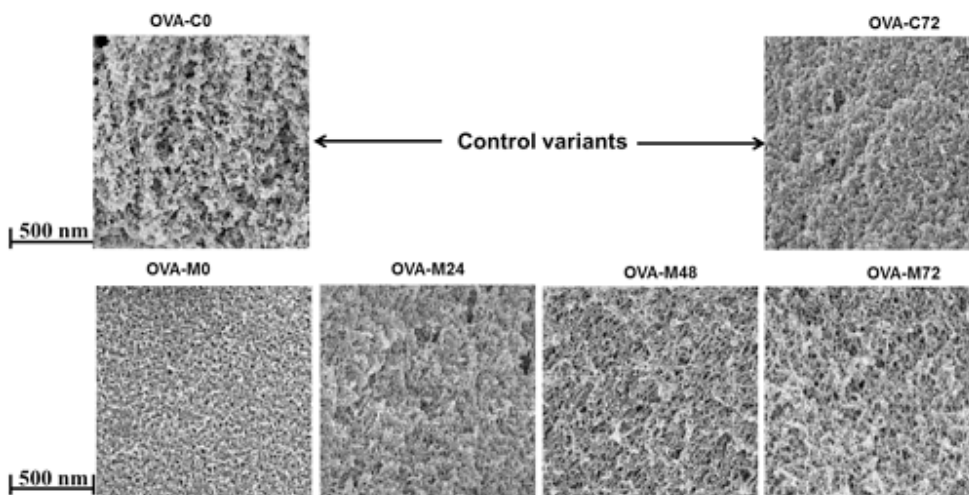


Fig. 4a

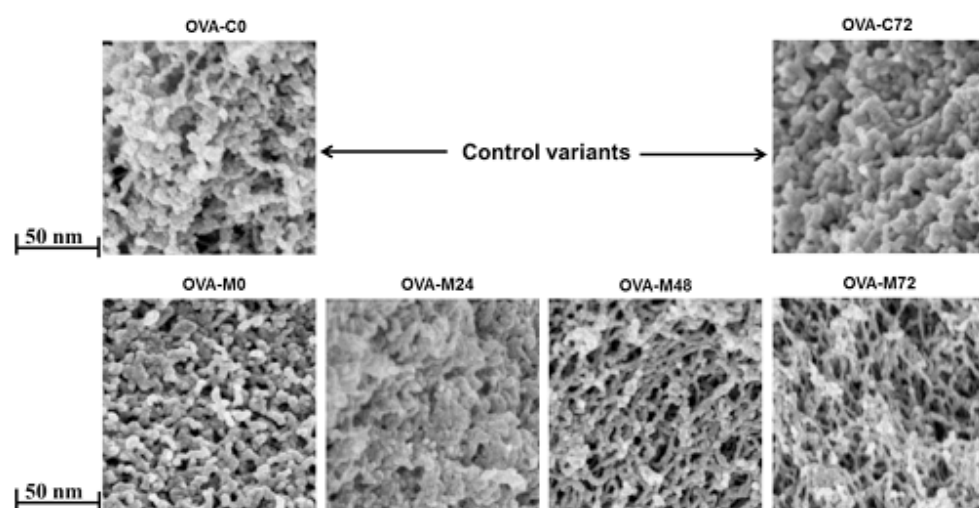


Fig. 4b

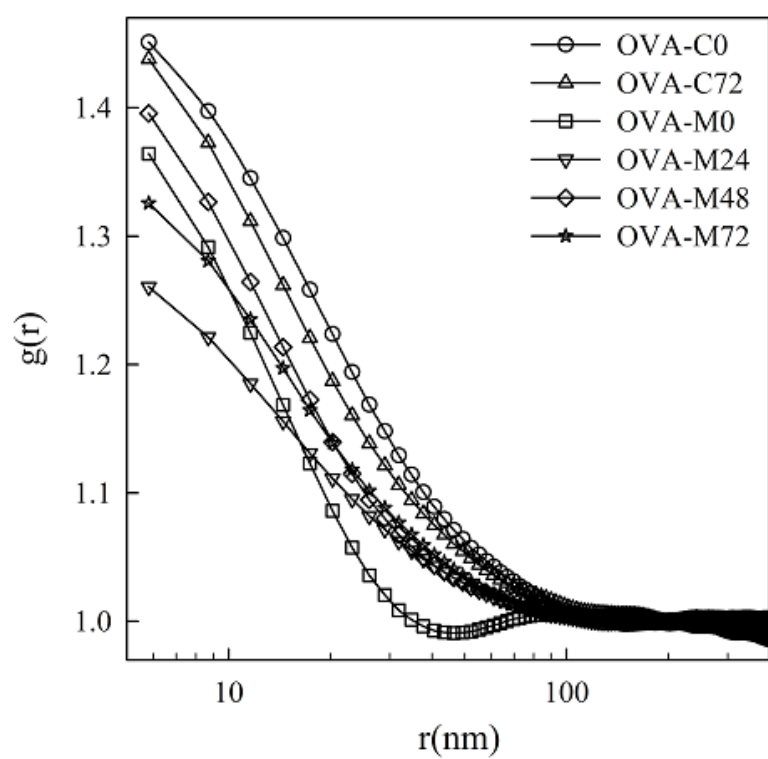


Fig. 4c

Figure 4: SEM micrographs of ovalbumin gels prepared from OVA-Mo, OVA-M24, OVA-M48, and OVA-M72 variants are shown in **Figure 4**. OVA-Co and OVA-C72 were included to study the effect of dry heating to ovalbumin samples as shown in **Figure 4 a**. The scale bars represent 500 nm. **Figure 4 b** is a zoom into the OVA-C72, OVA-Mo, OVA-M24, OVA-M48, and OVA-M72 SEM micrographs. The scale bars represent 50 nm. For practical reasons, OVA-C24 and OVA-C48 variants were not included in the SEM analysis. **Figure 4 c** shows the semi-logarithmic representation of the pair correlation functions of ovalbumin variants OVA-Co, OVA-C72, OVA-Mo, OVA-M24, OVA-M48, and OVA-M72. The solid lines represent fits to Eq. (6).

$$g(r) = \frac{\sum_{i=1}^n \sum_{j=1}^m I_i I_j}{\sum_{i=1}^n I_i \sum_{j=1}^m I_j} \quad \text{with} \quad r = \left| \vec{i} - \vec{j} \right| \quad (5)$$

The fits through the data shown in **Fig. 4 c** are a stretched exponential function of Eq. (6): where g_0 is the contrast value at $r \rightarrow 0$, ξ the correlation length that characterizes the size of the domains, and β the stretched factor that characterizes the way the $g(r)$ decreases.

$$g(r) = g_0 \cdot e^{-(r/\xi)^\beta} + 1 \quad (6)$$

The ξ and β are shown in **Table 2**. The almost similar β shows that the $g(r)$ for ovalbumin variants could be superimposed within the experimental error by horizontal and vertical shifts. The ξ results show that the sizes of the local domains constituting the networks do not vary significantly (ξ values between $14 - 17 \pm 5$ nm) with an increase in DM (**Table 2**). The $g(r)$ profile shows a decrease in the local sizes of the aggregates from large (OVA-Co) to smaller aggregates (OVA-M72) where $g(r)$ is unity at a value that characterizes the size of the domains. This behavior means that interconnection of small domains dominate the structure which reduces with an increase in the DM.

Effect of modification on mechanical deformation properties of ovalbumin gels

To establish whether the microstructural changes observed in **Fig. 4** affect the mechanical deformation properties of ovalbumin spatial gel networks, the large deformation properties such as the fracture stress, fracture strain, and Young's modulus, of gels prepared from control and modified ovalbumin variants were determined as presented in **Fig. 5**.

Fracture stress

Fracture stress gives an indication of gel strength³⁴. Changes in the gel strength of ovalbumin variants are shown in **Fig. 5 A**.

There was an initial decrease in gel strength for gels prepared from OVA-C24 when compared to OVA-Co. With an increase in incubation time of ovalbumin variants without FOS, the gel strength increased. The gel strength of control ovalbumin variants was higher than that of variants incubated with FOS (**Fig. 5 A**). Upon incubation of ovalbumin in the presence of FOS, an initial decrease in fracture stress (gel strength) was observed in gels prepared from OVA-Mo.

Table 2: Changes in the apparent mesh size, apparent strand thickness (nm), ξ characterizing the size of the domains, and the β (Mean \pm SD) as measured by the use of ImageJ for scanning electron micrographs obtained from gels prepared from ovalbumin variants that were incubated in the presence of FOS and incubated for 0, 24, 48, and 72 h. Analysis of 0 and 72 h control variant incubated without FOS was included in the analysis. ^a

Ovalbumin variant	Strand thickness (nm)	Apparent mesh size (nm)	ξ	β
OVA-Co	83.28 \pm 6.5	93.0 \pm 2.8	12 \pm 5	0.8 \pm 0.1
OVA-C72	64.43 \pm 2.5	98.4 \pm 4.4	16 \pm 5	0.9 \pm 0.1
OVA-Mo	63.40 \pm 1.8	69.3 \pm 4.7	13 \pm 5	1.2 \pm 0.1
OVA-M24	54.25 \pm 4.2	118.0 \pm 6.3	14 \pm 5	0.8 \pm 0.1
OVA-M48	33.26 \pm 3.8	144.4 \pm 9.7	15 \pm 5	1.0 \pm 0.1
OVA-M72	19.28 \pm 2.7	180.8 \pm 17.9	16 \pm 5	0.9 \pm 0.1

A further increase in the incubation time of samples in the presence of FOS had only a marginal impact on the gel strength as observed in OVA-M24, OVA-M48, and OVA-M72. FOS treatment of ovalbumin resulted in lower gel strength (**Fig. 5 A**). This is in contrast to the findings of Sun and co-workers²¹ who observed an increase in breaking stress when ovalbumin was Maillardated with rare ketohexose (D-Psicose). The higher gel strength observed in gels prepared from control ovalbumin variants compared to gels prepared from modified ovalbumin variants may be linked to dry-heating as this has been shown to enhance the strength of protein gels following disulfide bond formation and interchange resulting in a firmer gel matrix³⁵.

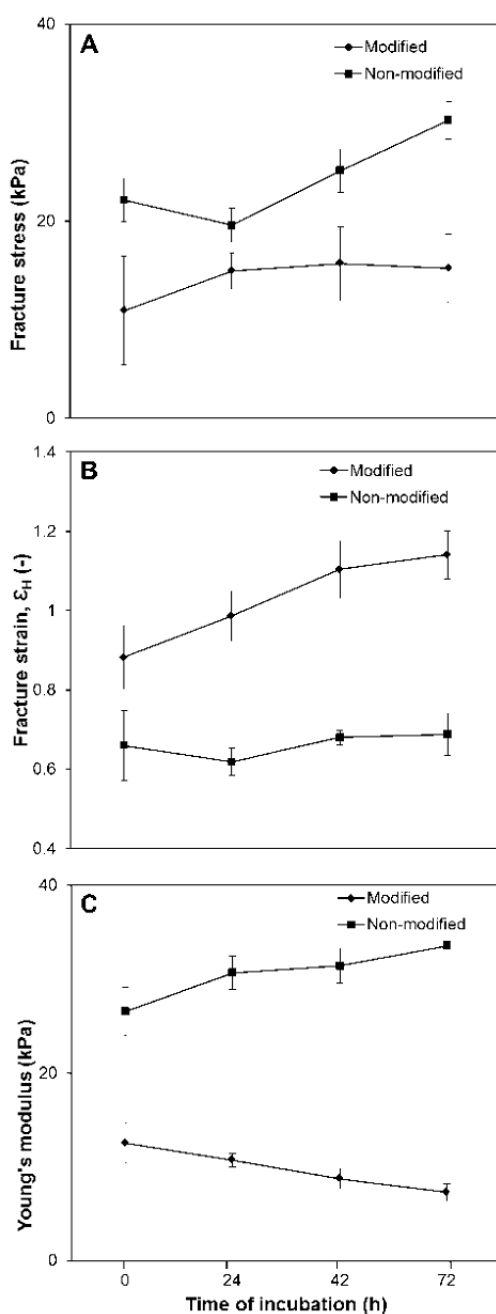


Figure 5: The fracture stress, fracture strain, Young's modulus for gels prepared from non-modified (control) (■) and modified (♦) ovalbumin variant gels. The error bars are derived from the standard error obtained from the standard deviations calculated from the variations of 3 - 4 samples.

Fracture strain

The fracture strain, which is a measure of brittleness of the gels³⁴ has been related to the curvature and length of network structures³⁶. To relate changes in the network structure to the brittleness of the gels, the fracture strain was measured for gels prepared from control ovalbumin variants as well as for modified ovalbumin variants (**Fig. 5 B**). The fracture strain of control samples was almost similar, suggesting that, the heat treatment alone did not affect the fracture strain of ovalbumin gels. Increased modification with FOS resulted in increased fracture strain, indicating that the samples became less brittle than the gels prepared from ovalbumin that had been mixed with FOS but not incubated (OVA-Mo).

In general, modification of ovalbumin resulted in higher fracture strain (less brittle gels), whereas the heat treatment of ovalbumin variants without the addition of FOS did not affect the fracture strain of the gels. The differences in the brittleness of the gels can be explained from the microstructure as seen in **Fig. 4**. With higher modification, the strands of the networks were rather finer (thinner), longer, more flexible, and stretchable, whereas the apparent aggregate size, and strand thickness decreased (**Table 2**). Taking into account the coarseness of the networks, defined as the inhomogeneity of the gel network as related to the thickness of the strands that span the networks³⁰, gels prepared from highly modified ovalbumin were finer than gels prepared from control samples or lowly modified ovalbumin (**Fig. 4 a and b**). Larger fracture strains observed in highly modified ovalbumin variants indicate that the strands are longer, and more curved, and thus, a higher degree of straightening might occur before fracture. Longer and curved strands were observed from the scanning electron micrographs of these network structures (**Fig. 4 a and b**). Increase in fracture strain upon an increase in modification was also observed for gels prepared from ovalbumin that had been Maillardated with rare ketohexose (D-Psicose)²¹.

Young's modulus

Young's (elasticity) modulus, which is the measure of the stiffness of a material⁹ was determined for gels prepared from control and modified ovalbumin variants as shown in **Fig. 5 C**. An initial increase in stiffness was observed when comparing OVA-Co to OVA-C24, after which only a marginal increase in stiffness of the gels occurred (**Fig. 5 C**). The results show that the gels became slightly stiffer when the duration of incubation was prolonged without the addition of FOS.

Gels made from modified variants showed a more than two-fold decrease in stiffness compared to gels made from non-modified (control) variants. With an increase in the incubation time in the presence of FOS, a further decrease in stiffness of gels was observed (**Fig. 5 C**). The decrease in the stiffness of the gels coincided with an increase in fracture strain (**Fig. 5 B**), an indication that the gels become more elastic. The differences in the stiffness of the gels could be related to differences in the curvature of the networks structure similar to the observed effect on fracture strain as previously reported³⁶.

With a higher DM, the strands become thinner (finer) and more curved. Given that the bending of cylinder scales with the diameter³⁷, thin strands are easier to bend than thick strands, which implies a lower modulus with thinner strands.

The ability of ovalbumin gels to elastically store energy

The recoverable energy (energy stored in the networks) of gels prepared from non-modified (control) and modified forms of ovalbumin is shown in **Fig. 6**.

No remarkable changes in the recoverable energy were observed for the controls upon increased incubation. The recoverable energy was higher in gels prepared from control samples than the gels prepared from FOS-modified samples, where a decrease in recoverable energy was observed with increasing FOS groups ligated (**Fig. 6**). The observed differences in the recoverable energy of ovalbumin can be related to the apparent coarseness of the microstructure. From **Fig. 4 a** and **b**, the network structures appear to be more open and finer (thinner), indicating an increase in apparent mesh size, whereas the apparent strand thickness is reduced upon increased modification of ovalbumin. With higher modification the gel structure became less compact, with thinner (finer) strands (**Table 2**, **Fig. 4 a**, and **b**), and larger pores between the aggregates (**Table 2**), and subsequently less connectivity between strands. The larger pore sizes indicate an increase in apparent mesh size as already described under section 3.3. The increase in apparent mesh size, pore sizes, and less connectivity between protein aggregates resulted in lower ability to store energy elastically within the network.

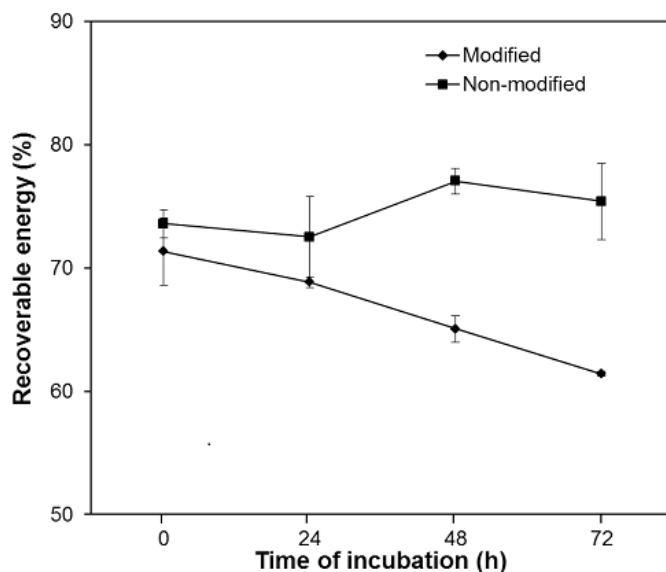


Figure 6: The recoverable energy of gels prepared from non-modified (control) (■) and modified (♦) ovalbumin variants. The error bars are derived from the standard error obtained from the standard deviations calculated from the variations of 3 - 4 samples.

Assuming equal solubility in all ovalbumin variants, and that all the protein is incorporated in to the networks, the decrease in recoverable energy with an increase in DM could also indicate that the local clustering (knots) of protein aggregates of thickness of about 16 ± 5 nm (**Table 2**) observed in the highly modified variants compared to non-modified variants (**Fig. 4 a and b**) acts as weak points interrupting with the connectivity of the networks.

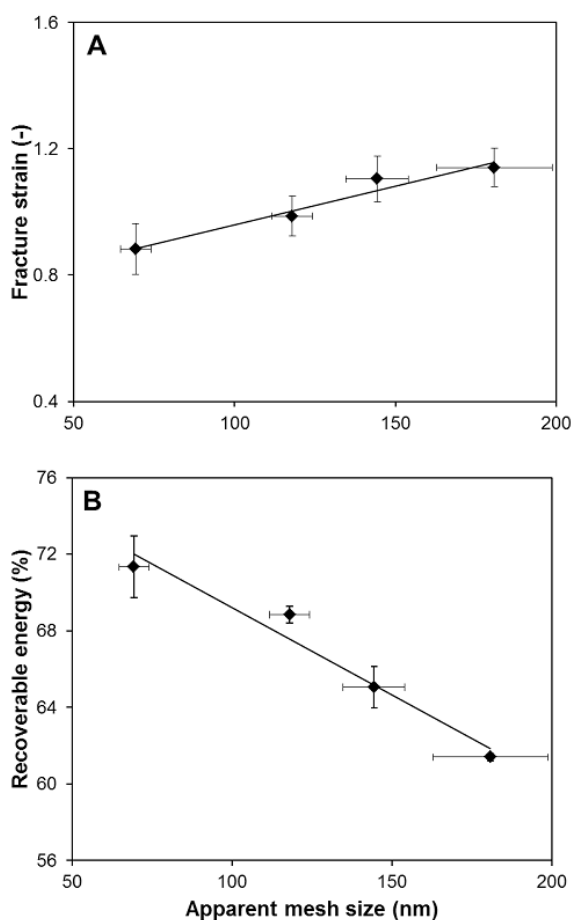


Figure 7: The correlation plot of the apparent mesh size with the fracture strain, and the recoverable energy for gels prepared from modified ovalbumin incubated for varying durations of time. The error bars are derived from the standard error obtained from the standard deviations calculated from the variations of 3 - 4 samples. The R^2 for the linear regression was 0.9547 and 0.9597 for the correlation of the apparent mesh size with the fracture strain, and the correlation of the apparent mesh size with the recoverable energy respectively.

Thus, upon applied deformation, the inhomogeneities in the network as a result of increased local concentration of protein aggregates coupled with the thinner strands networks interferes with the networks ability to elastically store energy.

Correlations between mesh size, fracture strain and recoverable energy

The apparent mesh size was correlated to recoverable energy and the fracture strain of gels prepared from ovalbumin variants. The correlation plots for Maillardated ovalbumin variants are presented in **Fig. 7**. The results show a strong positive significant ($P < 0.05$) correlation between the apparent mesh size and the fracture strain (**Fig. 7 A**). An increase in apparent mesh size with higher modification resulted in a concurrent increase in the fracture strain. The results shows an increase in apparent mesh size, results in increased stretchability of the networks, and thus, the network-strands do not snap easily, but will require more deformation to be applied to the network before fracture can occur. Thus, higher fracture strains were recorded with higher modification as a result of an increase in apparent mesh size.

The paired sample correlation of the apparent mesh size with the fracture strain and the apparent mesh size with the recoverable energy gave significance values of 0.023 and 0.020 respectively (**Table 3**). The apparent mesh size was correlated to the recoverable energy as shown in **Fig. 7 B**. The results show that the mesh size is significantly negatively correlated ($P < 0.05$) to the recoverable energy as seen from the pair correlation results (**Table 3**).

Taking in to consideration the energy dissipation modes listed in equation 1, one may expect the oligofructosylation of ovalbumin to result in the occurrence of changes in the intrinsic viscosity of the network, and as a consequence, changes in how serum flows (serum properties) around the networks. Changes in the properties of the serum phase of the networks would then result in an impact on the ability of the networks to elastically store energy.

However, given that the solutions with modified protein were extensively dialyzed against MilliQ water, it is assumed that all non-covalently attached FOS was dialyzed away. An estimation of the residual amounts of FOS in the network provided typically a concentration of maximally 0.5 wt/v % FOS, suggesting that oligofructosylation of ovalbumin does not have an influence on the intrinsic viscosity of the serum phase. Additionally, it is documented that FOS does not contribute significantly to intrinsic viscosity of the aqueous phase^{38, 39}, and hence will not result in changes in the properties of the serum phase of the networks. Furthermore, covalent coupling of FOS to β -lg was shown to result in a two-fold decrease in the intrinsic viscosity of FOS- β -lg conjugates interpreted to be the result of diminished protein-protein interaction²⁵. Thus, the decrease in recoverable energy in this study is postulated to be due to the changes in the apparent mesh size (apparent mesh sizes increase >100 nm) and not due to changes in the intrinsic viscosity of the serum phase.

At increased mesh sizes, water molecules become able to move freely from the networks in relative motions, and as a result energy is lost via viscous dissipation at the expense of the storage of energy. Gels with pore sizes > 100 nm have been shown to be capable of releasing water on application of force without breaking⁴⁰.

Conclusions

The results from this study show that ovalbumin-FOS conjugates can be obtained in a controlled manner where the integrity of the secondary and tertiary structure of the protein is preserved. Modification of ovalbumin yields microstructural changes of gels including an increase in the apparent mesh size and a reduction in the apparent strand thickness as observed from SEM micrographs. The gels from modified ovalbumin variants were less strong, and showed reduced brittleness, reduced stiffness, and reduced ability of the networks to elastically store energy. The reported effects of ovalbumin modification on the large deformation properties are related to microstructural changes in the network structures of ovalbumin gels as a result of modification. The results from this paper provides an insight into the influence of structural aspects of the networks, such as apparent mesh size and apparent strand thickness, on the large deformation properties of ovalbumin gels including the ability of ovalbumin gels to store energy elastically in the material. The impact of modification on the networks ability to elastically store energy shows that the introduction of bulky oligo-sugar moieties onto ovalbumin may have an effect on the presumed crumbliness of the gels. The reported effects of modification on the networks structure by attachment of oligo-sugar moieties offers opportunities for efficient designing and optimizing desirable structures from proteins of diverse sources that can have an impact of the physico-chemical properties of food materials.

Acknowledgements

Maike Nieuwland is appreciated for meaningful discussions. Tiny Franssen-Verheijen is acknowledged for her help with scanning electron microscopy.

Komla Ako is acknowledged for the help with the image analysis and the interpretation of the results. The fructooligosaccharide was a gift from Sensus BV, the Netherlands.

References

- (1) Wilkinson, C.; Dijksterhuis, G. B.; Minekus, M., From food structure to texture. **Trends Food Sci. Technol.** 2000, **11**, 442-450.
- (2) Weijers, M.; Barneveld, P. A.; Cohen Stuart, M. A.; Visschers, R. W., Heat-induced denaturation and aggregation of ovalbumin at neutral pH described by irreversible first-order kinetics. **Protein Sci.** 2003, **12**, 2693-2703.
- (3) Clark, A. H.; Kavanagh, G. M.; Ross-Murphy, S. B., Globular protein gelation—theory and experiment. **Food Hydrocolloid** 2001, **15**, 383-400.
- (4) Mine, Y., Recent advances in the understanding of egg white protein functionality. **Trends Food Sci. Technol.** 1995, **6**, 225-232.
- (5) Weijers, M.; Van De Velde, F.; Stijnman, A.; Van De Pijpekamp, A.; Visschers, R. W., Structure and rheological properties of acid-induced egg white protein gels. **Food Hydrocolloid** 2006, **20**, 146-159.
- (6) Peleg, M., On fundamental issues in texture evaluation and texturization—A view. **Food Hydrocolloid** 2006, **20**, 405-414.
- (7) van Vliet, T., Large deformation and fracture behaviour of gels. **Curr. Opin. Colloid Interface Sci.** 1996, **1**, 740-745.
- (8) van den Berg, L.; Carolas, A. L.; van Vliet, T.; van der Linden, E.; van Boekel, M. A. J. S.; van de Velde, F., Energy storage controls crumbly perception in whey proteins/polysaccharide mixed gels. **Food Hydrocolloid** 2008, **22**, 1404-1417.
- (9) Çakir, E.; Daubert, C. R.; Drake, M. A.; Vinyard, C. J.; Essick, G.; Foegeding, E. A., The effect of microstructure on the sensory perception and textural characteristics of whey protein/κ-carrageenan mixed gels. **Food Hydrocolloid** 2012, **26**, 33-43.
- (10) van Vliet, T.; Luyten, H.; Walstra, P., Fracture and yielding of gels. In **Food polymers, gels and colloids**, E. Dickinson (ed.). **R. Soc. Chem., Cambridge** (1991) 392-403., 1991.
- (11) van Vliet, T., **Rheology and Fracture Mechanics of Foods**. CRC Press: Boca Raton, FL, USA, 2013; p 363.
- (12) de Jong, S.; van Vliet, T.; de Jongh, H. J. H., The contribution of time-dependent stress relaxation in protein gels to the recoverable energy that is used as tool to describe food texture **Mech. Time-Depend. Mater.** 2014, **Submitted**.
- (13) Kitabatake, N.; Tani, Y.; Doi, E., Rheological properties of heat-induced ovalbumin gels prepared by two-step and one-step heating methods. **J. Food Sci.** 1989, **54**, 1632-1638.
- (14) Martin, A. H.; Baigts Allende, D.; Munialo, C. D.; Urbonaite, V.; Pouvreau, L.; de Jongh, H. H. J., Modulating protein interaction on a molecular and microstructural level for texture control in protein based gels. In **Gums and Stabilisers for the Food Industry 17: The Changing Face of Food Manufac-**

ture: The Role of Hydrocolloids, The R. Soc. Chem.: 2014; pp 64-70.

- (15) Renkema, J. M. S.; van Vliet, T., Heat-induced gel formation by soy proteins at neutral pH. **J. Agric. Food. Chem** 2002, **50**, 1569-1573.
- (16) Hinsch, H.; Wilhelm, J.; Frey, E., Quantitative tube model for semiflexible polymer solutions. **Eur. Phys. J. E** 2007, **24**, 35-46.
- (17) Broersen, K.; Van Teeffelen, A. M. M.; Vries, A.; Voragen, A. G. J.; Hamer, R. J.; De Jongh, H. H. J., Do sulfhydryl groups affect aggregation and gelation properties of ovalbumin? **J. Agric. Food. Chem** 2006, **54**, 5166-5174.
- (18) Bhaduri, A.; Matsudomi, N.; Das, K. P., Effect of acetylation of ovalbumin on its adsorption behavior at solid/liquid interface. **Biosci., Biotechnol., Biochem.** 1996, **60**, 1559-1564.
- (19) Martins, S. I. F. S.; Jongen, W. M. F.; van Boekel, M. A. J. S., A review of Maillard reaction in food and implications to kinetic modelling. **Trends Food Sci. Technol.** 2000, **11**, 364-373.
- (20) Kato, A., Industrial applications of Maillard-type protein-polysaccharide conjugates. **Food Sci. Technol. Res.** 2002, **8**, 193-199.
- (21) Sun, Y.; Hayakawa, S.; Izumori, K., Modification of ovalbumin with a rare ketohexose through the Maillard reaction: Effect on protein structure and gel properties. **J. Agric. Food. Chem** 2004, **52**, 1293-1299.
- (22) Ma, X. J.; Chen, H. B.; Gao, J. Y.; Hu, C. Q.; Li, X., Conformation affects the potential allergenicity of ovalbumin after heating and glycation. **Food Addit. Contam., Part A** 2013, **30**, 1684-1692.
- (23) Matsudomi, N.; Nakano, K.; Soma, A.; Ochi, A., Improvement of gel properties of dried egg white by modification with galactomannan through the Maillard reaction. **J. Agric. Food. Chem** 2002, **50**, 4113-4118.
- (24) Broersen, K.; Voragen, A. G. J.; Hamer, R. J.; de Jongh, H. H. J., Glycoforms of β -lactoglobulin with improved thermostability and preserved structural packing. **Biotechnol. Bioeng.** 2004, **86**, 78-87.
- (25) Trofimova, D.; de Jongh, H. H. J., Modification of β -Lactoglobulin by Oligofructose: Impact on Protein Adsorption at the Air–Water Interface. **Langmuir** 2004, **20**, 5544-5552.
- (26) Kusters, H. A.; Broersen, K.; de Groot, J.; Simons, J. W.; Wierenga, P.; de Jongh, H. H., Chemical processing as a tool to generate ovalbumin variants with changed stability. **Biotechnol Bioeng** 2003, **84**, 61-70.
- (27) Munialo, C. D.; Martin, A. H.; van der Linden, E.; de Jongh, H. H. J., Fibril formation from pea protein and subsequent gel formation. **J. Agric. Food Chem.** 2014, **62**, 2418-2427.
- (28) de Jongh, H. H. J.; Goormaghtigh, E.; Killian, J. A., Analysis of circular dichroism spectra of oriented protein-lipid complexes: Toward a general application. **Biochemistry** 1994, **33**, 14521-14528.
- (29) Munialo, C. D.; de Jongh, H. H. J.; Broersen, K.; van der Linden, E.; Martin, A. H., Modulation

of the Gelation Efficiency of Fibrillar and Spherical Aggregates by Means of Thiolation. **J. Agric. Food Chem.** **2013**, **61**, 11628-11635.

(30) Munialo, C. D.; van der Linden, E.; de Jongh, H. H. J., The ability to store energy in pea protein gels is set by network dimensions smaller than 50 nm. **Food Res. Int.** **2014**, **64**, 482-491.

(31) Rasband, W. 2009. ImageJ, U.S National Institutes of Health, Bethesda, Maryland, USA. <http://rsb.info.nih.gov/ij/>

(32) Chamani, J.; Moosavi-Movahedi, A. A.; Hakimelahi, G. H., Structural changes in β -lactoglobulin by conjugation with three different kinds of carboxymethyl cyclodextrins. **Thermochim. Acta** **2005**, **432**, 106-111.

(33) Ako, K.; Durand, D.; Nicolai, T.; Becu, L., Quantitative analysis of confocal laser scanning microscopy images of heat-set globular protein gels. **Food Hydrocolloid** **2009**, **23**, 1111-1119.

(34) Walstra, P., **Physical chemistry of foods**. CRC Press: 2002; Vol. 121.

(35) Mine, Y., Effect of pH during the dry heating on the gelling properties of egg white proteins. **Food Res. Int.** **1996**, **29**, 155-161.

(36) Renkema, J. M. S., Relations between rheological properties and network structure of soy protein gels. **Food Hydrocolloid** **2004**, **18**, 39-47.

(37) Young, W. C.; Budynas, R. G., **Roark's formulas for stress and strain**. McGraw-Hill New York: 2002; Vol. 7.

(38) Roberfroid, M., **Inulin-type fructans: functional food ingredients**. CRC Press: 2004.

(39) Lomer, M.; Whelan, K., Advanced Nutrition and Dietetics in Gastroenterology. In Wiley Online Library: 2014.

(40) Aguilera, J.; Lillford, P.; Hermansson, A.-M., Structuring Water by Gelation. In **Food Materials Science**, Springer New York: 2008; pp 255-280.

Appendix to Chapter 6: Modification of ovalbumin fibrillar aggregates with fructooligosaccharides: consequences for network morphology and mechanical deformation responses

In this appendix, a study is reported where the ligation of oligo-sugar moieties was carried out on fibrillar aggregates prepared from ovalbumin, rather than on the native molecules as described in Chapter 6. In this study it was attempted to affect more directly the mesh size of fine-stranded networks to modulate the rheological responses.

Introduction

The behavior of proteins upon heating is of interest because, when well understood, protein denaturation and aggregation events can be directed to result in novel materials with diversity in size and functional properties^{1,2}. Heat treatment of proteins can result in the formation of fine or coarse-stranded networks. Fine-stranded networks that include linear aggregates that will be referred to as ‘fibrillar’ (‘fibrils’) aggregates in this study are formed when electrostatic repulsion between the protein molecules is large, such as at a pH away from IEP or at low ionic strength³ and can have the thickness in the order of a few nanometers and be a few μm long⁴.

This study focuses on Maillardation of fibrillar aggregates made from ovalbumin and on the comparison of the structural and rheological characterization of modified and non-modified fibrillar-based ovalbumin gels. Maillardation of pre-established fibrils with oligofructose was performed as a more direct way to affect the mesh size.

After Maillardation of fibrillar aggregates was achieved, the next step was to assemble these aggregates into a spatial network.

Experimental

Materials

Albumin (A5503) from chicken egg white (ovalbumin) (grade V, > 98 % pure by agarose electrophoresis, crystallized and lyophilized, Lot # SLBB4340V), Glucono- δ -lactone (GDL), ortho-phthaldialdehyde (OPA), NaOH pellets, HCl, N,N-dimethyl-2-mercaptoethyl-ammoniumchloride (DMA), di-sodiumtetraborate decahydrate (Borax), sodiumdodecylsulfate (SDS), uranyl acetate, glutaraldehyde, and dimethyl sulfoxide (DMSO) were obtained from Sigma-Aldrich (Steinheim, Germany). Frutafit[®] HD with an average degree of polymerization (DP) of ≈ 10 and a content of fructooligosaccharides (FOS)

$\geq 90\%$ were provided as a gift by Sensus (Roosendaal, The Netherlands). Thioflavin T (Th T) was obtained from Acros organics (Geel, Belgium). Sodium nitrite (NaNO_2) and paraffin oil were obtained from Merck (Darmstadt, Germany). All reagents were of analytical grade and used without further purification. All solutions were prepared with MilliQ water.

Preparation of ovalbumin protein solutions and fibril formation

Native ovalbumin solutions were prepared by dispersing 50 mg/mL ovalbumin powder in MilliQ water (Millipore Corp., Billerica, MA), followed by adjusting the pH of the samples to pH 7 using 1 M HCl. The solutions were then stirred at 4 °C, 300 rpm overnight. Subsequently, the protein solutions were centrifuged at $20000 \times g$ for 30 min at 4 °C. The supernatant was filtered through a 0.45 μm (Millex-SV, Millipore Corp., Bedford, MA) filter. The determination of the protein concentration using DUMAS (NA 2100 Protein, CE instruments, Milan, Italy) with a conversion factor of 6.25 showed that negligible losses in protein concentration occurred in the course of this process. These protein solutions were used in the preparation of fibrillar aggregates as described below.

Fibril preparation was carried out according to a previously described protocol⁵ with modification in which aliquots of 20 mL of 50 mg/mL protein solutions at pH 7 prepared as described above were incubated at 82 ± 1 °C for 22 h in a temperature-controlled water bath, and continuously stirred at 300 rpm. After the heat treatment, samples were cooled in an ice bath and stored at 4 °C until further use. Th T fluorescence assay was used to evaluate the formation of β -sheet aggregates as previously described⁵.

Maillardation of ovalbumin structural building blocks

Maillardation was carried out on ovalbumin as previously described⁶. Fibrillar ovalbumin solutions at pH 7 were mixed with 9 wt % FOS solutions to give a final molar ratio of FOS-reducing ends relative to the number of primary amino groups on the protein of about 3:1 (assuming a molecular mass for FOS of 1800 Da from an average DP \approx 10). The pH of the mixtures of fibrillar ovalbumin and FOS were adjusted to $\text{pH } 8.0 \pm 0.1$ using 1 M NaOH. The mixed solutions (ovalbumin + FOS) at pH 8 were freeze-dried (Christ Alpha 2-4 LD plus, Shropshire, UK), and the freeze dried powder were incubated at 60 °C in an oven (Fischer Scientific Venticell 111, MMM Medcenter, Belgium) at a relative humidity of 65 % (exposed to a saturated NaNO_2 solution) for 0, 24, 48, and 72 h. Following the incubation step, dry-powders were resuspended in 10 mM phosphate buffer and subsequently dialyzed against MilliQ water at 4 °C. Finally the samples were freeze-dried and stored at -20 °C until use. Control samples were also prepared by incubation (dry-heating) of the protein solutions without FOS under similar conditions and for the equivalent time intervals as described. Maillardation carried out in this way resulted in the formation of six ovalbumin variants.

Characterization of ovalbumin structural building blocks

The number of primary amines (lysines and the protein N-terminal amine groups) was determined using chromogenic ortho-phthaldialdehyde (OPA) assay as previously described⁷. Chromogenic OPA assay was carried out in duplicate and the results were used to determine the degree of modification (DM) of amines with FOS.

The molecular weight of ovalbumin variants at an approximate concentration of 10 mg/mL was analyzed using sodium dodecyl sulfate polyacrylamide gel electrophoresis (SDS-PAGE) under reducing and non-reducing conditions according to a previously described procedure⁸.

Microscopic and spectrophotometric characterization of ovalbumin structural building blocks

Unmodified and modified ovalbumin fibrillar aggregates were prepared for transmission electron microscopy (TEM) by negative staining according to the previously described protocol⁸.

Far-UV circular dichroism (CD) spectra of 0.1 mg/mL ovalbumin samples at pH 7 were recorded at 20 °C in the spectral range from 190 to 260 nm with a spectral resolution of 0.5 nm on a Jasco J-715 spectropolarimeter (Jasco Corporation, Japan) according to a previously described procedure⁸. Noise reduction was applied to the recorded spectra based on inverse Fourier transformation method using the supplier's software. The far-UV CD spectra of ovalbumin variants were analyzed for the secondary structural elements using non-linear least-squares fitting procedure as described previously⁹.

Intrinsic tryptophan fluorescence spectra of 50 µg/mL ovalbumin samples were obtained using a Cary eclipse fluorescence spectrophotometer (Agilent technologies, The Netherlands) according to a previously described procedure⁵.

Preparation and analysis of ovalbumin fibrillar-based protein gels

Preparation of gels from unmodified and modified fibrillar aggregates made using ovalbumin at a protein concentration of 50 mg/mL was carried out by acid-induced cold gelation using GDL according to a previously described procedure⁵. A stress-controlled rheometer (ARG2, TA Instruments, Leatherhead, UK) with a concentric cylinder geometry (C14: cup diameter, 15.4 mm; bob diameter, 14.04 mm;) was used to determine storage modulus (G') as a function of time (frequency, 1 Hz; temperature, 25 °C; strain, 0.05, 10 h). After 10 h, oscillation amplitude was performed (frequency, 1 Hz; temperature, 25 °C; strain, 0.001 - 100). Duplicate measurements were performed in all cases. Measurements were performed within the linear region which was in the strain % range of between 0.001 and 10.

Results and Discussion

Maillardation of ovalbumin based fibrillar protein aggregates to study its effect on the mesh size of the structural building blocks yielded six variants differing in degree of modification (DM). Ovalbumin fibrillar aggregates pH 7 will be referred to as OVA-F, unheated (native) ovalbumin will be referred to as OVA-N, ovalbumin fibrillar aggregates that had been treated with FOS but not incubated will be referred to as OVA-FO whereas, ovalbumin fibrillar aggregates prepared at pH 7, followed by the incubation of the samples for 24 h will be referred to as OVA-F24, 48 h as OVA-F48, and 72 h as OVA-F72.

Characterization of non-modified ovalbumin-fibrils variants

Thioflavin T (Th T) assay was carried out on ovalbumin variants to confirm the presence of β -sheet aggregates as a typical characteristic for the formation of fibrillar aggregates¹⁰.

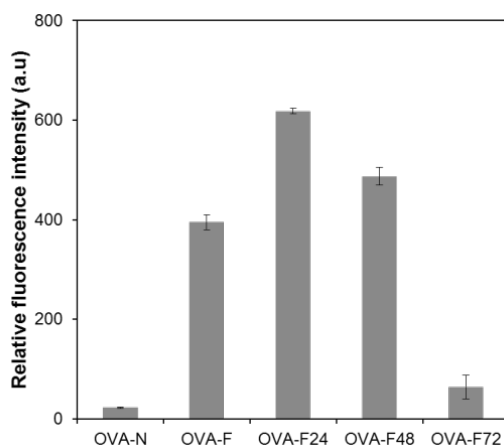


Figure 1: Average relative fluorescence intensities probed by Th T fluorescence at 485 nm wavelength for OVA-N, OVA-F, OVA-F24, OVA-F48, and OVA-F72.

The fluorescence intensities of OVA-F in comparison to OVA-N are shown in **Fig. 1**. The fluorescence intensity for OVA-F was higher than that of OVA-N. As expected the formation of fibrillar aggregates resulted in an increase in fluorescence intensity.

To characterize the building blocks of ovalbumin prior to modification, changes in the molecular weight were analyzed using SDS-PAGE. The electrophoretograms are shown in **Fig. 2** (for native and fibrillar ovalbumin aggregates). Monomers present in unheated OVA-N are shown in the band that appears at around 45 kDa although a small proportion of the materials appears as at around 90 kDa in lane 2 (**Fig. 2 A**) and lane 3 (**Fig. 2 B**).

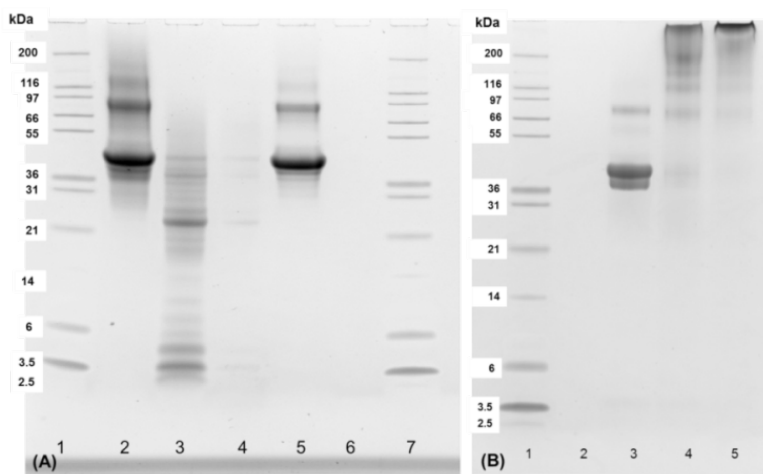


Figure 2: SDS-PAGE electrophoretograms are shown in **Fig. 2 (A)** for standard marker (lane 1 and 7), OVA-N (lane 2), OVA-F heated ovalbumin at pH 2 (lane 3), and OVA-F heated ovalbumin at pH 7 (lane 5), under reducing conditions. **Fig. 2 (B)** shows non-reducing SDS-PAGE profiles of OVA-N (lane 3), OVA-F prepared at pH 7 (lane 4) and OVA-F24 i.e. modified fibrils incubated for 24 h (lane 5).

Following the heating of ovalbumin solutions (22 h, 82 °C), changes in the molecular weight were observed at pH 7, as some bands around 116 kDa disappeared with extensive heating of ovalbumin (lane 5). However, hydrolysis, which has been reported to be the mechanism for fibril formation as extensively investigated and reported in other globular proteins such as lysozyme¹¹, soy β -conglycinin¹², and pea protein⁸, was not observed at this pH (lane 5). To confirm whether hydrolysis is an important step in the formation of ovalbumin fibrillar aggregates, ovalbumin was also heated at pH 2 at 82 °C for 22 h, (lane 3, **Fig. 2 A**) and the molecular weight bands were compared to samples heated at pH 7 (lane 5, **Fig. 2 A**) under reducing conditions. Following heating of ovalbumin at pH 2 (lane 3), hydrolysis of ovalbumin into peptides that form the building blocks for fibril assembly was shown to occur. There were two major groups of peptides, one around 20 - 25 kDa and another around 3 - 6 kDa (**Fig. 2**). A reduction of the molecular weight of ovalbumin at low pH and high temperature has been reported previously¹³.

From this analysis it can be concluded that the formation of fibrillar aggregates from ovalbumin at pH 7 occurs without the initial step of hydrolysis. In this case, aggregation takes place following partial unfolding of the native globular protein (due to heat treatment), resulting in the exposure of hydrophobic regions that are hidden in the core of the globular native state¹⁴. It is however important to note that, similar to fibril formation that requires hydrolysis, the aggregation of ovalbumin at pH 7 is also stabilized by the formation of cross β -structures as indicated by Th-T fluorescence binding (**Fig. 2**), in agreement with previous reports¹⁵. For SDS-PAGE carried out under non-reducing conditions (**Fig. 2 B**), the bands around 45 kDa seem to disappear upon the formation of fibrillar aggregates (lane 4).

Table 1: Chemical characterization of ovalbumin variants modified with a ratio of 3:1 FOS-reducing ends: amines. OVA-N and OVAF0 are control variants.

	Dry heating time (h)	Free amino group (%)	DM (%)
OVA-N	control	100 ± 0.78	0 ± 0.0
OVA-F0	0	100 ± 0.3	0
OVA-F24	24	94 ± 3.9	6 ± 1.0
OVA-F48	48	78 ± 4.5	22 ± 1.5
OVA-F72	72	76 ± 0.46	24 ± 0.5

Chemical characterization of fibrillar ovalbumin upon modification

To evaluate the degree of Maillardation, the number of free amino groups that react with the reducing end of the FOS in unmodified and modified ovalbumin variants was determined and shown in **Table 1**.

The degree of modification (DM) increases with an increase in incubation time (**Table 1**). The content of free amino groups in fibrillar aggregates decreased most significantly during the first 48 h of incubation. Longer incubations did not lead to substantial or more extensive Maillardation products to be formed. The significant decrease in the number of free amino groups within the first 48 h may be related to a decrease in the availability of reactive groups with the progression of the reaction resulting in the slowdown of the reaction rate. From the DM, an estimation of an ensemble averaged number of FOS residues linked per ovalbumin molecule was determined to be about 0.96 after 24 h of incubation, 3.5 after 48 h of incubation, 3.9 after 48 h of incubation, and 5.2 after 72 h of incubation. These calculations were made based on a free amino group (lysine) content per mmol of ovalbumin fibrils solutions made at pH 7, that was assumed to be 16 as calculated from the chromogenic OPA assay.

Characterization of modified fibrils by the use of SDS-PAGE was carried out (**Fig. 2 B**). The modification of ovalbumin was shown to result in a similar disappearance in the bands around 45 kDa (lane 5 for OVAF-24), although no significant changes in molecular weight were observed between the unmodified (OVA-F) and modified fibrillar variants (OVA-F24) as not all the proteins were able to enter the gel (**Fig. 2 B**).

To evaluate whether the Maillardation affected the degree of fibrillization, the Th T-assay was performed on the ovalbumin fibrillar aggregates that had been treated with FOS followed by the incubation of the samples for 24 h (OVA-F24), 48 h (OVA-F48), and 72 h (OVA-F72) as shown in **Fig. 1**. Upon modification, the fluorescence intensity of OVA-F48 increased further than OVA-F variant. A decrease in the fluorescence intensity was observed with prolonged incubation (for OVA-F48 and OVA-F72).

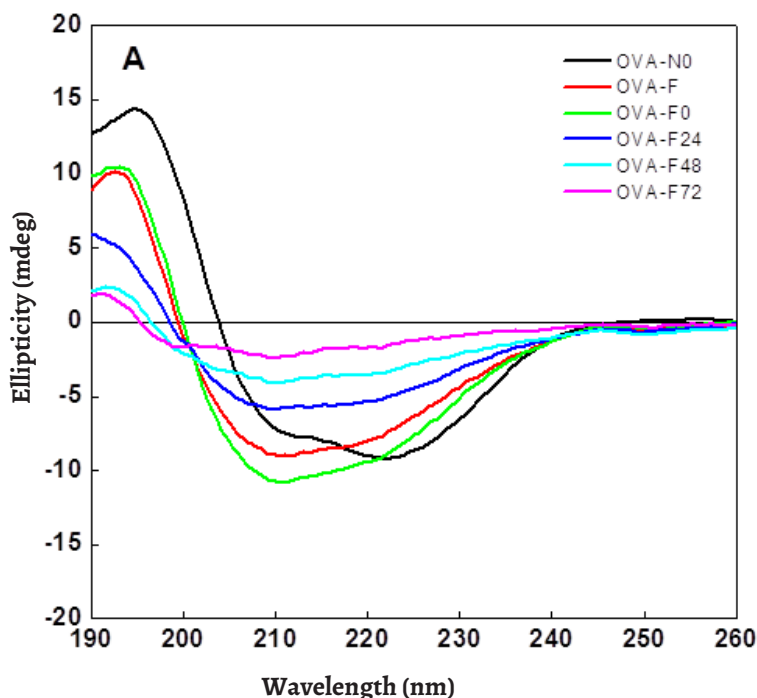


Figure 3: Changes on a secondary structural level for fibrillar ovalbumin variants analyzed by the use of circular dichroism.

The reduction in fluorescence intensity could be attributed to a reduced efficiency of Th T to bind to the protein, due to inaccessibility of Th T binding grooves¹⁶ as a result of higher degrees of modification or to a (partial) disassembly of the fibrils.

Analysis of the secondary structure of FOS-Maillardated fibrillar ovalbumin

The changes in secondary structure as a result of Maillardation of ovalbumin fibrils were probed using far-UV CD. The spectra (**Fig. 3**) show that upon the formation of fibrillar aggregates (OVA-F) from monomeric (native) ovalbumin (OVA-N), a shift of the zero crossing to lower wavelength is observed.

This suggests that partial unfolding of the protein occurs following the heating step. The presence of FOS to fibrillar aggregates without the incubation step (OVA-Fo) did not result in further changes in the CD spectrum.

With incubation of fibrillar aggregates in the presence of FOS, a progressive shift in the zero crossing to below 200 nm was observed indicating a considerable loss of β -sheet structure¹⁷.

Analysis of the tertiary structure of fibrillar ovalbumin

Changes at the tertiary folding level of the protein-fibrils by Maillardation were probed by monitoring the microenvironment of the tryptophan residues using fluorescence spectroscopy as shown in **Fig. 4**.

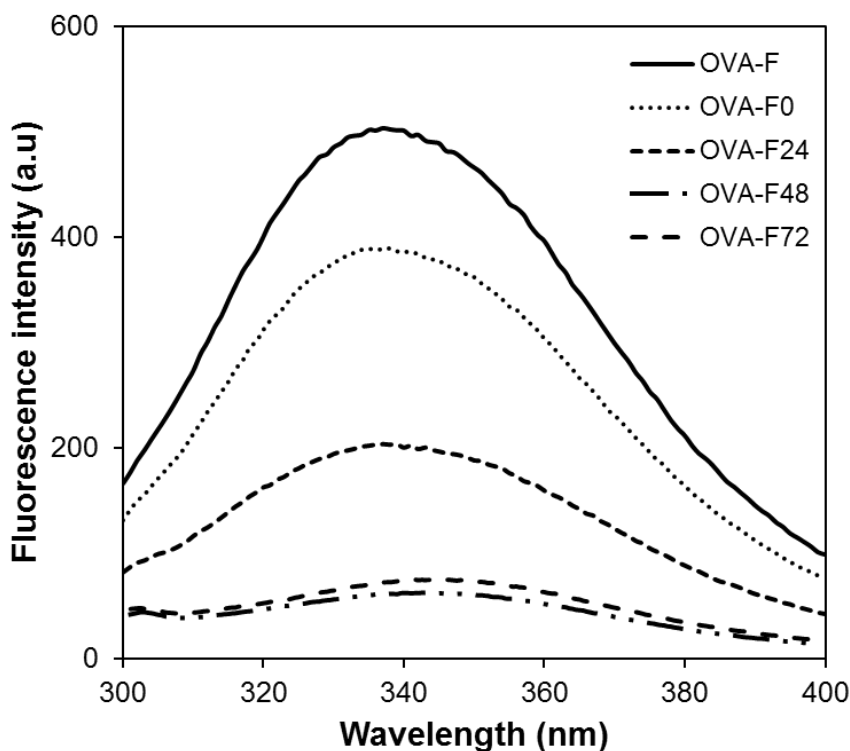


Figure 4. Analysis of the tertiary structure of OVA-F, OVA-Fo, OVA-F24, OVA-F48, and OVA-F72 by tryptophan fluorescence.

A maximum in the fluorescence of OVA-N was observed at 334 nm (not shown; see Chapter 6). Following the formation of fibrillar aggregates and the modification of these aggregates, the emission maxima shifted slightly by around 3 nm (red shift) at all conditions (**Fig. 4**), suggesting that tryptophan residues reside in a more polar environment upon fibril formation and the modification of the fibrillar aggregates in comparison to the native state of ovalbumin. For comparison, full solvent exposed tryptophans would emit around 355 nm. A decrease in the fluorescence intensity was observed with an increase in DM, which could be the result of a decrease in energy transfer efficiency between tryptophan and tyrosine. A similar decrease in fluorescence intensity without a significant red shift was previously reported for heated ovalbumin¹⁸.

Effect of Maillardation on the microstructure of fibrillar ovalbumin

The microstructure of fibrillar ovalbumin network structures was probed using TEM. The presence of fibrillar aggregates following heating of ovalbumin (pH 7.0, 22 h, 82 °C) was confirmed with TEM micrographs (**Fig. 5**). Ovalbumin fibrils can be described as being short, curly, highly flexible, and 'worm-like' (**Fig. 5**, OVA-F). Following the treatment of ovalbumin fibrillar aggregates with FOS and without the incubation step, the morphology of fibrillar aggregates was not altered (**Fig. 5**, OVA-Fo). Some fibrillar aggregates were still visible when ovalbumin fibrillar aggregates were incubated for 24 h in the presence of FOS (**Fig. 5**, OVA-F24).

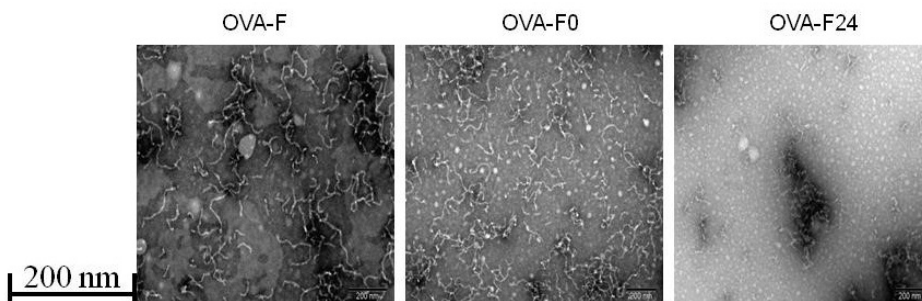


Figure 5. TEM micrographs of OVA-F, OVA-Fo, and OVA-F24. The scale bars represent 200 nm

The number of fibrils for OVA-F24 was however lower as well as the fibrillar aggregates appeared to be shorter, despite the strong Th T-binding (see **Fig. 1**). Following the resuspension of the modified fibrils in 10 mM phosphate buffer at pH 7, aggregation and clustering of the fibrillar aggregates occurred as observed with TEM, which coincided with a reduction in solubility of the fibrillar aggregates. This made it not possible to image the fibrillar aggregates that were modified for longer durations of 48 h and 72 h (not shown). The loss of solubility could be related to chemical cross-linking that is favored at higher pHs¹⁹, or alternatively may be explained by the lower net charge upon Maillardation²⁰.

Effect of Maillardation on gelation of fibrillar ovalbumin

The assembly of (modified and unmodified) fibrillar aggregates of ovalbumin into a spatial network by acidification to pH 4.8 using GDL was monitored using small deformation rheology. Changes in G' (**Fig. 6 A**) and G'' (**Fig. 6 B**) as a function of incubation time during the 10 h of gelation at 25 °C for ovalbumin fibrillar were monitored.

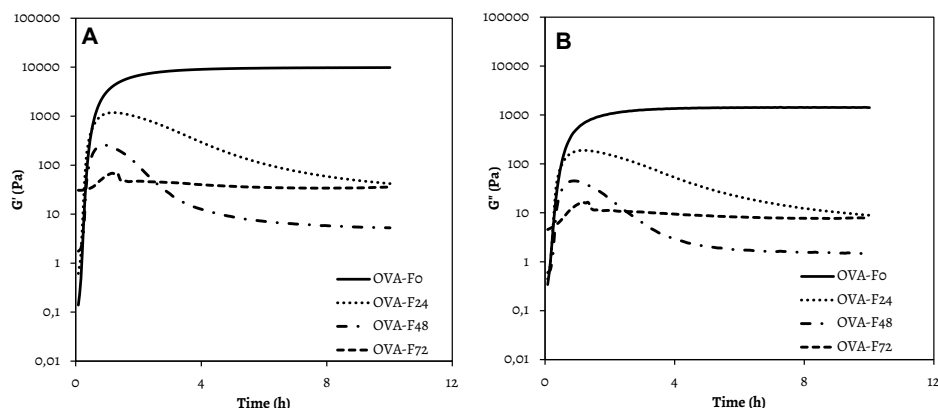


Figure 6: Changes in storage modulus (G' , Pa) and loss modulus (G'' , Pa) over time for OVA-Fo, OVA-F24, OVA-F48, and OVA-F72.

Gelation was assumed to have occurred when $\tan \delta$ of the solution was less than 1 ($G' > G''$)²¹. Non-modified fibrillar variants of ovalbumin, formed stiffer gels with higher G' values than modified variants. The G' was lower with higher modification than that of non-modified variants as well as those variants modified to low degrees (**Fig. 6**). The G' and G'' were all shown to decrease after an incubation of around 1 h at 25 °C. The decrease in G' and G'' over time suggests the breakdown and rearrangement of the network. This could be related to clustering of the fibrillar aggregates resulting in the formation of a weak network stabilized by electrostatic interaction between these clusters. Upon application of shear during small deformation rheological characterization of the fibrillar-based gels, the break down and rearrangement of the network could occur resulting in a decrease in the G' . The stiffness measured by the Young's modulus for gels of the various ovalbumin variants was also shown to decrease with an increase in DM (Chapter 6, **Fig. 5**). This illustrates that the attachment of FOS to ovalbumin either in its native or pre-aggregated form decreases the stiffness of the gels, which may be related to the impact on the curvature of the strands and the mesh size as discussed in detail in Chapter 6.

For ovalbumin fibrillar aggregates, no large deformation was performed as it was not possible to concentrate the samples (because of the yield obtained from the fibrillar aggregates) to levels where self-supporting gels could be formed to allow for the study of large deformation responses of the gels, including the recoverable energy.

Conclusions

Pre-assembled fibrils of ovalbumin were subjected to Maillardation with the purpose to affect the mesh size in gels more directly than by modification of native ovalbumin as reported in chapter 6. The differences between modifying fibrils versus native protein are firstly that changes in the secondary structural of the protein were observed when Maillardation was carried out on fibrillar aggregates, in contrast to glycation of native ovalbumin. Secondly, the fluorescence intensity of modified ovalbumin fibrillar and native variants decreased with an increase in the degree of modification. The fluorescence intensity of ovalbumin fibrillar aggregates was however reduced substantially at higher degrees of modification than when Maillardation was carried out using native protein. Maillardation with fructooligosaccharides of both native and fibrillar-aggregated ovalbumin resulted in a decreased stiffness of the gels with an increase in the DM. The reduced solubility of Maillardated fibrillar aggregates prohibited substantial concentration of the material to allow the assembly in spatial networks leading to self-supportive gels that could be used to test mechanical responses, like the recoverable energy and fracture behavior.

Thus the influence of Maillardation of fibrils on recoverable energy of ovalbumin networks remains unresolved. However, this work shows that one is able to modify the functional properties of pre-formed fibrillary aggregates, for example with larger steric moieties as oligosaccharides, in a controlled manner. Such tuned microstructural building blocks may offer new potentials in the formulation of food applications where tailored fibers are included.

Acknowledgements

The authors acknowledge help with transmission electron microscopy by Harry Baptist, scanning electron microscopy by Tiny Franssen-Verheijen. Maaïke Nieuwland is appreciated for fruitful discussions.

References

- (1) Qi, P. X.; Onwulata, C. I., Physical properties, molecular structures, and protein quality of texturized whey protein isolate: Effect of extrusion temperature. **J. Agric. Food. Chem** **2011**, *59*, 4668-4675.
- (2) Zúñiga, R. N.; Tolkach, A.; Kulozik, U.; Aguilera, J. M., Kinetics of formation and physicochemical characterization of thermally-induced β -Lactoglobulin aggregates. **J. of Food Sci** **2010**, *75*, E261-E268.
- (3) Langton, M.; Hermansson, A. M., Fine-stranded and particulate gels of beta-lactoglobulin and whey protein at varying pH. **Food Hydrocolloid** **1992**, *5*, 523-539.
- (4) Kroes-Nijboer, A.; Sawalha, H.; Venema, P.; Bot, A.; Floter, E.; den Adel, R.; Bouwman, W. G.; van der Linden, E., Stability of aqueous food grade fibrillar systems against pH change. **Faraday Discuss.** **2012**, *158*, 125-138.
- (5) Munialo, C. D.; de Jongh, H. H. J.; Broersen, K.; van der Linden, E.; Martin, A. H., Modulation of the gelation efficiency of fibrillar and spherical aggregates by means of thiolation. **J. Agric. Food. Chem** **2013**, *61*, 11628-11635.
- (6) Matsudomi, N.; Nakano, K.; Soma, A.; Ochi, A., Improvement of gel properties of dried egg white by modification with galactomannan through the Maillard reaction. **J. Agric. Food. Chem** **2002**, *50*, 4113-4118.
- (7) Kusters, H. A.; Broersen, K.; de Groot, J.; Simons, J. W.; Wierenga, P.; de Jongh, H. H., Chemical processing as a tool to generate ovalbumin variants with changed stability. **Bio-technol Bioeng** **2003**, *84*, 61-70.
- (8) Munialo, C. D.; Martin, A. H.; van der Linden, E.; de Jongh, H. H. J., Fibril formation from pea protein and subsequent gel formation. **J. Agric. Food. Chem** **2014**, *62*, 2418-2427.
- (9) de Jongh, H. H. J.; Goormaghtigh, E.; Killian, J. A., Analysis of circular dichroism spectra of oriented protein-lipid complexes: Toward a general application. **Biochemistry** **1994**, *33*, 14521-14528.
- (10) Naiki, H.; Higuchi, K.; Hosokawa, M.; Takeda, T., Fluorometric determination of amyloid fibrils invitro using the fluorescent dye, thioflavine T. **Anal. Biochem.** **1989**, *177*, 244-249.
- (11) Mishra, R.; Sörgjerd, K.; Nyström, S.; Nordigården, A.; Yu, Y.-C.; Hammarström, P., Lysozyme amyloidogenesis is accelerated by specific nicking and fragmentation but decelerated by intact protein binding and conversion. **J. Mol. Biol.** **2007**, *366*, 1029-1044.
- (12) Tang, C.-H.; Wang, S.-S.; Huang, Q., Improvement of heat-induced fibril assembly of soy β -conglycinin (7S Globulins) at pH 2.0 through electrostatic screening. **Food Res Int.**

2012, **46**, 229-236.

(13) Lara, C.; Gourdin-Bertin, S.; Adamcik, J.; Bolisetty, S.; Mezzenga, R., Self-assembly of ovalbumin into amyloid and non-amyloid fibrils. **Biomacromolecules** 2012, **13**, 4213-4221.

(14) Chiti, F.; Dobson, C. M., Amyloid formation by globular proteins under native conditions. **Nat Chem Biol** 2009, **5**, 15-22.

(15) Azakami, H.; Mukai, A.; Kato, A., Role of amyloid type cross β -structure in the formation of soluble aggregate and gel in heat-induced ovalbumin. **J. Agric. Food. Chem** 2005, **53**, 1254-1257.

(16) Li, H.; Rahimi, F.; Sinha, S.; Maiti, P.; Bitan, G.; Murakami, K., Amyloids and protein aggregation—analytical methods. In **EAC**, John Wiley & Sons, Ltd: 2006.

(17) de Jongh, H. H. J.; Robles, C. L.; Timmerman, E.; Nordlee, J. A.; Lee, P.-W.; Baumert, J. L.; Hamilton, R. G.; Taylor, S. L.; Koppelman, S. J., Digestibility and IgE-Binding of Glycosylated Codfish Parvalbumin. **BioMed Research International** 2013, **2013**, 10.

(18) Tani, F.; Murata, M.; Higasa, T.; Goto, M.; Kitabatake, N.; Doi, E., Molten globule state of protein molecules in heat-induced transparent food gels. **J. Agric. Food. Chem** 1995, **43**, 2325-2331.

(19) Mine, Y., Effect of dry heat and mild alkaline treatment on functional properties of egg white proteins. **J. Agric. Food. Chem** 1997, **45**, 2924-2928.

(20) Lee, C. M.; Sherr, B.; Koh, Y. N., Evaluation of kinetic parameters for a glucose-lysine Maillard reaction. **J. Agric. Food. Chem** 1984, **32**, 379-382.

(21) Ross-Murphy, S. B., Incipient behaviour of gelatin gels. **1991**, **30**, 401-411.

Chapter 7

Modulation of the serum phase viscosity and its contribution to energy dissipation upon mechanical deformation of whey protein gels

The viscosity of the entrapped serum phase of a gelled network has an influence on the textural and sensorial properties of many foods and food systems. However, the role of the viscosity of the serum phase and its influence on the ability of food gels to elastically store energy due to an effect on the dissipation of energy is unclear. This chapter focused on understanding the role of the serum phase viscosity on the ability to elastically store energy in whey protein gels by energy dissipation upon mechanical deformation of gels. Whey protein gels were used as a model system and high (HM) and low (LM) methylated negatively charged pectin or the neutral pullulan were added to modulate the viscosity of the serum phase. The addition of the three different polysaccharides resulted in gels that showed differences in rheological responses such as fracture stress, fracture strain, Young's modulus and the recoverable energy.

This chapter is to be submitted as:

Munialo, C.D.; van der Linden, E.; Ako, K.; Nieuwland, M.; Van As, H.; de Jongh, H. H. J. Modulation of the serum phase viscosity and its impact on the ability of whey protein gels to either store or dissipate energy upon mechanical deformation. ***Food Hydrocolloids*** 2015.

Introduction

The rise in the global human population poses a challenge to the food industry to diversify on the available protein sources to feed the growing population. This diversification can encompass replacing proteins with proteins from other sources or the addition of other components, such as polysaccharides to the protein gels. However, exchangeability of proteins can be a great challenge when the functional characteristics such as gel network formation and its responses to mechanical deformation are not fully understood.

Gel formation by proteins contributes to a large extent to the textural and sensorial attributes of food gels, and thereby to the consumer acceptance of food products¹. Heat induced gel formation occurs following thermal (partial) unfolding of native proteins which results in exposure of non-polar residues, and this leads to clustering of aggregates to form a spatial gel network². At sufficiently high protein concentrations, these gels can be self-supporting. The formation of self-supporting gels under specified conditions is essential in defining the quality characteristics, (such as the fracture properties of food gels) which determine the functional behavior (such as cutting and handling) of the gels³.

In linear elastic fracture mechanics, the energy that is applied to materials is initially stored and can be used in the propagation of fracture. However, in many gels only part of the energy supplied is stored, whereas the other part is dissipated⁴. The ability to store energy is often measured in terms of the recoverable energy and has been correlated to crumbliness perception of food gels⁵. Crumbliness is one of the textural attributes that determines consumer acceptance of several food products, such as processed meat or confectionary, and hence it is often used as a parameter for quality control during manufacture⁵. However, to tailor this parameter, physical properties that relate to crumbliness, such as the recoverable energy, have to be understood.

Energy dissipation can occur via the following modes (i) fracturing events, (ii) friction between structural elements upon deformation of gels, (iii) viscous serum flow of the liquid that is entrapped by the network, (iv) de-bonding of physical contacts that make up the network, (v) plastic deformation, and (vi) relaxation of structural elements⁶. A detailed account of how each of these dissipation modes contribute to the loss of energy loss can be found elsewhere⁶.

Energy dissipation can be affected when the coarseness of the gel, defined as inhomogeneity of gel networks as related to the thickness of the strands that spans the networks⁷ is varied, or due to morphological differences caused by changes in the porosity of the networks⁸. Changes in the pore sizes have been shown to be related to the amount of energy that is dissipated via serum flow of the entrapped liquid during mechanical deformation⁸. Recently, it was shown that time-dependent contribution of energy dissipation are partly related to structural rearrangements during the time-span of the experiments⁶.

Longer experimental time-spans were shown to result in changes in the type of reversible microstructural rearrangements of protein gels. Energy dissipation caused by viscous flow of the liquid entrapped by the network for protein gels has also been reported⁶. Predominance of higher impulse-conditions or larger deformation rates were reported to be necessary for permeable gels, and this was interpreted to be related to the liquid being able to be squeezed faster through the network-pores provoking higher friction forces. However, a detailed account on how the viscosity of the serum phase can be modulated whilst preserving the integrity of the gel morphology, and how this contributes to energy dissipation at the expense of storage of energy has not yet been reported. Knowledge of the mechanism by which energy dissipation results in a decrease in the storage of energy in protein gels, emanating from changes in the viscosity of the serum is however important for the development of desirable properties in food products.

To modulate the viscosity of the serum phase and to study the influence of this modulation on the energy balance of food gels, an approach was taken in this study to prepare gels from whey proteins (WP). WP, are important in the food industry, not only as components of dairy products, but also as ingredients in many non-dairy food products^{9, 10}. WP gels were formed as such, or following the addition of pectins or pullulan to WP. Pectins are linear homopolysaccharide polyelectrolytes bearing a negative charge¹¹. Pectins varying in degree of methylation and thus in charge density will have different interactions with WP¹². Pullulan on the other hand is a neutral non-gelling homopolysaccharide¹³.

The aim of this study was to understand the role of the serum phase viscosity on the ability to either store or dissipate energy upon mechanical deformation of heat-induced whey protein gels. To this end, WP-pectin and WP-pullulan gels were prepared at a fixed 13 wt % protein concentration, whereas the polysaccharide concentrations were chosen and varied such that their presence had no or only a limited effect on gel morphology. The microstructure of the formed gels was visualized using confocal laser scanning and scanning electron microscopy. Following imaging of the gel networks, quantitative analysis of the network structures was carried out using the pair correlation function. Subsequently, the large deformation properties of the protein gels were studied using uniaxial compression. The self-diffusion coefficients and T_2 relaxation times of enclosed water, and the water holding capacity of these gels were also measured to be able to differentiate between the contribution of the gel porosity and inherent viscosity on energy dissipation in WP gels.

Experimental

Materials

Whey protein isolate (WPI, Bipro™) was obtained from Davisco Food International (Le Sueur, MN). According to the manufacturers specifications, the powdered WPI was constituted of 97.6 wt % protein, 2.1 wt % ash, and 0.3 wt % fat (dry weight basis) and 4.5 wt % moisture (wet weight basis).

Low methylated (LM) pectin (Pectin Classic CU-L 027/10) with a degree of esterification (DE) of 32 % and a galacturonic acid content of 88 %, and highly methylated (HM) block-wise pectin (Pectin Classic CU-L 028/10) with a DE of 70 % and a galacturonic acid content of 87 % (both derived from citrus peels), were purchased from Herbstreith & FOX KG (Neuenbürg, Germany). Pullulan (average molecular weight 150 kDa Lot # E47JGNH) was obtained from Tokyo Chemical Industry (Tokyo, Japan). NaOH pellets, HCl, Rhodamine B, acetone, and glutaraldehyde were purchased from Sigma-Aldrich (Steinheim, Germany), paraffin oil was obtained from Merck (Darmstadt, Germany). Omnifix® syringes were obtained from Braun (Melsungen, Germany). All materials were of analytical grade and used without further purification. All solutions were prepared with MilliQ water.

Sample preparation

WPI stock solutions (16 wt %) were prepared by slowly dissolving the protein in MilliQ water (Millipore, 18.2 MΩ), with continuous stirring for 6 h at room temperature (20 °C, 300 rpm) and stored at 4 °C overnight in the presence of 0.02 % sodium azide to prevent microbial growth. Stock polysaccharide solutions (4 wt %) were prepared by adding and hydrating the polysaccharide at 85 °C for about 2 h under continuous stirring. These solutions were then stored overnight at 4 °C to allow complete hydration. The solutions were left to equilibrate to room temperature (20 ± 2 °C) prior to mixing at the appropriate protein-polysaccharide ratios with the final protein concentration of 13 wt % and at pH 6.7 ± 0.2 . Subsequently, the mixed protein-polysaccharide solutions were degassed and transferred to 20 mL Omnifix® syringes with an internal diameter of 19.7 mm, which had been coated with paraffin oil for lubrication. The solutions were then heated (30 min, 95 °C) and allowed to set at room temperature (20 ± 2 °C) prior to testing.

Characterization of the microstructure of the gels

Confocal laser scanning microscopy (CLSM)

CLSM was used to visualize the gel microstructure according to a previously described procedure¹⁴ with modifications. Sample solutions were labeled with 20 μL/mL of aqueous solution of the fluorochrome Rhodamine B (0.2 % w/w) prior to heat treatment. Rhodamine B binds non-covalently to the protein network. Samples were then inserted between a concave slide and a coverslip and hermetically sealed. Subsequently, the samples were heated at 95 °C for 30 min. The visualization of the microstructure was performed using a Leica TCS SP5 microscope (Leica Microsystems (CMS) GmbH, Mannheim, Germany) configured with an inverted microscope. An Ar/Kr laser was used for excitation in the fluorescence single-photon mode. Images were taken with two different objective lenses: HCX PL APO 63×/1.20 W.CORR.CS and HC PL APO 20×/0.70 IMM/CORR.CS, at a scan depth of 20 μm. The incident light was emitted by a laser beam at 561 nm, and the emission of Rhodamine was recorded between 570 and 725 nm. Digital image files were acquired in 1024 × 1024 pixel resolution.

Scanning electron microscopy (SEM)

Gels for SEM were essentially prepared according to the previously described procedure^{7, 8} with modifications in which the obtained gels were cross-linked in 2.5 % (v/v) glutaraldehyde solution for 8 h instead of 1 % glutaraldehyde that was previously used. Additionally, following the cross-linking step, the gels were washed in MilliQ water overnight followed by exchanging of the MilliQ water with acetone in steps of 10- 30- 50- 70- 100 % acetone. The samples were then dried by critical point drying (CPD 030 BalTec, Liechtenstein) followed by breaking the gels to smaller pieces and gluing onto a SEM sample holder using carbon glue (Leit-C, Neubauer Chemicalien, Germany). The samples were subsequently stored overnight under vacuum. After drying of the carbon cement, the samples were sputter coated with 10 nm iridium in SCD 500 (Leica EM VCT 100, Leica, Vienna, Austria) prior to imaging. All samples were analyzed with a field emission scanning electron microscope (Magellan XHR 400L FE-SEM, FEI, Eindhoven, the Netherlands) at room temperature (20 ± 2 °C) at a working distance of 4 mm with SE detection at 2 kV. To determine the filament sizes, quantitative analysis was carried out in terms of the pair correlation function ($g(r)$) accordingly to a previously described procedure¹⁴. The images were analyzed using the pair correlation function according to

$$g(r) = g_0 \cdot e^{-(r/\xi)^\beta} + 1 \quad (1)$$

where g_0 is the contrast value at $r \rightarrow 0$, ξ is the correlation length characterizing the size of the domains, and β a stretched exponential factor. Six images were used for SEM analysis, over pairs of 874×874 pixels representing one SEM image. To reduce the dimensional effect the 2D SEM images, an average of the dark intensity from the raw images represented by the threshold level was measured and subtracted from the images as previously described. The $g(r)$ presented is an average of these images.

Rheological characterization of pea protein gels

Dynamic rheological measurements

Dynamic rheological characterization of whey protein (WP) gels was carried out according to the previously described procedure¹⁴ with modifications. An Anton Paar MCR 502 rheometer (Anton Paar, Graz, Austria) was used to determine rheological changes which occurred during in situ thermal processing of WP gels. The measuring system consisted of an oscillating cup and a fixed bob attached to a 13.2 torque bar. The protein solutions were carefully poured into the cup at 20 °C, and covered with a thin layer of paraffin oil to prevent water evaporation during experiments. Gels were formed by heating the samples from 20 °C to 95 °C at a constant rate of 1 °C/min, holding at 95 °C for 30 min, cooling down to 20 °C at a constant rate of 1 °C/min, and then holding at 20 °C for 30 min. An angular frequency of 6.28 rad/s and a maximum strain of 0.5 were used to measure the storage modulus (G') and loss modulus (G'') of the samples during the entire thermal treatment.

The experiments were performed in triplicate and the obtained results were averaged. Testing frequency and strain during gelation process was selected based on preliminary experimental results from strain and frequency sweeps of thermally induced gels to minimize damage to the gel network and to ensure that the linear visco-elastic behavior of the samples was retained.

Uniaxial compression

To determine the fracture properties of the gels, compression tests were performed on cylindrical gel samples (19.7 mm in diameter and 20 mm in height) compressed by a Texture Analyzer fitted with a 50 kg load cell and P/75 probe (TA.XTPlus, Stable Micro Systems, Surrey, UK). The cylindrical gel samples were obtained following heating of the protein or protein-polysaccharide solutions (95 °C, 30 min) followed by allowing the samples to set at room temperature overnight as aforementioned. The fracture properties were studied by a uniaxial compression test up to a 90 % deformation of the specimen height at a rate of 1 mm/s according to the previously described procedure^{7, 8}. The determined fracture properties included the true fracture stress and the true fracture strain. The true fracture stress and true fracture strain which will be designated as the fracture stress and fracture strain throughout this paper were calculated at each point from time zero to time of final deformation according to a previously described procedure^{7, 8}. The Young's modulus was calculated from the slope of the linear region of the stress-strain curve as previously described¹. Experiments were performed at least in triplicates.

Recoverable energy

The recoverable energy measurements were carried out on the cylindrically cut specimen described above according to the previously described procedure^{7, 8} with modification. Compression and decompression of the specimen was analyzed on the above described Texture Analyzer. Twenty percent of the maximum strain before fracture was applied to determine the energy release during decompression at a deformation speed of 1 mm/s. The percentage of recoverable energy of the gels was calculated from the area under the force-deformation curve as being the ratio of the amount of energy that was recovered after applying the stress over the amount of energy that was applied during the compression of the gels⁵. Each specimen was analyzed at least in triplicates.

Stress relaxation

To determine the fraction of energy dissipated via reversible structural rearrangements, stress-relaxation measurements were carried out as previously described⁶. During stress-relaxation, the WP-polysaccharide gels were compressed in the same way as for recoverable energy, however, the gels remained compressed at the set strain for 300 s before decompression. During these 300 s, the network had time to relax and over time, the force on the probe decreased due to stress relaxation.

The data recorded over time was fitted to Eq. 1, in which τ_1 is the short relaxation time, τ_2 is the long relaxation time, A_0 is the fraction of stress which did not dissipate, A_1 is the fraction of stress dissipated at τ_1 and A_2 is the fraction of stress dissipated at τ_2 .

$$Y = A_0 + (A_1 \times e^{x/\tau_1}) + (A_2 \times e^{x/\tau_2}) \quad (2)$$

Shear and intrinsic viscosity measurements

The shear viscosity of the serum phase was measured with an Anton Paar MCR 502 rheometer (Anton Paar, Graz, Austria) using a double concentric cylinder measuring unit with a gap of 0.5 mm. Samples were heated from 20 °C to 95 °C at a heating rate of 5 °C/min, followed by holding the samples at 95 °C for 30 min while recording the viscosity at a shear rate of 300 s⁻¹. Subsequently, the samples were cooled to 20 °C and held at 20 °C for 30 min while recording the viscosity at a shear rate of 300 s⁻¹. The intrinsic viscosity was obtained by plotting the changes in the shear viscosity as a function of the polysaccharide concentration and the extrapolation of the plot of the changes in the viscosity as a function of polysaccharide concentration to zero was taken to be the intrinsic viscosity.

Water Holding Capacity (WHC)

WHC of the gels was determined using the centrifugation procedure as adapted from Kocher and Foegeding¹⁵. A microcentrifuge filtration unit composed of an inner spin tube and a 2 ml Eppendorf tube (Axygen Biosciences, Inc., Union City, USA) was used in this experiment. Gels were cut in 10 mm height and 4.8 mm diameter cylinders and placed on the bottom of the spin tube which was covered with a 5.5 mm diameter filter paper to reduce grid size. Centrifugation was carried out at 3,000 and 10,000 × g for 10 min at 20 °C. Released serum from the gels was collected at the bottom of the Eppendorf tube and weighed. The WHC was then calculated as a percentage using Eq (3).

$$WHC = \frac{W_T - W_g}{W_T} \times 100 \quad [\%] \quad (3)$$

where W_T is the total amount of water in the sample (g) and W_g denotes the amount of water removed from the sample (g) at given centrifugation force (3,000 and 10,000 × g). Measurements were performed in duplicate.

Nuclear magnetic resonance (¹H-NMR) spectroscopy

¹H-NMR measurements were carried out on a home build ¹H-NMR spectrometer at room temperature (21 ± 1 °C) following heating of the samples at 95 °C for 30 min. A Maran Ultra NMR spectrometer (0.72 T magnetic field strength, 30.7 MHz proton resonance frequency) was used, controlled by RINMR software (Resonance Instruments Ltd., Witney, United Kingdom).

A modified Bruker RF and gradient probe (Bruker, Karlsruhe, Germany) with a cylindrical sample space with an inner diameter of 1.0 cm was used for the T_2 and T_2 correlated self-diffusion measurements. All ^1H -NMR measurements were performed in a glass tube (inner diameter, 7 mm) containing about 150 μL of sample.

Transverse relaxation (T_2) decay curves were measured using a conventional CPMG pulse sequence. T_2 relaxation decays were analyzed as a discrete sum of exponents by SplMod and as a continuous distribution of exponents by Contin¹⁶. T_2 correlated self-diffusion coefficients were determined using Diffusion Relaxation time COrrrelation SpectroscopY (DRCOSY)¹⁷. Extracting diffusion constants from echo-time-dependent PFG NMR data was done using relaxation-time information¹⁸. Typical acquisition parameters were as follows: repetition time, 3 s (four averages); spectral width, 50 kHz, number of echoes, 4,000 or 8000, with five data points per echo and an inter echo time of 200 or 300 μs , depending on the decay rates. The gradient pulses had a duration of 2 ms; the observation time Δ , the time between the gradient pulses, was 25 ms, the amplitude of the gradient pulses (G) was varied between 0.12 and 1.0 T/m in 16 logarithmically distributed steps. 2D Laplace inversion of the data yielded diffusion- T_2 correlation maps¹⁹.

Statistical analysis

Data are reported as mean values \pm standard deviations (SD) for all data points. Significant differences in mechanical properties were evaluated by determining the correlation between experimental data using one sample t-test with minimum significance set at the 5 % level ($P < 0.05$) using SPSS (version 19, International Business Machines, Armonk, NY, USA).

Results and Discussion

The aim of this study was to determine the role of the serum phase viscosity on the recoverable energy of whey protein (WP) gels by energy dissipation via viscous serum flow upon mechanical deformation. In order to describe physical properties underlying energy dissipation, various gels were prepared at a fixed 13 wt % protein concentration with the polysaccharide concentration being varied as a tool to modulate the viscosity of the serum phase. In all experiments in which WP-pectin samples were prepared, the polysaccharide concentrations were kept sufficiently low to prevent the occurrence of macro-scale phase separation events leading to gels with a substantial different morphology and thereby different rheological responses such as Young's modulus and/or fracture stress. For this reason, the pectin concentrations were kept at a maximum of 0.2 wt %. In the case of pullulan, much higher concentrations could be used, up to 5 wt %.

Gel microstructure

To visualize the microstructure of the formed gels, confocal laser scanning microscopy (CLSM) and scanning electron microscopy (SEM) were used to analyze the network structure at a supra-micrometer (CLSM) and submicron (SEM) level as shown in **Fig. 1**. From the CLSM micrographs, the protein network, stained with Rhodamine B is represented as the bright areas and non-protein phase, which will be referred to here as the serum phase, is depicted by the dark areas. The gels appear to be homogenous on lengths scales larger than $0.5\ \mu\text{m}$, and therefore show no features visible with CSLM. At higher pectin concentrations and in particular for HM pectin local inclusions can be observed. The gels appear to be homogenous and no macroscopic phase separation was observed, consistent with other reports^{20, 21}. It is important to note that with an increase in pectin concentration above 0.2 wt %, phase separation events are observed and coarse-stranded network structures were found at a supra-micrometer level (results not shown).

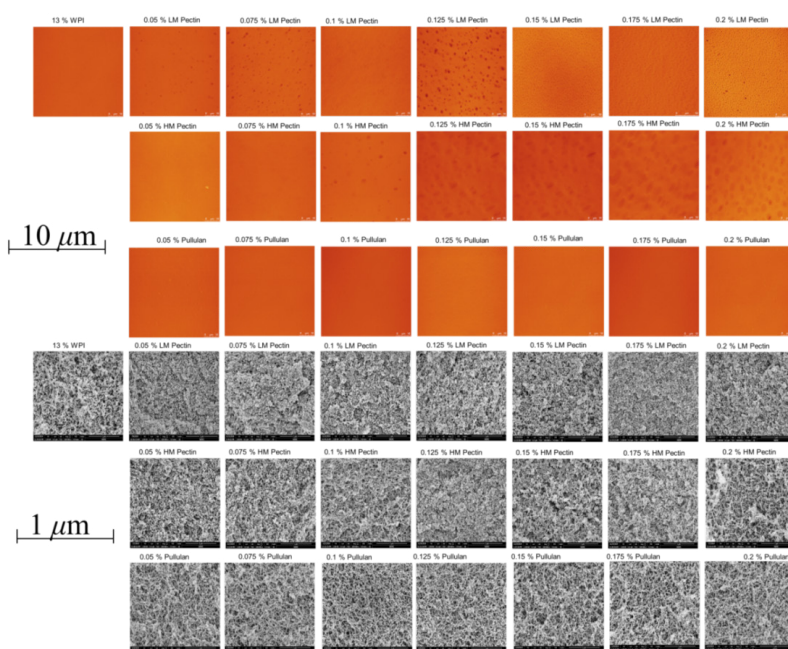


Figure 1a: The CLSM and SEM micrographs for WP gels made in the presence and absence of polysaccharides.

As may be expected based on the inherent difference between WP and the polysaccharide, the incompatibility of the biopolymers²² is the most probable occurrence in WP-pectin gels at the low pectin concentrations used in this study, as opposed to phase separation which is the most likely outcome of the gelation of mixed biopolymer solutions²³ and is usually driven by the incompatibility of the biopolymers which is a fundamental property of many protein-polysaccharide mixtures²⁴.

Due to the resolution of CLSM, the morphology of the formed gels in terms of aggregate size, shape and the connectivity of WP gels could not be reported (**Fig. 1**). Additionally, the spatial distribution of the polysaccharide in the gels could not be determined as the polysaccharides were not fluorescently labeled before imaging with CLSM.

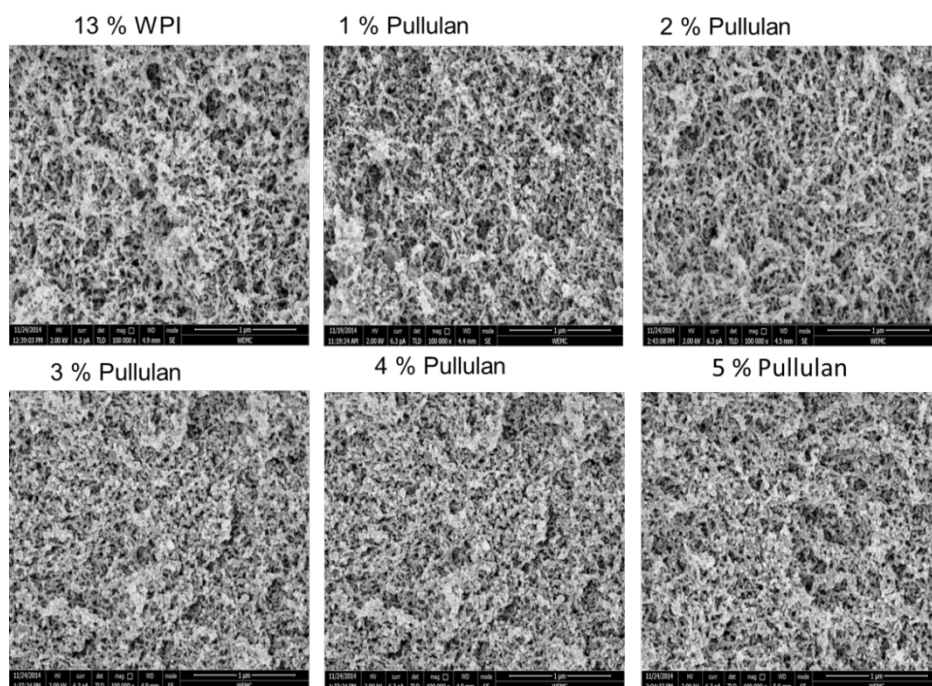


Figure 1 b: SEM micrographs for WP gels made at higher pullulan concentrations (1 – 5 wt %).

To visualize the microstructure at a submicron level, SEM was used and the obtained micrographs are shown in **Fig. 1 a**. In **Fig. 1 a**, no major variations were observed in the network structures in terms of pore sizes, strand thickness, and coarseness, at low pullulan concentrations, hence images were also obtained for whey protein gels at higher pullulan concentrations as shown in **Fig. 1 b**.

In the employed concentration regimes no major differences are observed in morphology; as they are what is considered to be all fine-stranded networks in the range of around 70 – 280 nm (**Fig. 2**). Gels prepared from WP without the addition of polysaccharides have ‘thread-like’ filaments connecting different protein aggregates with relatively small distances between the junctions that connect these aggregates. For the gels prepared with WP-pullulan at similar concentration as LM and HM pectin, the networks appear to be more open, and to have larger pores. An increase in the pullulan concentration up to 0.2 wt % did not result in significant changes in the pore and filament sizes (**Fig. 1 a**).

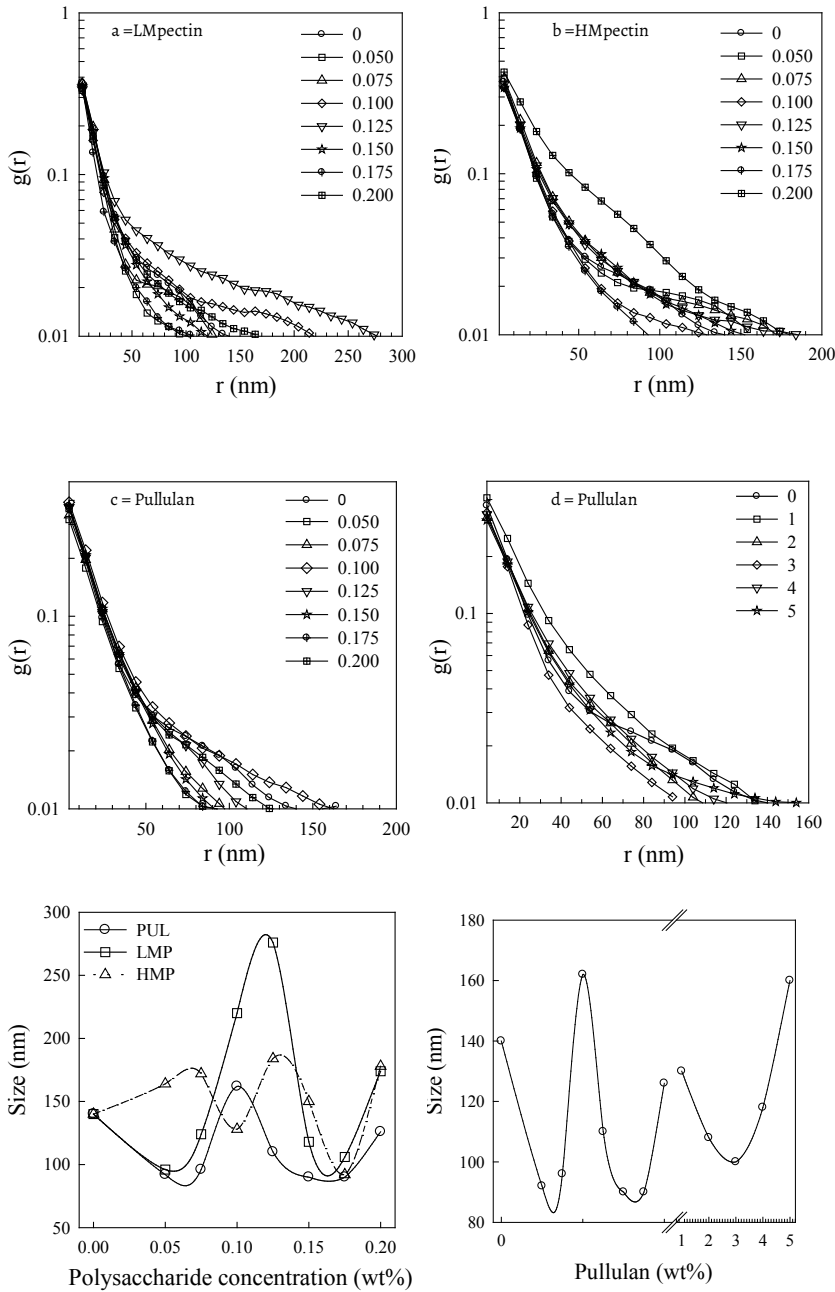


Figure 2: Log-linear plot for $g(r)$ for different concentrations of a = LM pectin; b = HM Pectin; c = Pullulan low concentration; d = Pullulan high concentration. The filament sizes of whey protein network structures as a function of polysaccharide concentration are plotted in Fig. 2 e, whereas the pullulan samples at low and higher concentrations are plotted in Fig. 2 f. The results were obtained by quantitative analysis of SEM images. The solid lines in Fig. 2 a, b, c and d, are fits to Eq. 1.

The size of the filaments was shown to decrease when up to 3 wt % pullulan was added followed by an increase with an increase in pullulan concentration beyond 3 wt %. For WP-pullulan gels prepared at 5 wt % pullulan, the network structure seems to form local clusters connected with interwoven filaments (**Fig. 1 b**).

The variations in the filament sizes were also observed when quantitative analyses of the SEM images (**Fig. 2**) was carried out according to a previously described procedure^{8 14}. Changes in filament sizes were observed with an increase in polysaccharide concentration as well as changing the type of polysaccharide.

The changes in the filament sizes can be observed in $g(r)$ plots for the various polysaccharide concentration for LM pectin (**Fig. 2 a**), HM pectin (**Fig. 2 b**), pullulan low concentrations i.e. 0.05 – 0.2 wt % (**Fig. 2 c**) and pullulan at higher concentrations i.e. 1 – 5 wt % (**Fig. 2 d**) plotted in log-linear representation.

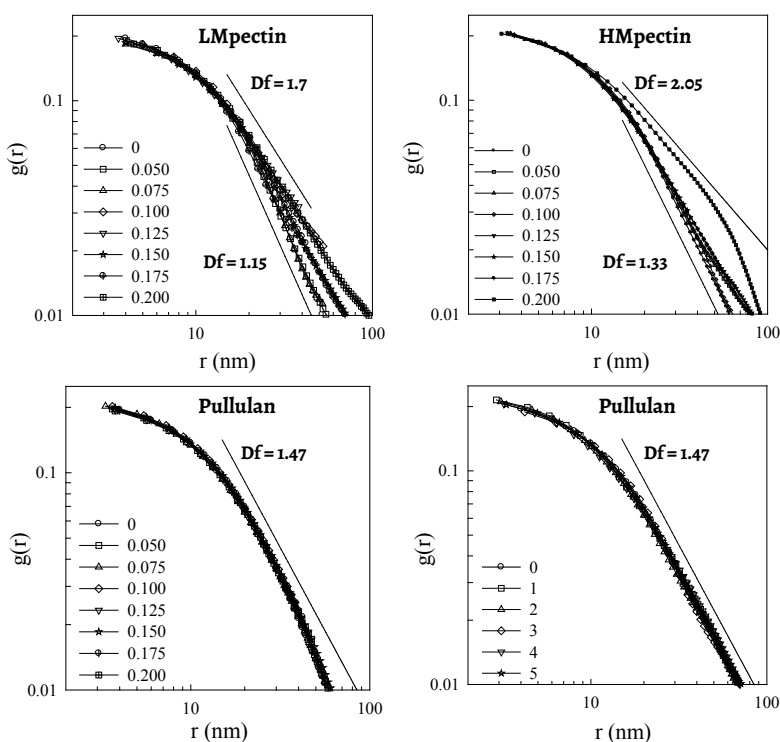


Figure 3: the plots showing the fractal dimension of whey protein gels obtained from 2D images for a = LM pectin, b = HM Pectin, c = pullulan at low concentration, and d = pullulan at high concentration

From the plots in **Figs. 2 a - d**, the correlation length (nm) for the filament size (nm) was obtained as shown in **Fig. 2 e** for whey protein gels made in the presence of LM pectin, HM pectin and pullulan at varying concentrations (0.05 – 0.2 wt %).

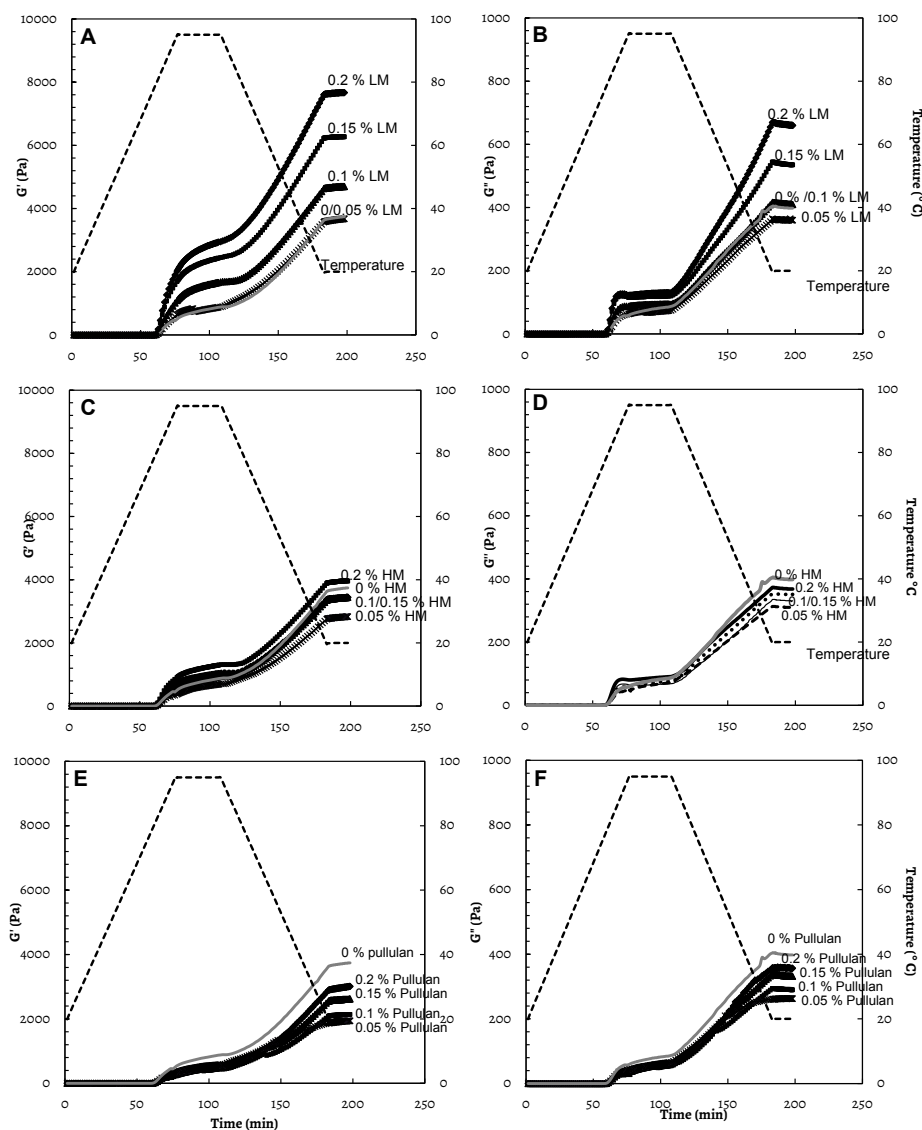


Figure 4: Changes in G' as a function of time for WP-LM pectin (**A**), WP-HM pectin (**C**), and WP-pullulan (**E**) and G'' for WP-LM pectin (**B**), WP-HM pectin (**D**), and WP-Pullulan (**F**) gels prepared at varying polysaccharide concentrations. The dotted line shows the temperature history during gel formation.

In **Fig. 2 f** changes in the filament sizes of whey protein gels made in the presence of low and higher pullulan concentration are presented. For WP gels prepared in the presence of the polyelectrolyte pectin (LM and HM), the networks are connected with filaments with short distances between the junctions of the various strands that connect to the protein aggregates (**Fig. 1 a**).

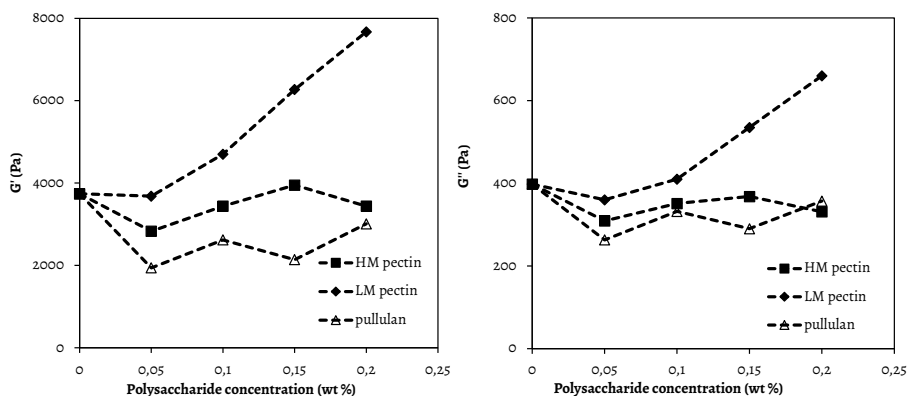


Figure 5: Changes in the final G' (A) and G'' (B) as a function of polysaccharide concentration (wt %) for gels prepared from WP in the presence of LM and HM pectin as well as pullulan.

The filament sizes vary with an increase in polysaccharide concentration (**Fig. 2 e** and **f**). For gels made from LM pectin, the filament sizes were shown to decrease with the addition of 0.05 wt % LM pectin (**Fig. 2 e**).

With further increase in the LM pectin concentration up to 0.125 wt %, the filament sizes increased. Addition of 0.175 wt % and 0.2 wt % of LM pectin resulted in a further increase in filament sizes. The lack of a clear trend in changes in the filament sizes with an increase in polysaccharide concentration was also observed for whey protein gels made in the presence of HM pectin although the filament sizes for whey protein- HM pectin gels were smaller at some concentrations (**Fig. 2 e**). The fluctuation in the filament sizes observed in pectin samples could indicate the occurrence of micro-scale phase separation that introduces inhomogeneity in the network structure. Thus, during imaging of the samples the zones in which the images were obtained from could either be 'protein rich' or 'pectin rich' domains resulting in the observed differences in the filament sizes. The size fluctuation was however higher in HM pectin compared to LM pectin samples. For this gels, local inclusion were also observed from CLSM images (**Fig. 1 a**). In the case of pullulan, this effect is minimal and the filament size fluctuates between 70 – 160 nm (**Fig. 2 f**).

Fig. 3 shows the fractal dimensions obtained from the analysis of 2D images of whey protein gels. Changes in the protein concentration resulted in variation in the fractal dimension which could indicate structural changes from finer to coarser networks. Addition of pullulan to even higher concentrations did not result in a change in the fractal dimension and this shows that pullulan does not have an influence of the gel morphology.

It can thus be concluded that distinctively, the addition of the three different polysaccharides to WP results in the formation of networks that show morphological differences. For networks made at increasing pullulan concentrations i.e. from 0.05 wt % to 0.2 wt % pullulan (similar to concentrations as pectins), the integrity of the network structure was preserved. For samples prepared with pectins, variations in the filament sizes are observed which range between 70 – 280 nm, although the filament sizes for WP-LM pectin network structures were considerably larger than WP-HM network structures at all concentrations except for the lowest concentrations used.

Dynamic visco-elastic properties of whey protein gels

To study whether the presence of a polysaccharide influences the mechanism of gel formation as well as to relate the viscous modulus (which gives information on the energy dissipated via heat during gel formation) to the viscosity of the serum phase, the changes in visco-elastic properties of WP gels were recorded as a function of time during heating of the WP-polysaccharide solutions. The storage modulus (G') and the loss modulus (G'') developed equally with an increase in the incubation time although the G' were significantly higher in magnitude than the G'' (**Figs. 4 and 5**).

The time for the onset of gelation (T_{onset}) for WP gels remained the same with an increase in the polysaccharide concentration (around 60 min) as can be observed from **Figs. 4 A – 4 F**. The gelling temperature (T_{gel}), defined as the temperature at which the G' began to increase in the heating process also remained the same at around 80 °C for WP gels prepared with and without the addition of either pectin (either LM or HM) or pullulan (**Figs. 4 A, C, and E**). The strength of the gels increased with an increase in polysaccharide concentration, with WP gels made upon the addition of LM pectin being the strongest (most firm) (**Fig. 4 A**). The G'' for WP gels prepared in the presence of LM pectin was also the highest (**Fig. 4 B**). No significant changes in the G' and G'' were observed during heating of the samples from 20 °C - 95 °C. Upon holding of the samples at 95 °C the stiffness of the gels was shown to increase and further increased upon cooling of the samples to 20 °C. Holding of the samples at 20 °C after gel formation did not further enhance the firmness of the gels (**Figs. 4 A, C, and E**). A similar trend was observed for the changes in the G'' (**Figs. 4 B, D, and F**).

The differences in the firmness of the gels in the presence of different polysaccharides may be related to the contribution of the viscosity of the serum phase on the visco-elastic properties of the formed gels.

When the intrinsic viscosity of the different polysaccharides was determined, pullulan samples had the lowest intrinsic viscosity of 1 dl/g, HM pectin had the highest intrinsic viscosity of about 15 dl/g, whereas LM pectin had an intermediate intrinsic viscosity of 6 dl/g (results not shown). Gels prepared from polysaccharides with the lowest intrinsic viscosity (pullulan) were the least firm. Gels with intermediate intrinsic viscosity (LM pectin) were the most firm whereas for gels that had the highest intrinsic viscosity, the effect on the firmness of the gels was moderate. Thus, it can be concluded that the modulation of the serum viscosity of WP results in firmer gels (increased gel strength) although the mechanism of gel formation (as observed from the Tgel) as well as the kinetics of gel formation (determined from the tonset) are not changed with the presence of the polysaccharide when gel formation is induced. The HM pectin samples which had the highest intrinsic viscosity, in this case can induce phase separation which affects the gel strength. The analysis of the images in **Fig. 2** pointed at the occurrence of micro-phase separation and this corresponds to the highest intrinsic viscosity measured for this samples which could also contribute to the differences observed in the gel strength.

Changes in G' (**Fig 6 A**) and G'' (**Fig. 6 B**) during heating and cooling were recorded for WP gels as a function of polysaccharide concentration and normalized for the changes in viscosity of the polysaccharide as a function of G' (**Fig. 6 C**) and G'' (**Fig. 6 D**).

The ratio of the increase in G' during heating ($\Delta G'_{\text{heat}}$) to that during cooling ($\Delta G'_{\text{cool}}$), has been reported to reflect the relative contributions of the intermolecular interactions to the final value of $G'^{25, 26}$ and is therefore an indicator for the gelation mechanism. With an increase in LM and HM pectin, the ratio of $\Delta G'_{\text{heat}}/\Delta G'_{\text{cool}}$ increased for up to 0.15 wt % after which this ratio was not affected for WP-LM pectin whereas a slight reduction was observed for WP-HM pectin gels (**Fig 6 A**).

A similar trend was observed for the ratio of $\Delta G''_{\text{heat}}/\Delta G''_{\text{cool}}$ although a slight reduction in this ratio was observed for WP-LM pectin at 0.2 wt % (**Fig. 6 B**).

For gels prepared from WP-pullulan no clear trend was observed as an increase followed by a decrease and a subsequent increase in this ratio was observed when the pullulan concentration was increased. An increase $\Delta G'_{\text{heat}}/\Delta G'_{\text{cool}}$ ratio with an increase in pectin concentration suggests that an increase in polysaccharide concentration appears to enhance intermolecular interactions which enhance the gel formation. When the $\Delta G'_{\text{heat}}/\Delta G'_{\text{cool}}$ (**Fig 6 C**) and $\Delta G''_{\text{heat}}/\Delta G''_{\text{cool}}$ (**Fig 6 D**) was normalized for the changes in the viscosity, the $\Delta G'_{\text{heat}}/\Delta G'_{\text{cool}}$ ratio was shown to increase steeply with an increase in the viscosity of the serum phase for WP-LM pectin gels.

With further increase in the viscosity, this ratio does not change further. For WP-HM pectin gels, this ratio seems not to be affected initially until when the viscosity increases to around 0.5 mPa.s. With a further increase in the viscosity, the $\Delta G'_{\text{heat}}/\Delta G'_{\text{cool}}$ ratio increases though the slope is not as steep as that of WP-LM pectin gels. A further increase in the shear viscosity beyond 1.5 mPa.s, resulted in a decrease in $\Delta G'_{\text{heat}}/\Delta G'_{\text{cool}}$ ratio.

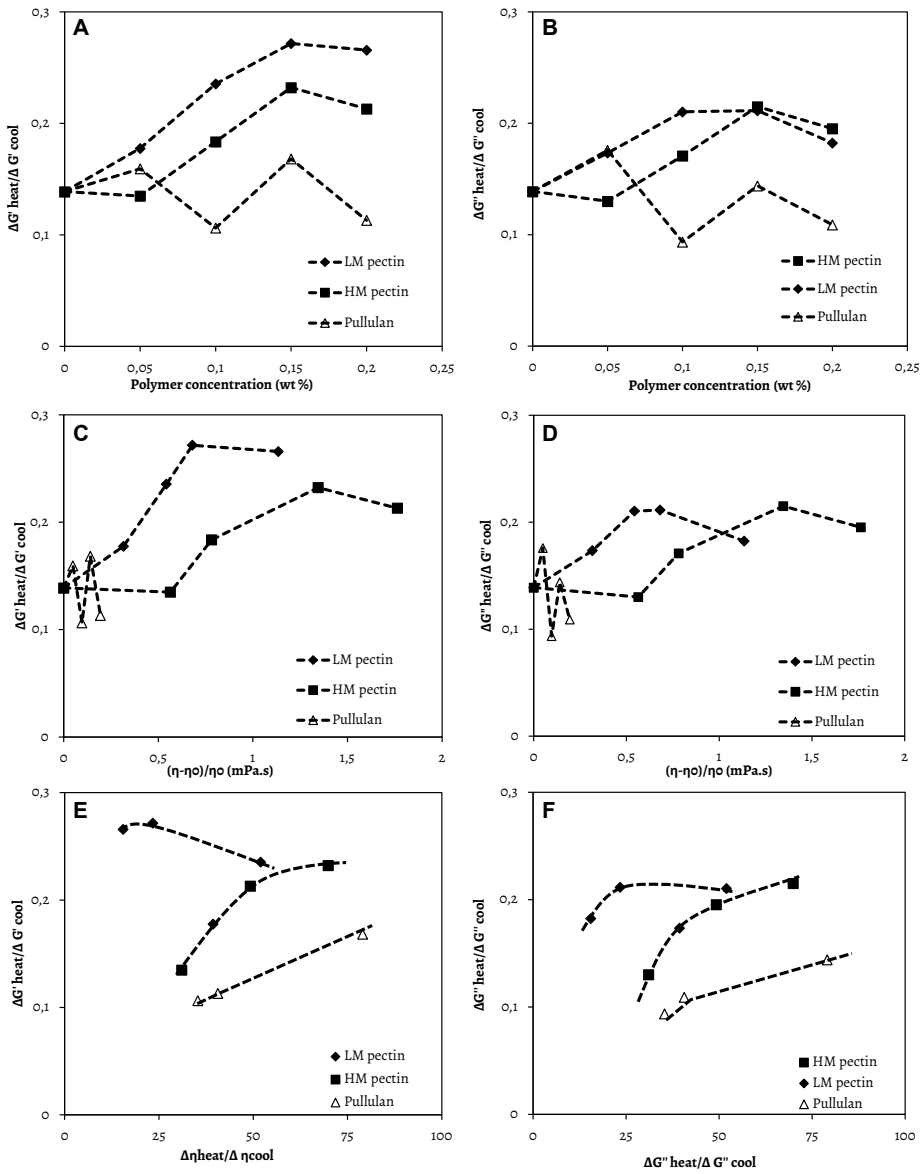


Figure 6: Relationship among pea protein and $\Delta G' \text{ heat} / \Delta G' \text{ cool}$ and $\Delta G'' \text{ heat} / \Delta G'' \text{ cool}$ values of whey protein gels at a fixed 13 wt % whey protein concentration plotted as a function of varying polysaccharide concentration for the relationship between G' (A) and G'' (B) during heating and cooling, as a function of changes in viscosity of the serum phase for the relationship between G' (C) and G'' (D) during heating and cooling, and as a function of the change in viscosity during heating and cooling for the relationship between G' (E) and G'' (F). For clarity, the samples in which 0.05 wt % pullulan and 0.1 wt % HM pectin have been left out in **Figs. 6 E and F**.

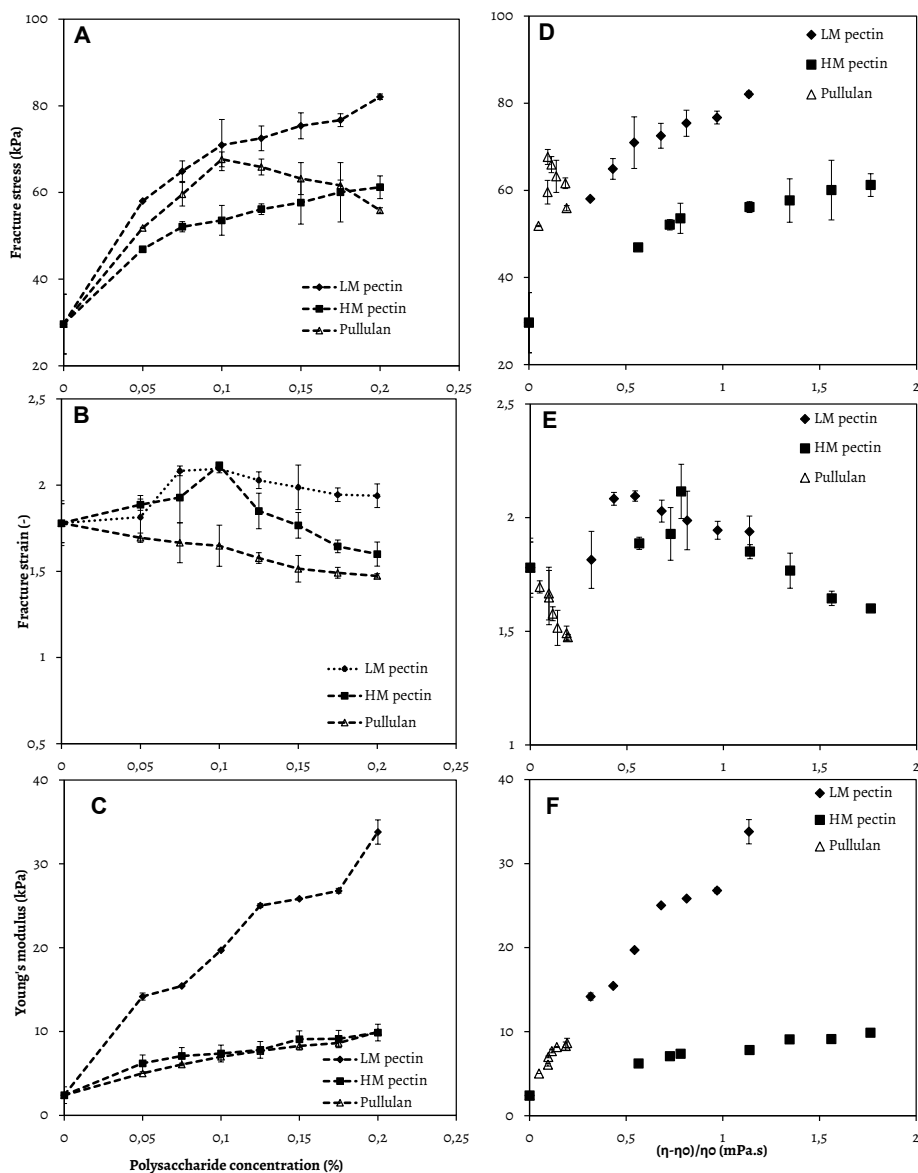


Figure 7: Mechanical deformation properties (fracture stress, fracture strain, and Young's modulus) of whey protein gels are shown in **Fig. 7 A** (fracture stress), **B** (fracture strain), and **C** (Young's modulus). These data were normalized for the changes in viscosity as shown in **Fig. 7 D** (fracture stress), **E** (Fracture strain), and **F** (Young's modulus). The error bars are derived from the SE calculated from the SD of the variations of 5 – 6 samples.

The results suggest that the type of polysaccharide affects the contribution of the intermolecular interactions such as hydrogen bonding on gel formation. As in the case of the concentration, no clear trend was observed for pullulan gels which suggest that pullulan does not have a straight forward influence on the contribution of intermolecular interactions on gel formation. The change in $\Delta G'_{\text{heat}}/\Delta G'_{\text{cool}}$ (**Fig. 6 E**) and $\Delta G''_{\text{heat}}/\Delta G''_{\text{cool}}$ (**Fig. 6 F**) plotted as a function of the $\Delta \eta_{\text{heat}}/\Delta \eta_{\text{cool}}$ show an increase in both $\Delta G'_{\text{heat}}/\Delta G'_{\text{cool}}$ and $\Delta G''_{\text{heat}}/\Delta G''_{\text{cool}}$ ratio when the viscosity of the serum phase was changed during the heating of the samples to allow for gel formation. This result confirms the suggestion that changes in the viscosity of the serum phase play a major role in the formation and the strength of WP gels.

Rheological properties at large deformation

The fracture properties of WP-polysaccharide gels were measured by uniaxial compression at a deformation constant speed of 1 mm/s as shown in **Fig. 7**.

Table 1: τ_1 values for a selected number of mixed WP-polysaccharide gels. The measurements were carried out by compressing the gels up to 20 % strain followed by holding of the gels at the maximal loading strain for 5 min.

WP + polysaccharide (%)	τ_1 (s)	Fraction of total stress
0 polysaccharide	6.65 ± 0.4	0.18 ± 0.01
0.05 HM pectin	6.84 ± 0.21	0.16 ± 0.01
0.1 HM pectin	7.54 ± 0.40	0.15 ± 0.02
0.15 HM pectin	7.87 ± 0.63	0.12 ± 0.02
0.05 LM pectin	7.01 ± 0.08	0.16 ± 0.01
0.1 LM pectin	7.75 ± 0.16	0.14 ± 0.01
0.15 LM pectin	8.09 ± 0.30	0.12 ± 0.01
1 % pullulan	6.5 ± 0.01	0.17 ± 0.01
2 % pullulan	6.89 ± 0.33	0.16 ± 0.01
3 % pullulan	7.07 ± 0.23	0.15 ± 0.23

Fracture

The fracture stress and strain were determined from the macroscopic fracture point, which corresponds to the maximum in stress versus strain curve and the results of the stress response for WP gels upon deformation at an applied compressive strain for a compression rate of 1 mm/s are shown in **Fig. 7**.

An increase in the concentration of LM pectin resulted in an increase in the fracture stress (**Fig. 7 A**) which corresponds to an increase in the viscosity of the serum phase (**Fig. 7 D**). A similar trend was observed by the addition of HM pectin although the gel strength was significantly lower for HM compared to LM pectin. The development of stronger gels with the addition of pectin to a certain concentration was also observed for acid-induced WP-LM pectin complex gels ²⁷. In general, WP gels in the presence of LM-pectin formed the strongest gels that showed the highest fracture stress values. Contrarily, the addition of more pullulan resulted in an increase in the gel strength but only up to 0.1 wt % pullulan after which the gels became weaker (**Fig. 7 A**). The strength of the gels also decreased with changes in the viscosity of the serum phase due to an increase in pectin concentration as shown in the fracture stress results normalized for viscosity (**Fig. 7 D**). The decrease in fracture stress with further increase in the pullulan concentration beyond 0.1 wt % could give an indication of the presence of the polysaccharides interfering with the formation of the network structures even though, the addition of non-surface active anionic polysaccharide to protein gels is not expected to contribute to the network formation. In WP-pullulan samples, the pullulan is expected to act as an inert filler, defined as a component that is not involved in the network formation and does not have any affinity to the network forming molecule, and this was shown to result in the decrease in gel strength. The reduction in strength of the gels could also be related to stress concentration at contact points between the polysaccharide and the protein molecules leading to inhomogeneities in the matrix and as a result lower fracture stress.

The fracture strain, a measure of the brittleness of gels was determined for gels made with and without the addition of polysaccharides as a function of polysaccharide concentration (**Fig 7 B**) and normalized for the viscosity of the serum phase (**Fig. 7 E**). The addition of 0.075 wt % LM pectin resulted in an increase in fracture strain. Beyond 0.075 wt % LM pectin, no significant changes in the fracture strain were observed, an indication that the gels were equally brittle. An increase in HM pectin concentration to 0.1 wt % also resulted in an increase in the fracture strain, an indication that the gels were less brittle at these LM and HM pectin concentrations. Beyond 0.1 wt % HM pectin concentration, the fracture strain of the gels decreased an indication that the gels became more brittle. In general, WP gels prepared with the addition of pullulan resulted in the formation of the most brittle gels whereas the WP-LM pectin gels were the least brittle. In the case of the addition of pullulan, the fracture strain of the gels also decreased linearly, an indication that the gels were more brittle.

Changes in the viscosity of the serum phase resulted in an increase in the fracture strain but only up to the viscosity equivalent to around 1 mPa.s for both LM and HM pectin after which the fracture strain decreased with further changes in the viscosity (**Fig. 7 E**), an indication that higher viscosity results in more brittle gels. For gels made with WP-pullulan, further changes in the viscosity of the serum phase resulted in a further decrease in the fracture strain which also shows that higher viscosity results in more brittle gels than lower viscosity.

The Young's modulus, the measure of the stiffness of gels was measured for WP gels in the presence and absence of polysaccharides (**Fig. 7 C**) and normalized for the viscosity of the serum phase (**Fig. 7 F**). In all cases, the gel stiffness increased with an increase in the polysaccharide concentration. WP gels made in the presence of LM pectin were at all concentrations and viscosity changes the most stiff, whereas there were no significant differences in the stiffness of the gels prepared at various concentrations of HM pectin and pullulan with an increase in the polysaccharide concentration (**Fig. 7 C**).

The increase in the stiffness of the gels could be related to increased local concentration and enhanced connectivity among protein aggregates leading to increased gel stiffness where higher forces were required for deformation.

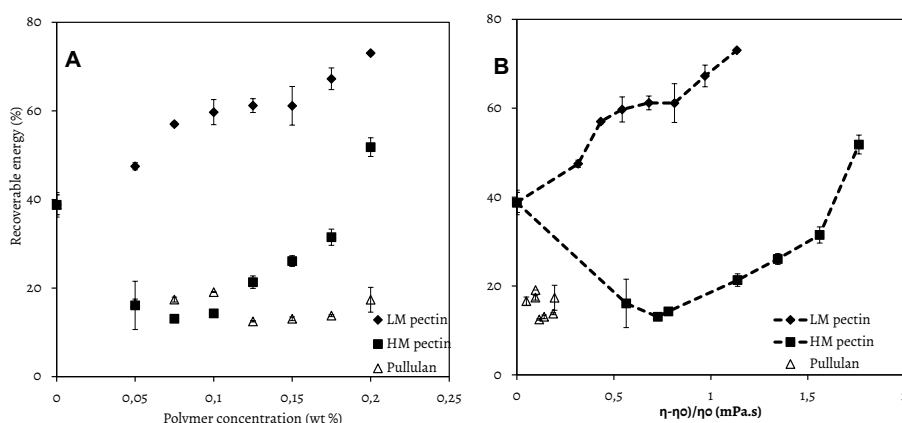


Figure 8: The recoverable energy of gels formed by WP-polysaccharide with different concentration of polysaccharides (A) and the recoverable energy normalized for the shear viscosity (B). The measurements were carried out at 20 % of the maximum strain before fracture.

Additionally, the observed enhanced stiffness of the gels could be related to the microstructure of the gels. The modulus of gels has been reported to be proportional to the number of the effective strands and the modulus of the strands²⁰. For the homogenous networks formed in this study, it can be hypothesized that the modulus of the gels is dominated by the modulus of the strands and not the number of effective strands. The differences in the strands can be observed in **Figs. 1** and **2**.

Stress relaxation

To get insights on time-dependent contribution of energy dissipation that is related to structural rearrangements of WP gels, stress relaxation properties of selected gels were determined (**Table 1**).

The true stress of the obtained data was normalized and plotted as a function of time (s).

The plots of the normalized stress as function of time for the gels were fitted according to Eq. (2) yielding longer relaxation times (τ_2) typical in the range of 118 – 148 s, a range negligible for recoverable energy measurements (Results not shown) and τ_1 values, (Table 1). Typical R^2 values for fitted data were close to 0.99 in all cases.

The τ_1 values are the short relaxation times which are relevant for recoverable energy measurements that typically take 8 s (2*20 % of 20 mm at 1 mm/s = 8 s). The stress was monitored during 5 min after applying the compression load at 1 mm/s deformation rate. The results show that the stress build-up in the gels decays in this time-span to about 12 - 18 %. The τ_1 value for WP without the addition of polysaccharide was 6.65 ± 0.4 s. An increase in the HM pectin concentration resulted in an increase in the τ_1 value from 6.65 to 7.87 ± 0.63 for WP gels made in the presence of 0.15 HM pectin (Table 1). A similar trend was observed for WP gels made in the presence of different concentrations of LM pectin and pullulan, where the τ_1 values continued to increase with an increase in the polysaccharide concentration. The differences observed in τ_1 values are however not significantly different when the polysaccharides are varied, and this indicates that structural rearrangements explained by stress relaxation do not contribute significantly to energy dissipation in WP gels.

The ability of the gels to store energy

From the energy balance model described by van Vliet and co-workers (1991) upon the application of deformation to gels⁴, the energy can dissipate via the mechanism described in the introduction⁶, whereas the other part of the energy can be stored⁴. In this work, structural rearrangements were shown not to result in significant energy dissipation as explained by the stress relaxation measurements (Table 1). If one considers plastic deformation to be an irreversible structural rearrangement that cannot relax⁶, it makes sense to check whether this events occurred during deformation as they can contribute to energy dissipation. Careful analysis of the loading-unloading profiles showed that the build-up of resilience stress were similar in all cases. Recently, it was hypothesized that plastic deformation might depend on the impulse moment acting on the gel and as such, irreversible structural rearrangements require an activation energy to bring the material to a new chemical state⁶. However, there were no obvious indications for such behavior in this study. This suggests that the loss of energy as a result of irreversible structural rearrangements was minimal and hence can be assumed to be negligible. The recoverable energy was thus determined for WP gels as a measure of the energy that is stored within the gel network. The recoverable energy for WP gels was about 39 % (Fig. 8 A). An increase in LM and HM pectin concentration resulted in a concurrent significant increase ($P < 0.05$) in the recoverable energy. An increase in the recoverable energy can be related to a number of factors. Firstly, the contribution of the viscosity of the serum phase to the flow of the serum around the network when it deforms.

The pectin samples were shown to be more viscous and in a closed packed system such as a gelled network, more serum could be entrapped in the networks with biopolymers that contribute a higher effective viscosity and hence higher capillary forces will be required to expulse the entrapped serum. Thus, the energy loss via dissipation in this case due to viscous serum flow is reduced and this results in a higher recoverable energy. The influence of the viscosity of the serum phase on the recoverable energy was observed when the recoverable energy results were plotted as a function of changes in the viscosity of the serum phase (**Fig. 8 B**), where the recoverable energy was normalized for changes in the viscosity of the serum phase. Secondly, depending on the charge density, an enhanced interaction between the protein and the polysaccharide at relatively high pectin concentration is envisioned compared to lower pectin concentrations resulting in stiffer networks that do not deform easily and hence have higher energy storage. Thirdly, the network structure also plays an important role in the energy that can be stored within a network. In the case of whey protein-pectin gels, the networks are finer and composed of smaller pores with varying filament sizes from around 70 – 280 nm (**Fig. 2**). The low porosity of the network gives low serum release during deformation resulting in higher energy storage.

The addition of pullulan to the protein gels was shown to result in a decrease in the recoverable energy when the recoverable energy was normalized for changes in the viscosity of the serum phase (**Fig. 8 B**), whereas no significant changes in the recoverable energy were observed when pullulan concentration was further increased (**Fig. 8 A**). The decrease in the recoverable energy with an increase in the pullulan concentration may be related to a number of factors. Firstly, the friction between the polysaccharide (filler) phase and the protein continuous phase due to the lack of protein-polysaccharide interaction can result in more energy being lost via dissipation at the expense of the storage of energy, and this result in lower recoverable energy values. Secondly, the contribution of the microstructure to energy dissipation can result in a decrease in the recoverable energy within the network. Upon the addition of pullulan to WP, the network structures become more stretched, more open, and “fibrillar like” with bigger mesh sizes and larger porosity (**Fig. 1 a and b**). Hence, upon applied deformation, higher serum could be released from the network resulting in energy loss at the expense of storage. Thus, it can be concluded that the differences in the recoverable energy observed here are related to friction caused by serum flow which depends on (i) network porosity, which is set by the morphology, and (ii) the viscosity of the serum phase.

Serum flow

From the above results, it is clear that recoverable energy does depend on type and amount of polysaccharide included in the serum phase. Just evaluating the gel morphology is not sufficient enough to differentiate between the gel porosity and inherent viscosity. For this purpose two types of experiments were performed to elucidate on the mobility of serum within the gel: water holding measurements and T_2 -relaxation times of the aqueous phase.

Table 2: The T₂ values and the self-diffusion coefficient for WP-polysaccharide gels

Polysaccharide concentration (%)	T ₂ (ms)	Self-diffusion coefficient ($\times 10^{-9} \text{ m}^2 \text{ s}^{-1}$)
0	102	1.74
Pullulan		
1	66	1.56
2	75	n.d. [*]
3	77	1.54
4	70	n.d. [*]
5	67	1.32
HM pectin		
0.05	72	1.59
0.075	64	n.d. [*]
0.1	72	n.d. [*]
0.125	63	n.d. [*]
0.15	72	1.61
0.175	73	n.d. [*]
0.2	77	1.61
LM pectin		
0.05	70	1.54
0.075	73	n.d. [*]
0.1	68	n.d. [*]
0.125	66	n.d. [*]
0.15	67	1.51
0.175	62	1.53
0.2	62	1.52

Water holding experiments

To measure the serum that can be displaced from the gel by applying centrifugational forces (at 3000 and 10000 $\times g$) is referred to here as the water holding capacity (WHC). The WHC for WP gels without the addition of polysaccharides was to 100 % (results not shown).

The addition of polysaccharides to WP up to 0.2 wt % for LM and HM pectin did not affect the WHC of the mixed gels. For gels where up to 5 % pullulan was added, the WHC was also not affected (results not shown). This shows that the type of networks that are formed are homogenous and protein continuous. Thus, the amount of water release remained the same given that the aqueous phase was still entrapped throughout the protein network structure. Another possible reason for the high WHC with the addition of polysaccharides and especially in this case the addition of pectin below 0.2 wt % may also be due to the fact that WP are highly hydrophilic molecules which are mainly formed by polar amino acids²⁸. At low pectin concentrations, the interaction between the protein and pectin is less and thus more hydrophilic sites remain available during the gel formation that are available to bind water. This explanation also holds in the case of pullulan, a non-charged polysaccharide, which does not interact with WP. Hence, more hydrophilic sites are exposed on the surface of the protein upon heating to induce gel formation that can favor the binding of water during gelation. From the WHC results, it can be concluded that given that the porosity of the networks is too small and stiffness is high; all the entrapped water moves with the network during deformation and this results in higher WHC. Therefore, the contribution of the serum flow to energy dissipation in WP gels is regarded as being small in this case and this is one of the reasons why the gels made in this study were shown to have higher recoverable energy especially so in the case where LM and HM pectin gels were made. For pullulan, this contribution is not straight forward as the recoverable energy is still lower compared to WP-LM pectin or WP-HM pectin gels although at the applied centrifugal forces the WHC is not different when gels made from whey-pullulan are compared to those of whey-pectin.

NMR

To obtain more details on the diffusion of water molecules within the gelled networks and their sensed apparent viscosity, ¹H-NMR was used to characterize apparent diffusion coefficients in combination with T_2 . The T_2 spin-spin relaxation time for unheated WP is in the order of about 2.4 s. Upon heating of 13 wt % WP, to induce gel formation, it was shown that all water becomes more immobilized and hindered in its motion resulting in a change in the T_2 spin-spin relaxation time from about 2.4 s to 100 ms (**Table 2**).

The T_2 spin-spin relaxation time for the different polysaccharides alone (without the addition of protein) was ~ 2.4 s for all the three different polysaccharides studied here (results not shown). For WP gels formed in the presence of the polysaccharide, the T_2 spin-spin relaxation time decreased from around 100 ms (for WP gels only) to between 62 – 77 ms depending on the type and concentration of the polysaccharide that was added to WP gels (**Table 2**).

From the measurement of the self-diffusion coefficients of water in WP gels, gels that were made from WP without the addition of any polysaccharides had a self-diffusion coefficient $1.7 \times 10^{-9} \text{ m}^2 \text{ s}^{-1}$ (**Table 2**) which is lower than that of pure water which is about $2.3 \times 10^{-9} \text{ m}^2 \text{ s}^{-1}$ ²⁹. Upon the addition of the polysaccharides, the self-diffusion coefficients decreased in comparison to the WP gels made without the addition of any polysaccharides. The addition of LM pectin resulted in about 12 % decrease in the self-diffusion coefficient as shown in **Table 2**. This decrease was observed at low wt % of LM pectin (0.05 wt %). With further addition of higher LM pectin to WP gels, the diffusion coefficient was almost the same (**Table 2**). For WP gels prepared in the presence of 0.05 wt % HM pectin, the diffusion coefficients decreased by around 10 %. Upon the addition of higher HM pectin, the diffusion coefficients were not affected. The addition of up to 3 wt % pullulan to WP gels resulted in a comparable decrease in the diffusion coefficient as gels made when 0.05 wt % of LM pectin was added to WP.

In general, it is expected that samples with lower viscosities will have a higher self-diffusion coefficients and vice versa. This was observed for WP gels which had self-diffusion coefficients in the order of $1.7 \times 10^{-9} \text{ m}^2 \text{ s}^{-1}$. Surprisingly, gels made with the highest concentration of pullulan (5 wt %) had the lowest diffusion coefficient of $1.32 \times 10^{-9} \text{ m}^2 \text{ s}^{-1}$ and the highest decrease (about 25 % decrease) in the self-diffusion coefficient in comparison to gels made from WP only.

These results suggest that the exchange between bound and free water occurs at higher pullulan concentration leading to slow movement of the gel matrix resulting in the observed low self-diffusion coefficient. These results may also show that at higher pullulan concentrations, the diffusion is most hindered due to most free (not interacting) pullulan concentration in serum. The pullulan samples also had the lowest shear viscosity (Results not shown), the lowest intrinsic viscosity 1 dl/g (results not shown) and the lowest recoverable energy (**Figure 8**).

Upon heating of 13 wt % WP, to induce gel formation, it was shown that all water begins to get more immobilized and restricted in its motion resulting in a change in the T_2 relaxation time from about 2 s to 100 ms (**Table 2**). The T_2 spin-spin relaxation time for the polysaccharides alone was about 2.4 s with the exception of 0.15 wt % pullulan which had a T_2 spin-spin relaxation time of 1.9 s. For WP gels formed in the presence of the polysaccharide, the T_2 spin-spin relaxation time decreased from around 100 ms (for WP gels only) to between 62 – 77 ms depending on the type and concentration of the polysaccharide that was added to WP gels (**Table 2**). From the measurement of the self-diffusion coefficients of water in WP gels, gels that were made from WP alone without the addition of any polysaccharides had a self-diffusion coefficient very close to that of pure water which is about $2.3 \times 10^{-9} \text{ m}^2 \text{ s}^{-1}$. Upon the addition of the polysaccharides, the self-diffusion coefficients decreased in comparison to the WP gels made without the addition of any polysaccharides. The addition of LM pectin resulted in about 12 % decrease in the self-diffusion coefficient as shown in **Table 2**. The decrease was observed at low wt % of LM pectin (0.05 wt %). With further addition of higher LM pectin to WP gels, the diffusion coefficient increased by about 2 % (**Table 2**).

For WP gels prepared in the presence of HM pectin, the diffusion coefficients decreased by around 30 % and with the addition of higher HM pectin, the diffusion coefficients were not affected. The addition of up to 3 wt % pullulan to WP gels resulted in a comparable decrease in the diffusion coefficient as gels made when 0.05 wt % of LM pectin was added to WP. Surprisingly, gels made with the highest concentration of pullulan (5 wt %) had the lowest diffusion coefficient and the highest decrease (about 25 % decrease) in the self-diffusion coefficient in comparison to gels made from WP only. The pullulan samples also had the lowest viscosity and the lowest recoverable energy.

In general, it is expected that samples with lower viscosities will have a higher self-diffusion coefficients and vice versa. This was observed for WP gels which had self-diffusion coefficients in the order of $1.7 \times 10^{-9} \text{ m}^2 \text{ s}^{-1}$. For pullulan samples which had the lowest intrinsic viscosity of 1 dg/L, the self-diffusion coefficient was the lowest $1.32 \times 10^{-9} \text{ m}^2 \text{ s}^{-1}$ at the highest pullulan concentration used here (5 wt %). This result suggests that the exchange between bound and free water occurs at higher pullulan concentration leading to slow movement of the gel matrix resulting in the observed low self-diffusion coefficient.

Serum flow and self-diffusion coefficients in relation to recoverable energy

When the water holding (WHC) was measured for WP gels, the WHC was close to 100 %. The results show that, the contribution of the viscous serum flow in this case appears to be minimal. Hence, the serum flow has a less significant effect on the ability of the gels to elastically store energy. However, for gels made in the presence of pullulan, given that there is no interaction between the polysaccharide and the protein, friction between microstructural elements occurs resulting in energy dissipation, and as a result, reduced ability of the networks to store energy. Changes in the porosity of the networks with the modulation of the viscosity of the serum phase upon the addition of polysaccharides were observed from the SEM images and this contributes significantly to energy dissipation. This in turn has an influence on the amount of energy that is stored within the gel network. Changes in the viscosity of the serum phase can alter network morphology including the porosity of the network and this contributes to either energy storage or dissipation in spatial gel networks.

Conclusions

The results from this study show that the contribution of stress relaxation from microstructural rearrangements, plastic deformation, and de-bonding do not affect recoverable energy as a result of the dissipation phenomenon of whey protein gels. The determination of the fracture properties also showed higher fracture strain and stress values, which show the likelihood of the micro crack formation, which favor energy dissipation at the expense of storage, to be minimal. The study to check for the contribution of the serum to energy dissipation using water holding measurements showed that no serum could be expelled from the gels at the applied centrifugation forces at the determined

network dimensions. The findings suggest that changes in serum properties due to the presence of non-interacting polymer cause friction which influences the energy dissipation at the expense of storage. A relation between the serum phase viscosity, gel microstructure, and the recoverable energy was established. The findings from this study suggest that the viscosity of the serum phase matters for the energy dissipation but to different extent for different polymers. However, explaining the different extent is difficult, given that the interplay between structure and flow is unknown, as is the influence of the different polymers on these two aspects. The contribution of the viscosity of the serum phase does not however have a single-handed effect on energy dissipation. Energy dissipation arises from multifaceted effect arising from the combinatorial influence of serum phase viscosity, and the changes in the morphology of the network structure, in particular, the porosity and the deformability of the networks, and both result in an effect on the energy dissipation via friction of the squeezed liquid phase, and a concurrent influence on the recoverable energy. Thus, to be able to get details on how the serum phase viscosity directs the recoverable energy, it may be necessary to carry out studies on confined flow profiles. The results from this study show that to engineer the textural attributes of food materials, correcting for the viscosity of the serum phase is important for tailoring or (re) formulation of protein-based products where high recoverable energies are desirable.

Acknowledgements

We thank Tiny Franssen-Verheijen for the help with SEM imaging.

References

- (1) Çakir, E.; Daubert, C. R.; Drake, M. A.; Vinyard, C. J.; Essick, G.; Foegeding, E. A., The effect of microstructure on the sensory perception and textural characteristics of whey protein/κ-carrageenan mixed gels. **Food Hydrocolloid** 2012, **26**, 33-43.
- (2) Clark, A. H.; Kavanagh, G. M.; Ross-Murphy, S. B., Globular protein gelation—theory and experiment. **Food Hydrocolloid** 2001, **15**, 383-400.
- (3) van Vliet, T., Large deformation and fracture behaviour of gels. **Curr. Opin. Colloid Interface Sci.** 1996, **1**, 740-745.
- (4) van Vliet, T.; Luyten, H.; Walstra, P., **Fracture and yielding of gels**. 1991; p 392-403.
- (5) van den Berg, L.; Carolas, A. L.; van Vliet, T.; van der Linden, E.; van Boekel, M. A. J. S.; van de Velde, F., Energy storage controls crumbly perception in whey proteins/polysaccharide mixed gels. **Food Hydrocolloid** 2008, **22**, 1404-1417.
- (6) de Jong, S.; van Vliet, T.; de Jongh, H. J. H., The contribution of time-dependent stress relaxation in protein gels to the recoverable energy that is used as tool to describe food texture **Mech. Time-Depend. Mater.** 2015, *In press*.
- (7) Munialo, C. D.; van der Linden, E.; de Jongh, H. H. J., The ability to store energy in pea protein gels is set by network dimensions smaller than 50 nm. **Food Res. Int.** 2014, **64**, 482-491.
- (8) Munialo, C. D.; Ortega, R. G.; van der Linden, E.; de Jongh, H. H. J., Modification of ovalbumin with fructooligosaccharides: Consequences for network morphology and mechanical deformation responses. **Langmuir** 2014.
- (9) Flett, K. L.; Corredig, M., Whey protein aggregate formation during heating in the presence of κ-carrageenan. **Food Chem.** 2009, **115**, 1479-1485.
- (10) Li, J.; Ould Eleya, M. M.; Gunasekaran, S., Gelation of whey protein and xanthan mixture: Effect of heating rate on rheological properties. **Food Hydrocolloid** 2006, **20**, 678-686.
- (11) Carpita, N. C.; Campbell, M.; Tierney, M.; Willats, W. T.; McCartney, L.; Mackie, W.; Knox, J. P., Pectin: cell biology and prospects for functional analysis. In **Plant Cell Walls**, Springer Netherlands: 2001; pp 9-27.
- (12) Zhang, S.; Vardhanabhuti, B., Acid-induced gelation properties of heated whey protein-pectin soluble complex (Part II): Effect of charge density of pectin. **Food Hydrocolloid** 2014, **39**, 95-103.
- (13) Milani, J.; Maleki, G., Hydrocolloids in food industry. **Food industrial processes—methods and equipment, InTech, Croatia** 2012, 17-38.
- (14) Munialo, C. D.; van der Linden, E.; Ako, K.; de Jongh, H. H. J., Quantitative analysis of the network structure that underlines the transitioning in mechanical responses of pea protein gels. **Food**

Hydrocolloid 2015, Submitted.

- (15) Kocher, P. N.; Foegeding, E. A., Microcentrifuge-Based Method for Measuring Water-Holding of Protein Gels. **J. Food Sci.** 1993, **58**, 1040-1046.
- (16) Provencher, S. W., A constrained regularization method for inverting data represented by linear algebraic or integral equations. **Computer Physics Communications** 1982, **27**, 213-227.
- (17) Vandusschoten, D.; Dejager, P. A.; Vanas, H., Extracting Diffusion Constants from Echo-Time-Dependent PFG NMR Data Using Relaxation-Time Information. **Journal of Magnetic Resonance, Series A** 1995, **116**, 22-28.
- (18) Washburn, K. E.; Callaghan, P. T., Tracking pore to pore exchange using relaxation exchange spectroscopy. **Phys Rev Lett** 2006, **97**, 175502.
- (19) Venkataramanan, L.; Song, Y. Q.; Hürlimann, M. D., Solving Fredholm integrals of the first kind with tensor product structure in 2 and 2.5 dimensions. **IEEE Transactions on Signal Processing** 2002, **50**, 1017-1026.
- (20) de Jong, S.; van de Velde, F., Charge density of polysaccharide controls microstructure and large deformation properties of mixed gels. **Food Hydrocolloid** 2007, **21**, 1172-1187.
- (21) van den Berg, L.; van Vliet, T.; van der Linden, E.; van Boekel, M. A. J. S.; van de Velde, F., Breakdown properties and sensory perception of whey proteins/polysaccharide mixed gels as a function of microstructure. **Food Hydrocolloid** 2007, **21**, 961-976.
- (22) Laneuville, S. I.; Paquin, P.; Turgeon, S. L., Effect of preparation conditions on the characteristics of whey protein—xanthan gum complexes. **Food Hydrocolloid** 2000, **14**, 305-314.
- (23) Morris, V., Multicomponent gels. **Gums and stabilisers for the food industry** 1986, **3**, 87-99.
- (24) Braudo, E. E.; Gotlieb, A. M.; Plashina, I. G.; Tolstoguzov, V. B., Protein-containing multicomponent gels. **Nahrung** 1986, **30**, 355-364.
- (25) Bowland, E. L.; Allen Foegeding, E.; Hamann, D. D., Rheological analysis of anion-induced matrix transformations in thermally induced whey protein isolate gels. **Food Hydrocolloid** 1995, **9**, 57-64.
- (26) Ikeda, S.; Foegeding, E. A., Dynamic viscoelastic properties of thermally induced whey protein isolate gels with added lecithin. **Food Hydrocolloid** 1999, **13**, 245-254.
- (27) Zhang, S.; Hsieh, F.-H.; Vardhanabhuti, B., Acid-induced gelation properties of heated whey protein–pectin soluble complex (Part I): Effect of initial pH. **Food Hydrocolloid** 2014, **36**, 76-84.
- (28) Picone, C. S. F.; da Cunha, R. L., Interactions between milk proteins and gellan gum in acidified gels. **Food Hydrocolloid** 2010, **24**, 502-511.
- (29) Tanaka, K., Self-diffusion coefficients of water in pure water and in aqueous solutions of several

electrolytes with ^{18}O and ^2H as tracers. ***Journal of the Chemical Society, Faraday Transactions 1: Physical Chemistry in Condensed Phases*** 1978, **74**, 1879-1881.

Appendix to Chapter 7: Modulation of the serum phase viscosity and its contribution to energy dissipation upon mechanical deformation of pea protein in comparison to whey protein gels

Introduction

The viscosity of the serum phase was shown to affect the mechanical deformation properties of whey protein gels (Chapter 7). The presence of an inert polysaccharide i.e. pullulan resulted in gels that had lower recoverable energy and also a lower gel strength and stiffness (Chapter 7). The reduced recoverable energy was attributed to an enhanced friction caused by flow of the serum through the network-pores during mechanical deformation when the viscosity of this serum phase was increased. To test the genericity of this insight, a study was carried out to evaluate whether the addition of pullulan to another protein, in this case pea protein, will result in a similar impact on the mechanical responses of the gels including the ability of the networks to elastically store energy. Alternatively, the molecular weight of the polysaccharide added was also varied to evaluate the impact having a similar volume fraction of polysaccharides, but different intrinsic viscosities of the aqueous phase. To vary the molecular weight of the polysaccharide, dextran, which has a molecular weight of around 40 kDa, was used and the obtained results were compared with pullulan which has a molecular weight of around 150 kDa. Both dextran and pullulan are non-ionic polysaccharides where the first one is a branched glucan composed of many glucose units, and the latter is a linear maltotriose chain.

Experimental

Materials

Pea protein isolate was extracted from pre-dried dehulled commercial green pea seeds with a protein content of 22 g/100 g (dry weight basis) according to a previously described procedure (see Chapter 3, 4, and 5)^{1,2}. Following the extraction process, pea protein isolate was kept at 4 °C in the presence of 0.02 % sodium azide to prevent microbial growth. Pea protein extracted in this way will be referred to as “native” pea protein. The protein content of native pea protein was around 12.3 wt %, with a dry matter content of 12.13 %. The protein content was determined using Kjeldahl with a conversion factor of 6.25. Native pea protein was concentrated to the desired protein concentration using ultrafiltration, where an Amicon Stirred Cell (EMD Millipore Corporation, Billerica, MA, USA) paired with 30 kDa filter membrane under pressured nitrogen gas (not more than 5 pSi) was used. The protein content of native pea protein was measured using Kjeldahl method with conversion factor 6.25. The peak denaturation temperature of native pea protein was 80.4 ± 0.8 °C.

The enthalpy change of the major endotherm was 1.48 J/g_{protein}. Dextran with a molecular weight of around 40 kDa was obtained from Sigma Aldrich (Steinheim, Germany) whereas Pullulan (average molecular weight 150 kDa Lot # E47JGNH) was obtained from Tokyo Chemical Industry (Tokyo, Japan). Pullulan in water gives viscosity of about 22000 mPa.s (25 % w/w)³. Whereas dextran has viscosity of about 4 mPa.s (10 % w/w) in water⁴ which is noticeably lower than that of pullulan.

Pea protein gel formation

The preparation of pea protein gels as such (without the addition of polysaccharide) was carried out according to the previously described procedure². The pH of the protein concentration was adjusted to pH 3.0 ± 0.2 using 2 M HCl, and the protein concentration was varied from 10 – 15 wt %.

30 wt % stock polysaccharide solutions were prepared by adding and hydrating the polysaccharide at 85 °C for about 2 h under continuous stirring. These solutions were then stored overnight at 4 °C to allow complete hydration. The next day, the protein stock solutions at 15 wt % concentration and polysaccharide solutions were left to equilibrate to room temperature (20 ± 2 °C) prior to mixing at the appropriate protein-polysaccharide ratios. The final protein concentration was kept constant at 10 % (w/w) for samples where polysaccharides were added before gelation. The polysaccharide addition was carried out in a protein-polysaccharide ratio that resulted in final effective protein concentration of 11 wt % - 15 wt % (in respect to the ratio of protein: water). The effective concentration of 11 - 15 wt % here refers to the protein concentration calculated as follows:-

$$\frac{\text{protein (g)}}{\text{protein (g)} + \text{water (g)}} \times 100 \% = \text{protein concentration (\%)} \quad (1)$$

The final pH for the either pea protein as such or mixed protein-polysaccharide solutions was kept at pH 3.0 ± 0.2. Subsequently, the protein or mixed protein-polysaccharide solutions were degassed and transferred to 20 mL Omnifix[®] syringes with an internal diameter of 19.7 mm, which had been coated with paraffin oil for lubrication. The solutions were then heated (30 min, 95 °C) and allowed to set at room temperature (20 ± 2 °C) prior to testing.

Characterization of pea protein gels

The microstructure was visualized by the use of confocal laser scanning (CLSM) and scanning electron microscopy (SEM) according to the procedure described in Chapter 7. The determination of the mechanical deformation properties of the gels as well as the recoverable energy was carried out according to the procedures described in Chapter 7.

Results and Discussion

To evaluate whether the role of serum viscosity on the dissipation of energy in protein-based gels is protein or polysaccharide specific, the structural as well as mechanical responses, including the ability of pea protein gels to elastically store energy, were studied. Pea protein gels were prepared in the presence and absence of different concentrations of non-charged polysaccharides i.e. either pullulan or dextran to result in an effective protein concentration of 10 – 15 %. The results are compared to the situation where the effective protein concentration ranged from 10 - 15 wt% in the absence of polysaccharide.

The microstructure

Gels were prepared from pea protein at different wt % protein concentration in the absence and presence of the polysaccharides. Visually all gels appeared to be translucent (not shown). The network morphology was characterized using CLSM and SEM. In **Fig. 1** we show an example of gels prepared at 13 wt % pea protein, pea-pullulan at an effective protein concentration of 13 wt %, and pea-dextran at an effective concentration of 13 wt %. The results for 13 wt % are shown only, as in Chapter 7, the whey protein concentration was also kept at 13 wt %. This makes it easier to compare the microstructure of gels prepared with the two different proteins.

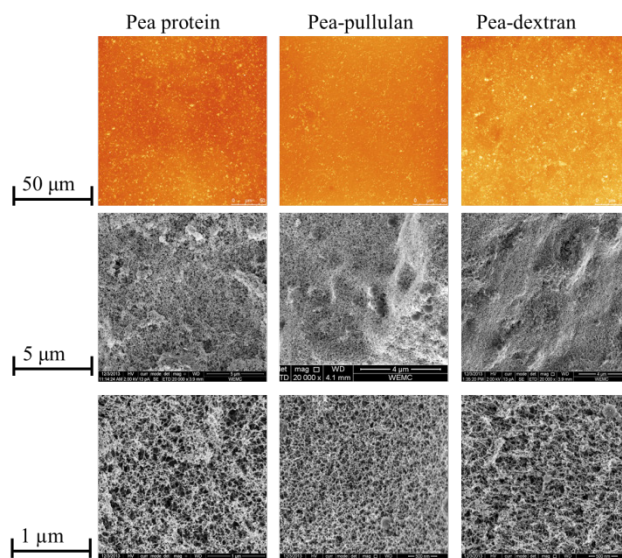


Figure 1: Confocal laser scanning micrographs and scanning electron micrographs for pea protein, pea-pullulan and pea-dextran. The protein concentration was kept constant at 13 wt % with polysaccharide added to bring the effective concentration to 13 %.

The addition of both polysaccharides to pea protein did not result in significant changes in the network structure at the micrometer level (as observed from the CLSM micrographs in **Fig. 1**).

At this length scale, homogenous network structures were observed both in the presence and absence of the polysaccharides. To obtain more details on the size of the aggregates as well as the thickness of the strands, SEM was used to visualize the network structures at a higher resolution (**Fig. 1**).

These micrographs showed that fine-stranded pea protein gels were made from strands that had an apparent coarseness of around 70 nm (**Fig. 1**). For gels prepared in the presence of the polysaccharide, no significant differences were observed in the network structures (**Fig. 1**). Similar to what was observed for whey proteins (Chapter 7 **Fig. 1a** and **b**), an increase in the pullulan or dextran concentration to bring the effective concentration to 13 wt % did not result in structural changes in pea protein (**Fig. 1**).

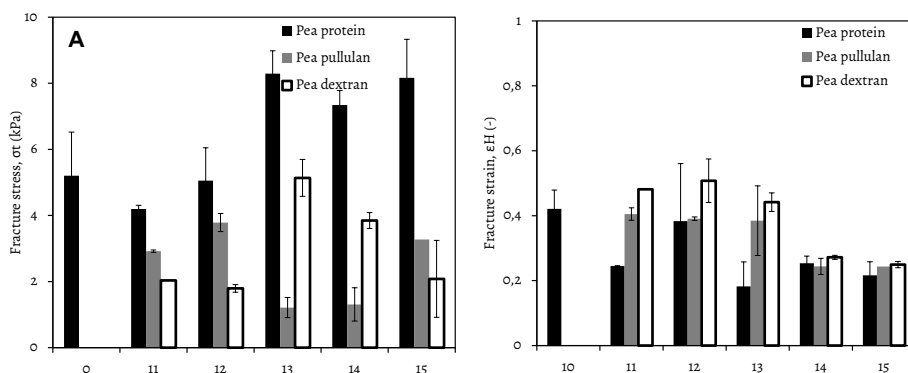


Figure 2: Comparisons of fracture stress (**A**), fracture strain (**B**), for pea protein, pea-pullulan and pea-dextran gels prepared at various effective concentrations (11 – 15 wt %). The pea protein concentration was kept at 10 wt % in all cases.

In Chapter 7, the addition of pullulan up to 5 wt % to whey proteins did not show morphological differences.

Rheological measurements at large deformation

Fig. 2 A shows the fracture stress and fracture strain of pea protein at varying protein concentrations (black bars).

An increase in the pea protein concentration up to 13 wt % resulted in a two-fold increase in the gel strength.

Above 13 wt % no differences in the gel strength are apparent. Increase in gel strength may be related to increased local concentration and enhanced connectivity between protein aggregates thus, higher forces are required to create a fracture during deformation.

Alternatively, when evaluating at a fixed protein concentration of 10 wt% and increasing amounts of pullulan (grey bars) or dextran (white bars), it can be observed that the addition of polysaccharides in general decreased the gel strength except for those gels in the presence of dextran at an effective concentration of 13 wt % and 14 wt %, the decrease was more pronounced in the presence of dextran compared to the same volume fraction of pullulan (**Fig. 2 A**). Despite the non-ionic character of the polysaccharides used, the decrease in the gel strength could indicate that the polysaccharides do interfere to some extent with the formation of the network.

Comparing gels prepared from pea protein-pullulan and whey protein-pullulan, an initial increase in the gels strength was observed when the effective concentration increased from 11 wt % - 12 wt % for pea-pullulan gels. The gel strength subsequently decreased at 13 wt % and 14 wt % for pea-pullulan gels (**Fig. 2 A**). A similar trend was observed when pullulan was added to whey protein gels, where the gel strength initially increased followed by a decrease (Chapter 7, **Fig. 7 B**).

The addition of polysaccharides to 10 % pea protein to result in an effective concentration of 11 - 13 wt % resulted in an increase of the brittleness of the gels (higher fracture strains) as shown in **Fig. 2 B**, but at higher concentrations of polysaccharide, no significant effect was observed. Pea-dextran gels were less brittle than pea-pullulan and gels prepared from pea protein alone. Higher fracture strains indicate that the gels become less brittle with the addition of polysaccharide in comparison to gels made from pea protein only which are more brittle.

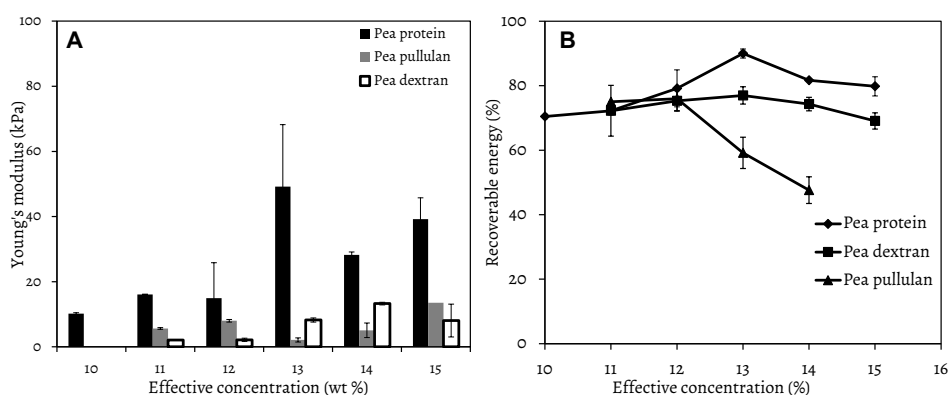


Figure 3: Comparisons of Young's modulus (**A**), and the recoverable energy (**B**), for pea protein, pea-pullulan and pea-dextran gels prepared at various effective concentrations (11 – 15 wt %). The pea protein concentration was kept at 10 wt % in all cases.

A similar trend was observed in the fracture strain when pullulan was added to whey protein gels (Chapter 7, **Fig. 7 B**), and this shows that the effect of pullulan on the brittleness of the gels is not protein specific.

The Young's modulus (**Fig. 3 A**) follows the same trend as observed for the fracture stress (**Fig. 2 A**).

The addition of polysaccharides to the pea protein resulted in a substantial decrease in stiffness of the gels, although in general pea-dextran gels were stiffer than pea-pullulan gels. The reduction in the stiffness of the gels can be related to the size of the polysaccharide. Given that the molecular weight of dextran is almost three times smaller than pullulan, upon interaction with pea proteins, the packing by dextran is better than that of pullulan and hence results in stiffer networks compared to pullulan gels. Contrarily, the stiffness of the gels increased steadily when pullulan was added to whey proteins even at higher concentrations (Chapter 7, **Fig. 7 B**).

The recoverable energy (elastically stored energy) was determined of the pea protein gels with increasing concentration polysaccharide (**Fig. 3 B**). An increase in pea protein concentration (without the addition of polysaccharides) resulted in gels that showed an increase in recoverable energy up to a concentration of 13 wt %. A further increase in the protein concentration beyond 13 wt % resulted in a slight decrease in the recoverable energy. The addition of dextran to a 10 wt % protein sample did not result in significant changes in recoverable energy, remaining constant at ~74 % as observed for the sample without polysaccharide. However, when pullulan was added a strong decrease in recoverable energy was observed yielding a value of around 50 % at an effective protein concentration of 14 wt % in the presence of pullulan. The decrease in recoverable energy in these gels may be related to changes in the viscosity of the serum phase, similar to what was observed for WPI-pullulan gels in Chapter 7, where the addition of pullulan to whey protein gels resulted in around 50 % decrease in the recoverable energy. Additionally, the reduction in the recoverable energy may be related to higher energy dissipation that may have occurred via fracture events. Pea protein-pullulan gels had lower fracture stress (**Fig. 2 A**), and this increases the likelihood of the occurrence of micro-cracks, resulting in higher energy dissipation at the expense of storage. The reduction in recoverable energy of the gels could also be related to stress concentration at contact points between the polysaccharide and the protein molecules, resulting in higher energy dissipation due to friction between structural elements upon deformation of gels at the expense of storage. When pullulan was added to whey protein, an initial decrease in the recoverable energy was observed, after which no remarkable changes in the recoverable energy were observed (Chapter 7, **Fig. 8 A**). The results show that the effect of the addition of polysaccharides on the ability of the networks to store energy is influenced by the size (observed in **Fig. 3 B**), and type of polysaccharide (**Fig. 3 B**), as well as the network morphology which depends on the type of protein (Comparison on whey protein in chapter 7, and pea protein discussed in this appendix).

Conclusions

The objective of this appendix was to show that the role of the serum phase viscosity in influencing mechanical responses including the recoverable energy of protein gels also holds for another protein system and the type and size of non-ionic polysaccharide. The modulation of the viscosity of the serum phase of pea protein gels was shown to have a significant impact on the recoverable energy. In the case of mixtures of pea protein-pullulan, pea protein-dextran, or whey protein-pullulan, it was possible to obtain gels that vary in recoverable energy, though the morphology of the gel was not affected. The results from this study show that the influence of the viscosity of the serum phase on the large deformation properties of protein gels including the ability of the networks to elastically store energy is modulated by the size and type of polysaccharide, and is more general for gels from different protein sources. The impact on the recoverable energy may be related to coarseness of the networks which affects the serum flow, which contributes to friction of serum resulting in energy dissipation. These insights allow food industries to work with the serum viscosity to tailor semi-solids for texture properties, when the coarseness is sufficiently large to allow serum flow to occur during mechanical deformation of the gel.

References

- (1) Munialo, C. D.; Martin, A. H.; van der Linden, E.; de Jongh, H. H. J., Fibril formation from pea protein and subsequent gel formation. **J. Agric. Food. Chem** 2014, **62**, 2418-2427.
- (2) Munialo, C. D.; van der Linden, E.; de Jongh, H. H. J., The ability to store energy in pea protein gels is set by network dimensions smaller than 50 nm. **Food Res. Int.** 2014, **64**, 482-491.
- (3) Leathers, T. D., Pullulan. In **Biopolymers Online**, Wiley-VCH Verlag GmbH & Co. KGaA: 2005.
- (4) Tolstoguzov, V., Functional properties of protein-polysaccharide. **Functional properties of food macromolecules** 1998, 252.

Chapter 8

Activation energy of the disruption of gel networks in relation to elastically stored energy in fine-stranded ovalbumin gels

To determine the activation energy of the disruption of ovalbumin network structures and to relate this to energy storage and dissipation obtained from mechanical deformation tests, ovalbumin gels were prepared at a fixed volume fraction and pH, but varying incubation temperatures. These network structures were visualized by the use of microscopy, and rheological characterization of the gels was carried out. The disruption of ovalbumin networks was shown to follow the first-order behavior. Increasing incubation temperature to form the gels was shown to result in gradual increase of this activation energy up to a factor of 8 going from 65 to 95 °C. For gels prepared following heating of ovalbumin at higher temperatures, the recoverable energy was steady although the disruption energies increased for these gels. When gels were obtained at incubation temperatures below the denaturation temperature, the recoverable energy was significantly lower, just like rheological properties such as the fracture stress and strain. At higher incubation temperatures the recoverable energy remained constant around 75 %.

This chapter is to be submitted as:

Munialo, C.D.; van der Linden, E.; de Jongh, H. H. J. Molecular dissociation energy in relation to energy storage and dissipation upon mechanical deformation of fine-stranded ovalbumin gels. ***Langmuir***, 2015.

Introduction

An increase in the global human population has consequences for the demand for food. This can result in a constraint on the supply of food and a concomitant effect on the availability of balanced diets that include protein-rich foods¹. This provides a challenge to the food industries to formulate new products or to adopt alternative protein sources in order to tailor product development to catch up with the demand. However, to enable the exchangeability of the proteins in food products, an understanding of various parameters that affect the rheological behavior, and the resulting textural and sensory attributes of food and food products, is essential.

Egg white proteins (albumins), including ovalbumin as the main constituent, are used in a wide range of foods because of their functional properties. For most functional applications of egg white proteins, denaturation, and subsequent aggregation of the protein is essential². At sufficiently high protein concentrations, these aggregation events can result in the formation of spatial gel networks. The formation of spatial networks occurs following the heating of proteins above their denaturation temperature, leading to (partial) unfolding, and thereby, exposure of non-polar residues resulting in intermolecular association, and clustering of protein aggregates³. Fine-stranded networks, where the thickness of the strands can be in the order of nanometers⁴, are formed when electrostatic repulsion between the protein molecules is large, such as at pHs away from the protein's iso-electric point (IEP) and/or at low ionic strength⁵.

At sufficiently high protein concentrations the spatial networks can be self-supporting and this allows for the study of mechanical (large) deformation properties of these gels. Large deformation properties are the main quality characteristics that determine the functional properties of gels such as cutting, handling, oral processing, and sensory/mouthfeel perception^{6, 7}. Mechanical deformation of gels in the laboratory can be used to mimic the "palating" (between tongue and palate) process, and this can be used to predict oral processing, and sensory/mouthfeel perception of food gels⁸.

The characterization of the structural aspects that constitute the gel networks is important to understand the responses to mechanical deformation¹. Structural aspects dominating a network include the mesh size⁹, strand thickness¹⁰⁻¹², strand stiffness¹³, and the interaction energy in the physical contacts of the individual strands making up the network¹⁰. The interaction energy is believed to determine the strand dissociation energy within the network and thereby the ability to respond to mechanical deformation¹⁴. However a study on how the dissociation energy can be determined and how this quantity relates to the ability of the networks to elastically store energy, often measured in terms of the recoverable energy¹⁵, is not reported. The recoverable energy is one of characteristics that define the fracture mechanisms of gels by controlling the energy balance within the gel structure during deformation¹⁵.

The effect of the heating rate of globular proteins on their gel strength has been reported¹⁶. The lower the heating rate, the higher the gel strength obtained. The effect of incubation temperature on stiffness of gels has also been reported¹⁷. In most of the studies where the heating temperature was varied, and the formation of spatial gel networks evaluated, the investigation was carried out using small deformation rheology¹⁸. However, the effect of heating temperature during gel formation on rheological responses of protein gels under large deformation is not reported. Conceptually, it has been suggested that a property like the recoverable energy is set by the extent of interactions between the different microstructural elements. However, a study to elucidate if such a relation exists or not has never been documented. Moreover, the lack of a correlation between fracture stress and recoverable energy¹⁹ also questions this concept.

The aim of this study was to relate the activation energy of the disruption of ovalbumin network structures to the elastically stored energy (i.e. recoverable energy) obtained from mechanical deformation tests. To this end, gels were made from ovalbumin at a neutral pH and a fixed volume of approximately 9 vol % (12 wt % protein and assuming a protein density of 1.42 g/cm³). Ovalbumin was chosen as a model system as its aggregation and gelation mechanisms are well studied^{20, 21}. Moreover, no significant chemical cross-linking occurs in heat-set ovalbumin gels, as evaluated by SDS-PAGE-analysis under non-reducing conditions²². The energies of activation were determined from the first-order kinetics of monitoring the dissociation of gel pieces in urea-solutions in time. The Arrhenius equation was used to derive activation energy. The dissociation was monitored by following the protein concentration from absorbance measurements carried out using the UV-VIS spectrophotometer. Subsequently, the large deformation properties of the gels were studied by uniaxial compression. The microstructure was visualized by the use of confocal laser scanning and scanning electron microscopy. To evaluate the different energy dissipation modes, the stress relaxation and water holding capacity of ovalbumin gels were determined.

Experimental

Materials

Albumin (A5503) from chicken egg white (ovalbumin) (grade V, > 98 % pure by agarose electrophoresis, crystallized and lyophilized, Lot # SLBB4340 V), acetone, NaOH pellets, glutaraldehyde, urea, and potassium phosphate monobasic were obtained from Sigma-Aldrich (Steinheim, Germany). Anhydrous dipotassium hydrogen phosphate was obtained from ThermoFisher Scientific (Dreieich, Germany). Paraffin oil was obtained from Merck (Darmstadt, Germany). Omnifix[®] syringes were obtained from Braun (Melsungen, Germany). All reagents were of analytical grade and used without further purification. All solutions were prepared with MilliQ water.

Sample preparation

Ovalbumin solutions were prepared by dispersing 120 mg/mL ovalbumin powder in MilliQ water (Millipore Corp., Billerica, MA), followed by adjusting the solutions to pH 7.0 using 1 M NaOH. The solutions were then stirred at 4 °C, 300 rpm, overnight. Subsequently, ovalbumin solutions were degassed in a vacuum chamber to remove small air bubbles, and transferred to 20 mL syringes with an internal diameter of 19.7 mm, whose walls had been pre-coated with paraffin oil for lubrication, and closed at the bottom with sterile luer lock closures. Subsequently, the solutions were heated at 65 °C, 68.5 °C, 70 °C, 72.5 °C, 75 °C, 80 °C, 85 °C, 90 °C, and 95 °C (± 2 °C) in a water bath for 30 min, followed by cooling at room temperature (20 ± 2 °C) overnight. The gels obtained were cut with a gel slicer into 20 mm in height and 19.7 mm diameter cylinders. Each sample was prepared at least in duplicate.

Determination of activation energy of disruption

Ovalbumin gels prepared as described above were cut into small pieces. These gel pieces were then weighed and MilliQ water added to dilute the samples to a final concentration of 0.22 mM. These mixtures (gel pieces + MilliQ water) were then turraxed using Ultra Turrax T25 basic (IKA-Werke GmbH & Co. KG, Germany) at a speed of 1/min equivalent to 6,500 rpm to mechanically breakdown the gels. Subsequently, 100 μ L of 0.22 mM ovalbumin gel suspensions were added to 0, 200, 400, 600, 800, 900, and 1000 μ L of 10 M urea prepared in the presence of 50 mM phosphate buffer. These volumes of urea correspond to 0, 2, 4, 6, 8, 9, and 10 M final concentrations of urea respectively. To bring the final volume to 1000 μ L, 10 mM phosphate buffer or MilliQ water was added to the mixtures of protein and urea (or MilliQ water), where necessary. These solutions (protein + urea + 10 mM phosphate buffer or MilliQ water) were then mixed and incubated at 20 °C, 24 °C, 28 °C, and 32 °C (± 0.2) in a UV-1800 UV-vis spectrophotometer (Shimadzu Corporation, Japan) equipped with a CPS-temperature controller. The absorbance was monitored in time for up to 2 h at 280 nm using quartz cuvettes with a 10 mm path length at the temperatures indicated above. Subsequently, the obtained absorbance values were used to calculate the changes in effective protein concentration using an absorption coefficient of $\epsilon = 0.698 \text{ L g}^{-1} \text{ cm}^{-121}$. The changes in the protein concentration were used to determine the order of reaction and the rate constant. The rate constant was used to calculate the activation energy of the disruption of ovalbumin gel networks using the Arrhenius equation as follows:-

$$k = Ae^{-Ea/(RT)} \quad (1)$$

where **k** is the rate constant of the reaction, **T** is the temperature in Kelvin, **A** the prefactor, **Ea** the activation energy, and R the universal gas constant (8.314×10^{-3} J/mol·K). Duplicate measurements were carried out on each sample for a urea-titration range from 0 up to 10 M (at 20 °C, 24 °C, and 28 °C).

Rheological characterization of ovalbumin gels

Uniaxial compression

To determine the fracture properties of the gels, compression tests were performed on cylindrical gel specimens (19.7 mm in diameter and 20 mm in height) compressed by a Texture Analyzer fitted with a 5 kg load cell and P/75 probe (TA.XTPlus, Stable Micro Systems, Surrey, UK). The fracture properties were studied by a uniaxial compression test up to a 90 % deformation of the specimen height at a rate of 1 mm/s according to the previously described procedure²³. The determined fracture properties included the true fracture stress and the true fracture strain. The true fracture stress and true fracture strain which will be designated as the fracture stress and fracture strain throughout this paper were calculated according to a previously described procedure²³. The Young's modulus was calculated from the slope of the linear region of the stress-strain curve as previously described¹⁵. Experiments were performed at least in triplicates.

Recoverable energy

The recoverable energy measurements were carried out on the cylindrically cut specimen described above according to the previously described procedure¹⁵ with modification. Compression and decompression of the specimen was analyzed on the above described Texture Analyzer. 20 % of the maximum strain before fracture was applied to determine the energy release during decompression at a deformation speed of 1 mm/s. The percentage of recoverable energy of the gels was calculated from the area under the force-deformation curve as being the ratio of the amount of energy that was recovered after applying the stress over the amount of energy that was applied during the compression and decompression of the gels⁷. Each specimen was analyzed at least in triplicates.

Stress relaxation

To determine the fraction of energy dissipated via reversible structural rearrangements, stress-relaxation measurements were carried out according to a previously described procedure²⁴. During stress-relaxation, ovalbumin gels were compressed in the same way as for recoverable energy. The gels however remained compressed for 300 s before decompression. During these 300 s, the networks had time to relax and over time, the force on the probe decreased due to structural rearrangements. The data recorded over time was fitted to Eq. 2, in which A_0 is the fraction of energy which did not dissipate, A_1 is the fraction of energy dissipated at τ_1 and A_2 is the fraction of energy dissipated at τ_2 .

$$Y = A_0 + (A_1 \times e^{x/\tau_1}) + (A_2 \times e^{x/\tau_2}) \quad (2)$$

Characterization of the microstructure

Confocal laser scanning microscopy (CLSM)

Gels for CLSM were prepared according to a previously described procedure^{11, 24, 25}. Visualization of the microstructure was performed using a LEICA TCS SP5 confocal laser scanning microscope, equipped with an inverted microscope and Ar/Kr lasers (Leica Microsystems (CMS) GmbH, Mannheim, Germany) for excitation in the fluorescence single-photon mode. The excitation was performed at 561 nm, and the emission of Rhodamine B was recorded between 570 and 725 nm. Leica objective lenses HC PL APO 20x/0.70 IMM/CORR CS and HCX PL APO 63x/1.20 W CORR CS were used. Digital image files were acquired in 1024 × 1024 pixel resolution, taken at a penetration depth of 15 µm.

Scanning electron microscopy (SEM)

Gels for SEM were prepared according to the previously described procedure^{1, 11, 25} with modifications in which the obtained gels were cross-linked in 2.5 % (v/v) glutaraldehyde solution for 8 h instead of 1 % glutaraldehyde that was previously used²⁵. Furthermore, following the cross-linking step, the gel pieces were washed in MilliQ water overnight followed by the exchange of the MilliQ water with acetone in steps of 10 – 30 – 50 – 70 – 100 % acetone. Subsequently, the gels were dried by critical point drying (CPD 030 BalTec, Liechtenstein). This step was followed by breaking of the gels to smaller pieces and gluing these pieces onto a SEM sample holder using carbon glue (Leit-C, Neubauer Chemicalien, Germany). The gels were then stored overnight under vacuum. After drying of the carbon cement, the gel specimen were sputter coated with 15 nm iridium in SCD 500 (Leica EM VCT 100, Leica, Vienna, Austria) prior to imaging. All samples were analyzed with a field emission scanning electron microscope (Magellan XHR 400L FE-SEM, FEI, Eindhoven, the Netherlands) at room temperature (20 ± 2 °C) at a working distance of 4 mm with SE detection at 2 kV. Following the SEM imaging, the apparent aggregate and pore sizes of the network structure were determined from ImageJ according the previously described procedure¹.

Water Holding Capacity (WHC)

WHC of the gels was determined using the centrifugation procedure as adapted from Kocher and Foegeding²⁶. A microcentrifuge filtration unit composed of an inner spin tube and a 2 ml Eppendorf tube (Axygen Biosciences, Inc., Union City, USA) was used in this experiment. Gels were cut in to cylinders with 10 mm height and 4.8 mm diameter, and placed on the bottom of the spin tube which was covered with a 5.5 mm diameter filter paper to reduce grid size. Centrifugation was carried out over a range of g-forces ($20 - 1000 \times g$) for 10 min at 20 °C. Released serum from the gels was collected at the bottom of the Eppendorf tube and weighed. The WHC was then calculated as a percentage using Eq (3).

$$\text{WHC} = \frac{W_T - W_g}{W_T} \times 100 \quad [\%] \quad (3)$$

where W_T is the total amount of water in the sample (g) and W_g denotes the amount of water removed from the sample (g) at given centrifugation force ($20 - 1000 \times g$). Measurements were performed in duplicate.

Results and Discussion

The aim of this study was to relate the activation energy of the disruption of ovalbumin network structures to the elastically stored energy (i.e. recoverable energy) obtained from mechanical deformation tests. To this end, gels were prepared from ovalbumin at a fixed protein concentration to result in a fixed volume of approximately 9 vol % (for protein gels made at 12 wt % assuming a protein density of 1.42 g/cm³), a fixed ionic strength (where no salts were added to the samples to adjust the ionic strength), and a fixed pH at pH 7.0. The denaturation temperature of ovalbumin under these conditions is reported to be around 75 °C²⁷. Given that ovalbumin is a typical multi-domain protein²⁸, a significant part of the structure will still remain intact at the denaturation temperature. Following incubation at higher temperatures, ovalbumin will lose the folded domains further, and, thereby affects the aggregation propensity. By varying the incubation temperature from just below (65 °C) up to 90 °C, the kinetics of association is affected. It is hypothesized that at higher temperatures, more unfolded species are involved in aggregate formation. Samples were thus prepared at varying incubation temperatures and are referred to according to their heating temperature (e.g. OVA65 refers to a sample heated for 30 min at 65 °C). These gels were evaluated for the disruption energy using Arrhenius equations. Rheological and structural properties of these gels were also determined by the use of uniaxial compression and confocal laser scanning and scanning electron microscopy respectively.

Activation energy of disruption of ovalbumin gel networks

The activation energy of gel disruption by the chaotropic agent urea was used in this study as measure for the strength of the interactions between the assembled microstructures that form the network. To determine the activation energy, urea was used to destabilize the network. As a first step to allow urea to access the structure better, ovalbumin gels were mechanically broken down and the resultant suspensions were incubated at 0.22 mM protein concentration in the presence of different concentrations of urea ranging from 0 to 10 M. Urea is a commonly used protein-dissociating and denaturation agent²⁹. To quantify the amount of re-dissolved or re-dispersed protein, the absorbance at 280 nm was recorded as a function of time. Examples of the changes in effective protein concentration over time at different urea concentrations are shown in **Fig. 1**. An increase in urea concentration increased the rate of disruption of the ovalbumin gel networks (example shown with the addition of 0 M vs. 9 M urea concentrations to OVA75 in **Fig. 1 A** and the addition of 0 – 9 M urea to OVA80 presented in **Fig. 1 B**).

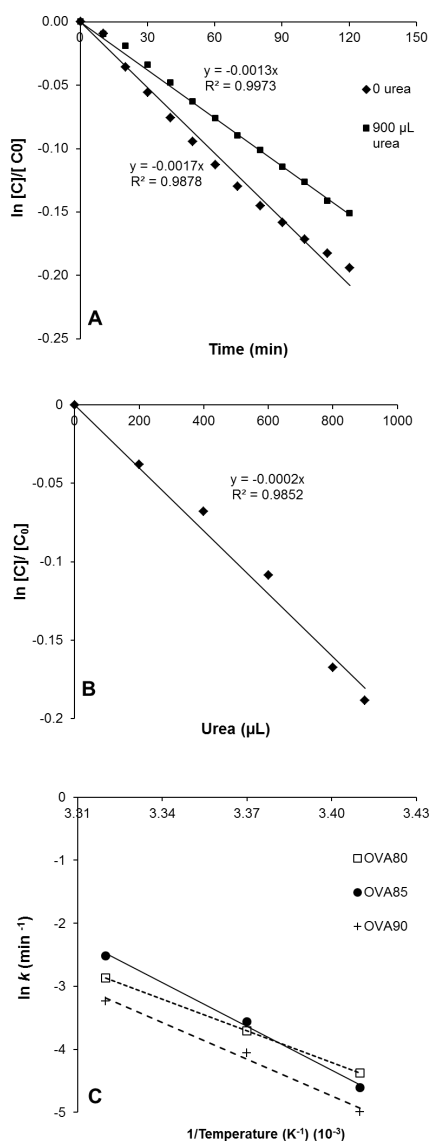


Figure 1: Examples of the plot for the change in the protein concentration of OVA variants as a function of time for OVA75 (A). The results were obtained following the incubation of OVA75 as a function of time in the presence of 0 and 9 M urea monitored at 20 °C. An example of changes in the rate constant as a function of urea concentration (from 0 – 9 M of urea) for OVA80 incubated at 20 °C, 24 °C, and 28 °C are shown in Fig. 1 B. Examples of plot of the rate constants at time zero (k_0) for different ovalbumin variants as a function of $1/\text{temperature}$ are shown in Fig. 1 C. First-order rate constants changes with temperature as described in the Arrhenius equation (Eq. 1); the energy of activation are shown in Fig. 2.

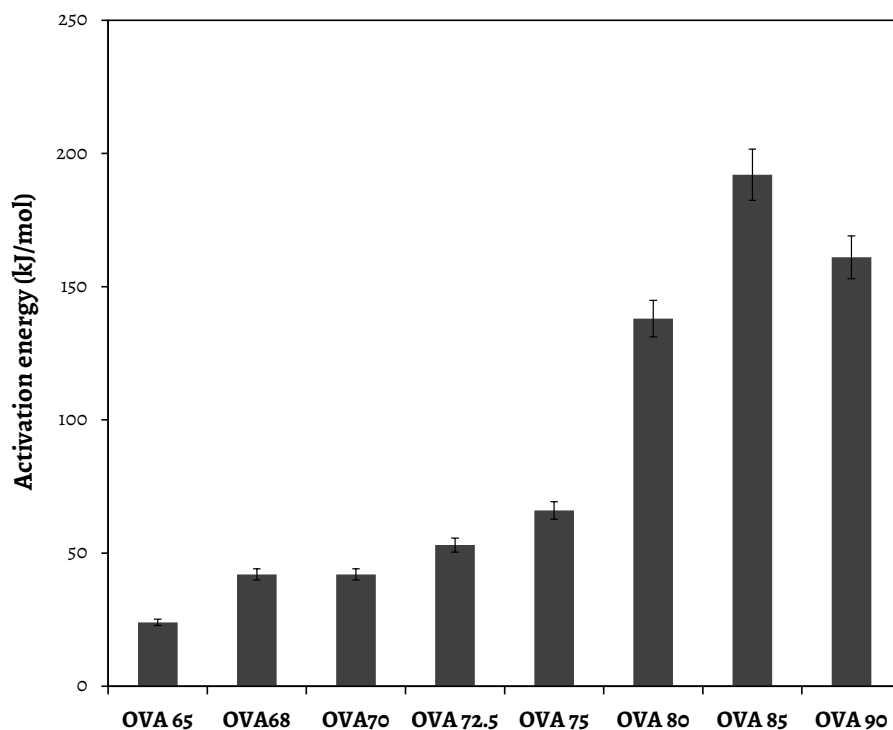


Figure 2: The activation energy for the disruption of ovalbumin gels prepared following heating of samples at varying temperatures at pH 7.0 for 30 min.

The disruption of the gelled network is attributed to the chaotropic effect of urea that results in the interference of hydrogen bonds that are formed during the setting of ovalbumin gels. The assembly process of ovalbumin followed a first order²¹, and thus we assume that the disruption follows a first order as well. In all condition used, disruption of ovalbumin was shown to follow the first-order behavior (example shown in **Fig. 1**).

It is however important to note that given the multiple steps involved in the disruption of the gels, it is not known whether the activation energy determined is from a number of kinetically trapped strands or monomers that are still present in the solution. Here we use the activation energy to denote a combination of the disruption of the gel networks into strands plus the dissociation of the strands into more individual molecules. Given that the activation energy belongs to the rate limiting step and we have no insight which one that is, for simplicity we refer in this work to the activation energy for disruption. As its determination relies on the evaluated protein concentration as it appears ‘dissolved’ by urea, and reflects an indirect method it needs to be mentioned that the activation energies determined are ‘effective’ numbers.

The activation energies of disruption of the different ovalbumin gels are shown in **Fig. 2**. The activation energy gradually increased from 24 kJmol⁻¹ for OVA65 to around 190 kJmol⁻¹ for OVA85. For this latter gel the activation energy was about 8-fold compared to OVA65. Incubation at 90 °C resulted in a slightly lower activation energy (**Fig. 2**).

The activation energies observed here were however lower than those reported by other workers who found activation energy of 430 kJmol⁻¹ during gel assembly at 80 °C². The lower values observed here show that the energy required to cause the disruption of ovalbumin gel networks is lower than the energy required for the denaturation and association of ovalbumin to form the spatial gel network.

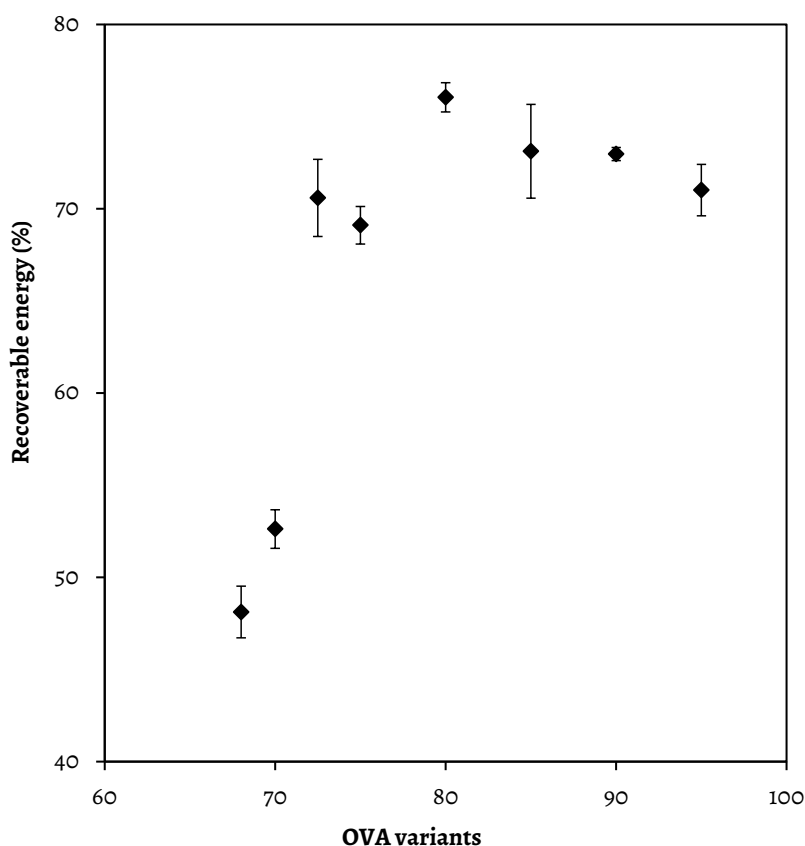


Figure 3: Changes in the recoverable energy of the different ovalbumin gels. The gels were formed following the heating of 120 mg/mL ovalbumin at varying temperatures for 30 min at pH 7.0. OVA65 gels are left out as the gels were relatively weak and hence the recoverable energy results of these gels are not included in Fig. 3.

The ability of ovalbumin gels to store energy

The ability of ovalbumin gels to store energy was determined from the recoverable energy measurements. The recoverable energy was determined by application of the loading and unloading force to a specimen at a deformation rate of 1 mm/s and up to 20 % compressive strain. **Fig. 3** shows the recoverable energy for ovalbumin gels prepared following heating of the samples at varying temperatures for 30 min.

OVA65 gels were weak gels and hence the recoverable energy of these gels is not included in **Fig. 3**.

OVA68 had a recoverable energy of around 50 %. An increase in the heating temperature resulted in an increase in the recoverable energy from around 50 % to around 75 % (a 33 % relative increase) for OVA72.5. At higher temperatures, the recoverable energy remained constant, with the exception of OVA80 that appeared to have a slightly higher recoverable energy.

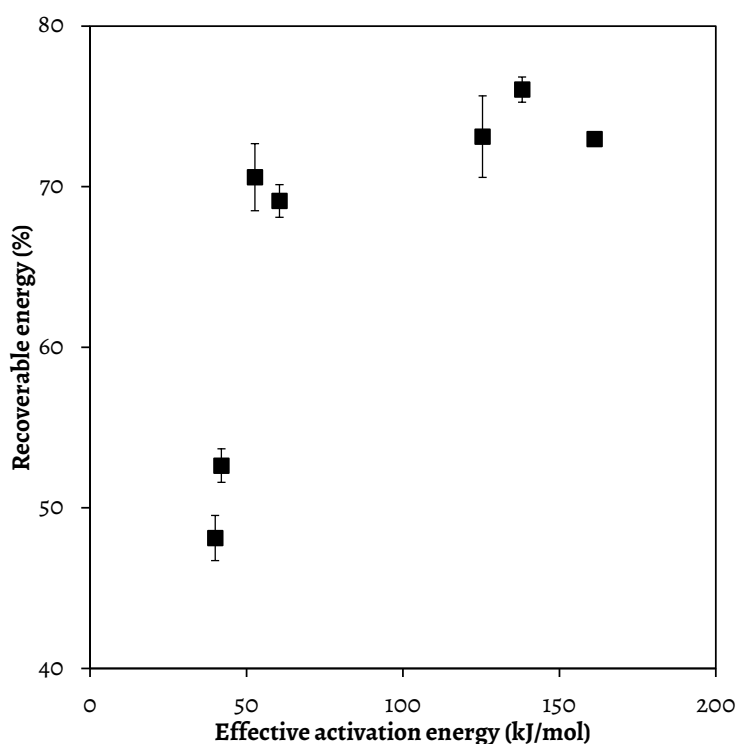


Figure 4: The recoverable energy of ovalbumin gel variants prepared at varying incubation temperatures plotted against the activation energy for the disruption of ovalbumin gel networks.

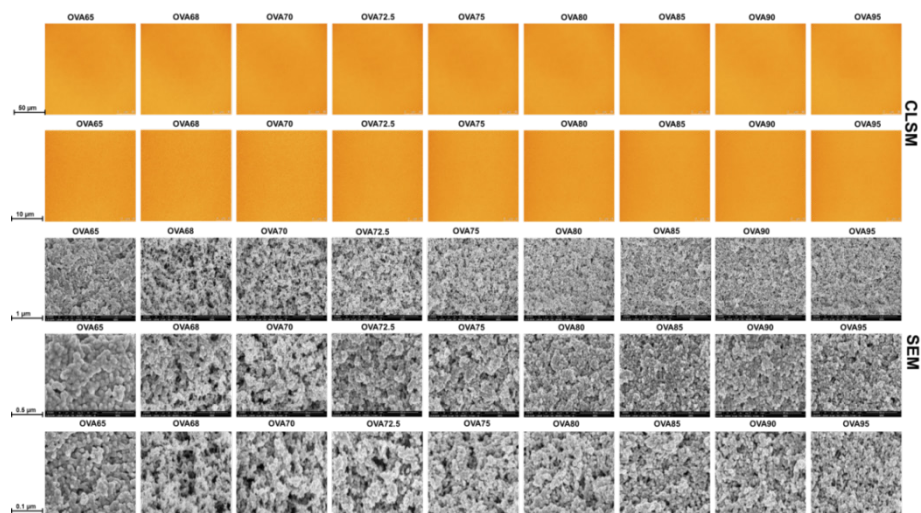


Figure 5: Confocal laser scanning and scanning electron micrographs of gels prepared from ovalbumin following the incubation of the samples at various temperatures using the conditions specified in the materials and methods

Recoverable energy related to the activation energy for the disruption of ovalbumin gel networks

Changes in the recoverable energy of the heat-set ovalbumin gels **Fig. 3** were plotted as a function of the activation energy for the disruption of ovalbumin gels shown in **Fig. 2**. The result is shown in **Fig. 4**. OVA68 and OVA70 had the lowest recoverable energy and these gels also had the lowest activation energy (**Fig. 4**).

An increase in the incubation temperature to around or above the denaturation temperature resulted in an increase in the activation energy for the disruption of gels but it does not coincide with a higher recoverable energy. It has been suggested that the activation energy of a network dissociation is related to the weakest links ³⁰.

The weakest links in gel networks are the points at which crack initiation and propagation or just displacement of two strands relative to each other can occur paving the way for energy dissipation via fracture at the expense of energy storage.

The fact that an increase in the activation energy for the disruption of gels does not coincide with a higher recoverable energy suggests that the recoverable energy is independent of how much effort it takes to physically disrupt the networks. The results also suggest that molecular associations are not related to the network's ability to store energy. This must then also be reflected by the conservation of the different energy dissipation mechanisms for the different gels prepared. The recoverable energy is set by six dissipation modes²⁴. (i) the de-bonding of physical contacts and the subsequent rehydration of structural elements that form the networks, (ii) the events that initiate and propagate fracture events, (iii) friction between microstructural elements, (iv) viscous serum flow of the liquid entrapped by the network, (v) plastic deformation of the material which can result in different irreversible structural rearrangements, and (vi) the structural rearrangements within the network upon the application of force, which lead to energy dissipation by the relaxation of these structure element. A detailed explanation of how these modes can result in the dissipation of energy to result in a concurrent effect on the ability of the networks to store energy can be found elsewhere ²⁴. The contribution of these modes upon mechanical deformation of ovalbumin gels was evaluated and is subsequently discussed.

Dissipation modes that can affect the recoverable energy

The recoverable energy measured following mechanical deformation of ovalbumin gels at a compressive strain of 20 % varied between 50 - 75 % (**Fig. 3**). This implies that 50 – 25 % of total energy applied in the time scale of deformation (compression-decompression) dissipates. Typically, with a deformation speed of 1 mm/s and a compression of 20 % of 20 mm, a recoverable energy measurement takes about 8 seconds. To find out possible modes by which the energy dissipation occurs, water holding capacity, stress relaxation, and the fracture properties of ovalbumin gels were determined. However, energy dissipation can also occur via plastic deformation, de-bonding, and microstructural friction as aforementioned.

Serum flow

To evaluate the contribution of serum flow to energy dissipation in ovalbumin gels, the microstructure of the gels was imaged using microscopy. Structural changes have been reported previously to affect how serum flows through gel networks ¹, which in turn can result in energy dissipation. Water holding measurements were also carried out to evaluate whether serum can be displaced from the networks, and if this could be used to quantify the proportion of energy dissipated via serum flow. In this latter approach the extent of water exudation depends both on the morphology and deformability of the network³¹.

Microstructure

Changes in structural aspects, such as coarseness defined as heterogeneity of the density of the aggregates that span the networks²⁵, and porosity defined as the distance or the void between filament strands or network constituents of the networks can result in a variation of how the serum flows with the protein networks, and this can contribute to viscous dissipation in protein gels^{1,11}. The gels studied in this work appeared macroscopically to be translucent (results not shown), which is a typical characteristic of fine-stranded networks. The visualization of the network structures at a micron level was carried out by the use of confocal laser scanning microscopy (CLSM), whereas the network structures at a submicron level were evaluated using scanning electron microscopy (SEM). The CLSM and SEM micrographs obtained for the different gels are shown in **Fig. 5**.

The gels are homogeneous on lengths scales larger than 0.5 μm , and therefore show no distinguishable features by CSLM.

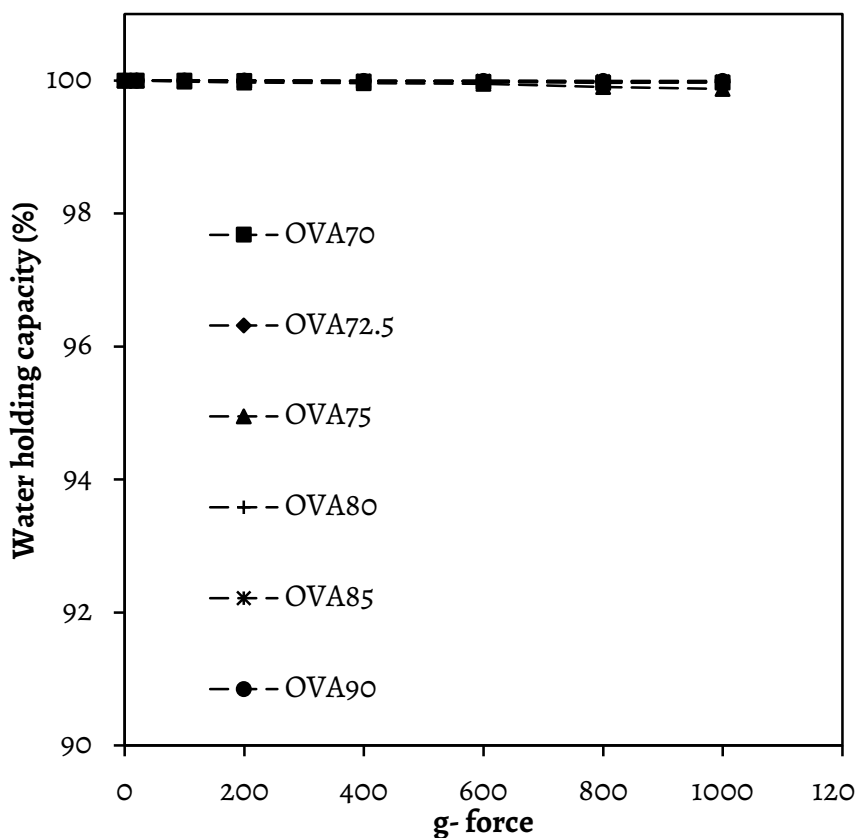


Figure 6: Changes in water holding capacity as a function of g-force for the different ovalbumin variants.

Table 1: The apparent size of aggregates and the pores sizes of ovalbumin network structures. The apparent aggregate and pore sizes were determined from SEM micrographs shown in **Fig. 5** using image analysis.

	Aggregate sizes (nm)	Pore sizes (nm)
OVA 65	103.2 ± 9.9	114.8 ± 15.6
OVA68	92.6 ± 16.7	118.9 ± 13.6
OVA70	104.8 ± 22.8	102.2 ± 13.4
OVA 72.5	96.9 ± 13.3	84.7 ± 12.4
OVA 75	91.5 ± 12.1	81.4 ± 9.1
OVA 80	97.0 ± 14.2	76.3 ± 8.2
OVA 85	83.2 ± 9.3	77.8 ± 7.4
OVA 90	90.7 ± 9.8	64.4 ± 5.5
OVA 95	67.7 ± 8.1	50.3 ± 9.4

At a submicron level some small differentiation between the OVA gels can be observed using SEM. From image analysis it follows that all ovalbumin gels, except OVA95, have apparent aggregate building blocks of around 95 nm and pore sizes that range from about 115 nm at low temperatures to smaller sizes (around 65 nm) for OVA90. OVA95 shows both the smallest aggregate and pore size (**Table 1**). At higher incubation temperatures, the networks appear to become denser (**Fig. 5**) with smaller apparent aggregate and pore sizes (**Table 1**). The increase in the density of the network could indicate that following heating of ovalbumin at higher temperatures, more protein is incorporated in the networks than at lower incubation temperatures. The decrease in the aggregate size also indicates that more aggregates are formed and as a result of that a finer structure can be assembled.

Water holding capacity

To determine the serum that can be displaced within and become exudated from the gel by applying centrifugational forces, the water holding capacity (WHC) of ovalbumin gels was measured. The WHC measurements were carried out at varying centrifugational forces for all gels except for OVA65, and OVA68.5 as shown in **Fig. 6**.

OVA65 and OVA68 gels were relatively weak to handle and as a result, the gel broke down into pieces during centrifugation, making it impossible to obtain an accurate value for the exudated serum. For this reason, the WHC for these two gels are not shown.

The WHC for all ovalbumin gels was close to 100 % at all centrifugational forces (up to $1000 \times g$). The high WHC in all cases is related to the fact that the formed gels are all fine-stranded (as seen in **Fig. 5**). Fine-stranded gels have been shown to be capable of holding high amounts of water³². The reason for the high WHC in ovalbumin gels is related to the pore sizes. Ovalbumin gels obtained in this study have pore sizes in the range of up to around 120 nm (**Table 1**). Previously, it was reported that water could hardly be removed from gels with pore sizes below 130 nm. This is due to the fact that no water can move freely upon applied pressures as these pore sizes are below the threshold for water flux³¹.

Fine-stranded gels having higher stiffness, and small pore sizes (< 130 nm) were shown to have higher WHC³¹. Gels having higher stiffness require higher deformability/forces to result in a velocity gradient for serum to be released from the networks.

Table 2: τ_1 , and the fraction of total stress at τ_1 values for ovalbumin gels. The measurements were carried out by compressing the gels up to 20 % strain followed by holding of the gels at the maximal loading strain for 5 min and these data was obtained from normalized stress as function of time for the gels fitted according to Eq. (2). The typical R^2 values for fitted data were close to 0.99 in all cases.

Variant	τ_1 (s)	Fraction of total stress at τ_1
OVA68	8.5 ± 0.6	0.16 ± 0.01
OVA70	8.8 ± 0.2	0.16 ± 0.02
OVA72.5	8.5 ± 0.1	0.16 ± 0.01
OVA75	8.4 ± 0.1	0.15 ± 0.01
OVA80	8.5 ± 0.1	0.15 ± 0.04
OVA85	8.6 ± 0.1	0.14 ± 0.01
OVA90	8.8 ± 0.3	0.14 ± 0.01
OVA95	8.6 ± 0.1	0.14 ± 0.01

Ovalbumin gels prepared at higher incubation temperatures in this study also had higher stiffness as derived from the Young's modulus measurements (results not shown). These gels also have higher WHC (**Fig. 6**). The high WHC observed here illustrate that energy dissipation via serum flow is minimal in ovalbumin gels and its contribution to energy dissipation will not be different for the various OVA gels studied.

Stress relaxation

To assess the time-dependent contribution of energy dissipation related to structural rearrangements during the time-span of the experiment, stress relaxation properties of ovalbumin gels were determined at a compressive strain of 20 % and a deformation speed of 1 mm/s, similar to the recoverable energy measurements described above. The true stress of the obtained data was normalized and plotted as a function of time (s). These plots were fitted according to Eq. (2) yielding longer relaxation times (τ_2) typical in the range of 123 – 138 s for the different gels (results not shown), and short τ_1 values in the order of ~ 9 s (**Table 2**).

The τ_1 values are relaxation times relevant to take into account for recoverable energy measurements that require around 8 s ($2 \times 20\%$ of 20 mm at 1 mm/s = 8 s).

However, these relaxation times are comparable for all gels studied.

Moreover, the fraction of the total stress that decays with the characteristic time does not change significantly when ovalbumin is heated at different temperatures.

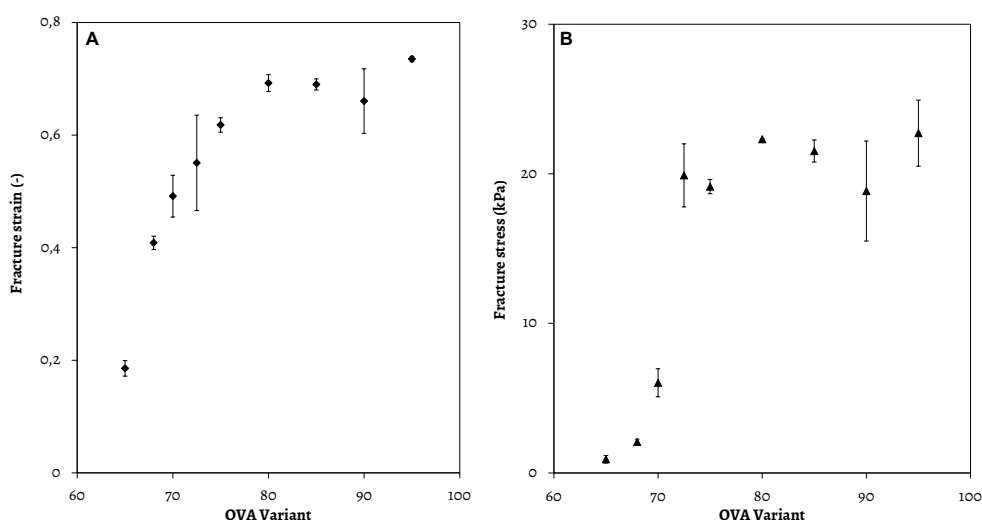


Figure 7: The fracture strain (-), fracture stress (kPa), and the Young's modulus (kPa) of ovalbumin gels formed following the heating of 120 mg/mL of ovalbumin at pH 7.0 for 30 min at varying temperatures.

The results suggest that the amount of energy dissipated via structural rearrangement in ovalbumin gels can be treated as a constant (~15 % of total stress in the recoverable energy measurement) for all ovalbumin gels tested.

Fracture

Fig. 7 shows the stress responses of the different ovalbumin gels following the application of 90 % compressive strain at a rate of 1 mm/s. The fracture stress and strain were determined from the macroscopic fracture point, which corresponds to the maximum of the stress versus strain curve. OVA65 had the lowest fracture strain of around 0.19. An increase in the incubation temperature from 65 °C to 80 °C resulted in a concurrent increase in the fracture strain (**Fig. 7 A**); at higher temperatures it remained constant around 0.7. These findings show that for gels prepared at lower incubation temperature, the occurrence of fracture events resulting in energy dissipation cannot be excluded, given that the 20 % compressive strain used in recoverable energy measurements is close to the measured fracture strain value of 0.2 and 0.4 for gels incubated < 70 °C (**Fig. 7 A**).

An increase in fracture stress, a measure of the gels strength, was observed with an increase in incubation temperature but only up to heating of the samples to temperatures 72.5 °C. At higher temperatures, no significant changes in the fracture stress were observed giving a fracture stress of around 20 - 23 kPa (**Fig. 7 B**). The lower gel strength for the gels incubated up to 70 °C may indicate that during heating ovalbumin below the denaturation temperatures, not all the protein is unfolded and thus not all of it participates in the network formation.

As a result there is less protein present in the serum phase resulting in gels with lower strength. The low gel strength could indicate that micro cracks may form upon deformation of the gels due to the low fracture stress levels in these gels and these results in an increase in energy dissipation.

The findings from the determination of the fracture properties of ovalbumin gels show that even though OVA68 and OVA70 might have a reasonable fracture strain, the fracture stress is low for these gels. Hence, there is a possibility that micro crack formation occur during deformation of the material and this will contribute to energy dissipation at the expense of storage.

Plastic deformation, de-bonding, and microstructural friction

The possibility of energy dissipation to occur via plastic deformation, defined here as the structural rearrangement that cannot relax on the relevant time scale, was evaluated. Careful analysis of all unloading profiles of the gels where the occurrence of resilience stress is an indication for extensive plastic deformation did not show any indications for this behavior (results not shown). Hence, this contribution to energy dissipation is regarded as being constant and negligible for the gels evaluated here.

The energy that is applied upon deformation can also result in the de-bonding of physical contact points³³ and subsequent rehydration of microstructural elements of the networks to occur²⁴. This contribution has been reported to scale with the number of interaction points or junctions of microstructural elements but little is known about the magnitude of de-bonding energies²⁴.

In this study, it was observed that different ovalbumin samples do not change substantially at the network level. Moreover, the structural building blocks are spherical aggregates rather than elongated filaments (**Fig. 5**). This justifies our assumption that this contribution is negligible and not different for the various OVA gels.

Given that all ovalbumin gels were prepared at the same volume fraction of ~ 9 vol % it is unlikely that friction between microstructural elements during a compressive strain of 20 % will contribute significantly to energy dissipation upon deformation of the gels. It is improbable that at this volume fraction, the friction between microstructural elements will vary for different ovalbumin gels as both the protein concentration as well as the fine-strandedness is comparable (**Fig. 5**, and **Table 1**).

Hence, the contributions of plastic deformation, de-bonding, and microstructure friction are postulated to be constant and/or negligible for all ovalbumin gels prepared in this study. As a result, these modes are not considered to contribute to significant energy dissipation at the expense of storage upon mechanical deformation of ovalbumin gels.

Conclusions

In summary, this work shows that whilst the activation energy of ovalbumin gels increases with increasing heating temperature, this does not correlate to the recoverable energy of the gel. This is surprising, as the recoverable energy is often considered as a property of a network to hold energy in the strand network. However, all ovalbumin gels appear to be fine-stranded with pores sizes in the range of up to 120 nm, having high water holding capacities, suggesting that serum flow caused by network deformation will at least be constant for the various gels. Moreover, it was observed that gels had a comparable stress relaxation mechanism. As the gels prepared above 70 °C had a similar fracture behavior, it can thus be expected that the recoverable energy will not differ for the different gels, despite their strongly increasing activation energy for disruption of the gel network. Clearly this latter process is not related to the ability of a material to hold energy as elastically stored energy. The gels incubated at temperatures ≤ 70 °C had relatively lower fracture strain and stress which may indicate the higher probability for the formation of (micro) fractures during deformation. From the recoverable energy results, it was observed that ovalbumin gels prepared at temperatures ≤ 72.5 °C had relatively lower recoverable energy. Additionally, these gels have larger cavities which could influence the way serum flows around the networks. This could also contribute to energy dissipation, which would explain their lower values for the recoverable energy. The results from this study show that ovalbumin can be incubated at varying temperatures to result in the formation of gel networks that require different activation energies to disrupt the networks. The findings suggest that strand-strand interactions do not set the ability of a network to store energy. These insights offer opportunities for efficient designing and optimizing desirable structures from proteins. The results from this study could be exploited in product development to predict, tune, and tailor food materials with desirable techno-functional applications.

Acknowledgements

We thank Tiny Franssen-Verheijen for the help with SEM imaging and Jan Klok for CSLM samples preparation and imaging.

References

- (1) Munialo, C. D.; Ortega, R. G.; van der Linden, E.; de Jongh, H. H. J., Modification of ovalbumin with fructooligosaccharides: Consequences for network morphology and mechanical deformation responses. **Langmuir** 2014.
- (2) Weijers, M.; Barneveld, P. A.; Cohen Stuart, M. A.; Visschers, R. W., Heat-induced denaturation and aggregation of ovalbumin at neutral pH described by irreversible first-order kinetics. **Protein Sci.** 2003, **12**, 2693-2703.
- (3) Clark, A. H.; Kavanagh, G. M.; Ross-Murphy, S. B., Globular protein gelation—theory and experiment. **Food Hydrocolloid** 2001, **15**, 383-400.
- (4) Clark, A. H.; Judge, F. J.; Richards, J. B.; Stubbs, J. M.; Suggett, A., Electron microscopy of network structures in thermally-induced globular protein gels. **Int. J. Pept. Protein Res.** 1981, **17**, 380-392.
- (5) Langton, M.; Hermansson, A.-M., Fine-stranded and particulate gels of β -lactoglobulin and whey protein at varying pH. **Food Hydrocolloid** 1992, **5**, 523-539.
- (6) van Vliet, T., Large deformation and fracture behaviour of gels. **Curr. Opin. Colloid Interface Sci.** 1996, **1**, 740-745.
- (7) van den Berg, L.; Carolas, A. L.; van Vliet, T.; van der Linden, E.; van Boekel, M. A. J. S.; van de Velde, F., Energy storage controls crumbly perception in whey proteins/polysaccharide mixed gels. **Food Hydrocolloid** 2008, **22**, 1404-1417.
- (8) Chen, J.; Stokes, J. R., Rheology and tribology: Two distinctive regimes of food texture sensation. **Trends Food Sci. Technol.** 2012, **25**, 4-12.
- (9) Hinsch, H.; Wilhelm, J.; Frey, E., Quantitative tube model for semiflexible polymer solutions. **Eur. Phys. J. E** 2007, **24**, 35-46.
- (10) Martin, A. H.; Baigts Allende, D.; Munialo, C. D.; Urbonaite, V.; Pouvreau, L.; de Jongh, H. H. J., Modulating protein interaction on a molecular and microstructural level for texture control in protein based gels. In **Gums and Stabilisers for the Food Industry 17: The Changing Face of Food Manufacture: The Role of Hydrocolloids**, The R. Soc. Chem.: 2014; pp 64-70.
- (11) Munialo, C. D.; van der Linden, E.; de Jongh, H. H. J., The ability to store energy in pea protein gels is set by network dimensions smaller than 50 nm. **Food Res. Int.** 2014, **64**, 482-491.
- (12) Kitabatake, N.; Tani, Y.; Doi, E., Rheological properties of heat-induced ovalbumin gels prepared by two-step and one-step heating methods. **J. Food Sci.** 1989, **54**, 1632-1638.
- (13) Renkema, J. M. S.; van Vliet, T., Heat-induced gel formation by soy proteins at neutral pH. **J. Agric. Food. Chem** 2002, **50**, 1569-1573.
- (14) Fernandes, A. M.; Rocha, M. A.; Freire, M. G.; Marrucho, I. M.; Coutinho, J. A.; Santos, L. M., Evaluation of cation–anion interaction strength in ionic liquids. **J. Phys. Chem. B** 2011, **115**, 4033-4041.
- (15) Çakir, E.; Daubert, C. R.; Drake, M. A.; Vinyard, C. J.; Essick, G.; Foegeding, E. A., The effect of

microstructure on the sensory perception and textural characteristics of whey protein/ κ -carrageenan mixed gels. **Food Hydrocolloid** 2012, **26**, 33-43.

(16) Camou, J. P.; Sebranek, J. G.; Olson, D. G., Effect of heating rate and protein concentration on gel strength and water loss of muscle protein gels. **J. Food Sci.** 1989, **54**, 850-854.

(17) Shim, J.; Mulvaney, S. J., Effect of heating temperature, pH, concentration and starch/whey protein ratio on the viscoelastic properties of corn starch/whey protein mixed gels. **J. Sci. Food Agric.** 2001, **81**, 706-717.

(18) Renkema, J. M. S.; Gruppen, H.; van Vliet, T., Influence of pH and ionic strength on heat-induced formation and rheological properties of soy protein gels in relation to denaturation and their protein compositions. **J. Agric. Food Chem.** 2002, **50**, 6064-6071.

(19) van den Berg, L.; van Vliet, T.; van der Linden, E.; van Boekel, M. J. S.; van de Velde, F., Physical Properties Giving the Sensory Perception of Whey Proteins/Polysaccharide Gels. **Food Biophys** 2008, **3**, 198-206.

(20) Weijers, M.; Van De Velde, F.; Stijnman, A.; Van De Pijpekamp, A.; Visschers, R. W., Structure and rheological properties of acid-induced egg white protein gels. **Food Hydrocolloid** 2006, **20**, 146-159.

(21) Weijers, M.; de Hoog, E. H. A.; Cohen Stuart, M. A.; Visschers, R. W.; Barneveld, P. A., Heat-induced formation of ordered structures of ovalbumin at low ionic strength studied by small angle X-ray scattering. **Colloids Surf., A** 2005, **270-271**, 301-308.

(22) Photchanachai, S.; Mehta, A.; Kitabatake, N., Heating of an ovalbumin solution at neutral pH and high temperature. **Biosci. Biotechnol. Biochem** 2002, **66**, 1635-1640.

(23) Renkema, J. M. S.; Knabben, J. H. M.; van Vliet, T., Gel formation by β -conglycinin and glycinin and their mixtures. **Food Hydrocolloid** 2001, **15**, 407-414.

(24) de Jong, S.; van Vliet, T.; de Jongh, H. J. H., The contribution of time-dependent stress relaxation in protein gels to the recoverable energy that is used as tool to describe food texture **Mech. Time-Depend. Mater.** 2015, *In press*.

(25) Munialo, C. D.; van der Linden, E.; Ako, K.; de Jongh, H. H. J., Quantitative analysis of the network structure that underlines the transitioning in mechanical responses of pea protein gels. **Food Hydrocolloid** 2015, **49**, 104-117.

(26) Kocher, P. N.; Foegeding, E. A., Microcentrifuge-Based Method for Measuring Water-Holding of Protein Gels. **J. Food Sci.** 1993, **58**, 1040-1046.

(27) Mine, Y., Recent advances in the understanding of egg white protein functionality. **Trends Food Sci. Technol.** 1995, **6**, 225-232.

(28) Huntington, J. A.; Stein, P. E., Structure and properties of ovalbumin. **J. Chromatogr. B** 2001, **756**, 189-198.

- (29) Chandra, B. S.; Prakash, V.; Rao, M. N., Association-dissociation of glycinin in urea, guanidine hydrochloride and sodium dodecyl sulphate solutions. **J. Biosci.** **1985**, **9**, 177-184.
- (30) Denisov, E. T.; Tumanov, V., Estimation of the bond dissociation energies from the kinetic characteristics of liquid-phase radical reactions. **Russ. Chem. Rev.** **2005**, **74**, 825-858.
- (31) Urbonaite, V.; H.H.J., d. J.; van der Linden, E.; Pouvreau, L., Permeability of gels is set by the impulse applied on the gel. **Food Hydrocolloid** **2015**, **Accepted**.
- (32) Çakır, E.; Foegeding, E. A., Combining protein micro-phase separation and protein-polysaccharide segregative phase separation to produce gel structures. **Food Hydrocolloid** **2011**, **25**, 1538-1546.
- (33) Hang, F.; Gupta, H. S.; Barber, A. H., Nanointerfacial strength between non-collagenous protein and collagen fibrils in antler bone. **J. R. Soc. Interface** **2014**, **11**, 20130993.

Chapter 9

General Discussion

Introduction

Foods and food products are multi-component systems, whose spatial volume is often set by a protein-continuous network, such as in dairy products like cheese and butter, jellies, tofu, or confectionary products¹. However, with an increase in human population and a concurrent increase in demand for protein, the food industry is challenged to diversify the available protein sources or to come up with alternative proteins to meet the increasing demand. Alternative proteins should have a similar functionality to the original protein and, most importantly, the end products should still have a similar texture. However, proteins from different sources such as animal or plant protein sources have inherent functional properties that profoundly differ e.g. in solubility, denaturation, aggregation propensity, and thereby the network-forming properties. This makes the exchangeability of protein sources without altering the textural and sensorial properties of the final product a difficult target.

To efficiently search for alternative protein sources for food gels, the relation between protein network properties and texture must be better understood. This provides a challenge to understand the fundamental relations between characteristics of the constituting proteins and the conditions of the network formation such as pH, ionic strength, protein concentration, and incubation temperature, to produce a wide range of network properties. Such knowledge will give guidelines on the limits of exchangeability of protein sources in food products and can be used to tailor products accordingly.

In most food products such as confectionaries, crumbliness is one of the main texture parameters that control consumer acceptance. The ability to store energy, often measured in terms of the recoverable energy, has been shown to correlate to perceived crumbliness of food gels². The term ‘recoverable energy’ is used in literature as shorthand for the amount of energy available after deformation of a (gel) network. The recoverable energy is equivalent to the amount of energy stored in the network upon deformation. Though from a thermodynamic point of view the term ‘recoverable energy’ is debatable, it is used in this thesis as defined above.

To use proteins in food applications or to select alternative protein sources, it is important to understand, predict, and direct the ability to elastically store energy in a network upon mechanical deformation. Mechanical deformation is a key step in oral processing of foods.

By applying mechanical deformation, one can mimic the “palating” (between tongue and palate) process given that mechanical properties of foods are widely used to understand and predict mouth flow properties and to establish relationships with sensory perception³. For instance, slipperiness perception in the oral cavity, was observed in the mixed lubrication regime at typical entrainment speeds between 10 and 100 mm/s⁴ with tongue-palate contact pressures of 10 – 33 kPa⁵. These pressures are in the same order as the observed fracture stress determined from mechanical deformation of protein gels¹. Additionally, an understanding of how the energy dissipation upon mechanical deformation is influenced by several factors, such as the microstructure of the network is of great significance for the food industry to be able to modulate products towards desired sensory properties, especially when new or alternative proteins sources are involved.

To change the ability of globular protein networks to store energy (as opposed to energy dissipation), several approaches can be followed. One approach is to change the morphological aspects of the networks as set by system conditions resulting in networks that can vary e.g. in coarseness and strand thickness. The assembled networks can either be composed of fine or coarse strands. Fine-stranded networks have a typical submicron scale, and are known to have less energy dissipation via e.g. serum flow, which results in higher amounts of stored energy than it is the case for coarse-stranded networks^{6,7}. Other approaches include the modification of proteins⁸, or the addition of other components, such as polysaccharides to protein gels².

Changes in the network preparation can result in variation of the structural aspects that dominate a stranded network such as the strand thickness, strand stiffness, strand-strand interaction energy, and the mesh size. These structural aspects emanate from the aggregation behavior of the protein, which is determined by molecular characteristics, and their ability to interact during processing. An assembled microstructure may consist of molecules that have a dimension of a few nanometers, or protein molecules that are assembled into flexible fine-stranded structure elements, coarse-stranded or particle shaped structure elements⁹. Modulation of the structural elements that dominate a stranded network can result in the variation of the aggregate size and thickness of the strands of the protein networks. This in turn has an influence on the mechanical properties of protein gels and their interactions with the food matrix.

In this thesis, fine and coarse-stranded protein networks formed under defined conditions such as heating temperature, ionic strength, and pH, were investigated. The aim of this thesis was to understand how structural aspects affect the ability of protein gels to store versus dissipate energy. This thesis was divided into sections. In the introduction we gave an overview of the relevant literature and the goals and strategies of the thesis project. Next, we showed how conditions can be manipulated to vary the strand thickness. Thereafter, the strand stiffness of the network structure was varied, followed by the modulation of the structural aspects of stranded networks, in particular the mesh size, via chemical modification of the protein.

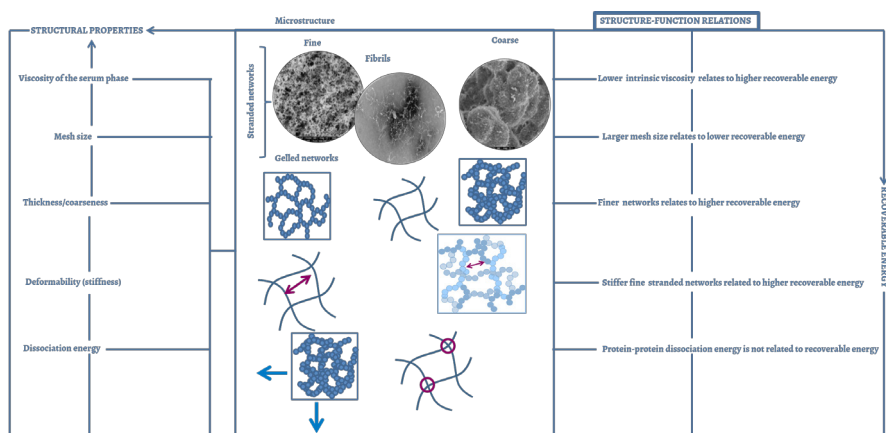


Figure 1: Schematic presentation of thesis content

Subsequently, we discussed the relevance of the viscosity of the serum phase on energy dissipation via serum flow and how this affects the rheological responses of gel networks. Finally, the activation energy of disruption of protein networks was discussed in relation to recoverable energy. The content of the thesis and its main findings is summarized schematically in **Fig. 1**.

In this final chapter of the thesis, we put the findings of the previous chapters into perspective, by evaluating the mechanisms responsible for the modulation of energy storage in protein networks. First, a short review on how the term recoverable energy is used in food versus material science is presented. Thereafter, we discuss the structures that were assembled in this thesis, the length scales that show the network dimensions of these structures, and how the aspects of these structures can be altered. The conditions that were used in the preparation of protein networks are reviewed in the context of the relevant literature. Subsequently, the functional properties of these networks are addressed, as well as the mechanisms responsible for the main findings in each study. In the final part, we comment on the relevance of the findings of this thesis for application in food technology and possible future research.

Recoverable energy: A review based on food and material science

In this section of the discussion, special attention is given to understanding the recoverable energy in relation to relevant literature from food and material sciences. Even though the term ‘recoverable energy’ is common in food and/or material science, one should note that it is a shorthand term for the elastically stored energy, or the part of the energy applied during compression that is available for work during subsequent decompression. If one looks at it from a thermodynamic point of view, the term ‘recoverable energy’ is debatable, as aforementioned.

Recoverable energy has been described in various ways and related to different sensorial properties of food gels^{2, 7}. The microstructure was shown to play a crucial role in the recoverable energy of food gels making it a material property of gels. Homogenous gels were shown to have higher recoverable energy than particulate networks⁷. Attempts were also made to relate energy dissipation via various modes such as friction and viscous flow to the recoverable energy.

Gels that had higher energy dissipation were reported to have lower recoverable energy¹⁰. However, the big questions remain: “Does the recoverable energy really exist?” and “is it a material property or not?” An understanding of the recoverable energy is important as this provides a tool to engineer materials with the desired physical (textural) as well as sensorial properties.

In food science, the recoverable energy is measured as the ratio of the amount of energy that is recovered after applying stress over the amount of energy that is applied during the compression and subsequent decompression of the gels. Recently, the recoverable energy was reported to be applied energy assumed implicitly to be 100 % minus the energy dissipated over six (and perhaps more) modes described in the introduction¹. However, several parameters of the methods used to determine recoverable energy, such as the applied strain, have an influence on the recoverable energy. If the relation between strain and deformation is linear over a certain range, one can work with just one strain. However, if the relation is non-linear, different strain levels will give different results. Moreover, some of the dissipation modes display a rate-dependence, for instance the friction caused by serum flow through porous networks is dependent on the deformation speed. Thus, if the recoverable energy is in a non-linear relationship to the strain applied, the determined recoverable energy may not be the actual amount of energy stored in the networks. This is due to the fact that non-linear processes change the way the elastic energy is conveyed toward the crack tip¹¹ and fracture events could already result in energy dissipation at the expense of elastic storage.

The deformation rate can also affect the recoverable energy of the gels as aforementioned. A clear correlation was reported between the sensory crumbly scores and the recoverable energy of whey protein gels determined at a deformation speed of 20 mm/s ($R^2 = 0.87$), but not at a deformation speed of 1 mm/s¹⁰. The deformation speed of 20 mm/s is in the same order as the biting and palating speeds applied in humans⁴. A relation was also established between the recoverable energy and the crumbly effect of gels. Crumbly gels were shown to have a higher recoverable energy of 70 - 80 %, which implies that the reaction on applied deformation has a higher elastic component. Contrarily, gels with low crumbly scores were shown to have a lower recoverable energy (30 - 40 %)². This implies that the reaction on applied deformation for gels with a low crumbliness score has a lower elastic component. Weak gels and concentrated solutions also exhibit viscoelastic behavior^{12, 13}. These materials display deformations that are time scale dependent. At short deformation time scales, the materials exhibit elastic storage of energy, but relax into viscous flow when the deformation time is prolonged¹⁴.

Apart from the studies relating the recoverable energy to either the microstructure or to the crumbly effect of food gels^{2,10}, not much attention has been paid to understanding the mechanism responsible for the storage of energy in gel networks. Recently, it was shown that to determine the ability of network structures to store energy, an understanding of the modes by which energy is dissipated is essential, given that only part of the applied energy is stored¹.

Structural aspects of gels such as the mesh size were shown to affect the fraction of energy dissipated via serum flow which in turn influences the ability of the protein networks to elastically store energy as the mesh size has an influence on how water flows within the networks¹⁵. Previously, the recoverable energy was related to the water/serum entrapped in the network which was shown to depend on the coarseness of the networks⁶.

The recoverable energy was hypothesized to be related to energy stored in the network chains of biopolymer gels¹⁶. However, the problem with relating the number of network chains of biopolymer gels to the stored energy is that, the number of chains per unit volume of the network has to be determined to quantify the energy that is stored. However, for a number of reasons, this is not a straightforward explanation of the number of chains formed per unit volume and how this affects the stored energy. Firstly, even beyond the gel point, a part of the protein molecules or aggregates in the gels which are not physically attached to the infinite network, will still be existing and therefore will not contribute to elastic phenomena¹⁶. Secondly, even within the network, there will still be a number of chains which, at equilibrium, are not capable of supporting stress applied upon mechanical deformation¹⁶.

In the material sciences, the stored energy has been studied and related to various aspects. For instance, synthetic hydrogels containing slide-ring polymers are shown to be able to stretch to more than 10 times the initial length¹⁷. This quality is related to the resilience of the material and this has to do with the way energy is elastically stored within gels. Stretching of the gels was reported to result in the rupturing of the short-chain network which led to energy dissipation at the expense of storage¹⁸. The replacement of the sacrificial covalent bonds with non-covalent bonds was shown to result in glassy domains of gel with copolymers of triblock chains remaining intact, while the ionic crosslinks broke and dissipated energy¹⁹. Recoverable energy is shown to also be affected by hydrophobic associations^{20, 21}. In gels containing hydrophobic bilayers in a hydrophilic polymer network, stretching of the networks resulted in the bilayers dissociating and dissipating energy; on unloading, the bilayers re-assembled, leading to recovery²⁰. Other workers have shown that elastic energy is stored in semi-flexible networks primarily in the homogeneous extension and compression of filaments²². In collagen gels, the energy expended was reported to be stored as elastic strain energy when cells are embedded within monomeric collagen prior to polymerization²³. These few examples show that the use of the term recoverable energy or energy storage varies broadly. Hence, a study of how the recoverable energy can be modulated is crucial especially in food science where it is used as a tool to map texture.

Thus, in subsequent sections of this thesis, we looked in more detail at recoverable energy and how this parameter is used as a measure for energy dissipation.

Manipulation of the network structure to increase strand thickness

Stranded networks with varying structural aspects such as strand stiffness, strand thickness, strand interaction energy, and mesh size can be produced by different methods.

Proteins denature when heated above the denaturation temperature resulting in the formation of protein aggregates via hydrophobic and sometimes covalent interactions^{24, 25, 26}. It is well known that depending on the protein concentration, pH, heating conditions, the type and the amount of salt added, aggregates can be obtained varying in size, shape, microstructure, and functional behavior²⁵. Previous research has shown that prolonged heating of proteins at pHs far from the isoelectric point (IEP) can result in the formation of fibrillar aggregates²⁷. Fibrillar aggregates may be used in the formulation of low-caloric products because of their functionality, which ranges from gelling agents to stabilizers of foams and emulsions²⁸. The dimensions of fibrillar aggregates are a few nm in width and can be up to 1 μm in length.

To vary the size or thickness of fibrillar strands, various approaches can be followed. These can include the modification of proteins via methods such as thiolation, where thiol groups are attached to the proteins in a non-reactive state. These thiol groups can be made reactive, resulting in the formation of disulfide bonds that can alter the functional properties of protein gels. Modification of proteins can also be achieved via glycation^{29, 30}, oligofructosylation³¹, succinylation^{32, 33}, and phosphorylation³⁴. In most studies of these modifications, native proteins have been used, to which different groups are attached to a folded protein molecule. Subsequently, gel formation was induced by heat when the protein containing the attached groups was unfolded resulting in the formation of a spatial network.

In Chapters 2 and 3, fibrillar aggregates were formed with the aim of manipulating the strand thickness and stiffness of the networks. In Chapter 2, thiolation was carried out on pre-aggregated supra-molecular structures. Fibrillar aggregates as well as spherical aggregates made from whey protein isolate (WPI) were thiolated. Spherical aggregates served as control variants. It was hypothesized that the de-blocking of the thiol groups attached to the pre-formed aggregates would allow for the formation of intrastructural disulfide bonds, resulting in coupling of the aggregates, resulting in thicker strands. In Chapter 2, it was indeed shown that covalent attachment acetylthiogroups to preformed aggregates can be carried out. The attachment of thiol groups to preformed aggregates is judged to be better than using folded (native) protein, because starting with preformed aggregates allows the exposed functional groups to undergo direct cross-linking. Folded protein molecules, however, need to change conformation multiple times prior to “docking” into aggregates.

Additionally, a high degree of thiolation of natively folded protein inhibits the initial aggregation process, which in turn greatly inhibits strong gel formation³⁵.

The changes in the morphology of networks of thiolated aggregates were investigated using transition electron microscopy (TEM). However, the fibrillar aggregates appeared to overlap to a great extent making it difficult to distinguish between overlapping versus true coupling of fibrils.

Changing the protein source can also change the morphology of stranded networks. For instance, one can choose plant proteins instead of animal proteins.

Due to inherent differences between plant storage and animal proteins, such as in quaternary structure and solubility, variations in the structural aspects of the stranded networks like strand thickness and stiffness, are inevitable.

Previous studies have shown that proteins after being hydrolyzed into peptides at pHs away from the isoelectric point (IEP), and can be assembled into fibrils^{1,10-12}. Many proteins of animal origin such as whey proteins and ovalbumin have been reported to assemble in this way into fibrils³⁶⁻³⁹. Fibrils made using whey proteins are 1 μm long and a few nm thick⁴⁰. Fibrils were also prepared from plant storage proteins, such kidney bean phaseolin⁴¹, vicilin⁴², and soy proteins^{43,44}. Fibrils made from soy proteins exhibited different characteristics from those made from whey proteins such as being more branched and curly⁴³. In Chapter 3, fibrils were formed from pea proteins that were few nm thick and highly flexible compared to fibrillar aggregates formed from whey protein as shown in **Fig. 2**.

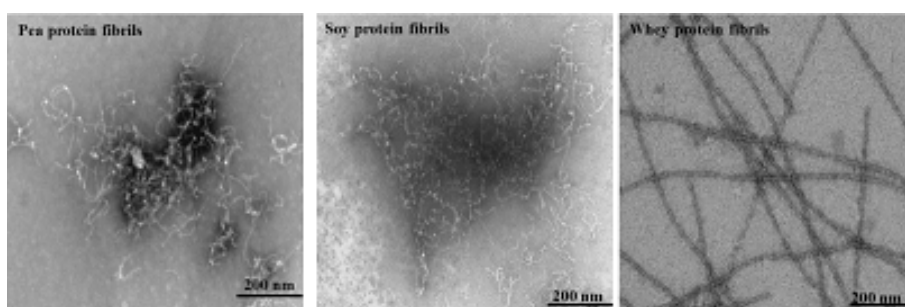


Figure 2: A comparison of fibrils made from pea protein, soy protein and whey proteins.

These two studies carried out in Chapters 2 and 3 show that changing the protein source to vary the strand thickness or to obtain stiffer structural motifs does not lead to differences in strand thickness, although changing the protein source results in variations in the strand stiffness.

The functional properties of fibrillar networks

The formation of stranded networks in an aqueous or gelled system has significant influence on the textural and rheological properties. Therefore, the physical properties of fibrillar aggregates (i.e., secondary and tertiary structural integrity of the proteins, microstructure, and rheological properties) were evaluated. Rheological properties of thiolated fibrillar aggregates formed from whey proteins were investigated in Chapter 2. The attachment of acetylthio groups to pre-aggregated WPI fibrillar and spherical aggregates was shown to result in conformational changes in these structural building blocks. Gels made from unthiolated WPI spherical aggregates were the least stiff as they had the lowest storage modulus (G' ; Pa). The attachment of acetylthio groups that were not de-blocked resulted in an increase in the stiffness of the gels as well as a decrease in the onset gelation time. Gels prepared from thiolated WPI fibrillar aggregates were two-fold stiffer than those of unthiolated fibrils.

Fibrils form gels with an order of magnitude lower protein concentration than conventional cold or heat-induced gelation⁴⁵. Upon the introduction of extra attractive interaction, gel formation can occur even at lower protein concentrations⁴⁵. Such attractive interactions were introduced to the supra-molecular structures by means of thiolation and this was shown to result in an increase in stiffness of the gels.

In this thesis, the mechanical deformation properties of gels such as Young's modulus, as a measure for stiffness, were assessed by compressing the gel specimen to 90 % compressive strain with 1 mm/s compression rate. Such tests are carried out on self-supporting gels. However, the yield of fibrillar aggregates obtained from the thiolation study (Chapter 2) was not sufficient to allow formation of self-supporting gels. Previous studies have demonstrated that the thiolation of native ovalbumin resulted in the formation of gels that showed lower Young's moduli than gels prepared from unthiolated ovalbumin³⁵. This was related to the fact that the final aggregate morphology, gel formation, and the stability of thiolated proteins are affected by rapid covalent network formation, which does not allow rearrangements into more stable networks³⁵. Although the methods used to determine stiffness are not directly comparable, the results show that when thiolation is carried out on pre-aggregated proteins, the stiffness of the gels is enhanced due to the formation of disulfide bridges. When thiolation was carried out on the proteins in their native state, the stiffness of the gels was however significantly reduced. The reduction in stiffness of the gels is likely related to the fact that the final aggregate morphology, gel formation, and the stability of thiolated proteins are affected as a result of rapid covalent network formation as aforementioned, which does not allow rearrangements into more stable networks³⁵.

In Chapter 3, fibrillar aggregates were prepared from pea protein. These aggregates were used in the formation of gels via slow acidification using GDL. The rheological responses of pea protein-based fibrillar gels were evaluated in comparison to soy and whey protein-based fibrillar aggregates.

Fibrils made from pea proteins were found to be highly flexible (**Fig. 2**) compared to fibrils made from whey protein which have been described as being semi-flexible^{46, 47}. Gels made from pea protein fibrils were less stiff than gels made from whey proteins fibrils at the same concentration as about 6 times more concentration of pea proteins was required to derive a comparable storage modulus (G') to whey protein-based fibrillar gels. The differences in gel strength may be related to inherent differences between plant and animal proteins as well as structural differences between the formed fibrils such as differences in the flexibility, and as a consequence, the deformability of the fibrils. Fibrils made from pea protein were also short as seen in **Fig. 2** and confirmed by steady-state birefringence analysis⁴⁸. These findings are discussed in detail in Chapter 3.

The gel strength of pea protein-based fibrillar gels was however comparable to that of soy protein-based fibrillar gels, just like the fibrillar structure. The fracture properties of pea protein-based fibrillar gels made at 160 mg/mL protein concentration were comparable to those of soy protein-based fibrillar gels made at 40 mg/mL and those of whey protein-based fibrillar gels made at 25 mg/mL. The observed differences in the strength of pea protein, soy protein, and whey protein-based fibrillar gels were due to variations in the strand stiffness/flexibility of the strands.

From the study on fibrillar aggregates assembly and rheological characterization, it was demonstrated that when using plant protein instead of animal protein, the stiffness of the resulting network structure affects the gel strength contrary to the strand thickness, which has no effect. Changes in the strand stiffness would change the deformability of the networks, and thereby, the rheological behavior due to variation in the flow of serum within the networks. Hence, a study was carried out to vary the conditions used in the preparation of pea protein gels to result in the formation of so-called fine or coarse-stranded networks, and to evaluate whether this can be a tool to understand the energy balance in protein-based gels.

Fine and coarse-stranded networks of pea proteins

When protein solutions are heated above their denaturation temperature, at higher concentrations than the minimum gelling concentration, at pH away from the IEP and at low ionic strength, the formation of fine-stranded gels is favored. Fine-stranded gels are often transparent and the strands are around 5 – 12 nm thick^{40, 41}. Contrarily, when protein solutions are heated at pHs closer to the IEP or at high ionic strength, the formation of coarse-stranded gels composed of particulate aggregates occurs⁴⁹. Coarse-stranded gels are usually turbid and these strands can be up to several micro-meters thick^{50, 51}. In Chapter 4, fine and coarse-stranded networks were formed following heating of pea protein solutions at varying pHs and ionic strength at a fixed protein concentration of 150 mg/mL, at 95 °C for 30 min. The typical length scales of the formed networks were characterized by image analysis with the aim to find a possible relation between degree of coarseness of protein networks and the recoverable energy.

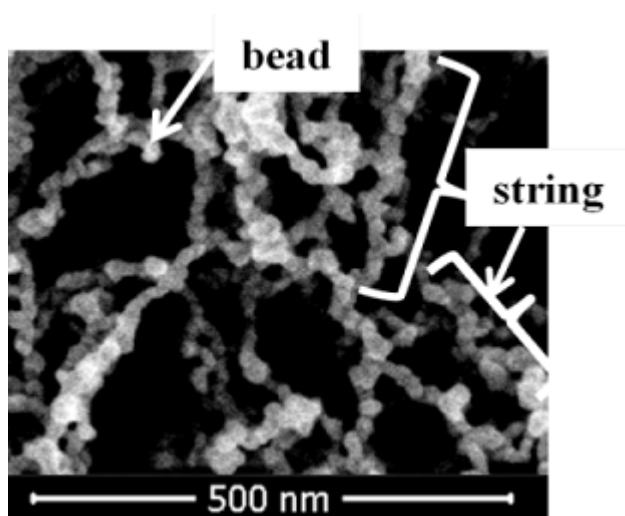


Figure 3: Representation of the local domains (“bead”) and (“string”) that characterizes pea protein network structure.

It was shown that gels varying in apparent coarseness, defined as the inhomogeneity of gel networks as related to the thickness of strands that span the networks, can be formed from pea proteins. A broad variety of network structures with differences in coarseness were created from pea proteins by varying the pH, ionic strength, and ionic species. Fine-stranded networks were composed of strands that were few nm thick whereas coarse-stranded networks were up to several μm thick depending on the gelation conditions. The pH ranges (3, 5, 7, and, 9) used in this study were, however, broad making it impossible to precisely determine the conditions at which structural transition from fine to coarse-stranded networks occurs, and to investigate the related consequences of rheological responses of the formed gels. In Chapter 5, the quantification of the network structures that underline the transition in the rheological responses of pea protein gels was carried out in more detail. The pH of pea protein solutions was varied at a fixed protein concentration and the protein concentration was varied at a fixed pH prior to gel formation. It was evident that a transition in the structure of pea protein gels occurs around pH 3.7 at typical domain size of 100 nm string size (illustration of string is shown in **Fig. 3**), based on SEM images. When image analysis was carried out on the micrographs obtained from CLSM, variations in correlation lengths were also observed at a micron level and the results also confirmed that the structural transition in pea protein at low pHs occurs around pH 3.7.

Functional properties of fine and coarse-stranded networks

In Chapter 4, gels were made at a fixed protein concentration and varying ionic strength. Under these conditions, a wide range of stranded networks was formed.

The networks varied from fine to coarse-stranded (as characterized by the use of CLSM and SEM) and in coarseness. Coarseness was defined as the inhomogeneity of the gel networks as related to the interplay between the network and the enclosed serum (based on CLSM images), or as the inhomogeneity of the gel networks as related to the thickness of the strands that span the networks (based on SEM micrographs as aforementioned). These networks differed in gel strength as measured from fracture stress. The fracture stress was higher for finer networks formed at pHs away from the IEP or at low ionic strength, as opposed to coarser networks formed closer to IEP or at higher ionic strength. These differences in the gel strength could be related to a number of factors. Firstly, differences in the connectivity of the networks. When the gel network shifts from the least coarse to coarser, the network becomes less dense with larger pore sizes. Less dense β -lactoglobulin networks have been reported to have a lower fracture stress⁵². Particulate whey protein isolate gels have also been reported to show discontinuous crack propagation during tensile fracture as visualized by CLSM⁵³. Therefore, the porous nature of coarse pea protein networks could cause step-wise crack formation due to micro-scale inhomogeneities between protein clusters in the form of cracks, or weak regions resulting in lower fracture stress. Changes in gelation conditions also resulted in changes in the fracture strain, a measure of the brittleness of the gels. Coarser networks had the highest fracture strain, an indication that the gels were rubber-like. Coarse-stranded networks also showed slightly higher fracture strains than fine-stranded networks. A higher fracture strain could indicate that a larger degree of straightening occurs before fracture. Coarse gels had the highest Young's moduli compared to finer networks. Given that the bending load of cylinders scales with the diameter⁵⁴, coarse strands are more difficult to bend than finer ones. Gels prepared at higher salt concentration also had higher Young's moduli. The modulus of gels has been reported to increase on the addition of salts⁵⁵. Gradual changes in Young's modulus with an increase in the coarseness of pea protein gels were observed which suggests that there may be an additional contribution that set the Young's modulus of pea protein gels at larger length scales. In general, there was no unequivocal relation between the fracture properties (such as fracture stress, fracture strain, and the Young's modulus) of the gels and the coarseness. A lack of correlation between the coarseness of the network structure and the Young's moduli of soy protein gels has been reported⁵⁶.

The recoverable energy measured at 1 mm/s deformation speed was higher in fine-stranded gels than in coarser gels, being an indication for a larger elastic component. Elasticity in gels is usually higher when more water is held within the gel network⁷. Visually, less dense gel networks showed a higher serum release during compression and this may suggest that, more energy is dissipated via viscous serum flow, resulting in lower recoverable energy. The typical dimensions of stranded networks that set the ability to store energy in pea protein gels were shown to be below 50 nm strand thickness, where the strand thickness was measured based on the bead size (illustration of bead size is shown in **Fig. 3**).

The structural changes of pea protein gels from fine- to coarse-stranded and the resulting transition in rheological properties of pea protein gels were studied in Chapter 5. An increase in string size and bead size was observed when the pH was increased above pH 3.6.

Gels prepared above pH 3.8 showed a remarkable decrease in the recoverable energy measured at 1 mm/s deformation speed. At around pH 3.8, a clear increase in the correlation length was also observed which shows that the dimensions that matter for recoverable energy are at a sub-micron level (below 100 nm string size).

Given that the recoverable energy has been shown to be deformation rate dependent⁵⁷, energy release in pea protein gels during relaxation was also measured at varying deformation speeds of 0.1, 0.25, 1, 2.5, and 10 mm/s for gels prepared at pHs 3.0 to pH 4.2 at a fixed protein concentration.

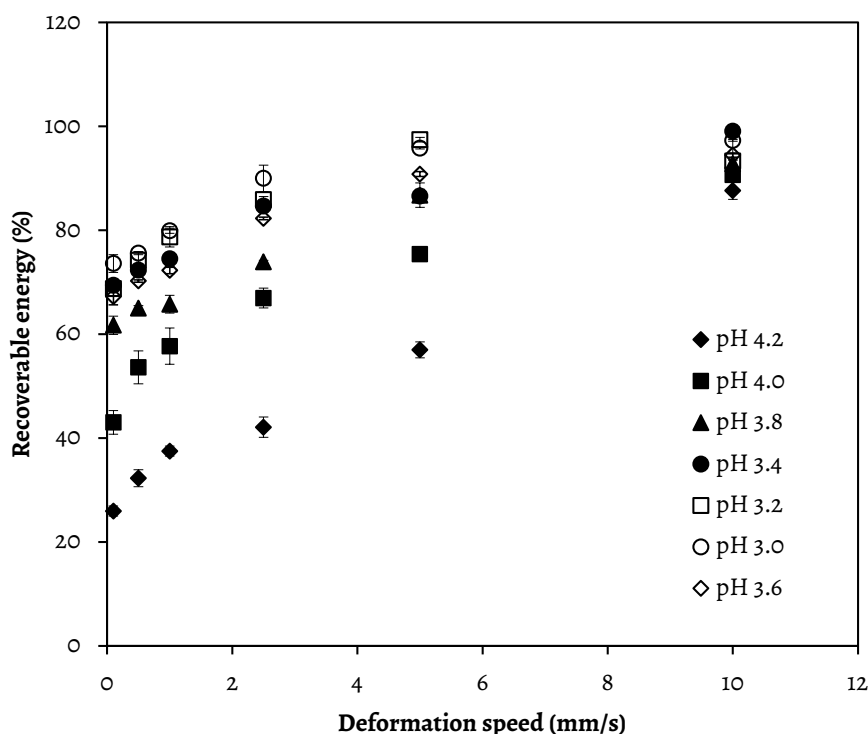


Figure 4: Changes in the recoverable energy as a function of deformation speed for pea protein gels prepared at varying pHs from pH 3.0 – pH 4.2 at a fixed protein concentration of 120 mg/mL.

This study was carried out to find out whether a change in the deformation rate results in differences in the recoverable energy of pea protein gels at varying pHs. The deformation rate (speed) dependence of recoverable energy was measured as shown in **Fig. 4**. At deformation speeds of up to 5 mm/s, a clear difference in the recoverable energy was observed between gels prepared at pH 3.8, pH 4.0 and pH 4.2 and the rest of the gels (**Fig. 4**). The gels prepared at pH 4.2 had the lowest recoverable energy at all deformation speeds lower than 5 mm/s. There was no significant difference in the recoverable energy as a function of deformation speed up to 5 mm/s for samples prepared at pH 3.0 - 3.6.

At the highest deformation speed applied in this study (10 mm/s), the recoverable energy at all pHs investigated was close to 100 %. The high recoverable energy at highest deformation speeds could be related to the amount of time allowed for the gels to recover after deformation. The measurements at 10 mm/s are the fastest and hence the samples have less time to deform and recover than at lower deformation speeds. The results from the study of the influence of deformation speed on the ability of the protein gels to store energy show that in addition to the influence of the microstructure, the deformation speed also affects the ability of pea protein gel networks to store energy but only up to the deformation speeds of 5 mm/s.

The substantially low recoverable energy observed at lower deformation speeds for gels made at pHs close to IEP could be related to increased formation of micro-cracks due to longer time taken to compress the gels, in addition to these gels being coarser resulting in occurrence of energy dissipation via fracture events or serum flow within the gel networks.

In the studies carried out in Chapter 4 and 5, it was shown that from fine to finer stranded networks quantified by the degree of coarseness, the recoverable energy did not change. For coarser networks, the recoverable energy was lower because of an increase in pore sizes, and the thickness of the strands. From the study of the transition in the network structure, it was shown that network dimensions that matter for recoverable energy are below 0.2 μm string sizes. In the introduction, the viscous flow was shown to result in energy dissipation resulting in lower recoverable energy. A typical dimension of pore size diameter that relates to water holding which is associated with energy dissipation lies in the range of 0.1 - 2 μm ⁵⁸. A study was carried out to evaluate whether manipulating the pore size and mesh sizes (distance between two strands) of protein networks by stretching the meshes by covalent ligation of large sugar-moieties to the protein network would affect the ability to store energy due to an increase or decrease in energy dissipation via viscous flow of the entrapped serum.

Modulation of the mesh size of protein networks affects the recoverable energy

During storage of food products or just as mixed ingredient powders, Maillard reaction of the reducing sugars with primary amine groups on the protein may occur spontaneously resulting in the formation of a number of end products. This process can also be carried out in a more controlled way so that the resultant effect on structural aspects can be monitored. Covalent coupling of ovalbumin with oligo-sugar moieties was carried out using fructooligosaccharides (FOS) with a degree of polymerization of around 10 and a FOS content > 92 % as described in Chapter 6. Ovalbumin variants that had been modified in their native state to varying degrees were used in heat-induced gel formation following heating of the protein at 95 °C for 30 min. The microstructure was visualized using SEM followed by the quantitative characterization of the correlation length by pair correlation. Pre-aggregated fibrils of ovalbumin were also subjected to Maillardation with the purpose to affect the mesh size in gels as discussed in the Appendix to Chapter 6.

The aggregates (beads) constituting the network structures of gels prepared from ovalbumin modified in its native state were shown to vary between 12 and 16 ± 5 nm, whereas the apparent mesh increased from around 93 – 180 nm, with an increase in the degree of modification.

The Functional properties of FOS-modified ovalbumin

The gel strength was higher for gels prepared from unmodified ovalbumin variants. Modification of ovalbumin in its native state resulted in higher fracture strain, an indication that these gels were less brittle. With a higher degree of oligofructosylation, the network structures became finer, longer, more flexible, and stretchable, and had an increased mesh size to around 180 nm. Thus, the higher fracture strains observed show that a higher degree of straightening is possible before fracture for gels prepared from modified ovalbumin variants. A reduction in the Young's modulus occurred when oligo-sugar moieties were attached to native ovalbumin. A similar decrease in the Young's modulus was observed when native ovalbumin was thiolated³⁵, which indicates that the modification of proteins in their pre-aggregated state could be a better option than chemical modification of proteins in their native state. Using native protein appears to be less efficient for modification than using pre-aggregated proteins, as the destabilization of the protein structure will disrupt the ion-pairing network on the protein 'surface' and thereby make the lysines more reactive. The lysine groups are the amino acids to which the sugar-moieties attach during modification. The efficiency of chemical modification, however, depends on the type of modification being carried out as well as the type of protein, as the stiffness of ovalbumin gels was observed to decrease when oligofructosylation was carried out on pre-aggregated ovalbumin as discussed in the Appendix to Chapter 6.

An increase in the degree of modification resulted in a decrease in recoverable energy.

This was attributed to an increase in mesh size beyond 100 nm. At increased mesh sizes, water molecules become more able to move within the network resulting in an increase in the energy directed toward dissipation at the expense of energy storage. Gels with pore sizes > 100 nm are capable of releasing water on application of force without breaking⁵⁹. The variation in the mesh size was shown to be the main factor that affects how water flows within the network resulting in increased energy dissipation via viscous flow and thus a reduction in the recoverable energy.

Modulation of the viscosity of the serum phase

Viscous serum flow of the liquid entrapped by the network contributes to energy dissipation and this can lead to a reduction in the energy storage¹. However, properties of the serum phase like viscosity can be altered and this can influence the mechanical deformation properties of the gels including the ability to store energy in the networks.

To understand the effect of the serum phase viscosity on the physical properties of protein gels, whey protein (WP) gels were prepared as discussed in Chapter 7. Various small polysaccharides were then added to the protein solutions to modulate the viscosity of the serum phase, whilst keeping the network structure unaltered as much as possible. In this case low methylated (LM) and high methylated (HM) pectins, which are negatively charged polymers, and pullulan, a neutral polymer, were added to WP solutions at constant WP concentration. The pectin and pullulan used in this study were both branched homopolysaccharides. The molecular weight of pullulan was 150 kDa whereas the pectins were assumed to be approximately 185 kDa⁶⁰. Gel formation was induced via heating of the mixed protein-polysaccharide solutions at 95 °C for 30 min. To test the genericity of the impact of the serum phase, a study was carried out to evaluate whether the addition of pullulan to another protein, in this case pea protein, would result in a similar impact on the mechanical responses of the gels, including the ability of the networks to elastically store energy. The findings from this study are discussed in the Appendix to Chapter 7.

Physical properties of the networks

The polysaccharides in the serum phase caused an increase in the fracture stress, with samples containing LM pectin being stronger than those containing HM pectin and pullulan. The fracture strain increased to a certain level with an increase in the viscosity of the serum phase after which the fracture strain decreased, which is an indication that the gels became less brittle. To determine the mobility of serum within the gel, water holding measurements and T_2 -relaxation times of the aqueous phase of the gel networks were measured. T_2 spin-spin relaxation time decreased from around 100 ms (for WP gels only) to between 74 – 86 ms depending on the type and concentration of the polysaccharide that was added to WP gels. The water holding results, which give an indication of the flow of the entrapped serum phase, showed that the flow of serum was not affected by the addition of the three polymers as all gels containing one of the three polysaccharides had higher water holding capacities. Even at larger centrifugal forces such as $10,000 \times g$, less than 1 % of the serum could be exudated from the networks. The results suggest that no water could be removed from these networks as no water could move freely upon applied pressures as these pore sizes are below the threshold for water flux⁶¹.

The recoverable energy increased with an increase in the serum viscosity of gels prepared in the presence of LM and HM pectin. However, the increase in the viscosity of the serum phase as a result of an increase in the pullulan concentration resulted in a decrease in the recoverable energy. These gels also showed an increase in the porosity of the networks, which suggests that more energy was lost via viscous flow due to changes in the intrinsic viscosity of the serum phase, and this resulted in a decrease in the recoverable energy. However, it is important to note that the serum flow in this case was not related to the water that could be exudated from the gels as the pore sizes are below the threshold for water flux as aforementioned.

The results from Chapter 7 and its appendix show that the influence of the viscosity of the serum phase on the large deformation properties of protein gels including the ability of the networks to elastically store energy is modulated by the size, and type of polysaccharide, as well as the type of protein. The main contribution to energy dissipation was shown to be due to the viscosity of the serum phase in combination with the changes in the porosity of the networks. The modulation of the viscosity of the serum phase of pea protein gels (Appendix to Chapter 7) was shown to have a significant impact on the recoverable energy of the gels. In the case of mixtures of pea protein-pullulan, pea protein-dextran, or whey protein-pullulan, it was possible to obtain gels that vary in recoverable energy though the morphology of the gel was not altered.

Activation energy of the disruption of gel networks in relation to the recoverable energy

To determine the effective activation energy of the disruption of ovalbumin network structures and to relate this to energy storage and dissipation obtained from mechanical deformation tests, ovalbumin gels were prepared at a fixed volume fraction and pH, but varying incubation temperatures. The dissociation energy in ovalbumin networks was determined by establishing the activation energy of the disruption of networks. In Chapter 8, fine-stranded ovalbumin gels were studied. The gels were formed following heating of ovalbumin solution at neutral pH at different temperatures for 30 min at a fixed 120 mg/mL protein concentration. Subsequently, the mechanical deformation properties of the obtained gels were studied. The gels were mechanically broken down and solubilized using urea as chaotropic agent. From the kinetics of solubilization and by studying this as a function of temperature, the corresponding activation energy of the dissociation of ovalbumin gels could be obtained. These numbers were used as a measure for the energy involved in the association of the microstructural elements that make up the network.

Activation energy of the disruption related to physical properties of ovalbumin gels

Heating of ovalbumin solutions at a fixed 120 mg/mL protein concentration for 30 min above 65 °C resulted in self-supporting gels. An increase in the activation energy was observed with an increase in the incubation temperature which means that more energy is required to disrupt networks formed at higher incubation temperatures. From SEM analysis it was shown that the pore sizes decreased with an increase in incubation temperature. An increase in the incubation temperature also resulted in an increase in the gel strength as derived from the fracture stress measurements as well as the brittleness, derived from the fracture strain. A 33 % increase in the recoverable energy was observed with an increase in the incubation temperatures ≤ 72.5 °C. The changes in the recoverable energy are important given that as minimal as 20 % change in recoverable energy was reported to be sensorically relevant⁶².

For gels heated at temperatures above the denaturation temperature of ovalbumin (around 75 °C), the recoverable energy remained steady or decreased slightly, whereas the activation energy of disruption of the gels increased. The results show that the recoverable energy is independent of how much effort it takes to disrupt the networks.

The findings presented in this thesis show that changes in various structural aspects of the networks such as the mesh size, strand thickness, and strand stiffness, influence the contribution of energy dissipated via various modes which has a concomitant effect on the recoverable energy. Other structural properties such as the viscosity of the serum phase and the dissociation energy also affect the recoverable energy. The relationship between the structural aspects and the energy balance in deformed protein-based networks identified in this thesis shows that to reformulate protein-based products by employing other protein sources, a focus on the ability of the networks to elastically store energy is essential. The findings offer opportunities to control and engineer the textural attributes of food materials via their microstructure and mechanical deformation properties. This will in turn influence the sensorial attributes of foods and food products, which to a major extent influence consumer perception and acceptance.

Applications

In the last part of this thesis, attention will be given to possible applications of the knowledge obtained in this thesis. Given that the main aim of this work was to investigate how the structural aspects dominating a stranded network affect the ability of protein networks to store energy, various network structures varying from fine to coarse-stranded were investigated. The formation of fine and coarse-stranded networks, and how their characteristics interact to affect the storage and energy dissipation in protein networks was also studied. Differences in the network characteristics such as strand thickness, coarseness, strand stiffness, changes in dissociation energy, and mesh size, resulted in networks that possess a wide range of functionalities such as gel stiffness and strength, and ability of the gel networks to elastically store energy.

Aggregated proteins can act as a nucleation prerequisite to induce gelation at high protein concentrations⁶³⁻⁶⁵. Fibrillar aggregates can form gels at relatively lower protein concentration than conventional gel formation carried out using native proteins⁴⁵. Fibrillar aggregates may be used in several applications such as thickening or as gelling agents, stabilizers of foams and emulsions or in the production of microcapsules^{28, 66-68}. Spherical aggregates on the other hand can be used as additives to improve creaminess or as thickening agents⁶⁹. Chapter 2 shows that the attachment of acetylthio groups to the proteins that are made reactive and allowed to form disulfide bonds may enhance the functional properties of pre-aggregated structures. Thiolated proteins can thus be used for various application such as in the enhancement of viscosity, texture of protein gels, improvement of thermal stability, and elasticity of protein gels as all these properties have been directly or indirectly linked to the sulfhydryl content of the protein³².

To make gels at relatively low protein concentration, fibrils made from pea proteins can be used as a replacement for animal based protein in fibrillar gels. At the protein concentrations employed in Chapter 3, the gel strength increased with an increase in the concentration of fibrils. The gel strength of pea fibril-based gels was similar to that of soy protein, which shows that pea protein-based aggregates can be used as a replacement for soy protein in various products. The improvement of the gel strength of pea protein-based fibrillar gels can thus enhance the opportunities of using pea proteins in various products to replace animal proteins.

The application of thiolated pre-aggregated fibrillar or spherical aggregates as well as pea protein fibrils in real foods or food systems, however, remains a challenge, given that the toxicological as well as organoleptic qualities of products made from chemically modified proteins or hydrolyzed proteins at low pHs have to be tested before they can be introduced in to the food chain.

The investigation of the deformation properties of gels is important as these affect how the products will be perceived in the mouth during oral processing. In Chapters 4, and 5, fine to coarse-stranded gel networks were made that differed in fracture stress, fracture strain, Young's modulus, and recoverable energy. Process parameters that determine the quality of the gels are pH, ionic strength, protein concentration, and gelation temperature. Fine-stranded pea protein gels were shown to have a recoverable energy comparable to fine-stranded gels formed from animal proteins such as whey proteins. This shows the potential usefulness of fine-stranded pea protein gels for application in the food industry. Coarser networks, on the other hand, had a lower ability to store energy as a result of higher viscous energy dissipation, at the expense of elastic energy storage. These findings show that it is important to understand which aspects of the network structures affect the energy dissipation, as this in turn affects the deformation properties of gels and, finally, the sensory perception during oral processing.

In this thesis it was shown that one can steer the gelling process by several parameters, including pH and salt concentration, to apply alternative proteins in food or food systems, as the process of gel formation seems to work similarly for both plant and animal proteins. However, the interaction between the parameters is complex, and hence one cannot give a simple overall recipe for the use of alternative proteins in the food industry. It was also clear that to direct the recoverable energy, it is important to assemble the protein into structures that have the ability to store energy. By employing image analysis on pea protein gels, it was clear that the network dimensions that set the ability to store energy in protein gels are at nano-scale (below 50 nm bead sizes, and 100 nm string size) as above these dimensions the recoverable energy significantly decreased to around 40 %. The determination of the dimensions that set the ability to store energy in protein gels is important as this makes it easier to relate textural properties to sensorial properties, in particular the perceived crumbliness of gels, which is correlated to recoverable energy².

An understanding of the relevant length scales that matter in storing energy can result in the formulation of products with desirable textural attributes. The study of structural transition at pH below IEP of pea proteins can result in the formulation of products with optimal shelf life stability. The study on recoverable energy provides a stepping stone to exchangeability of raw materials in formulation of products once a clear understanding of the possibilities and limitations is considered. Sustainability can be enhanced if more plant proteins are used instead of animal proteins.

An increase in the mesh size of ovalbumin gels resulted in a decrease in the ability of the networks to elastically store energy. A decrease in recoverable energy observed in gels when various structural aspects were varied is noteworthy, given that as little as 20 % decrease in recoverable energy has been reported to be sensorically relevant¹⁰. This shows that modulation of the mesh size can have a comparable impact on the presumed crumbliness of food gels.

Serum viscosity is another factor that influences large deformation and fracture properties of gels, and the study of serum viscosity enhances our understanding of the relation between mechanical deformation properties and the sensory qualities of gels. The formation of a homogenous microstructure at a micrometer length scale leading to low macroscopic serum release was observed when whey protein gels were made containing LM and HM pectin or pullulan. The results found from the study of the role of serum phase viscosity in energy dissipation upon mechanical deformation of gels can be of particular interest for products where high serum release is considered a defect.

The variation of the incubation temperature was shown to be important in setting the textural attributes of ovalbumin gels and also to play an important role in the dissociation mechanisms of ovalbumin networks. This influences the ability of the networks to store and dissipate energy upon mechanical deformation. The insights obtained from this study could be exploited in product development to predict, tune, and tailor the textural attributes of food and food products.

The different energy dissipation routes explained in this thesis can thus be explored and used to engineer the textural attributes of different food materials. This in turn will impact the sensorial attributes of food products, and as a consequence affect the consumer acceptance of food products.

Concluding remarks and outlook

This thesis focused on understanding how the structural aspects dominating a stranded network affect the ability of protein networks to elastically store energy as defined by the typical measurements described in the introduction. The gelation of thiolated aggregates showed that the gel strength is enhanced for fibrillar aggregates than spherical aggregates as shown in **Chapter 2**. In **Chapter 3**, we prepared fibrillar aggregates from more sustainable protein sources such as pea proteins.

It was observed that fibrillar aggregates can be prepared from pea proteins via the hydrolysis process. The structural aspects of fibrillar aggregates made from pea protein were shown to considerably influence the rheological behavior of the gels. More research on the determination of the strand thickness and the percolation length of fibrils made from pea proteins would be beneficial for the possible future applications of these aggregates.

We have studied the conditions that are necessary for the formation of fine and coarse-stranded protein networks using animal protein alternatives. In **Chapter 4**, fine and coarse-stranded protein networks were made from pea protein using the gelation conditions such as the pH and ionic strength to steer network coarseness. In **Chapter 4**, the image analysis of the network structures showed that the network dimensions that set the recoverable energy of pea protein gels are below 50 nm. In **Chapter 5**, the quantitative analyses of the network structures that result in the transitioning in the mechanical deformation properties of protein gels were determined. We have shown that the transition from fine to coarser networks occurs below isoelectric point at around pH 3.7 at a typical correlation length of 100 nm based on string size. From the studies carried out in these two chapters (4 and 5), it was shown that structural transition is correlated with energy dissipation and as a consequence, with the recoverable energy. An essential future research line would be the investigation of the transition in pea proteins at pHs above the IEP to find out the pH at which transition occurs above the IEP. This would provide a wider window for the formulation of products from pea proteins at varying pHs. It may also be essential to characterize the stranded networks to determine whether the number of branches per unit length is proportional to the pH or the protein concentration and whether this has an influence on the networks ability to store energy.

The relevance of the modulation of the mesh size and the consequences for the rheological behavior is studied in Chapter 6. The findings from **Chapter 6** suggest that for reformulation of protein-based products by employing other protein sources, a focus on the ability of the networks to store energy is important, as this can be used to engineer the texture attributes of food materials. Thus, to tailor products with alternative proteins, it is essential to modulate the structural aspects of the gels such as the mesh size and use the derivatized proteins in food systems or model systems. Hence, a study on the impact of controlled Maillard reaction on the sensorial perception of the food and food products in relation to the textural qualities is relevant for engineering food products.

In **Chapter 7**, we looked at the role of the serum phase viscosity on energy storage in whey protein gels. We found that the role of the viscosity of the serum phase is important in understanding the mechanism responsible for deformation properties of the protein gels. It was shown that the viscosity determines mechanical deformation properties of whey protein gels. The type of polymers used influenced the fracture properties in addition to the recoverable energy of the gels. In the case of the polyelectrolyte pectin, changes in the viscosity resulted in stronger gels that also had a higher ability to store energy.

To pin-point the exact mechanism responsible for the effect of the serum viscosity on mechanical properties of food gels, a study on serum flow using confined flow profiles may provide useful information to be used to understand the influence of the serum phase viscosity on energy dissipation of gels. A study to characterize the serum phase using for instance size exclusion chromatography following centrifugation of the samples to expulse the serum may provide information on whether the polysaccharides that are added to the serum phase are part of the gel network or not.

In **Chapter 8**, we looked at the gel structure disruption energy in relation to energy storage and dissipation upon mechanical deformation of fine-stranded ovalbumin gels. It was shown that by varying the incubation temperature, gels that vary in recoverable energy can be obtained. Higher activation energies were obtained when ovalbumin was incubated at higher temperatures. From the results obtained in **Chapter 8**, it was evident that varying the incubation temperature can result in gels that show variations in the mechanical deformation properties, and that gels that vary in mechanical deformation properties also vary in the dissociation energy. Thus, detailed studies on the disruption kinetics of food gels should be further explored.

Although we refer to the term “texture”, which is defined as “all the structural and rheological attributes of the product perceptible by means of mechanical, tactile and, where appropriate, visual and auditory receptors”⁷⁰, a number of times in this thesis, we never measured it. The insights obtained from this thesis, such as how rheological responses of protein-based gels are related to structural properties, can however be used to engineer food gels and materials that can be applied in future texture studies.

Conclusion

To understand the energy balance in protein-based gels, networks were prepared from different proteins. It was shown that by varying process parameters such as pH, derivatization of protein aggregates, ionic strength, ionic species, the addition of polysaccharide to the serum phase, the incubation temperature during gelation, and the protein type, the structural properties of the networks can be varied. Five different structural properties of the networks i.e. strand thickness, mesh size, viscosity of the serum phase, strand stiffness, and the dissociation energy were investigated. The influence of these structural properties on energy storage and dissipation in gels was evaluated. Gelled networks composed of finer strands had a higher recoverable energy than those composed of coarser strands. An increase in the mesh size resulted in a decrease in the recoverable energy. Stiffer fine-stranded networks had higher recoverable energy. Lower intrinsic viscosity coincided with an increase in the recoverable energy. Contrarily, no relation was found between network dissociation energy and the recoverable energy. This shows that molecular interactions do not set the ability of the networks to store energy.

The findings from this research indicate that changing the structural properties of gel networks has a direct effect on energy dissipation, which consequently impact on the recoverable energy. A wide range of mechanical deformation properties of protein-based gels, such as fracture stress and strain, and Young's modulus, were also obtained when structural properties of the gels were varied. This shows that ingredients and process parameters are the main tools to control deformation properties of protein-based gels. Structurally, the submicron length scales were shown to be the most important in controlling the energy storage and dissipation in protein-based gels upon mechanical deformation on seconds' time scale, i.e. time scales that are relevant for the study of textural attributes of gels.

References

- (1) de Jong, S.; van Vliet, T.; de Jongh, H. J. H., The contribution of time-dependent stress relaxation in protein gels to the recoverable energy that is used as tool to describe food texture **Mech. Time-Depend. Mater.** 2015, *In press*.
- (2) van den Berg, L.; Carolas, A. L.; van Vliet, T.; van der Linden, E.; van Boekel, M. A. J. S.; van de Velde, F., Energy storage controls crumbly perception in whey proteins/polysaccharide mixed gels. **Food Hydrocolloid** 2008, **22**, 1404-1417.
- (3) Chen, J.; Stokes, J. R., Rheology and tribology: Two distinctive regimes of food texture sensation. **Trends Food Sci. Technol.** 2012, **25**, 4-12.
- (4) Prakash, S.; Tan, D. D. Y.; Chen, J., Applications of tribology in studying food oral processing and texture perception. **Food Res. Int.** 2013, **54**, 1627-1635.
- (5) Kieser, J.; Singh, B.; Swain, M.; Ichim, I.; Waddell, J. N.; Kennedy, D.; Foster, K.; Livingstone, V., Measuring intraoral pressure: Adaptation of a dental appliance allows measurement during function. **Dysphagia** 2008, **23**, 237-243.
- (6) Munialo, C. D.; van der Linden, E.; de Jongh, H. H. J., The ability to store energy in pea protein gels is set by network dimensions smaller than 50 nm. **Food Res. Int.** 2014, **64**, 482-491.
- (7) Çakir, E.; Daubert, C. R.; Drake, M. A.; Vinyard, C. J.; Essick, G.; Foegeding, E. A., The effect of microstructure on the sensory perception and textural characteristics of whey protein/κ-carrageenan mixed gels. **Food Hydrocolloid** 2012, **26**, 33-43.
- (8) Munialo, C. D.; Ortega, R. G.; van der Linden, E.; de Jongh, H. H. J., Modification of ovalbumin with fructooligosaccharides: Consequences for network morphology and mechanical deformation responses. **Langmuir** 2014, **30**, 14062-14072.
- (9) Martin, A. H.; Baigts Allende, D.; Munialo, C. D.; Urbonaite, V.; Pouvreau, L.; de Jongh, H. H. J., Modulating protein interaction on a molecular and microstructural level for texture control in protein based gels. In **Gums and Stabilisers for the Food Industry 17: The Changing Face of Food Manufacture: The Role of Hydrocolloids**, The R. Soc. Chem.: 2014; pp 64-70.
- (10) van den Berg, L. Texture of food gels explained by combining structure and large deformation properties. Wageningen University, 2008.
- (11) Lefranc, M.; Bouchaud, E., Mode I fracture of a biopolymer gel: Rate-dependent dissipation and large deformations disentangled. **EML** 2014, **Accepted**.
- (12) Soby, L.; Jamieson, A. M.; Blackwell, J.; Choi, H. U.; Rosenberg, L. C., Viscoelastic and rheological properties of concentrated solutions of proteoglycan subunit and proteoglycan aggregate. **Biopolymers** 1990, **29**, 1587-1592.
- (13) Vadillo, D.; Tuladhar, T.; Mulji, A.; Mackley, M., The rheological characterization of linear

viscoelasticity for ink jet fluids using piezo axial vibrator and torsion resonator rheometers. **J. Rheol. (1978-present)** 2010, **54**, 781-795.

(14) Chavan-Shinde, J., Studies on Evaluation of Viscoelastic Material. **J. Adv. Drug Delivery** 2014, **1**, 38-44.

(15) Munialo, C. D.; Ortega, R. G.; van der Linden, E.; de Jongh, H. H. J., Modification of ovalbumin with fructooligosaccharides: Consequences for network morphology and mechanical deformation responses. **Langmuir** 2014.

(16) McEvoy, H.; Ross-Murphy, S. B.; Clark, A. H., Large deformation and ultimate properties of biopolymer gels: 1. Single biopolymer component systems. **Polymer** 1985, **26**, 1483-1492.

(17) Okumura, Y.; Ito, K., The polyrotaxane gel: A topological gel by figure-of-eight cross-links. **Adv. Mater.** 2001, **13**, 485-487.

(18) Yu, Q. M.; Tanaka, Y.; Furukawa, H.; Kurokawa, T.; Gong, J. P., Direct observation of damage zone around crack tips in double-network gels. **Macromolecules** 2009, **42**, 3852-3855.

(19) Sun, J.-Y.; Zhao, X.; Illeperuma, W. R. K.; Chaudhuri, O.; Oh, K. H.; Mooney, D. J.; Vlassak, J. J.; Suo, Z., Highly stretchable and tough hydrogels. **Nature/letter** 2012, **489**, 133-136.

(20) Haque, M. A.; Kurokawa, T.; Kamita, G.; Gong, J. P., Lamellar bilayers as reversible sacrificial bonds to toughen hydrogel: hysteresis, self-recovery, fatigue resistance, and crack blunting. **Macromolecules** 2011, **44**, 8916-8924.

(21) Tuncaboylu, D. C.; Sari, M.; Oppermann, W.; Okay, O., Tough and self-healing hydrogels formed via hydrophobic interactions. **Macromolecules** 2011, **44**, 4997-5005.

(22) Head, D.; Levine, A.; MacKintosh, F., Mechanical response of semiflexible networks to localized perturbations. **Phys. Rev. E** 2005, **72**, 061914.

(23) Koch, T. M.; Münster, S.; Bonakdar, N.; Butler, J. P.; Fabry, B., 3D Traction forces in cancer cell invasion. **PLoS One** 2012, **7**, e33476.

(24) Rediguieri, C. F.; de Freitas, O.; Lettinga, M. P.; Tuinier, R., Thermodynamic incompatibility and complex formation in pectin/caseinate mixtures. **Biomacromolecules** 2007, **8**, 3345-3354.

(25) de la Fuente, M. A.; Singh, H.; Hemar, Y., Recent advances in the characterisation of heat-induced aggregates and intermediates of whey proteins. **Trends Food Sci. Technol.** 2002, **13**, 262-274.

(26) Nicolai, T.; Britten, M.; Schmitt, C., β -Lactoglobulin and WPI aggregates: Formation, structure and applications. **Food Hydrocolloid** 2011, **25**, 1945-1962.

(27) Tang, C.-H.; Wang, S.-S.; Huang, Q., Improvement of heat-induced fibril assembly of soy β -conglycinin (7S Globulins) at pH 2.0 through electrostatic screening. **Food Res Int.** 2012, **46**, 229-236.

(28) Kroes-Nijboer, A.; Sawalha, H.; Venema, P.; Bot, A.; Floter, E.; den Adel, R.; Bouwman, W. G.; van der Linden, E., Stability of aqueous food grade fibrillar systems against pH change. **Faraday Discuss.** 2012, **158**, 125-138.

- (29) Van Teeffelen, A. M. M.; Broersen, K.; de Jongh, H. H. J., Glucosylation of β -lactoglobulin lowers the heat capacity change of unfolding; a unique way to affect protein thermodynamics. **Protein Sci.** **2005**, **14**, 2187-2194.
- (30) Rondeau, P.; Navarra, G.; Cacciabauda, F.; Leone, M.; Bourdon, E.; Militello, V., Thermal aggregation of glycosylated bovine serum albumin. **Biochim. Biophys. Acta** **2010**, **1804**, 789-798.
- (31) Trofimova, D.; de Jongh, H. H. J., Modification of β -lactoglobulin by oligofructose: Impact on protein adsorption at the air-water interface. **Langmuir** **2004**, **20**, 5544-5552.
- (32) Strange, E.; Holsinger, V.; Kleyn, D., Chemical properties of thiolated and succinylated caseins. **J. Agric. Food. Chem** **1993**, **41**, 30-36.
- (33) Strange, E. D.; Holsinger, V. H.; Kleyn, D. H., Rheological properties of thiolated and succinylated caseins. **J. Agric. Food. Chem** **1996**, **44**, 54-58.
- (34) Wegener, A.; Jones, L., Phosphorylation-induced mobility shift in phospholamban in sodium dodecyl sulfate-polyacrylamide gels. Evidence for a protein structure consisting of multiple identical phosphorylatable subunits. **J. Biol. Chem.** **1984**, **259**, 1834-1841.
- (35) Broersen, K.; Van Teeffelen, A. M. M.; Vries, A.; Voragen, A. G. J.; Hamer, R. J.; De Jongh, H. H. J., Do sulphhydryl groups affect aggregation and gelation properties of ovalbumin? **J. Agric. Food. Chem** **2006**, **54**, 5166-5174.
- (36) Durand, D.; Gimel, J. C.; Nicolai, T., Aggregation, gelation and phase separation of heat denatured globular proteins. **Phys. A** **2002**, **304**, 253-265.
- (37) Kavanagh, G. M.; Clark, A. H.; Ross-Murphy, S. B., Heat-induced gelation of globular proteins: part 3. Molecular studies on low pH β -lactoglobulin gels. **Int. J. Biol. Macromol.** **2000**, **28**, 41-50.
- (38) Veerman, C.; de Schifffart, G.; Sagis, L. M. C.; van der Linden, E., Irreversible self-assembly of ovalbumin into fibrils and the resulting network rheology. **Int. J. Biol. Macromol.** **2003**, **33**, 121-127.
- (39) Veerman, C.; Sagis, L. M. C.; Heck, J.; van der Linden, E., Mesostructure of fibrillar bovine serum albumin gels. **Int. J. Biol. Macromol.** **2003**, **31**, 139-146.
- (40) Bolder, S. G.; Hendrickx, H.; Sagis, L. M. C.; van der Linden, E., Fibril assemblies in aqueous whey protein mixtures. **J. Agric. Food. Chem.** **2006**, **54**, 4229-4234.
- (41) Tang, C.-H.; Zhang, Y.-H.; Wen, Q.-B.; Huang, Q., Formation of amyloid fibrils from kidney bean 7S globulin (Phaseolin) at pH 2.0. **J. Agric. Food. Chem.** **2010**, **58**, 8061-8068.
- (42) Liu, J.; Tang, C.-H., Heat-induced fibril assembly of vicilin at pH 2.0: Reaction kinetics, influence of ionic strength and protein concentration, and molecular mechanism. **Food Res Int.** **2013**, **51**, 621-632.
- (43) Akkermans, C.; van der Goot, A. J.; Venema, P.; Gruppen, H.; Vereijken, J. M.; van der Linden, E.; Boom, R. M., Micrometer-sized fibrillar protein aggregates from soy glycinin and soy protein isolate. **J. Agric. Food. Chem.** **2007**, **55**, 9877-9882.

- (44) Tang, C.-H.; Wang, C.-S., Formation and characterization of amyloid-like fibrils from soy β -conglycinin and glycinin. **J. Agric. Food. Chem.** 2010, **58**, 11058-11066.
- (45) Veerman, C.; Baptist, H.; Sagis, L. M. C.; van der Linden, E., A new multistep Ca^{2+} -induced cold gelation process for β -lactoglobulin. **J. Agric. Food. Chem.** 2003, **51**, 3880-3885.
- (46) Arnaudov, L.; de Vries, R.; Ippel, H.; van Mierlo, C., Multiple steps during the formation of β -lactoglobulin fibrils. **Biomacromolecules** 2003, **4**, 1614-1622.
- (47) Rogers, S. S.; Venema, P.; van der Ploeg, J. P. M.; van der Linden, E.; Sagis, L. M. C.; Donald, A. M., Investigating the permanent electric dipole moment of β -lactoglobulin fibrils, using transient electric birefringence. **Biopolymers** 2006, **82**, 241-252.
- (48) Munialo, C. D.; Martin, A. H.; van der Linden, E.; de Jongh, H. H. J., Fibril formation from pea protein and subsequent gel formation. **J. Agric. Food Chem.** 2014, **62**, 2418-2427.
- (49) Clark, A. H.; Judge, F. J.; Richards, J. B.; Stubbs, J. M.; Suggett, A., Electron microscopy of network structures in thermally-induced globular protein gels. **Int. J. Pept. Protein Res.** 1981, **17**, 380-392.
- (50) Langton, M.; Hermansson, A. M., Fine-stranded and particulate gels of beta-lactoglobulin and whey protein at varying pH. **Food Hydrocolloid** 1992, **5**, 523-539.
- (51) Stading, M.; Hermansson, A.-M., Large deformation properties of β -lactoglobulin gel structures. **Food Hydrocolloid** 1991, **5**, 339-352.
- (52) Öhgren, C.; Langton, M.; Hermansson, A. M., Structure-fracture measurements of particulate gels. **J. Mater. Sci.** 2004, **39**, 6473-6482.
- (53) Brink, J.; Langton, M.; Stading, M.; Hermansson, A.-M., Simultaneous analysis of the structural and mechanical changes during large deformation of whey protein isolate/gelatin gels at the macro and micro levels. **Food Hydrocolloid** 2007, **21**, 409-419.
- (54) Young, W. C.; Budynas, R. G., **Roark's formulas for stress and strain**. McGraw-Hill New York: 2002; Vol. 7.
- (55) van Vliet, T., Large deformation and fracture behaviour of gels. **Curr. Opin. Colloid Interface Sci.** 1996, **1**, 740-745.
- (56) Renkema, J. M. S., Relations between rheological properties and network structure of soy protein gels. **Food Hydrocolloid** 2004, **18**, 39-47.
- (57) van Vliet, T.; Walstra, P., Large deformation and fracture behaviour of gels. **Faraday Discuss.** 1995, **101**, 359-370.
- (58) Hermansson, A., Water and fat holding, Mitchell JR, Ledward DA, Functional properties of food macromolecules, 1986, 273-314. In Elsevier Applied Science Publishers, New York.

- (59) Aguilera, J.; Lillford, P.; Hermansson, A.-M., Structuring water by gelation. In **Food Materials Science**, Springer New York: 2008; pp 255-280.
- (60) Christensen, S. H.; Mathiesen, H. P.; Hansen, K. M., Pectin for heat stable bakery jams. In US Patent 20,080,166,465: 2008.
- (61) Urbonaite, V.; H.H.J., d. J.; van der Linden, E.; Pouvreau, L., Permeability of gels is set by the impulse applied on the gel. **Food Hydrocolloid** 2015, **Accepted**.
- (62) Berg, L. v. d., Texture of food gels explained by combining structure and large deformation properties. 2008.
- (63) Alting, A. C.; Hamer, R. J.; de Kruif, C. G.; Paques, M.; Visschers, R. W., Number of thiol groups rather than the size of the aggregates determines the hardness of cold set whey protein gels. **Food Hydrocolloid** 2003, **17**, 469-479.
- (64) Barbut, S.; Foegeding, E. A., Ca²⁺-induced gelation of pre-heated whey protein isolate. **J. Food Sci.** 1993, **58**, 867-871.
- (65) Ju, Z. Y.; Kilara, A., Aggregation induced by calcium chloride and subsequent thermal gelation of whey protein isolate. **J. Dairy Sci.** 1998, **81**, 925-931.
- (66) Sagis, L. M. C.; de Ruiter, R.; Miranda, F. J. R.; de Ruiter, J.; Schroën, K.; van Aelst, A. C.; Kieft, H.; Boom, R.; van der Linden, E., Polymer microcapsules with a fiber-reinforced nanocomposite shell. **Langmuir** 2008, **24**, 1608-1612.
- (67) Rossier-Miranda, F. J.; Schroën, K.; Boom, R., Mechanical characterization and pH response of fibril-reinforced microcapsules prepared by layer-by-layer adsorption. **Langmuir** 2010, **26**, 19106-19113.
- (68) Humblet-Hua, N.-P. K.; van der Linden, E.; Sagis, L. M. C., Microcapsules with protein fibril reinforced shells: Effect of fibril properties on mechanical strength of the shell. **J. Agric. Food. Chem** 2012, **60**, 9502-9511.
- (69) Cheftel, J. C.; Dumay, E., Microcoagulation of proteins for development of "creaminess". **Food Rev. Int.** 1993, **9**, 473-502.
- (70) Lawless, H. T.; Heymann, H., **Sensory evaluation of food: principles and practices**. Springer Science & Business Media: 2010; Vol. 5999.

Summary

This thesis describes how the structural aspects of stranded networks affect the ability of protein-based gel networks to store energy. Structural aspects such as strand thickness, stiffness, mesh size, and the strand-strand interaction energy were evaluated. The role of the serum phase viscosity on the energy dissipation at the expense of storage was also investigated. The physical properties studied included the microstructure, breakdown and large deformation properties of the gels, including the energy storage. In-depth understanding of the ability of the networks to elastically store energy is of prime importance in the tailoring and engineering of food products.

The strand thickness and stiffness control the deformability of the networks and both influence the ability of the networks to store energy. Therefore to make thicker network strand, fibrillar aggregates were prepared in different ways. In **Chapter 2**, fibrillar and spherical aggregates were prepared from whey protein isolate (WPI). These aggregates were thiolated to a substantial degree to observe any impact on functionality. Sulfur containing groups were introduced on these aggregates which could be converted to thiol groups by deblocking. Changes on a molecular and microstructural level were studied using tryptophan fluorescence, transmission electron microscopy, and particle size analysis. The average size (nm) of spherical aggregates increased from 38 nm to 68 nm (blocked variant) and 106 nm (deblocked variant) after thiolation, whereas the structure of fibrillar aggregates was not affected. Subsequently, gels containing these different aggregates were prepared. Rheological measurements showed that thiolation decreased the gelation concentration and increased gel strength for both WPI fibrillar and spherical aggregates. This effect was more pronounced upon thiolation of preformed fibrillar aggregates. The findings suggest that thiolation at a protein aggregate level is a promising strategy to increase gelation efficiency.

Chapter 3 describes how the strand stiffness can be altered to impact the rheological behavior of protein gels. To characterize fibrillar aggregates made using pea proteins, to assemble formed fibrils into protein-based gels, and to study the rheological behavior of these gels, micrometer-long fibrillar aggregates were observed after heating pea protein solutions for 20 h at pH 2.0. Following heating of pea proteins, it was observed that all the proteins were hydrolyzed into peptides and that 50 % of these peptides were assembled into fibrils. Changes on a structural level in pea proteins were studied using circular dichroism, transmission electron microscopy, and particle size analysis. During the fibril assembly process, an increase in aggregate size was observed which coincided with an increase in thioflavin T binding, indicating the presence of β -sheet aggregates. Fibrils made using pea proteins were more branched and curly. Gel formation of preformed fibrils was induced by slow acidification from a pH 7.0 to a final pH of around pH 5.0. The ability of pea protein-based fibrillar gels to fracture during an amplitude sweep was comparable to soy protein and whey protein-based fibrillar gels, although gels prepared from fibrils made using pea protein and soy protein were weaker than those of whey protein.

The findings show that fibrils can be prepared from pea protein which can be incorporated into protein-based fibrillar gels.

To identify which length scales set the ability to elastically store energy in pea protein network structures, various network structures were obtained from pea proteins by varying the pH and salt conditions during gel formation in **Chapter 4**. The coarseness of the network structure was visualized by the use of confocal laser scanning microscopy (CLSM) and scanning electron microscopy (SEM) and ranked from least coarse to most coarse networks. Least coarse networks were formed at a pH away from the isoelectric point (IEP) of pea proteins, and at a low ionic strength, whereas more coarse networks were formed at pH values close to the IEP, and at a high ionic strength during gel formation. Mechanical deformation properties of the gels such as elastically stored (recoverable) energy, Young's moduli (stiffness of gels), fracture stress (gel strength), and fracture strain (brittleness of the gels) were measured by the use of a texture analyzer and correlated to the coarseness of the networks structure. The influence of coarseness on the ability of the networks to elastically store energy was observed for length scales below 50 nm. The findings show that elastically stored energy of pea protein gels can be modulated via the creation of different network structures below 50 nm length scales. The results from this study contribute to a better understanding of the dimensions that set the ability to elastically storage in pea protein gels. If the ability of pea proteins to store energy can be understood, products can be better tailored for consumers.

To quantitatively analyze the network structure that underlines the transitioning in the mechanical responses, pea protein gels were prepared in **Chapter 5**. To observe structural transition, gels were prepared from pea proteins at varying pHs from 3.0 to 4.2 at a fixed 100 mg/mL protein concentration. Pea protein gels were also prepared by varying the protein concentration from 100 – 150 mg/mL at a fixed pH 3.0. Mechanical deformation properties of the gels were determined. An increase in protein concentration at a fixed pH 3.0 resulted in an increase in fracture stress and Young's modulus, although the fracture strain of the gels was not affected. Variation of the pH at a fixed protein concentration resulted in transitioning in mechanical responses such as fracture stress, fracture strain, and the recoverable energy. The network structures were visualized by the use of confocal laser scanning and scanning electron microscopy, and the characteristic length scales of these structures were quantitatively analyzed in terms of the pair correlation function. Variation of the protein concentration at a fixed pH did not significantly alter the microstructure of the gels, whereas variation of the pH at a fixed protein concentration resulted in significant changes in the gel structure. Transitioning from fine to coarse-stranded pea protein networks occurred around pH 3.7, corresponding to a typical domain size of about 100 nm (based on analysis of scanning electron micrographs). The findings from this study show the transitioning in rheological responses of pea protein gels as a result of structural changes and the length scales at which the structural changes occurs in pea protein networks. The results from this study offer opportunities to broaden the application of pea proteins in food products, as products with desirable rheological (textural) and structural properties can be designed from pea proteins.

In **Chapter 6**, Maillardation of ovalbumin to evaluate how the attachment of linear oligo-sugar moieties onto ovalbumin affects its aggregation, and network morphology, and consequently the mechanical deformation properties including the ability of the networks to elastically store energy in this material was studied. To potentially alter the morphology of the network structure, ovalbumin was modified by conjugating some of its amino groups with fructooligosaccharide (FOS) moieties via the Maillard reaction. It was demonstrated that the attachment of FOS to ovalbumin does not affect the integrity of the secondary and tertiary structure as characterized using circular dichroism and tryptophan fluorescence. Differences in the network morphology were observed by scanning electron microscopy for FOS-modified ovalbumin variants. Upon increased modification, the microstructure of the gels had more and larger pores, and had thinner strands than non-modified variants. Evaluation of the large deformation properties of the gels demonstrated that FOS-modified gels were less strong, less brittle, and showed lower stiffness than non-modified variants. The recoverable energy (elastically stored energy) of gels reduced with an increase in the degree of modification. The results show that the attachment of FOS to ovalbumin alters the structural and mechanical (large) breakdown properties of the protein gels. The consequences of the alteration of the network structure and large deformation properties of FOS-modified ovalbumin offer opportunities to efficiently design food materials with desirable techno-functional applications.

The role of the serum phase viscosity on the ability to elastically store energy in whey protein gels by energy dissipation via viscous serum flow upon mechanical deformation of gels was evaluated in **Chapter 7**. Whey protein gels were used as a model system and high (HM) and low (LM) methylated negatively charged pectin or the neutral pullulan were added to modulate the viscosity of the serum phase. The gels were then subjected to uniaxial compression and the recoverable energy was evaluated. Addition of pullulan did not enhance the recoverable energy, whereas for LM pectin, the recoverable energy increased with an increase in concentration. For HM pectin, an initial decrease in the recoverable energy was first observed followed by a subsequent increase with an increase in concentration. It was demonstrated that mechanical deformation properties of gels can be described better by correcting for the effect of the viscosity of the serum phase. The results from this study show that the viscosity of the serum phase can be modulated to result in an impact on mechanical deformation properties of food gels, and thus provides a tool to engineer food products with varying rheological responses.

The aim of the study in **Chapter 8** was to relate the activation energy of the disruption of ovalbumin network structures to the elastically stored energy (i.e. recoverable energy) obtained from mechanical deformation tests. To this end, heat-set ovalbumin gels were prepared at a fixed volume fraction and pH, but varying incubation temperatures. Subsequently, the network structures were visualized by the use of microscopy, and rheological characterization of the gels was carried out. The disruption of ovalbumin networks was monitored in time in the presence of different concentrations of urea.

The activation energy required to disrupt the gels was derived from the Arrhenius equation. Increasing incubation temperature from 65 to 95 °C during gel formation was shown to result in gradual increase of the activation energy up to a factor of around 8. Gels obtained just below or around the protein denaturation temperature had a significantly lower recoverable energy. These gels also had lower fracture stress and strain. At incubation temperatures above 70 °C the recoverable energy was constant around 75 %, although a steady increase in activation energy was observed. This demonstrates that storing energy elastically in a protein network is not directly related to the interactions that make up the network. A combination of electron microscopy, water holding, and stress relaxation experiments were performed to study the different energy dissipation modes. It was shown that the different dissipation modes for the different gels were the same, and this explains why the recoverable energy was similar, except that at lower incubation temperatures where (micro) fracture events could have occurred that lowered the recoverable energy. These results show that recoverable energy is not a network characteristic related to microstructural or smaller length scale interactions, but the result of various energy dissipation mechanisms, such as microstructural stress relaxation, or friction caused by serum flow.

The findings discussed in this thesis provide opportunities to control and engineer textural properties of food gels via their microstructure and mechanical properties, and this in turn can influence the sensorial properties of foods and food products.

Samenvatting

Deze thesis onderzoekt hoe structurele aspecten van netwerken opgebouwd uit strengen de capaciteit van eiwit gels om energie op te slaan beïnvloeden. Structurele aspecten, zoals de diameter van de strengen, stijfheid, maaswijdte en de energie van de interactie tussen strengen werden bestudeerd. De rol van de viscositeit van de vloeistof fase in de dissipatie van energie, ten koste van energieopslag, werd ook onderzocht.

De fysieke eigenschappen die bestudeerd werden waren onder andere de microstructuur, breuk- en mechanische vervormingseigenschappen van de gel, alsook de opslag van energie. Een goed begrip van de capaciteit van de netwerken om energie elastisch op te slaan is zeer belangrijk voor het ontwerpen en verfijnen van voedingsproducten.

De diameter en stijfheid van de strengen beïnvloeden de vervormbaarheid van het netwerk en beide eigenschappen beïnvloeden de capaciteit van het netwerk om energie op te slaan.

Om strengen van verschillende dikte te verkrijgen werden draadvormige eiwitaggregaten op verschillende manieren gemaakt. In **Hoofdstuk 2** werden draadvormige en bolvormige aggregaten geproduceerd van wei eiwitten (WPI). Aan deze aggregaten werden thiolgroepen gekoppeld om vast te stellen of dit de functionele eigenschappen beïnvloedt. Zwavelhoudende groepen werden aan de aggregaten gekoppeld en omgezet in thiolgroepen via deblokken. Veranderingen op moleculair en microstructureel niveau werden bestudeerd met tryptofaan fluorescentie, transmissie elektronenmicroscopie en deeltjesgrootte analyse. De gemiddelde grootte van de bolvormige aggregaten nam toe van 38 – 68 nm (geblokkeerde variant) tot 106 nm (gedeblokkeerde variant) na thiolering, maar de structuur van draadvormige aggregaten werd niet beïnvloed. Vervolgens werden gels gemaakt van deze verschillende types van aggregaten. Reologische metingen lieten zien dat thiolering de eiwitconcentratie waarbij gelvorming optreedt, verlaagt en leidt tot een sterkere gel voor zowel bolvormige als draadvormige WPI aggregaten. Dit effect was sterker bij thiolering van reeds gevormde draadvormige aggregaten. De resultaten suggereren dat thiolering van reeds geaggregeerde eiwitten een veelbelovende strategie is om de efficiëntie van gelvorming te verbeteren.

Hoofdstuk 3 beschrijft hoe de stijfheid van strengen gevarieerd kan worden om de reologische eigenschappen van eiwitgels te beïnvloeden. Draadvormige aggregaten van eiwit uit erwten met een lengte in de orde van grootte van micrometers werden geproduceerd door eiwitoplossingen 20 uur te verwarmen bij pH 2,0. Vervolgens werden de draadvormige aggregaten gekarakteriseerd, gels werden gemaakt van de aggregaten en de reologische eigenschappen van deze gels werden bestudeerd.

Na verhitting van erwteneiwit hydrolyseerde al het eiwit tot peptiden en 50% van deze peptiden vormde draadvormige aggregaten.

Structurele veranderingen in erwteneiwitten werden bestudeerd met circulair dichroïsme, transmissie elektronenmicroscopie en deeltjesgrootte analyse. Tijdens de opbouw van de draadvormige aggregaten werd een toename van de deeltjesgrootte geconstateerd, gelijktijdig met een toename in binding van thioflavin T, hetgeen de aanwezigheid van β -sheet structuren aangeeft. Draadvormige aggregaten van erwteneiwit waren meer vertakt en gekruld. Gelvorming van draadvormige aggregaten werd geïnduceerd door langzame verzuring van pH 7,0 tot uiteindelijk pH 5,0.

De breukeigenschappen van gels van draadvormige aggregaten van erwteneiwit waren vergelijkbaar met gels van draadvormige aggregaten van soja- en weiproteïne, maar gels van draadvormige aggregaten van erwten- en sojaproteïne waren zwakker dan gels van draadvormige weiproteïne aggregaten. De resultaten bewijzen dat draadvormige aggregaten gemaakt kunnen worden van erwtenproteïne en dat gels gevormd kunnen worden met deze aggregaten.

Om vast te stellen welke lengteschaal invloed heeft op het vermogen om energie elastisch op te slaan in erwtenproteïne netwerken werden verschillende netwerkstructuren gemaakt van erwteneiwit door de pH en het type en concentratie van zouten te variëren tijdens de vorming van gels (**Hoofdstuk 4**). De grofheid van de netwerkstructuren werd zichtbaar gemaakt met behulp van confocale laser scanning microscopie (CLSM) en scanning elektronenmicroscopie (SEM). De structuren werden gerangschikt van lage naar hoge grofheid. De minst grove netwerken werden gevormd bij een pH die ver verwijderd was van het isoëlectrisch punt (IEP) van erwtenproteïne en bij lage ionenconcentratie. Grovere netwerken werden gevormd bij pH waarden dicht bij het IEP en bij hogere ionenconcentratie. Mechanische vervormingseigenschappen, zoals elastisch opgeslagen (herwinbare) energie, Young's moduli (stijfheid van de gels) stress bij breuk (sterkte van de gel) en de opgelegde vervorming bij breuk van de gel werden gemeten met een textuur analyser en gecorreleerd met de grofheid van de netwerkstructuur. De invloed van de grofheid op de capaciteit van netwerken om energie elastisch op te slaan werd waargenomen op een lengteschaal onder 50 nm. De resultaten tonen dat elastische opslag van energie in erwtenproteïne gels gestuurd kan worden door het creëren van verschillende netwerkstructuren met een lengteschaal van onder 50 nm. De bevindingen van deze studie dragen bij aan een beter begrip van de netwerkdimensies die de capaciteit voor elastische energieopslag in erwtenproteïne gels bepalen. Een beter begrip van de capaciteit om energie op te slaan kan leiden tot beter ontworpen producten voor de consument.

Voor een kwantitatieve analyse van de netwerkstructuur die de overgang van de mechanische respons bepaalt, werden erwtenproteïne gels geproduceerd in **Hoofdstuk 5**. Om de overgang in mechanische eigenschappen te bestuderen werden gels gemaakt bij verschillende pH van 3,0 tot 4,2, bij een vaste eiwitconcentratie van 100 mg/ml. Erwtenproteïne gels werden ook gemaakt met een concentratiereeks van 100 – 150 mg /ml eiwit, bij een vaste zuurgraad van pH 3,0.

De mechanische vervormingseigenschappen van de gels werden bepaald.

Een toename van eiwitconcentratie bij een vaste zuurgraad (pH 3,0) resulteerde in een toename van de stress bij breuk en Young's modulus, maar de opgelegde vervorming bij breuk van de gels verschilde niet. Verschillen in pH bij een vaste eiwitconcentratie veroorzaakten een toename van stress bij breuk en Young's modulus, maar de opgelegde vervorming bij breuk van de gels werd niet beïnvloed. Verschillen in pH bij een vaste eiwitconcentratie resulteerden in een overgang in mechanische eigenschappen, zoals stress bij breuk, opgelegde vervorming bij breuk en herwinbare energie. De netwerkstructuren werden zichtbaar gemaakt met behulp van confocale laser scanning en scanning electronenmicroscopie en de karakteristieke lengteschaal van deze structuren werd kwantitatief geanalyseerd met de paar correlatiefunctie.

Variatie in de eiwitconcentratie bij vaste pH gaf geen significante verschillen in de microstructuur van de gels, maar variatie in pH bij een vaste eiwitconcentratie resulteerde wel in significante veranderingen in de gelstructuur. Rond pH 3.7 en een schaalgrootte van ongeveer 100 nm (gebaseerd op analyse met behulp van scanning electronenmicroscopie) trad een overgang op van fijne naar grove netwerken van erwtenproteïne strengen. De resultaten van deze studie tonen de overgang van reologische eigenschappen als gevolg van structurele veranderingen en de schaalgrootte waarop deze veranderingen plaatsvinden in erwtenproteïne netwerken. De uitkomst van het onderzoek maakt een bredere inzet mogelijk van erwtenproteïne omdat nu producten ontworpen kunnen worden op basis van erwtenproteïne die gunstige reologische textuur- en structurele eigenschappen hebben.

In **Hoofdstuk 6** wordt onderzocht hoe modificatie van ovalbumine door het aankoppelen van lineaire oligosaccharide ketens via de Maillard reactie de aggregatie en netwerk morfologie en de daarop gebaseerde mechanische vervormingseigenschappen evenals de capaciteit van de netwerken om elastisch energie op te slaan beïnvloedt. Om de netwerkstructuur te beïnvloeden werd ovalbumine gemodificeerd via conjugatie van een deel van de aminogroepen met fructoseoligosaccharide (FOS) ketens via de Maillard reactie.

Aangetoond werd dat conjugatie met FOS geen invloed heeft op de integriteit van de secundaire and tertiaire structuur van ovalbumine, die gekarakteriseerd werd met behulp van circulair dichroïsme en tryptofaanfluorescentie. Verschillen in netwerk morfologie werden onderzocht met behulp van electronenmicroscopie van FOS-ovalbumine varianten. Bij toenemende conjugatie met FOS hadden de gels meer en grotere poriën dan varianten zonder FOS. Evaluatie van de mechanische vervormingseigenschappen toonde aan dat gels van FOS-varianten minder sterk, minder bros en minder stijf waren dan niet gemodificeerde varianten. De herwinbare energie (elastisch opgeslagen energie) van gels was minder bij hogere modificatie. De resultaten tonen aan dat conjugatie van FOS aan ovalbumine de structurele en mechanische (vervormings-) eigenschappen van de eiwitgels verandert.

De consequenties van de verandering van de netwerkstructuur en de mechanische vervormingseigenschappen van FOS-ovalbumine conjugaten geven mogelijkheden om op een efficiënte manier voedsel ingrediënten te ontwerpen met gewenste technisch-functionele eigenschappen.

De rol van de viscositeit van de vloeistoffase in de capaciteit om energie elastisch op te slaan in weiproteïne gels via energie dissipatie door viskeuze stroming van de vloeistoffase bij deformatie van gels is onderzocht in **Hoofdstuk 7**.

Weiproteïne gels werden gebruikt als model systeem en negatief geladen pectine met een hoge (HM) of lage (LM) graad van methylering of het neutrale pullulan werden toegevoegd om de viscositeit van de vloeistoffase te variëren. De gevormde gels werden blootgesteld aan uniaxiale compressie en de herwinbare energie werd bepaald. Toevoeging van pullulan had geen effect op de herwinbare energie, maar toevoeging van LM pectine verhoogde de herwinbare energie in toenemende mate bij toenemende concentratie. Bij toevoeging van HM pectine werd bij lagere concentratie een daling in herwinbare energie vastgesteld, maar bij hogere concentratie nam de herwinbare energie toe. Aangetoond werd dat de mechanische vervormingseigenschappen van gels beter beschreven kunnen worden als een correctie toegepast wordt voor de viscositeit van de vloeistoffase. De resultaten van deze studie laten zien dat de viscositeit van de vloeistoffase gemodificeerd kan worden, resulterend in een effect op de mechanische vervormingseigenschappen van voedingsgels. Dit geeft mogelijkheden om voedingsingrediënten te ontwerpen met verschillende reologische eigenschappen.

Het doel van **Hoofdstuk 8** was een verband te leggen tussen de activeringsenergie van disruptie van ovalbumine netwerken en de capaciteit van het netwerk om energie elastisch op te slaan (herwinbare energie), gemeten met mechanische deformatietests.

Voor dit doel werden ovalbumine gels gemaakt met een vast volume en pH, maar bij verschillende temperaturen. Vervolgens werd de netwerkstructuur gevisualiseerd met microscopie en werden de gels reologisch gekarakteriseerd. De disruptie van ovalbumine netwerken werd gevolgd in de tijd bij verschillende concentraties van ureum. De activeringsenergie die nodig was voor de disruptie van de gels werd berekend met behulp van de Arrhenius vergelijking. Een toenemende incubatietemperatuur van 65 tot 95 °C tijdens de gelvorming leidde tot een graduele toename van de activeringsenergie tot ongeveer een factor 8. Gels die gemaakt werden net onder of rond de denatureringstemperatuur van het eiwit hadden een significant lagere herwinbare energie. Deze gels hadden ook een lagere stress bij breuk en opgelegde vervorming bij breuk. Bij incubatietemperaturen boven 70 °C was de herwinbare energie constant rond ongeveer 75 %, hoewel een voortdurende stijging van de activeringsenergie werd gevonden.

Dit resultaat toont aan dat elastische opslag van energie in een proteïne netwerk niet direct gerelateerd is met de interacties die het netwerk vormen. Een combinatie van elektronenmicroscopie, waterretentie en vervormingsexperimenten werden uitgevoerd om de verschillende manieren van energiedissipatie te bestuderen. De resultaten lieten zien dat de verschillende dissipatieroutes voor de verschillende gels het zelfde waren, wat verklaart dat de herwinbare energie niet verschilde tussen de gels, behalve bij de laagste

incubatietemperaturen, waar (micro)fracturen kunnen hebben plaatsgevonden, die de herwinbare energie verlagen. Deze resultaten tonen aan dat herwinbare energie niet een eigenschap van een netwerk is die gerelateerd is aan microstructuur of kleinschalige interacties, maar het gevolg van verscheidene energie dissipatiemechanismen, zoals microstructurele stress afname of wrijving veroorzaakt door stroming van de vloeistoffase.

De bevindingen die in deze thesis besproken worden geven mogelijkheden om textuureigenschappen van voedselgels te beheersen en te beïnvloeden via de microstructurele en mechanische eigenschappen en dit kan de sensorische eigenschappen van voedsel en voedingsproducten beïnvloeden.

Acknowledgements

The journey of doing a PhD has been to me like a roller coaster full of good and bad times. There have been times when everything seemed to fly high and to work well. These moments were always the best. However, there were also some moments that no matter how much effort I put in, everything seemed not to work. In the challenging moments, it would have been so easy to give up if I did not get the support, encouragement, and motivation from the many individuals who came my way. Some gave their support from near whereas others were from afar. However, all this support is greatly appreciated. I would have liked to acknowledge the many people who have been there for me all this far, but this may mean writing another thesis full of acknowledgements. For this reason, I will be limited to mentioning the names of few people. Should I miss out any names, it is just because the list of people who supported me is inexhaustible.

This thesis is an evidence of my dream that one day I will have a doctorate degree and that's why I am grateful to my Maker for His strength, and confidence that He provided for each day for me to achieve this dream.

I would like to express my greatest appreciation to my supervisors, Erik van der Linden, and Harmen de Jongh, for their guidance, help and encouragement. Dear Erik, many thanks for providing a platform to discuss my work with a lot of enthusiasm. I got to learn not only to initiate a discussion about my work but to also be able to engage other people as well as taking time to reflect on my research, qualities which were cultivated by interacting with you. To my co-supervisor Harmen de Jongh, thank you so much for believing in me. I am grateful for you giving me an opportunity not only to work with you but also to grow as a scientist. From the first time I got to meet you at Birmingham airport over four years ago, you have been there to support me in this journey. I enjoyed every single meeting we had despite the fact that sometimes you were left crying from laughter because of the silly things I said. In all I learnt to be objective and have developed a critical thinking and reflection on research for the years that I have worked with you. I learnt that everything is just a "piece of cake". I will always remember you having gotten to the same results using a post it to measure the strand thickness of networks and I got almost the same results with image treatment which is hilarious. This resulted in the famous proposition that "Nothing is more sensitive for change than the human eye (comparisons between mathematical and post it analysis)".

To Komla Ako (MBF), thanks for working together with me. It all started with an email and this resulted in a collaboration that made us write two papers together. Thanks for taking your time to discuss the results with me even if it meant staying to the wee hours of the night to finish up stuff. Your patience in explaining every detail is greatly appreciated. I would also like to thank Kerensa Broersen for every discussion, help, and encouragements.

I would also like to thank all of the people I have had the pleasure to meet and work with during these years. Special thanks go to the team members of Mechanical Behaviour of

Protein-based systems (FS001 TIFN project). Laurice thank you for taking care of the nitty gritty issues of the project and ensuring that all was well. Anneke thanks for partly supervising my work when Harmen was away. Carsten and Vaida, I shared the same office with you guys for the last four year. It was nice to all have those impromptu chats. I also enjoyed the dinner invitations although sometimes I disappointed you. Thanks also to other members of the team Jan Klok, Stacy, Arno, Jissy, Saskia, Maaïke, Lenka, and Eefjan. I would also like to gratefully acknowledge the people at TI Food and Nutrition. Corine, and Marion, thanks for every help.

I also would like to thank my colleagues from the Physics and Physical Chemistry of Foods group of Wageningen University. Els, you always made life around easy as I always knew that the practical stuff that needs to be sorted out for my work were taken care of. Thanks for always answering or directing me to the right place for all the answers I needed. Thanks to Elke, Paul, Leonard, Guido, Min, Alev, Laura, Maria, Auke, Jinfeng, Pauline, Jacob, Tijs, and Zhili. You all provided support to me in your own ways and this is much appreciated. Thanks to Harry and Miranda for your assistance in ensuring that the lab stuff were taken care of.

To my paranymphs, Anika Oppermann and Kun Liu. Thank you for every time you put in making this day special. Anika, it started with one day and the sports centre, and it moved in to time training together and in to friendship. Thanks for the quality time we spend burning those calories but also just listening. Kun, you were always willing to answer my questions and were always helpful. Thanks both of you for being on my side as I defend my thesis.

A big thank you goes to my students Remi, Claudia, Anya, Stella, Rodrigo, Sjors and Macedonio. I enjoyed every moment spent with you when you did your thesis with me. I learnt a lot from you and for some of the work that you did also contributed to the story in this thesis.

Apart from the people I interacted with in the lab, there are people who are part of my life that walked this path with me. Thus, I would also like to express my thanks to:

My best friend, partner, *'Jaoda'*, and the love of my life, Josh, I am grateful for you always believing in me, for your endless love and support. This journey could have been impossible if you did not walk it through with me. Through the sleepless nights, I knew you were there and always provided a shoulder to lean on when I needed one. It has been a long time apart but this journey is coming to an end, and I look forward to beginning a new life together.

To my dear family, I am very grateful to each one of you for being there for me throughout this journey. A big thank you to my mother Ruth Musimbi Munialo and my Father Andrew Mutambi Munialo for the love you always showed to me and providing an opportunity for me to go to school. Mummy, I know some times it was such a huge sacrifice for you to see to it that I was always comfortable at school. The sacrifices you always made are what have made me be what I am today. I will forever remain thankful to you.

My dear brothers (Kris & Bryan) and sisters (Connie, Cathy, Emily, Linda, Hedwick ('Shosho') and Divinia), thank you for your love and support throughout out this long journey that began many years ago. Special thanks to big sister Connie, I do not need to remind you of the far you have taken me. Thanks for opening the doors of your home to me, and for every little prayer that you made for me that has kept me going. I also thank Emily for always being on the other side of the line to listen to me. All the visits you made to cheer me up during this journey are much appreciated. Thanks for always bringing Xylia with you, and she did fill my heart with joy that kept me going. I also thank all my in-laws, for your invaluable assistance, support and guidance throughout. I am grateful to George (baba James), Lynne (mama James), and James for opening the doors of your home to host me. Every time I came to London, I did not have to worry of where to go to for you provided a home away from home for me.

When I arrived in the Netherlands in 2011, I desired to get a family away from home. Indeed this desire was fulfilled when I first attended the first Sunday church service at Amazing Grace Parish, Wageningen. Over time, the congregation became like a family to me. I am very grateful to my spiritual parents Pastor Farai Maphosa and Pastor Mrs Busi Maphosa. Thank you for taking care of my spiritual needs in Wageningen. It was always comforting to know that someone was praying for me. Thanks my dear sister Busi for the time we shared and the prayers we made together. Thanks to Pastor Adesuwa for opening the doors on your house to me. Thanks for making my birthdays special and for those 'jollof' dinners. I hope to become a 'jollof' specialist one day and to invite you to enjoy it. Thanks to Sunday and Maureen Makama. You were a blessing to me and I am grateful for you always asked about my wellbeing. Thanks to my bible study groups both in the Nude and in Lombardi. A special thanks to Elton and Ednah Zvinavashe for the warm hosting every Wednesday, for every word of prayer, as well as for being a source of encouragement to me throughout the journey of my PhD. You can be sure I always looked forward to the word and cake as well during the house fellowship. Thanks Elton for spending your time to work on the final quality and design of my thesis. Thanks Gerbert and Janet Kets, Samson Afolabi, Peter and Kumba Morsay for being part of this amazing journey.

In being a member of AGP, I also served in a number of ministries. I became a member of the Amazing Praise family. This family is made of wonderful people. You nurtured me in my singing and I grew in my love for music as a motivation from you guys. Over time, I was also privileged to become a mum, grand mum, sister etc. to some of you guys. Thanks Ernest Beckee for being a pillar to hold on. You are a friend that I will live to treasure. Thanks for the time you gave me a listening ear when things were not okay and your prayers that kept me going. Phamela Dube, though you were no longer in Wageningen, you never severed my friendship with you. Thanks Florence Taaka for always being there for me. During the write up of my thesis, you committed yourself to knowing about my welfare. Every text, phone call, Skype message throughout the period of writing my thesis meant so much to me. I hold you dear to my heart. Oluwapelumi Adameji (aka Philomena), Bethsheba Muchiri, Rahmat Quaigrane, and Lotte van Rangelrooij, you guys are amazing, you have been pillars to me. Ernest, Flo, Pelumi, Beth, Lotte, the talks to late hours of the night was never in vain.

I look forward to hearing the testimonies from you guys.

To Biaty, Mungai, Sebastian, Annie Mumo, Jane Ogova, Juma, Musa, thanks for being part of the “Omoriabati progressive Union”. This made the end of my stay in Wageningen a memorable time in my life. James Ledo, thanks for every word of encouragement. Irene Bwoga you were a special friend that I could always call for help at any time and I knew I won't be disappointed. George Agogo, not only did we run together but I really treasure each time we met and talked. Thanks for being that friend who cared.

To my housemates at Stadsbrink 413 Anna, Michael aka administrator, Angel, Gesine, Christina, Frans, Lisa, Arrigo, Nella, Alexandra, Paula, and Roberto, I enjoyed living in the same corridor with you. It was nice to have interacted with each one of you and realized how unique each person can be. Anna thanks for being more than a house mate. I enjoyed the ladies day out and every chat we had. Roberto, thanks for always honouring every invitation I extended to you.

Thanks to Hans Kok, what a friend I found in you. It was a real pleasure ministering together. With time, you became like my own brother, you critically read through my work as your own and even when I gave you very limited time to do so. Thanks for taking all the details in designing this thesis.

Special thanks go to Chris Betts for being that editor I needed in my scientific journey.

Last but not least, I would like to appreciate the Kenyans in WUR. Those I interacted with from near and far. I must say it was a pleasure to come for those meetings and parties. I really enjoyed your warm, the '*nyama choma*', and the nice food. Thanks Cyrus Njeru for always keeping me posted of the meetings.

Claire

List of publications

Munialo, C.D.; van der Linden, E.; Ako, K.; and de Jongh, H. H. J., Quantitative analysis of the network structure that underlines the transitioning in mechanical responses of pea protein gels. *Food Hydrocolloids*, 2015, 49, 104 - 117.

Munialo, C.D.; Ortega, R. G.; van der Linden, E.; and de Jongh, H. H. J., Modification of Ovalbumin with Fructooligosaccharides: Consequences for Network Morphology and Mechanical Deformation Responses. *Langmuir*, 2014, 30 (46), 14062 - 14072.

Munialo, C.D.; Martin, A.H.; van der Linden, E.; de Jongh, H. H. J., Formation of fibrils from pea protein and subsequent gelation. *Journal of Agricultural and Food Chemistry*, 2014, 62, 2418 – 2427.

Munialo, C.D.; van der Linden, E.; de Jongh, H. H. J., The ability to store energy in pea protein gels is set by network dimensions smaller than fifty nanometers. *Food Research International*, 2014, 64, 482 – 491.

Martin, A. H.; Baigts Allende, D.; Munialo, C. D.; Urbonaite, V.; Pouvreau, L.; de Jongh, H. H. J., Modulating Protein Interaction on a Molecular and Microstructural Level for Texture Control in Protein Based Gels. (Book chapter). *Gums and Stabilizers for the Food Industry 17: The Changing Face of Food Manufacture: The Role of Hydrocolloids*, The Royal Society of Chemistry, 2014, pp. 64 - 70.

Munialo, C.D.; Vassilis Kontogiorgos., An investigation into the degradation of ascorbic acid in solutions. *Journal of Food Research and Technology*, 2014, 2 (3), 106 – 112.

Munialo, C.D.; de Jongh, H. H. J.; Broersen, K.; van der Linden, E.; Martin, A.H., Modulation of the Gelation Efficiency of Fibrillar and Spherical Aggregates by Means of Thiolation. *Journal of Agricultural and Food Chemistry*, 2013, 61 (47), 11628 - 11635.

Munialo, C.D.; van der Linden, E.; Ako, K.; Nieuwland, M.; van As, H.; de Jongh, H. H. J. Modulation of the serum phase viscosity and its contribution to energy dissipation upon mechanical deformation of whey protein gels. Submitted to *Food Hydrocolloids*.

Munialo, C.D.; van der Linden, E.; de Jongh, H. H. J. Molecular dissociation energy in relation to energy storage and dissipation upon mechanical deformation of fine-stranded ovalbumin gels. Submitted to *Langmuir*.

Conference abstracts

Munialo, C.D., van der Linden, E., de Jongh, H. H. J. Mechanistic details of energy storage in protein gels during mechanical deformation. Arrested gels, dynamics, structure and applications conference; Gonville and Caius College, University of Cambridge, UK; March

2015, (Oral presentation).

Munialo, C.D., Choi, C., van der Linden, E., de Jongh, H. H. J. Recoverable energy of pea protein network structures. Food Colloids conference; Karlsruhe, Germany; April 2014, (Poster presentation).

Munialo, C.D., Martin, A.H., van der Linden, E., de Jongh, H. H. J. Characterization and rheological behavior of pea protein fibrils. Food Structure and Functionality Forum Symposium; Amsterdam, the Netherlands; April 2014, (Oral presentation).

Munialo, C.D., Martin, A.H., van der Linden, E., de Jongh, H. H. J. Rheological behavior of pea protein Fibrillar gels in comparison to soy and whey. Biopolymers conference; Nantes, France; December 2013, (Poster presentation).

Curriculum Vitae

Claire Darizu Munialo was born on 27th of February 1985 in Kakamega, Kenya. In 2008, she graduated from the department of Animal science, Egerton University, Kenya with a BSc. degree in Animal science (First class honours). After her graduation in December 2008, she worked at Kilifi Plantations Limited as the livestock/dairy manager.

In September 2009, she was awarded a Common wealth scholarship (with funding from DFID) to study for an MSc degree in Nutrition and Food Sciences at the University of Huddersfield, the UK. In November 2010, she received her MSc degree in Nutrition and Food Sciences (Distinction). In June 2011, she was appointed as a Ph.D. fellow of Top Institute Food & Nutrition (TI F&N) to perform her research at the Physics and Physical Chemistry of Food group at Wageningen University. The outcomes of her Ph.D. research are covered in the present dissertation. Claire looks forward to continuing with research in the area of food science and technology as well as lecturing in the same field.

OVERVIEW OF COMPLETED TRAINING ACTIVITIES

Discipline specific activities

Courses

1st International Food Structure and Rheology course, 2012, Wageningen, NL
International Course on Industrial Food Protein, 2013, Wageningen, NL

Conferences and Workshops

Physics@fom Conference, 2012, Veldhoven, NL
Bio-physics Protein and Stability Symposium, 2012, Liege, BE
TI Food and Nutrition Annual Conference, Amsterdam, NL
Bio-physics Protein and Stability Symposium, 2013, Liege, BE
Biopolymers Conference, 2013, Nantes, France
Food Structure and Functionality Forum Symposium, 2014, Amsterdam, NL
15th Food Colloids Conference, 2014, Karlsruhe, DE
Arrested Gels, Dynamics, Structure and Applications Conference, 2015, Gonville and Caius College, University of Cambridge, UK

General courses

Project and Time Management, 2012, Wageningen, NL
Effective Behaviour in Professional Surroundings, 2012, Wageningen, NL
PhD Course: Voice Matters, 2012, Wageningen, NL
Interpersonal Communication for PhD Students, 2012, Wageningen, NL
Workshop Presentation Skills, 2012, Wageningen, NL
Information Literacy Course Including Endnote, 2012, Wageningen, NL
Techniques for Writing and Presenting a Scientific Paper, 2012, Wageningen, NL
Philosophy and Ethics of Food Science and Technology, 2012, Wageningen, NL
Intellectual and Industrial Property (IP) Awareness Workshop, 2012, Wageningen, NL
Career Perspectives, 2014, Wageningen, NL
Reaction kinetics in food science, 2014, Wageningen, NL

Optional courses and activities

Mechanical Behaviour of Protein-based Systems (FSO01) Project Team Building, 2012, Valencia, ES
Partners Visit, 2011 – 2014, Eindhoven, NL, Ghent, BE, and Lausanne, CH
Participated in the PhD study Trip to USA and Canada, 2014
Project and Work Group Meetings T I Food and Nutrition and Physics and Physical Chemistry of Foods, 2011- 2015, Wageningen, NL
Expert Meetings for Mechanical Behaviour of Protein-based systems (FSO01) Project T I Food and Nutrition, 2011- 2015, Wageningen, NL

The research described in this thesis was financially supported by Top Institute Food & Nutrition.

Financial support from Wageningen University and Top Institute Food & Nutrition for printing this thesis is gratefully acknowledged.

Cover photo by Claire Munialo

Cover design by Hans Kok

Printed by Gildeprint, Enschede, Netherlands